WPW SCHOOL

WPW 2019

Imperial College London

17 June 2019

WPW SCHOOL

Welcome to the WPW2019 School

We are pleased to welcome you to the second Wireless Power Week School held in conjunction with the IEEE Wireless Power Week. In this one-day school we will cover a wide range of wireless powering topics including rectenna design, localization, communication, inductive powering regimes, system design and grid integration. We are proud to present a team of ten world leading experts to give the invited lectures on the topics of the school. With the selection of talks we believe that the school provides a good first introduction to newcomers in the field and many of its subfields, and, additionally, that its wide coverage will provide valuable to those who already are in the field but want to broaden their knowledge. In all, we wish you an intellectually challenging, inspiring and rewarding day here at Imperial College London.

Nuno Borges Carvalho
WPW School Chair

Paul D. Mitcheson and Hubregt J. Visser
Conference Co-Chairs

WPW2019 School Programme

Time	Monday 17th June 2019
08:00 - 08:30	Registration & Coffee
08:30 - 08:40	Introduction and Welcome (Nuno Borges Carvalho)
Session 1: Rectennas	
08:40 - 09:20	Lecture 1 - Ad Reniers: Practical Rectenna Design
09:20 - 10:00	Lecture 2 - Jiafeng Zhou: Multi-band Rectenna Design for Radio Frequency Energy Harvesting
10:00 - 10:40	Lecture 3 - Simon Hemour: Environment aware battery-less IoT Frontend
10:40 - 11:00	Break
Session 2: Systems and Practical Considerations	
11:00 - 11:40	Lecture 4 - Bruno Franciscatto: Battery-less UWB indoor location is the way forward for industry 4.0
11:40 - 12:20	Lecture 5 - Naoki Shinohara: How to detect position of user to keep high beam efficiency on wireless power transfer via radio waves
12:20 - 13:20	Lunch
Session 3: Simultaneous Communication and Power Transfer	
13:20 - 14:00	Lecture 6 - Bruno Clerckx: Optimize, Learn and Prototype Wireless Communications and Power Transfer
14:00 - 14:40	Lecture 7 - Nuno Borges Carvalho: Combining backscatter communications with WPT, the new Wireless Power Communication Paradigm
14:40 - 15:00	Break
Session 4: Inductive Power Transfer	

15:00 - 15:40	Lecture 8 - Giuseppina Monti: Inductive Resonant WPT: design equations for different operative regimes
15:40 - 16:20	Lecture 9 - Alessandra Costanzo: Analytical and numerical design of non-static WPT systems
16:20 - 17:00	Lecture 10 - Udaya Madawala: Wireless Grid Integration of EVs for V2G Applications : Challenges and Technologies
17:00 - 17:10	Closing remarks (Nuno Borges Carvalho), and head to Savoy Place for WPW2019 welcome reception

WPW SCHOOL

WPW2019 School Speakers

WPW2019 School Chair:

Nuno Carvalho - University of Aveiro, Portugal

Nuno Borges Carvalho (S'97–M'00–SM'05-F'15) was born in Luanda, Angola, in 1972. He received the Diploma and Doctoral degrees in electronics and telecommunications engineering from the University of Aveiro, Aveiro, Portugal, in 1995 and 2000, respectively. He is currently a Full Professor and a Senior Research Scientist with the Institute of Telecommunications, University of Aveiro and an IEEE Fellow. He coauthored Intermodulation in Microwave and Wireless Circuits (Artech House, 2003), Microwave and Wireless Measurement Techniques (Cambridge University Press, 2013) and White Space Communication Technologies (Cambridge University Press, 2014). He has been a reviewer and author of over 200 papers in magazines and conferences. He is the Editor in Chief of the Cambridge Wireless Power Transfer Journal, an associate editor of the IEEE Microwave Magazine and former associate editor of the IEEE Transactions on Microwave Theory and Techniques and IET Microwaves Antennas and Propagation Journal. He is the co-inventor of six patents. His main research interests include software-defined radio front-ends, wireless power transmission, nonlinear distortion analysis in microwave/wireless circuits and systems, and measurement of nonlinear phenomena. He has recently been involved in the design of dedicated radios and systems for newly emerging wireless technologies. Dr. Borges Carvalho is a member of the IEEE MTT ADCOM, the chair of the IEEE MTT-20 Technical Committee and the past-chair of the IEEE Portuguese Section and MTT-11 and also belong to the technical committees, MTT-24 and MTT-26. He is also the vice-chair of the URSI Commission A (Metrology Group). He was the recipient of the 1995 University of Aveiro and the Portuguese Engineering Association Prize for the best 1995 student at the University of Aveiro, the 1998 Student Paper Competition (Third Place) of the IEEE Microwave Theory and Techniques Society (IEEE MTT-S) International Microwave Symposium (IMS), and the 2000 IEE Measurement Prize. He is a Distinguished Microwave Lecturer for the IEEE Microwave Theory and Techniques Society.

WPW2019 School Speakers:

Ad Reniers - Eindhoven University of Technology, Netherlands

Ad Reniers received the Bachelor's degree in electrical engineering from Fontys University of applied sciences and is currently pursuing his Ph.D. degree at Eindhoven University of Technology (TU/e). From 1999 to 2009, he worked with TNO Industry and Technique in Eindhoven, The Netherlands on research projects, affiliated to antenna-based sensors, antenna miniaturization, RFID applications, and energy harvesting. Since 2009, he has been associated with the Electromagnetics Group, Department of Electrical Engineering, Eindhoven University of Technology, Eindhoven, The Netherlands as a research and education officer. He has extensive research and engineering experience in the field of antenna design and antenna measurement. His research interests include millimeter wave antenna measurement, antenna miniaturization for integrated mm-wave communication and wireless power transfer.

Jiafeng Zhou - University of Liverpool, UK

Dr. Jiafeng Zhou is with the Department of Electrical Engineering & Electronics at the University of Liverpool, UK since 2013. He has performed research on RF circuit design, radio signal receiving and transmitting for 15 years. During his PhD study at the University of Birmingham, UK, he implemented one of the world's smallest superconducting RF resonators and filters. After completing PhD, Dr. Zhou carried out research in the University of Birmingham to design advanced components for phased-array antennas for radio astronomy. Then he joined the University of Bristol, UK, where he developed power amplifiers with industrial leading performances for Toshiba. Dr. Zhou is currently an executive member of the IET Electromagnetics Professional Network and the IET Internet of Things Professional Network. His current research interests include microwave devices for satellite and wireless communication systems, wireless power transfer and energy harvesting for sensor networks, wearable and implantable devices.

Simon Hemour - University of Bordeaux, France

Dr. Simon Hemour is an Associate Professor at Bordeaux University, France. He holds a PhD degree in electrical engineering from Grenoble Institute of Technology. From 2011 to 2015, he was with Ecole Polytechnique de Montreal, Canada, where he lead a research team on Wireless Energy Transmission and Harvesting. Prior joining Polytechnic Montreal, he has been with the European Organization for Nuclear Research (CERN), Geneva, Switzerland, with the National Academy of Science of Ukraine (NASU), Lviv, Ukraine and with the national center for Micro and Nanotechnology (MINATEC) in Grenoble in France. He was the TPC chair of the wireless Power Transmission Conference WPTC2018. He is a member of the IEEE MTT technical committee TC-26 on "Wireless Energy Transfer and Conversion" and TC-10 on "Biological Effect and Medical Applications of RF and Microwave". He serves as a guest editor for the IEEE Journal of Electromagnetics, RF and Microwaves in Medicine and Biology on the WPT and RF energy harvesting special issue.

Bruno Franciscatto - UWINLOC, France

Bruno is the CTO of the French company UWINLOC, based on Toulouse - south of France. He holds more than 17 patent applications and more than 16 scientific papers published, he has 10 years of experience in Wireless Communications; Energy Harvesting; design, industrialization and deployment of IoT systems (HW and SW). Successful start-up experience (Executive board member) – IPO Valuation £225M. In 2014, Bruno obtained his PhD in optics and radiofrequency at Grenoble University (France) in a partnership between IMEP-LAHC laboratory and Multitoll Solutions. During his PhD, Bruno started to study the Wireless Energy Harvesting/Transfer. He succeeded in creating Wireless Energy Harvesters that were capable of recovering the RF energy to supply low-power devices. The results improved the state-of-the-art on Wireless Energy Harvesting and lead to high-level publications, one of them being awarded as the best student paper in the SBMO/IEEE MTT-S International Microwave and Optoelectronics Conference (IMOC) 2013. In 2010, Bruno obtained his M.Sc. degree in optics and radiofrequency from the University of Grenoble (France). Bruno obtained his B.E. degree in electronics and telecommunications at the Federal University of Campina Grande (Brazil) in 2010, with distinction and honoured with an excellence academic award.

Naoki Shinohara - Kyoto University, Japan

Naoki Shinohara received the B.E. degree in electronic engineering, the M.E. and Ph.D (Eng.) degrees in electrical engineering from Kyoto University, Japan, in 1991, 1993 and 1996, respectively. He was a research associate in Kyoto University from 1996. From 2010, he has been a professor in Kyoto University. He has been engaged in research on Solar Power Station/Satellite and Microwave Power Transmission system. He was IEEE MTT-S Distinguish Microwave Lecturer (2016-18), and is IEEE MTT-S Technical Committee 26 (Wireless Power Transfer and Conversion) chair, IEEE MTT-S Kansai Chapter TPC member, IEEE Wireless Power Transfer Conference founder and advisory committee member, URSI commission D vice chair, international journal of Wireless Power Transfer (Cambridge Press) executive editor, the first chair and technical committee member on IEICE Wireless Power Transfer, Japan Society of Electromagnetic Wave Energy Applications president, Space Solar Power Systems Society board member, Wireless Power Transfer Consortium for Practical Applications (WiPoT) chair, and Wireless Power Management Consortium (WPMc) chair. His books are “Wireless Power Transfer via Radiowaves” (ISTE Ltd. and John Wiley & Sons, Inc., “Recent Wireless Power Transfer Technologies Via Radio Waves (ed.)” (River Publishers), and “Wireless Power Transfer: Theory, Technology, and Applications (ed.)” (IET).

Bruno Clerckx - Imperial College London, UK

Bruno Clerckx received the M.S. and Ph.D. degrees in applied science from the Université Catholique de Louvain, Louvain-la-Neuve, Belgium, in 2000 and 2005, respectively. From 2006 to 2011, he was with Samsung Electronics, Suwon, South Korea, where he actively contributed to 3GPP LTE/LTE-A and IEEE 802.16m and acted as the Rapporteur for the 3GPP Coordinated Multi-Point (CoMP) Study Item. From 2014 to 2016, he was an Associate Professor with Korea University, Seoul, South Korea. He also held visiting research appointments at Stanford University, EURECOM, the National University of Singapore, and The University of Hong Kong. Since 2011, he has been with Imperial College London, first as a Lecturer from 2011 to 2015, then as a Senior Lecturer from 2015 to 2017, and now as a Reader. He is currently a Reader (Associate Professor) with the Electrical and Electronic Engineering Department, Imperial College London, London, U.K. He has authored two books, 150 peer-reviewed international research papers, and 150 standards contributions, and is the inventor of 75 issued or pending patents among which 15 have been adopted in the specifications of 4G (3GPP LTE/LTE-A and IEEE 802.16m) standards. His research area is communication theory and signal processing for wireless networks. He has been a TPC member, a symposium chair, or a TPC chair of many symposia on communication theory, signal processing for communication and wireless communication for several leading international IEEE conferences. He is an Elected Member of the IEEE Signal Processing Society SPCOM Technical Committee. He served as an Editor for the IEEE TRANSACTIONS ON COMMUNICATIONS from 2011 to 2015 and the IEEE TRANSACTIONS ON WIRELESS COMMUNICATIONS from 2015 to 2018, and is currently an Editor for the IEEE TRANSACTIONS ON SIGNAL PROCESSING. He has also been a (lead) guest editor for special issues of the EURASIP Journal on Wireless Communications and Networking, IEEE ACCESS and the IEEE JOURNAL ON SELECTED AREAS IN COMMUNICATIONS. He was an Editor for the 3GPP LTE-Advanced Standard Technical Report on CoMP.

Giuseppina Monti - University of Salento, Italy

Giuseppina Monti received the Laurea degree in Telecommunication Engineering (with honors) from the University of Bologna, Italy, in 2003, and the Ph.D. in Information Engineering from University of Salento (Italy), in 2007. She is currently with the Department of Innovation Engineering (University of Salento), where she is a temporary researcher and lecturer in CAD of Microwave circuits and Antennas. Since 2007, the research activities of G. Monti have been focused on the area of electromagnetic enabling technologies for energy autonomous smart systems. Special emphasis is put on reconfigurable devices for cognitive networks, wearable devices, energy harvesting, wireless power transmission (WPT). With regard to the development of technologies for WPT and energy harvesting, G. Monti is active both on: 1) the design of low-power long-range power links based on the use of rectennas, 2) the design and the theoretical analysis of high-power low/mid-range power links based on the use of electromagnetically coupled resonant systems (wireless resonant energy links). G. Monti has co-authored four book chapters and about 150 papers appeared in international conferences and journals.

Alessandra Costanzo - University of Bologna, Italy

Prof Alessandra Costanzo is a full professor at the University of Bologna, Italy since 2018. She is currently involved in research activities dedicated to design of entire wireless power transmission systems, based on the combination of EM and nonlinear numerical techniques, adopting both far-field and near-field solutions, for several power levels and operating frequencies. She has authored more than 200 scientific publications on peer reviewed international journals and conferences and several chapter books. She owns four international patents. She is co-founder the EU COST action IC1301 WiPE "Wireless power transfer for sustainable electronics", just ended where she chaired WG1: "far-field wireless power transfer". She was workshop chair of the EuMW2014. In 2018 she is ExCom chair of the WPTC2018 and TPC co-chair of the IEEE IMARC 2018. She is the past-chair (2016-2017) of the MTT-26 committee on wireless energy transfer and conversion and member of the MTT-24 committee on RFID. She serves as associate editor of the IEEE Transaction on MTT, of the Cambridge International Journal of Microwave and Wireless Technologies and of the Cambridge International Journal of WPT. Since 2016 she is steering committee chair of the new IEEE Journal of RFID. She is MTT-S representative and Distinguished Lecturer of the CRFID, where she also serves as MTT-S representative. She is IEEE senior member.

Udaya Madawala - The University of Auckland, New Zealand

Udaya K. Madawala graduated with a B.Sc. (Electrical Engineering) (Hons) degree from The University of Moratuwa, Sri Lanka in 1987, and received his PhD (Power Electronics) from The University of Auckland, New Zealand in 1993 as a Commonwealth Doctoral Scholar. At the completion of his PhD, he was employed by Fisher & Paykel Ltd, New Zealand, as a Research and Development Engineer to develop new technologies for motor drives. In 1997 he joined the Department of Electrical and Computer Engineering at The University of Auckland and, at present as a Full Professor, he focuses on a number of power electronics projects related to wireless grid integration of EVs for V2G applications and renewable energy. Udaya is a Fellow of the IEEE and a Distinguished Lecturer of the IEEE Power Electronic Society (PELS), and has over 30 years of both industry and research experience in the fields of power electronics and energy. He has served both the IEEE Power Electronics and Industrial Electronics Societies in numerous roles, relating to editorial, conference, technical committee and chapter activities. Currently, Udaya is an Associate Editor for IEEE Transactions on Power Electronics, and a member of both the Administrative Committee and Membership Development Committee of the IEEE Power Electronics Society. He was the General Chair of the 2nd IEEE Southern Power Electronics Conference (SPEC)- 2016, held in New Zealand, and is also the Chair of SPEC Steering Committee. Udaya, who has over 300 IEEE and IET journal and conference publications, holds a number of patents related to wireless power transfer (WPT) and power converters, and is a consultant to industry.

WPW SCHOOL

Practical Rectenna Design

Ad Reniers & Tom van Nunen
Eindhoven University of Technology

In this presentation we will give hands on instructions and tips to construct a 2.45GHz rectenna. We will start with designing a 50 Ohm rectangular microstrip patch antenna and realize this antenna on FR4 using copper tape, a ruler and a knife. After tuning the antenna to 50 Ohm, we will design a rectifying circuit using discrete Schottky diodes. For analyzing and designing the circuit we will make use of freeware circuit software. We will determine the input impedance and design a impedance matching circuit to connect the antenna to the rectifying circuit. Finally we will load the rectenna with a led and demonstrate the rectenna, using the signals leaked through the door of a microwave oven.

Practical Rectenna Design

Ad Reniers, Tom van Nunen,
Hubregt Visser
Eindhoven University of Technology
a.reniers@tue.nl

CONTENTS

1. INTRODUCTION

Rectenna = **Rect**ifying Ant**enna**

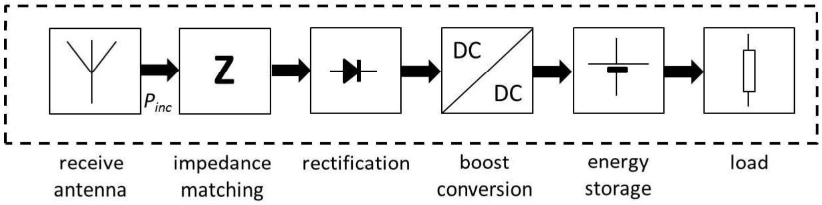

Powering at a distance

Using radio waves

Using a dedicated transmitter

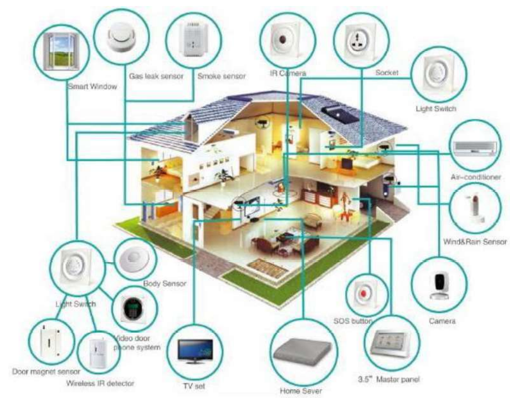

1. INTRODUCTION

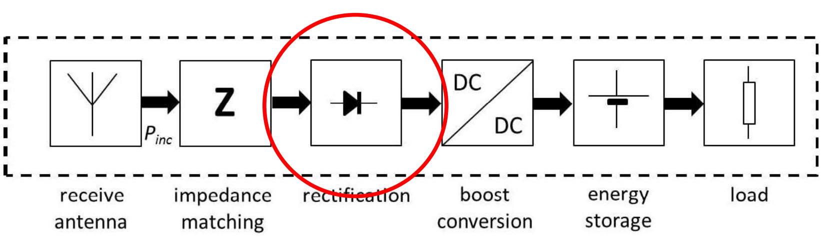

The core of a rectenna is the rectifier

Input impedance changes as a function of

frequency

RF input power

DC load

Need to know the input impedance with high degree of accuracy

1. INTRODUCTION

Analytical solutions to designing the antenna and the rectifier

Verified with Commercial Off The Shelf software validations

Since as a university we have access to that,
but not every company has

2. ANTENNA ANALYSIS

Inset-fed, rectangular microstrip patch antenna

- Can be integrated on PCB
- Radiation pattern cosine-like
- Design for 50Ω for easy evaluation

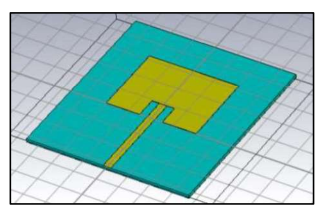

Start with microstrip transmission line

Width W, for given characteristic impedance Z_0, substrate thickness h and relative permittivity ε_r:

$$\frac{W}{h} = \begin{cases} \dfrac{8e^A}{e^{2A}-2} & \text{for } \dfrac{W}{h} < 2 \\ \dfrac{2}{\pi}\left[B - 1 - \ln(2B-1) + \dfrac{\varepsilon_r - 1}{\varepsilon_r + 1}\left\{\ln(B-1) + 0.39 - \dfrac{0.61}{\varepsilon_r}\right\}\right] & \text{for } \dfrac{W}{h} > 2 \end{cases}$$

$$A = \frac{Z_0}{60}\sqrt{\frac{\varepsilon_r + 1}{2}} + \frac{\varepsilon_r - 1}{\varepsilon_r + 1}\left(0.23 + \frac{0.11}{\varepsilon_r}\right)$$

$$B = \frac{377\pi}{2Z_0\sqrt{\varepsilon_r}}$$

D. Pozar, *Microwave Engineering, 4th edition*, John Wiley & Sons, New York, 2012.

2. ANTENNA ANALYSIS

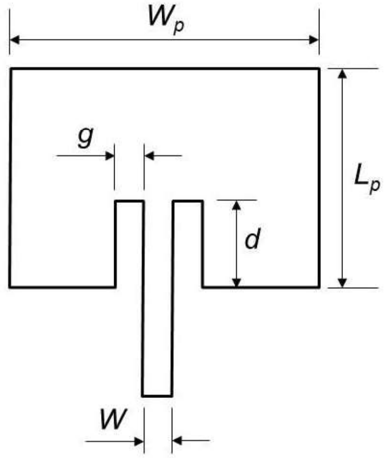

$$W_p = \frac{c}{2 f_0}\sqrt{\frac{2}{\varepsilon_r + 1}}$$

$$\varepsilon_{reff} = \frac{\varepsilon_r + 1}{2} + \frac{\varepsilon_r - 1}{2}\left[1 + 12\frac{h}{W_p}\right]^{-\frac{1}{2}}$$

$$\Delta L = 0.412h \frac{(\varepsilon_{reff} + 0.3)\left(\frac{W_p}{h} + 0.264\right)}{(\varepsilon_{reff} - 0.258)\left(\frac{W_p}{h} + 0.8\right)}$$

$$L_p = \frac{c}{2 f_0 \sqrt{\varepsilon_{reff}}} - 2\Delta L$$

$$g = W$$

$$d = 10^{-4}\left\{\begin{array}{l} 0.001699\varepsilon_r^7 + 0.13761\varepsilon_r^6 - 6.1783\varepsilon_r^5 \\ +93.187\varepsilon_r^4 - 682.69\varepsilon_r^3 + 2561.9\varepsilon_r^2 \\ -4043\varepsilon_r + 6697 \end{array}\right\}\frac{L}{2} \quad \text{for} \quad 2 \le \varepsilon_r \le 10$$

M.A. Martin and A.I. Sayeed, ‘A Design Rule for Inset-fed Rectangular Microstrip Patch Antenna’, *WSEAS Transactions on Communications*, Vol. 9, No. 1, pp. 63-72, January 2010.
M. Ramesh and Y. Kb, ‘Design Formula for Inset Fed Microstrip Patch Antenna’, *Journal of Microwaves and Optoelectronics*, Vol. 3, No. 3, pp. 5-10, December 2003.

2. ANTENNA ANALYSIS

Verification (f_0 = 1.8 GHz, ε_r = 3.55, h = 1.53 mm)

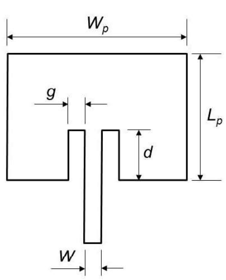

W = 3.42 mm L_p = 4.39 cm

W_p = 5.52 cm $g = W$ = 3.42 mm

ε_{reff} = 3.38 d = 12.49 mm

ΔL = 0.69 mm

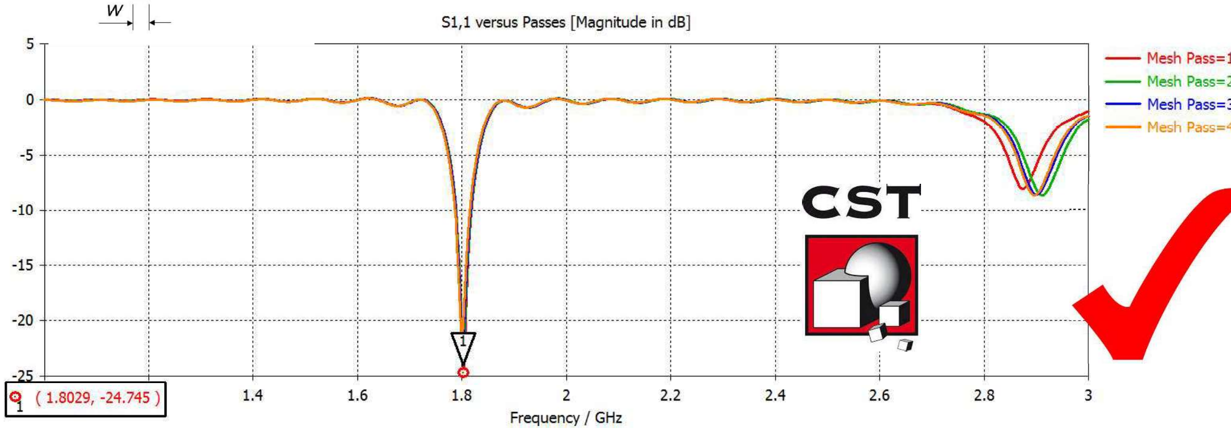

CST

3. RECTIFIER ANALYSIS

Rectifier based on Schottky diode

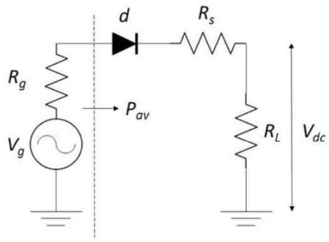

For the DC output voltage

$$B_0\left(\frac{q}{nkT}\sqrt{8R_gP_{av}}\right)=\left(1+\frac{V_0}{R_LI_s}\right)e^{\left(1+\frac{R_g+R_s}{R_L}\right)\frac{q}{nkT}V_0}$$

Electron charge
DC voltage
Temperature
Boltzmann's constant
Available power
Generator resistance
Saturation current
Ideality factor
Zero-order modified Bessel function of first kind
Load resistance

R.G. Harrison and X. Le Polozec, 'Nonsquarelaw Behavior of Diode Detectors Analyzed by the Ritz-Galérkin Method', *IEEE Transactions on Microwave Theory and Techniques*, Vol. 42, No. 5, pp. 840-846, May 1994.

3. RECTIFIER ANALYSIS

Input Impedance

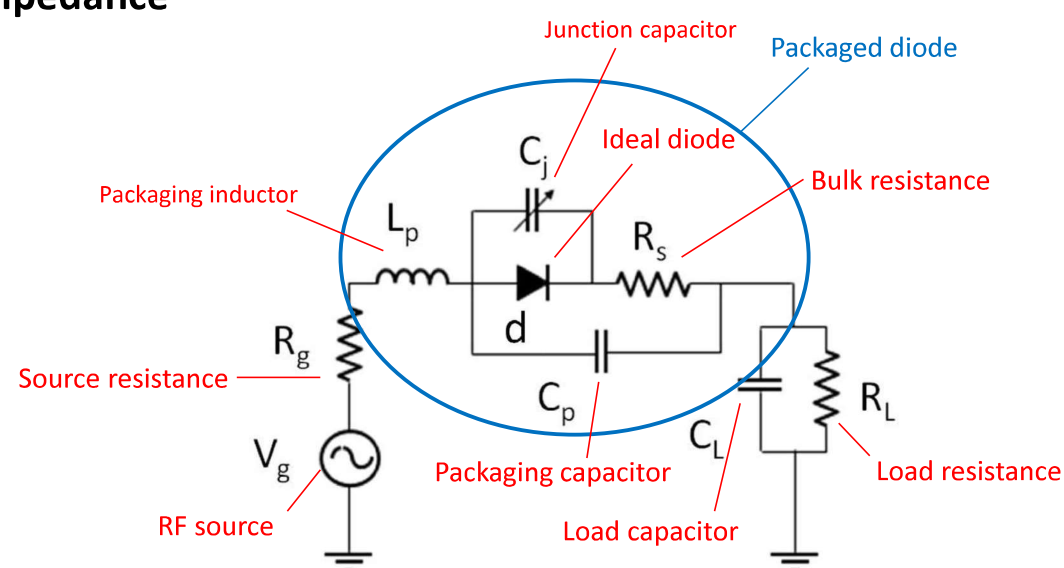

3. RECTIFIER ANALYSIS

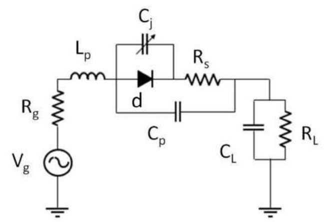

$$V_g = |V_g| \cos(2\pi f_0 t)$$

C_L large → behaves as open circuit

$$\frac{\partial V_d}{\partial t} = \frac{1}{R_s C_j}\left[V_g - I_g(R_g + R_L) - V_d - L_p I_X - \frac{I_s}{C_j}\left(e^{\frac{q}{nkT}V_d} - 1\right)\right]$$

$$\frac{\partial I_X}{\partial t} = \frac{1}{C_p L_p R_s}\left[V_g - V_d - I_g(R_g + R_L) - L_p I_X\right] + \frac{1}{L_p}\frac{\partial V_g}{\partial t} - \frac{(R_g + R_L)}{L_p} I_X - \frac{I_g}{C_p L_p}$$

$$\frac{\partial I_g}{\partial t} = I_X$$

MATLAB ODE solver for stiff equations, followed by FFT

3. RECTIFIER ANALYSIS

Verification

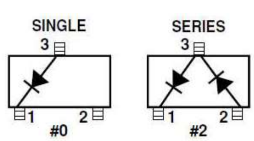

Parameter	HSMS-2820	HSMS-2850	Units
I_s	2.2E-8	3.0 E-6	A
n	1.08	1.06	-
R_s	6.0	25	Ω
C_j	0.7	0.18	pF
L_p	2.0	2.0	nH
C_p	0.08	0.08	pF
C_{23}	0.06	0.06	pF

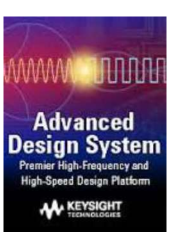

Schottky diode HSMS-2852

RF input power: -10dBm

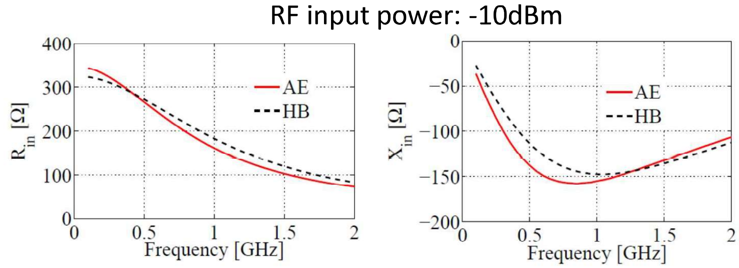

Schottky diode HSMS-2820

RF input power: -10dBm

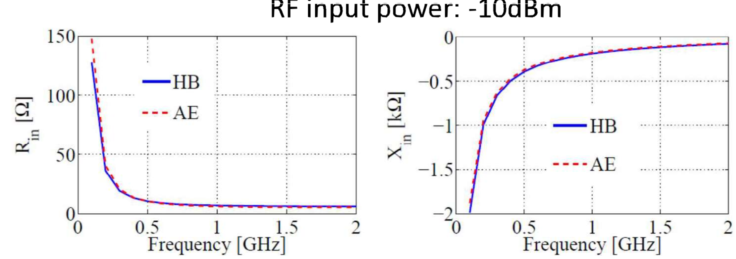

3. RECTIFIER ANALYSIS

Solving ODEs

GNU Octave

https://www.gnu.org/software/octave/

We now have an alternative for antenna and rectifier analysis, not relying on (expensive) COTS software.

However, it is restricted to one antenna type and one rectifier type.

NEXT: FREEWARE FULL-WAVE ANALYSIS

4. FREEWARE FULL-WAVE ANALYSIS - ANTENNA

Alternative Full-Wave EM simulation

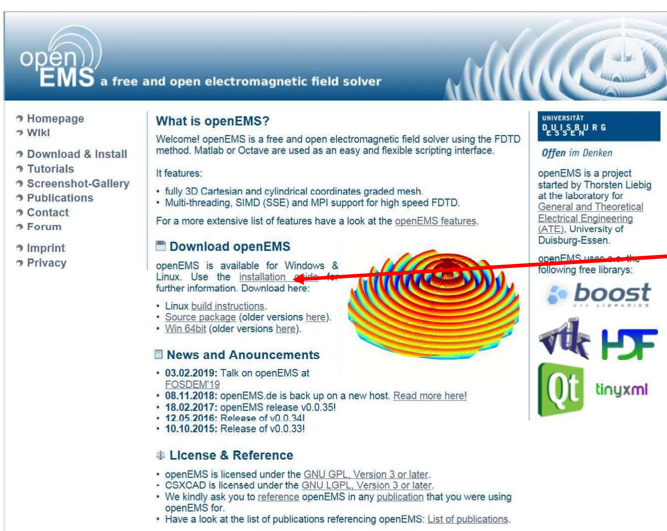

Download *.zip file

http://openems.de/start/index.php
https://archive.org/details/youtube-ThMLf0d5gaE
https://ftp.gnu.org/gnu/octave/windows/

4. FREEWARE FULL-WAVE ANALYSIS - ANTENNA

Alternative Full-Wave EM simulation

Install the folder as “openEMS” on your ‘C’ or ‘D’ directory (C:/openEMS/)

Open matlab file with your antenna code and add: addpath('D:/openEMS/matlab');

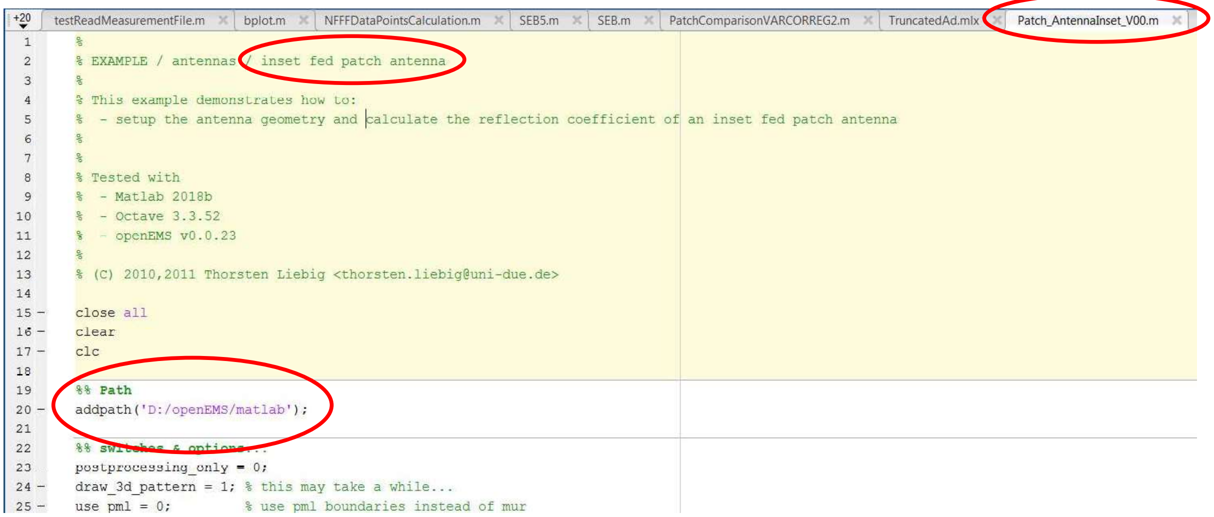

4. FREEWARE FULL-WAVE ANALYSIS - ANTENNA

Patch antenna design orientation

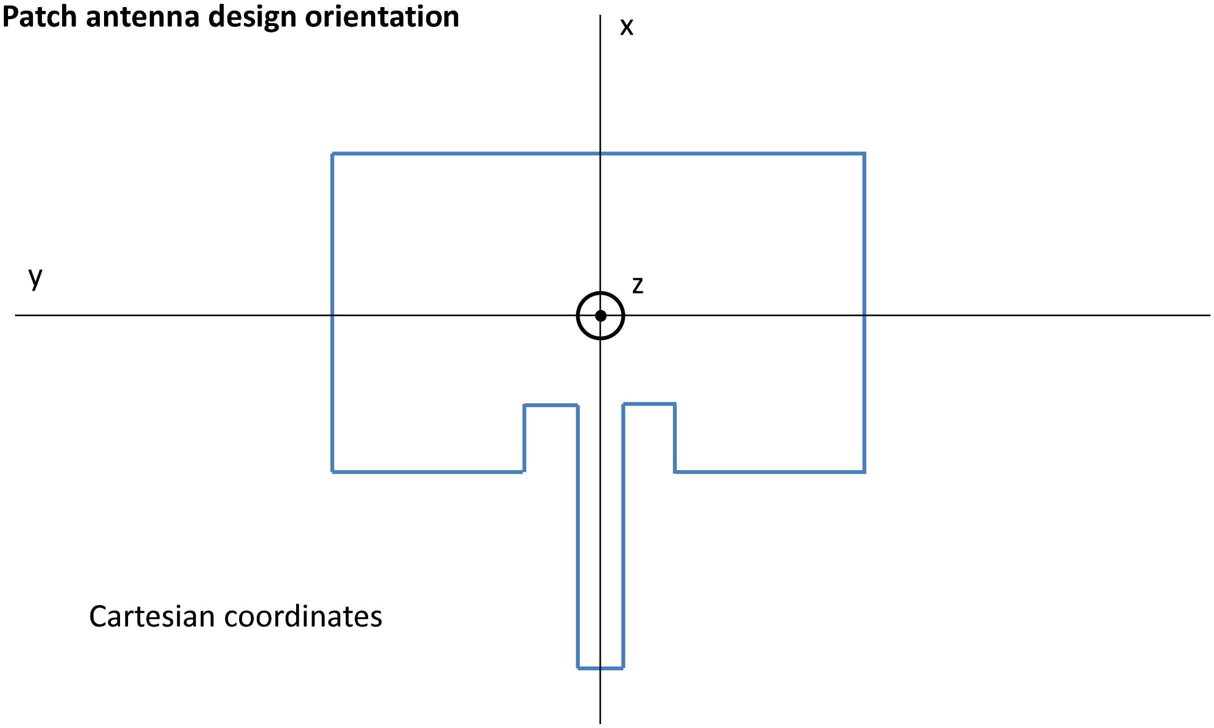

4. FREEWARE FULL-WAVE ANALYSIS - ANTENNA

Patch antenna design dimensions for 2.4 GHz

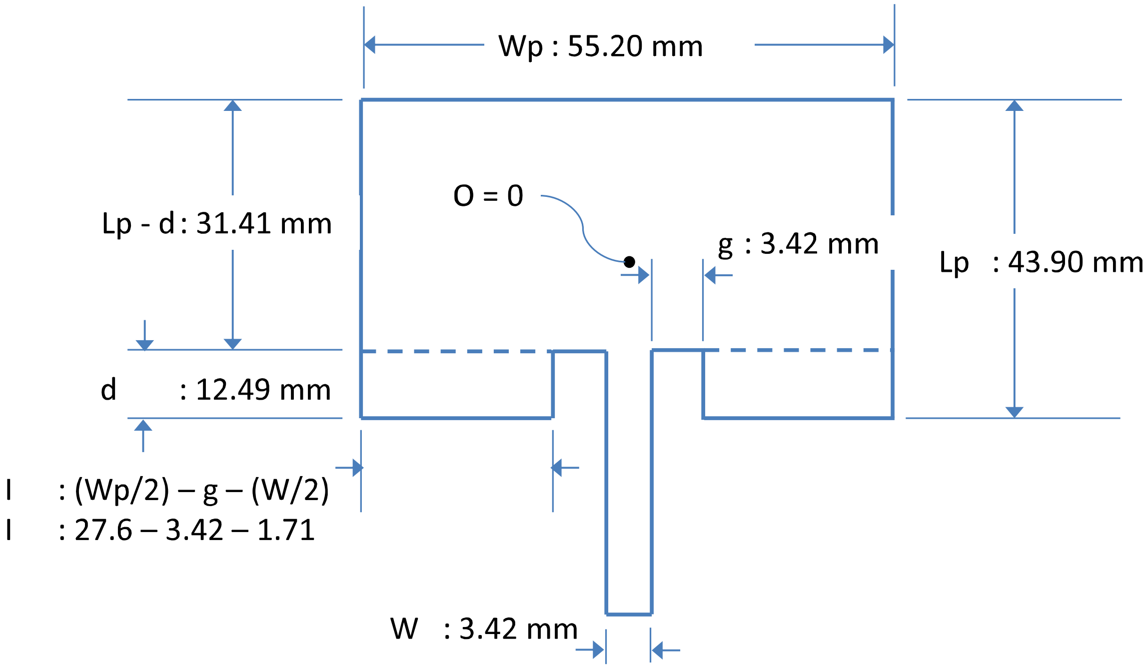

4. FREEWARE FULL-WAVE ANALYSIS - ANTENNA

Setting up a Full-Wave EM simulation of a patch antenna

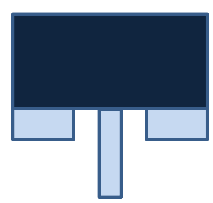

Patch geometry without inset

```
%% create patch
CSX = AddMetal( CSX, 'patch' ); % create a perfect electric conductor (PEC)
start           = [-(patch.length/2)+inset.length -patch.width/2 substrate.thickness];
stop            = [ patch.length/2  patch.width/2 substrate.thickness];
CSX             = AddBox(CSX,'patch',10,start,stop);
```

```
% width in x-direction
% length in y-direction
% main radiation in z-direction
patch.length         = 32.10; % resonant length 43.90 (x-axis)
patch.width          = 40.60; % (y-axis) 55.20

inset.width          = 3.41;  %Rectangular shape creating the inset 3.42
inset.length         = 9.13; % 12.49

line.width           = 3.41;  % 3.42
line.length          = 40.00;

substrate.epsR       = 3.55;
substrate.kappa      = 4e-3 * 2*pi*1.8e9 * EPS0*substrate.epsR;
substrate.width      = 100;
substrate.length     = 64.2;
substrate.thickness  = 1.524;
substrate.cells      = 4;

feed.pos             = -line.length;
feed.width           = 3.41;
feed.R               = 50; % feed resistance

% size of the simulation box
SimBox               = [160 160 50];
```

4. FREEWARE FULL-WAVE ANALYSIS - ANTENNA

Setting up a Full-Wave EM simulation of a patch antenna

Right patch extension

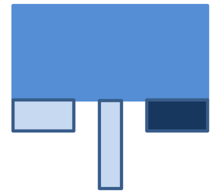

```
%% Create inset right
CSX             = AddMetal( CSX, 'insetright' ); % create a inset
start           = [-patch.length/2 -patch.width/2 substrate.thickness];
stop            = [-patch.length/2+inset.length 0-inset.width-feed.width/2 substrate.thickness];
CSX             = AddBox(CSX,'insetright',10,start,stop);
```

```
% width in x-direction
% length in y-direction
% main radiation in z-direction
patch.length         = 32.10; % resonant length 43.90 (x-axis)
patch.width          = 40.60; % (y-axis) 55.20

inset.width          = 3.41;  %Rectangular shape creating the inset 3.42
inset.length         = 9.13; % 12.49

line.width           = 3.41;  % 3.42
line.length          = 40.00;

substrate.epsR       = 3.55;
substrate.kappa      = 4e-3 * 2*pi*1.8e9 * EPS0*substrate.epsR;
substrate.width      = 100;
substrate.length     = 64.2;
substrate.thickness  = 1.524;
substrate.cells      = 4;

feed.pos             = -line.length;
feed.width           = 3.41;
feed.R               = 50; % feed resistance

% size of the simulation box
SimBox               = [160 160 50];
```


4. FREEWARE FULL-WAVE ANALYSIS - ANTENNA

Setting up a Full-Wave EM simulation of a patch antenna

Left patch extension

```
%% Create inset left
CSX = AddMetal( CSX, 'insetleft' ); % create a inset
start           = [-patch.length/2 patch.width/2 substrate.thickness];
stop            = [-patch.length/2+inset.length 0+inset.width+feed.width/2 substrate.thickness];
CSX             = AddBox(CSX,'insetleft',10,start,stop);
```


```
% width in x-direction
% length in y-direction
% main radiation in z-direction
patch.length         = 32.10; % resonant length 43.90 (x-axis)
patch.width          = 40.60; % (y-axis) 55.20

inset.width          = 3.41;  %Rectangular shape creating the inset 3.42
inset.length         = 9.13; % 12.49

line.width           = 3.41;  % 3.42
line.length          = 40.00;

substrate.epsR       = 3.55;
substrate.kappa      = 4e-3 * 2*pi*1.8e9 * EPS0*substrate.epsR;
substrate.width      = 100;
substrate.length     = 64.2;
substrate.thickness  = 1.524;
substrate.cells      = 4;

feed.pos             = -line.length;
feed.width           = 3.41;
feed.R               = 50; % feed resistance

% size of the simulation box
SimBox               = [160 160 50];
```

4. FREEWARE FULL-WAVE ANALYSIS - ANTENNA

Setting up a Full-Wave EM simulation of a patch antenna

Transmission line

```
%% Create transmission line
CSX          = AddMetal( CSX, 'line' ); % create a inset
start        = [-line.length -line.width/2 substrate.thickness];
stop         = [0 line.width/2 substrate.thickness];
CSX          = AddBox(CSX,'line',10,start,stop);
```

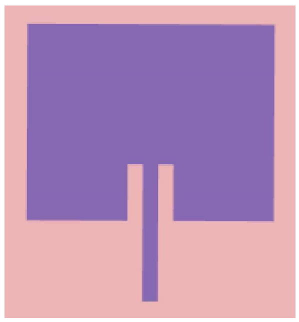

```
% width in x-direction
% length in y-direction
% main radiation in z-direction
patch.length        = 32.10; % resonant length 43.90 (x-axis)
patch.width         = 40.60; % (y-axis) 55.20

inset.width         = 3.41;  %Rectangular shape creating the inset 3.42
inset.length        = 9.13; % 12.49

line.width          = 3.41;  % 3.42
line.length         = 40.00;

substrate.epsR      = 3.55;
substrate.kappa     = 4e-3 * 2*pi*1.8e9 * EPS0*substrate.epsR;
substrate.width     = 100;
substrate.length    = 64.2;
substrate.thickness = 1.524;
substrate.cells     = 4;

feed.pos            = -line.length;
feed.width          = 3.41;
feed.R              = 50; % feed resistance

% size of the simulation box
SimBox              = [160 160 50];
```

https://github.com/thliebig/openEMS/blob/master/matlab/AddCoaxialPort.m

WPW 2019

WPW SCHOOL

4. FREEWARE FULL-WAVE ANALYSIS - ANTENNA

Setting up a Full-Wave EM simulation of a patch antenna

Substrate and ground

```
%% create substrate
CSX          = AddMaterial( CSX, 'substrate' );
CSX          = SetMaterialProperty( CSX, 'substrate', 'Epsilon', substrate.epsR, 'Kappa', substrate.kappa );
start        = [-substrate.width/2 -substrate.length/2 0];
stop         = [ substrate.width/2  substrate.length/2 substrate.thickness];
CSX          = AddBox( CSX, 'substrate', 0, start, stop );

%% create ground (same size as substrate)
CSX          = AddMetal( CSX, 'gnd' ); % create a perfect electric conductor (PEC)
start(3)     =0;
stop(3)      =0;
CSX          = AddBox(CSX,'gnd',10,start,stop);
```


```
% width in x-direction
% length in y-direction
% main radiation in z-direction
patch.length        = 32.10; % resonant length 43.90 (x-axis)
patch.width         = 40.60; % (y-axis) 55.20

inset.width         = 3.41;  %Rectangular shape creating the inset 3.42
inset.length        = 9.13; % 12.49

line.width          = 3.41;  % 3.42
line.length         = 40.00;

substrate.epsR      = 3.55;
substrate.kappa     = 4e-3 * 2*pi*1.8e9 * EPS0*substrate.epsR;
substrate.width     = 100;
substrate.length    = 64.2;
substrate.thickness = 1.524;
substrate.cells     = 4;

feed.pos            = -line.length;
feed.width          = 3.41;
feed.R              = 50; % feed resistance

% size of the simulation box
SimBox              = [160 160 50];
```

4. FREEWARE FULL-WAVE ANALYSIS - ANTENNA

Setting up a Full-Wave EM simulation of a patch antenna

Excitation

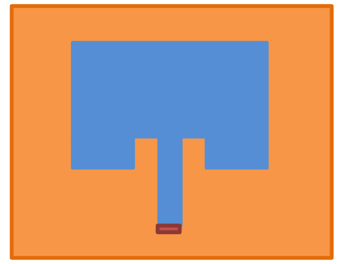

```
%% apply the excitation & resist as a current source
start           = [feed.pos-.1 -feed.width/2 0];
stop            = [feed.pos+.1 +feed.width/2 substrate.thickness];
[CSX]           = AddLumpedPort(CSX, 5 ,1 ,feed.R, start, stop, [0 0 1], true);
```

```
% width in x-direction
% length in y-direction
% main radiation in z-direction
patch.length        = 32.10; % resonant length 43.90 (x-axis)
patch.width         = 40.60; % (y-axis) 55.20

inset.width         = 3.41;  %Rectangular shape creating the inset 3.42
inset.length        = 9.13; % 12.49

line.width          = 3.41;  % 3.42
line.length         = 40.00;

substrate.epsR      = 3.55;
substrate.kappa     = 4e-3 * 2*pi*1.8e9 * EPS0*substrate.epsR;
substrate.width     = 100;
substrate.length    = 64.2;
substrate.thickness = 1.524;
substrate.cells     = 4;

feed.pos            = -line.length;
feed.width          = 3.41;
feed.R              = 50; % feed resistance

% size of the simulation box
SimBox              = [160 160 50];
```


4. FREEWARE FULL-WAVE ANALYSIS - ANTENNA

Setting up a Full-Wave EM simulation of a patch antenna

Frequency range

```
%% setup FDTD parameter & excitation function
max_timesteps = 30000;
min_decrement = 1e-5; % equivalent to -50 dB
f0 = 0e9; % center frequency
fc = 3e9; % 20 dB corner frequency (in this case 0 Hz - 3e9 Hz)
FDTD = InitFDTD( 'NrTS', max_timesteps, 'EndCriteria', min_decrement );
FDTD = SetGaussExcite( FDTD, f0, fc );
BC = {'MUR' 'MUR' 'MUR' 'MUR' 'MUR' 'MUR'}; % boundary conditions
if (use_pml>0)
    BC = {'PML_8' 'PML_8' 'PML_8' 'PML_8' 'PML_8' 'PML_8'}; % use pml instead of mur
end
FDTD = SetBoundaryCond( FDTD, BC );
```

4. FREEWARE FULL-WAVE ANALYSIS - ANTENNA

Setting up a Full-Wave EM simulation of a patch antenna

```
%% setup CSXCAD geometry & mesh
% currently, openEMS cannot automatically generate a mesh
max_res         = c0 / (f0+fc) / unit / 20; % cell size: lambda/20
CSX             = InitCSX();
mesh.x          = [-SimBox(1)/2 SimBox(1)/2 -substrate.width/2 substrate.width/2 feed.pos];
% add patch mesh with 2/3 - 1/3 rule
mesh.x          = [mesh.x -patch.width/2-max_res/2*0.66 -patch.width/2+max_res/2*0.33 patch.width/2+max_res/2*0.66 patch.width/2-max_res/2*0.33];
mesh.x          = SmoothMeshLines( mesh.x, max_res, 1.4); % create a smooth mesh between specified mesh lines
mesh.y          = [-SimBox(2)/2 SimBox(2)/2 -substrate.length/2 substrate.length/2 -feed.width/2 feed.width/2];
% add patch mesh with 2/3 - 1/3 rule
mesh.y          = [mesh.y -patch.length/2-max_res/2*0.66 -patch.length/2+max_res/2*0.33 patch.length/2+max_res/2*0.66 patch.length/2-max_res/2*0.33];
mesh.y          = SmoothMeshLines( mesh.y, max_res, 1.4 );
mesh.z          = [-SimBox(3)/2 linspace(0,substrate.thickness,substrate.cells) SimBox(3) ];
mesh.z          = SmoothMeshLines( mesh.z, max_res, 1.4 );
mesh            = AddPML( mesh, [8 8 8 8 8 8] ); % add equidistant cells (air around the structure)
CSX             = DefineRectGrid( CSX, unit, mesh );
```


4. FREEWARE FULL-WAVE ANALYSIS - ANTENNA

Alternative Full-Wave EM simulation

Press save and run (blue arrow). Go to opdrachtvenster type ‘yes’ (red arrow) and press enter.

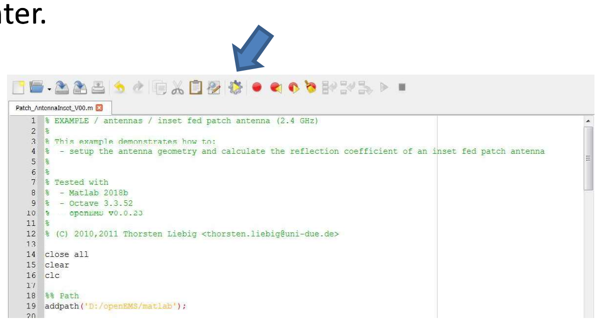

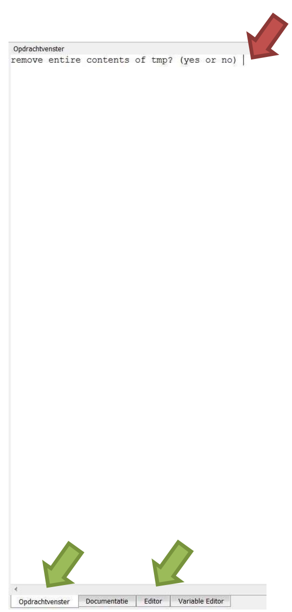

4. FREEWARE FULL-WAVE ANALYSIS - ANTENNA

Alternative Full-Wave EM simulation

Next appCSXCAD will open showing the patch antenna in 3D ….

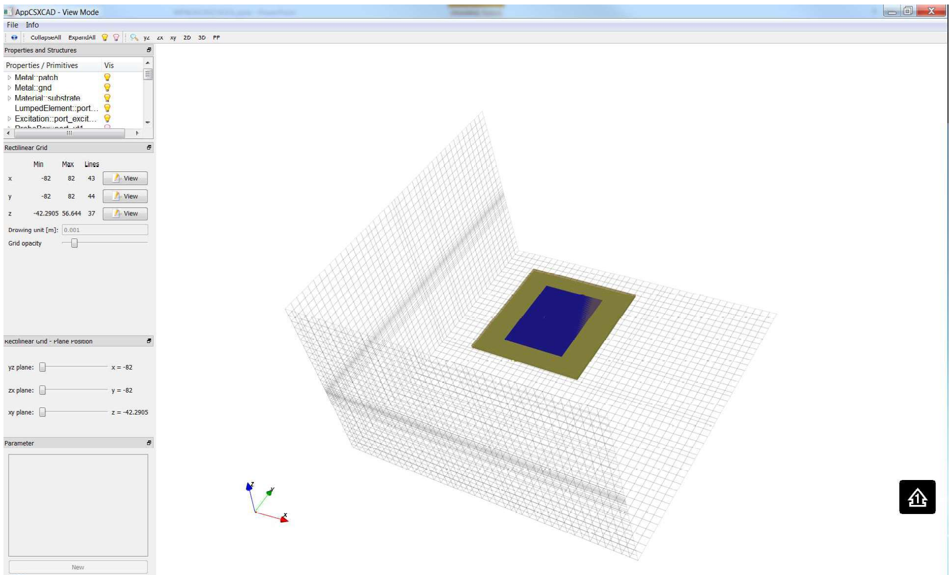

4. FREEWARE FULL-WAVE ANALYSIS - ANTENNA

Alternative Full-Wave EM simulation

…. Close the program and it will run.

```
remove entire contents of tmp? (yes or no) yes
invoking AppCSXCAD, exit to continue script...
QCSXCAD - disabling editing
 ----------------------------------------------------------------------
 | openEMS 64bit -- version v0.0.35
 | (C) 2010-2016 Thorsten Liebig <thorsten.liebig@gmx.de>  GPL license
 ----------------------------------------------------------------------
        Used external libraries:
                CSXCAD -- Version: v0.6.2
                hdf5   -- Version: 1.8.12
                          compiled against: HDF5 library version: 1.8.12
                tinyxml -- compiled against: 2.6.2
                fparser
                boost  -- compiled against: 1_57
                vtk -- Version: 6.1.0
                       compiled against: 6.1.0

Create FDTD operator (compressed SSE + multi-threading)
FDTD simulation size: 49x44x34 --> 73304 FDTD cells
FDTD timestep is: 1.49332e-012 s; Nyquist rate: 83 timesteps @4.03403e+009 Hz
Excitation signal length is: 480 timesteps (7.16794e-010s)
Max. number of timesteps: 30000 ( --> 62.5 * Excitation signal length)
Create FDTD engine (compressed SSE + multi-threading)
Running FDTD engine... this may take a while... grab a cup of coffee?!?
[@        4s] Timestep:          720 || Speed:   12.9 MC/s (5.694e-003 s/TS) || Energy: ~1.88e-013 (- 3
[@        8s] Timestep:         1460 || Speed:   13.5 MC/s (5.414e-003 s/TS) || Energy: ~3.21e-014 (-10
```

4. FREEWARE FULL-WAVE ANALYSIS - ANTENNA

Alternative Full-Wave EM simulation

The results

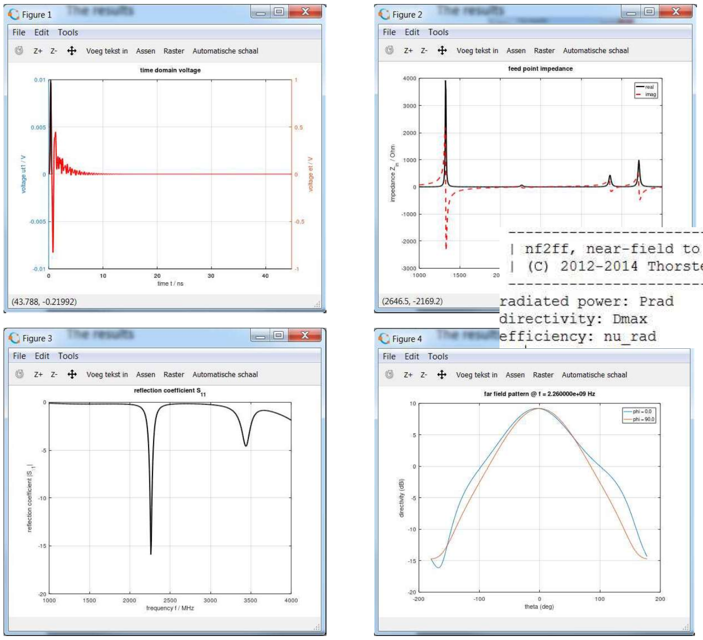


```
%% switches & options...
postprocessing_only = 0;
draw_3d_pattern     = 0; % this may take a while...
use_pml             = 0; % use pml boundaries instead of mur
openEMS_opts        = '';
```

```
------------------------------------------------------------------------
| nf2ff, near-field to far-field transformation for openEMS
| (C) 2012-2014 Thorsten Liebig <thorsten.liebig@gmx.de>  GPL license
------------------------------------------------------------------------
radiated power: Prad     = 2.5177e-26 Watt
directivity: Dmax        = 9.2002 dBi
efficiency: nu_rad       = 43.8264 %
```


5. FREEWARE FULL-WAVE ANALYSIS - RECTIFIER

QucsStudio

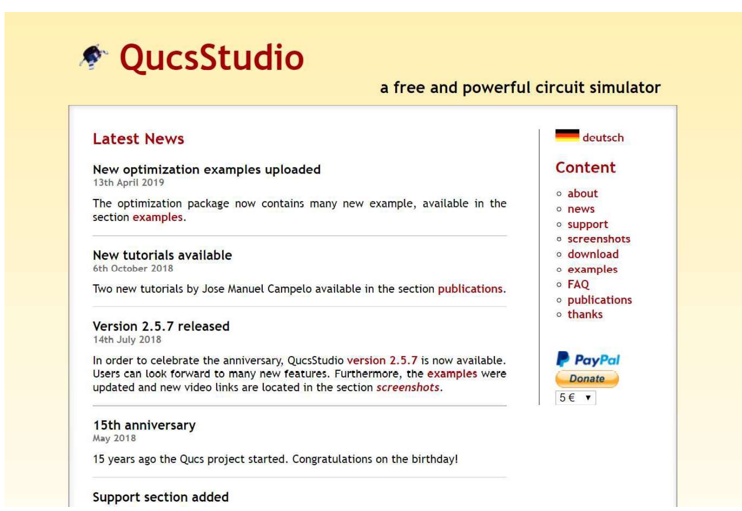

http://dd6um.darc.de/QucsStudio/qucsstudio.html

We will analyze a voltage doubler circuit (two diodes) as an example

5. FREEWARE FULL-WAVE ANALYSIS - RECTIFIER

Generate the circuit

Only the circuit, don't worry about sources or measurements yet

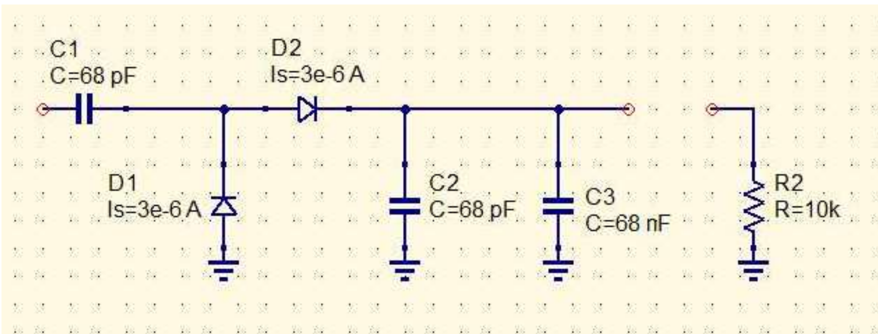

5. FREEWARE FULL-WAVE ANALYSIS - RECTIFIER

Generate the circuit

Only the circuit, don't worry about sources or measurements yet

Note: QUCS just regards those as if they are one capacitor of 68068 pF

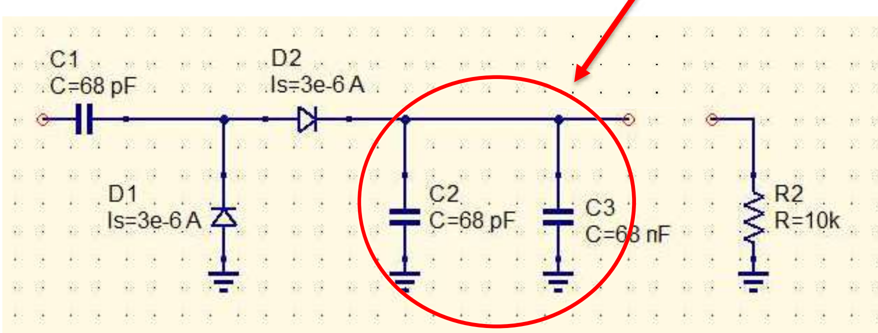

WPW SCHOOL

5. FREEWARE FULL-WAVE ANALYSIS - RECTIFIER

Generate the circuit

Only the circuit, don't worry about s

Diode parameters can be found in the datasheet.
If you can't find C_p, use 70~80 fF for a SOT-23 package

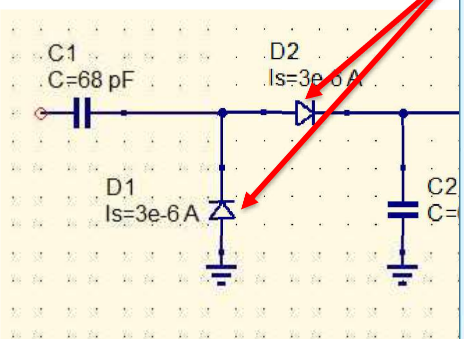

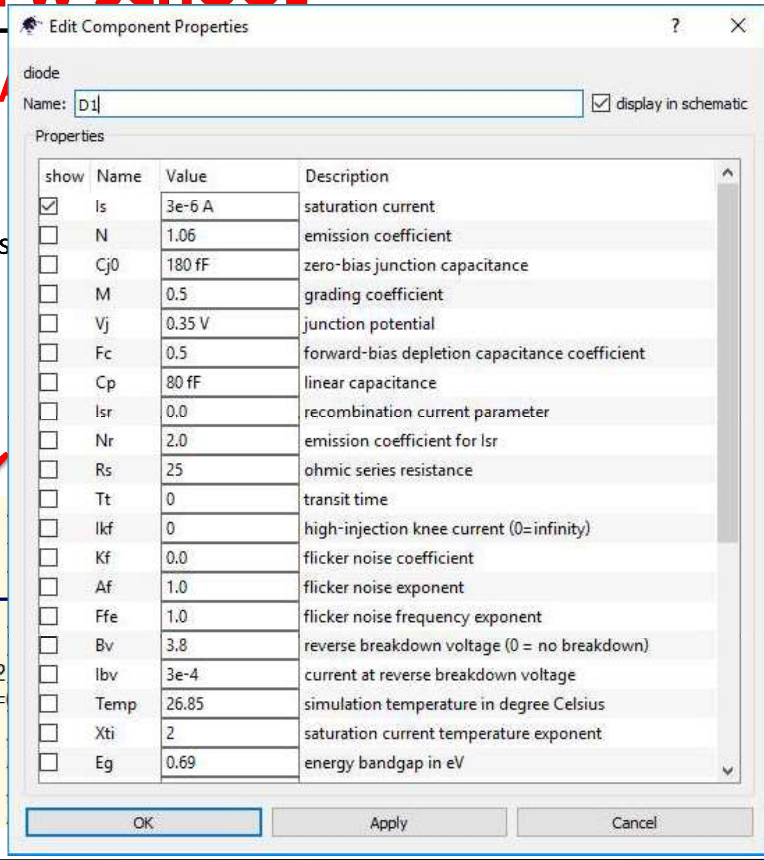
Edit Component Properties

diode

Name: D1 — display in schematic

Properties

show	Name	Value	Description
☑	Is	3e-6 A	saturation current
☐	N	1.06	emission coefficient
☐	Cj0	180 fF	zero-bias junction capacitance
☐	M	0.5	grading coefficient
☐	Vj	0.35 V	junction potential
☐	Fc	0.5	forward-bias depletion capacitance coefficient
☐	Cp	80 fF	linear capacitance
☐	Isr	0.0	recombination current parameter
☐	Nr	2.0	emission coefficient for Isr
☐	Rs	25	ohmic series resistance
☐	Tt	0	transit time
☐	Ikf	0	high-injection knee current (0=infinity)
☐	Kf	0.0	flicker noise coefficient
☐	Af	1.0	flicker noise exponent
☐	Ffe	1.0	flicker noise frequency exponent
☐	Bv	3.8	reverse breakdown voltage (0 = no breakdown)
☐	Ibv	3e-4	current at reverse breakdown voltage
☐	Temp	26.85	simulation temperature in degree Celsius
☐	Xti	2	saturation current temperature exponent
☐	Eg	0.69	energy bandgap in eV

OK Apply Cancel

WPW SCHOOL

5. FREEWARE FULL-WAVE ANALYSIS - RECTIFIER

Generate the circuit

Add

- AC voltage source
- Source impedance (exact value is not critical)
- Source current measurement

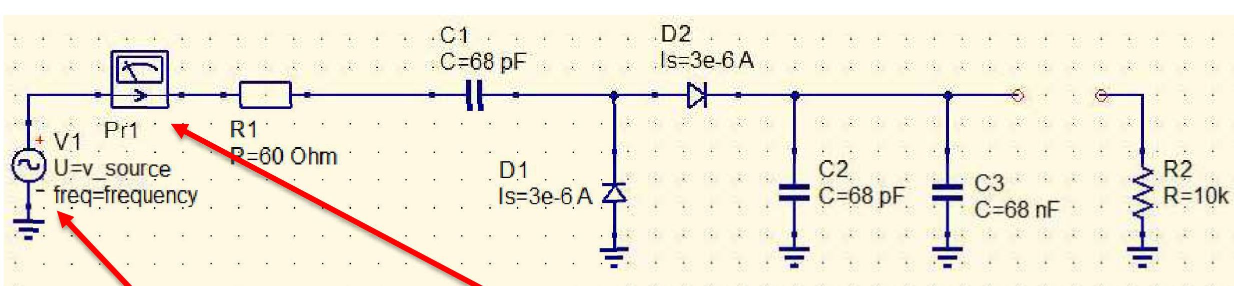

QUCS:
Sources/AC Voltage Source

QUCS:
Devices/Current Probe

5. FREEWARE FULL-WAVE ANALYSIS - RECTIFIER

Generate the circuit

Add

- AC voltage source
- Source impedance (exact value is
- Source current measurement

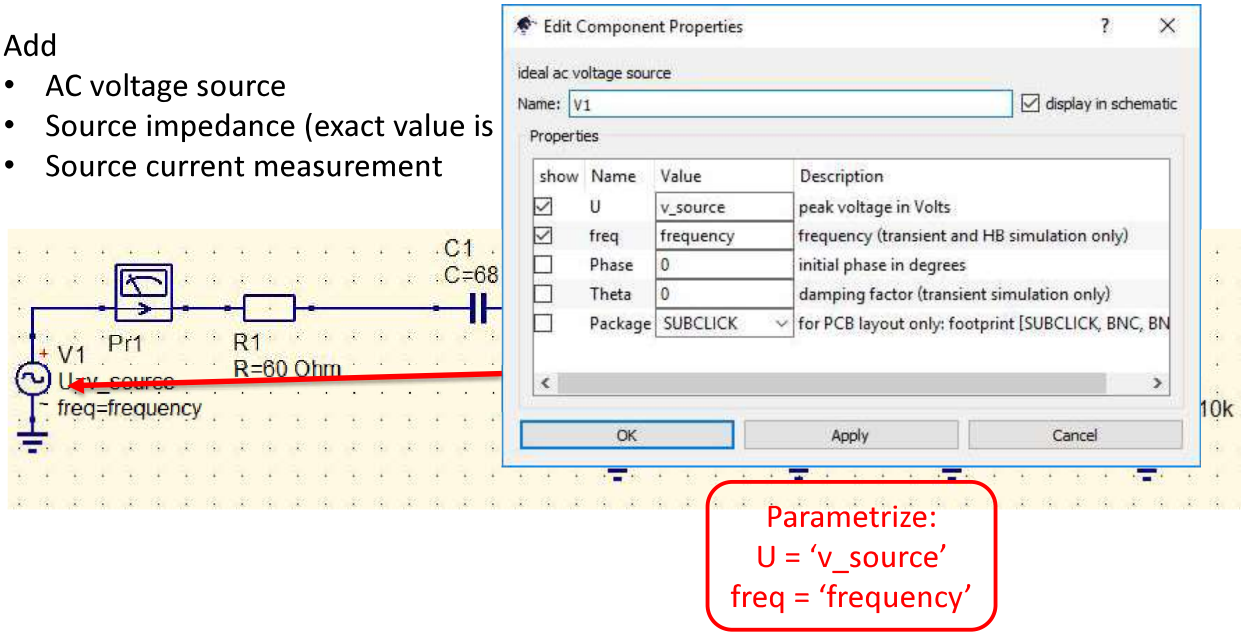

5. FREEWARE FULL-WAVE ANALYSIS - RECTIFIER

Generate the circuit

Add

- AC voltage source
- Source impedance (exact value is not critical)
- Source current measurement

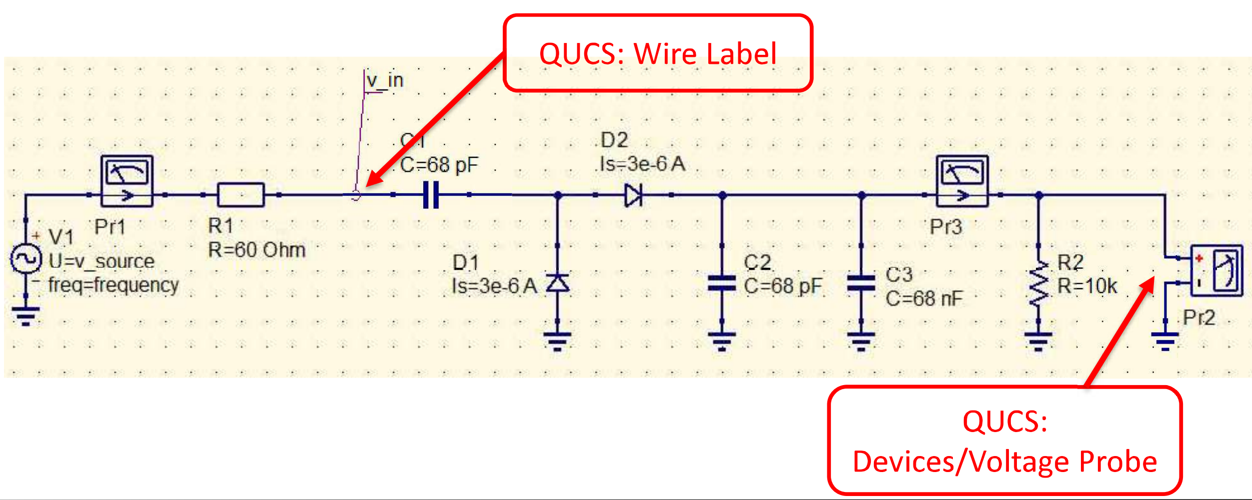

5. FREEWARE FULL-WAVE ANALYSIS - RECTIFIER

Generate the circuit

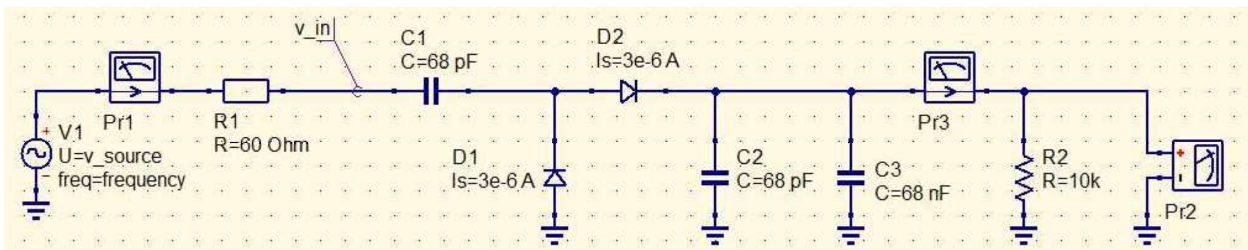

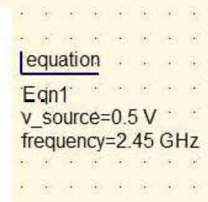

Add

- Equation

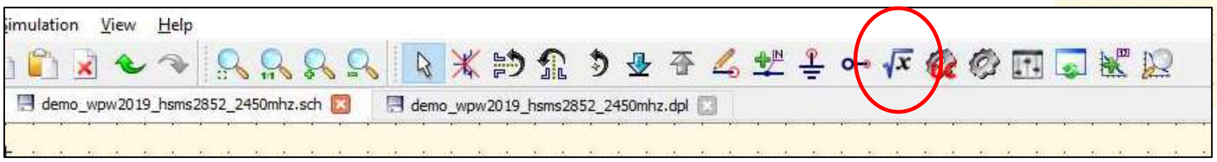

5. FREEWARE FULL-WAVE ANALYSIS - RECTIFIER

Generate the circuit

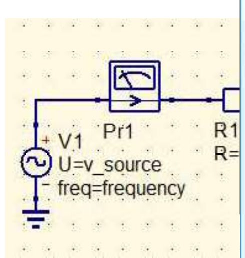

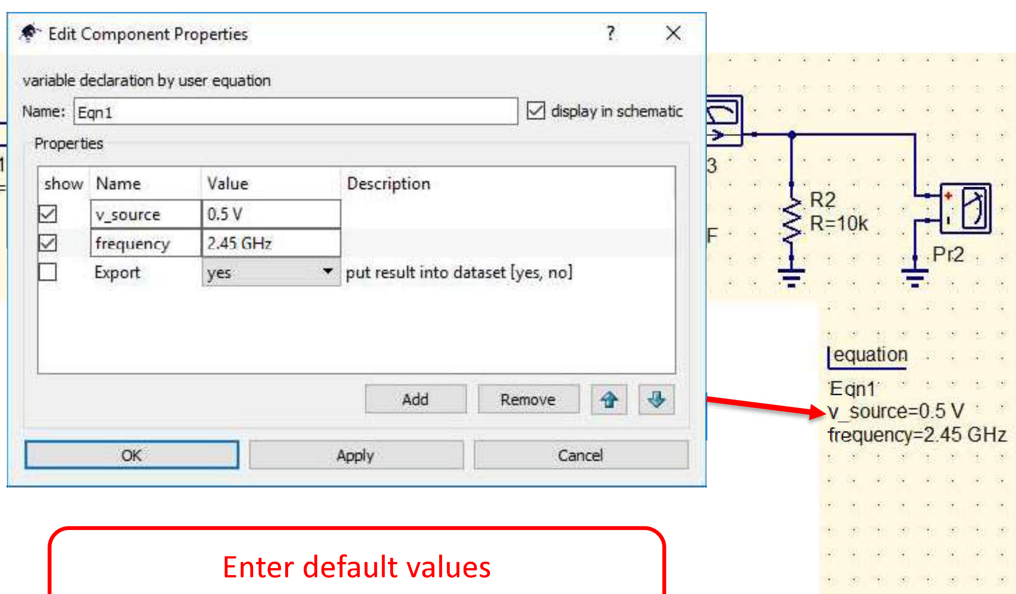

Add

- Equation

Enter default values
Can be overridden by a Parameter Sweep

5. FREEWARE FULL-WAVE ANALYSIS - RECTIFIER

Generate the circuit

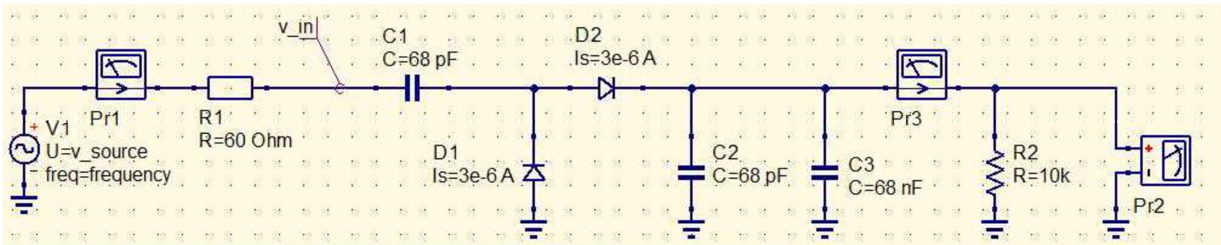

Add

- Harmonic Balance Simulation
  - Max order or harmonics = 8
  - Max number of iterations = 5000

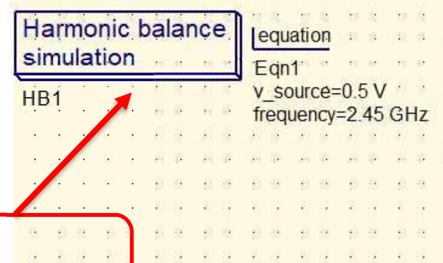

QUCS:
Simulations/Harmonic Balance

WPW SCHOOL

5. FREEWARE FULL-WAVE ANALYSIS - RECTIFIER

Generate the circuit

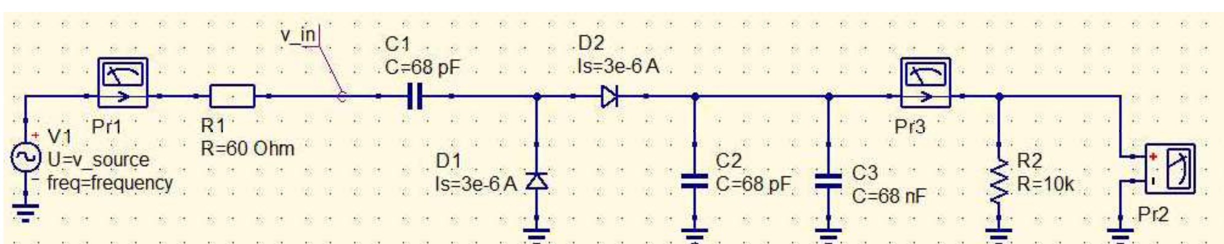

Add

- Parameter Sweep

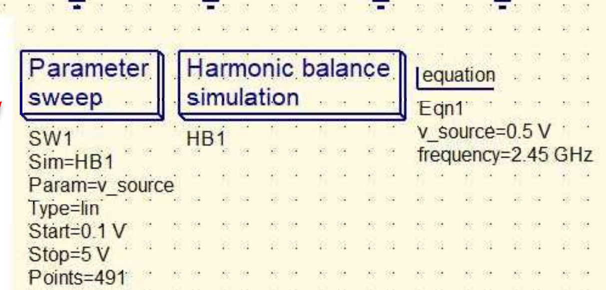

QUCS:
Simulation/Parameter Sweep

5. FREEWARE FULL-WAVE ANALYSIS - RECTIFIER

Generate the circuit

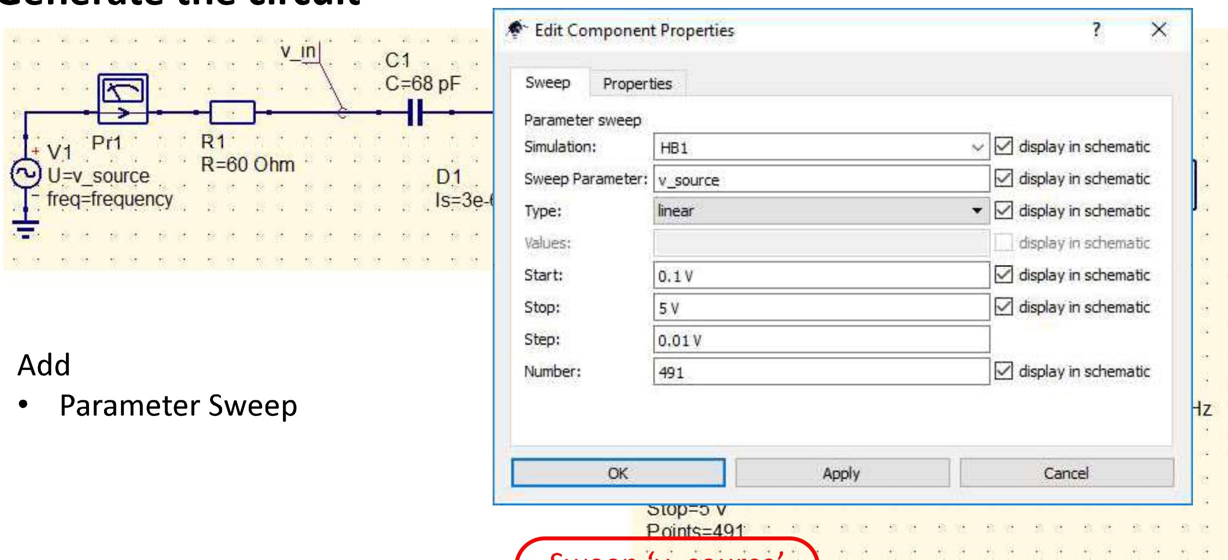

Add

- Parameter Sweep

Sweep 'v_source' from 0.1 to 5.0 V in 0.01 V steps linearly

5. FREEWARE FULL-WAVE ANALYSIS - RECTIFIER

Generate the circuit

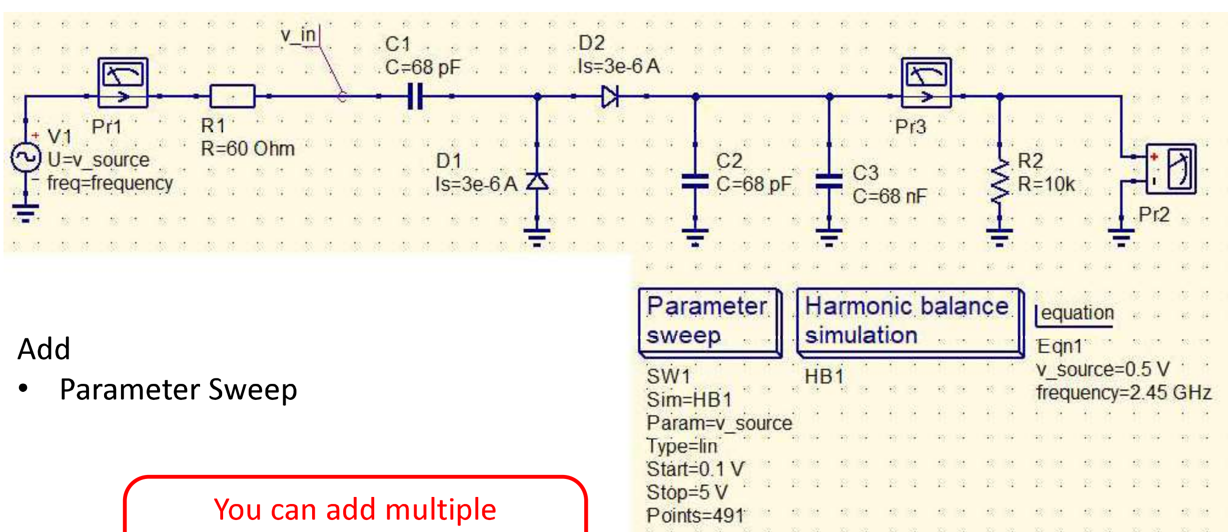

Add

- Parameter Sweep

You can add multiple parameter sweeps to create a multi-dimensional simulation

5. FREEWARE FULL-WAVE ANALYSIS - RECTIFIER
Run the Simulation

First run a DC simulation to check whether everything is OK

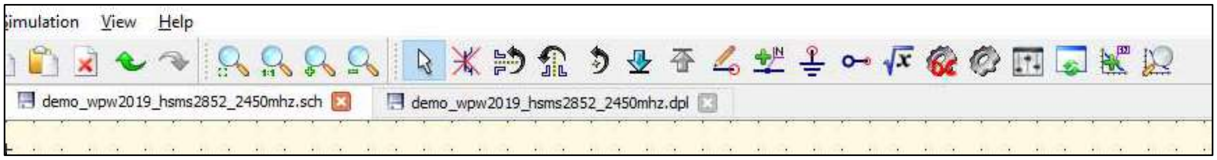

5. FREEWARE FULL-WAVE ANALYSIS - RECTIFIER
Run the Simulation

First run a DC simulation to check whether everything is OK

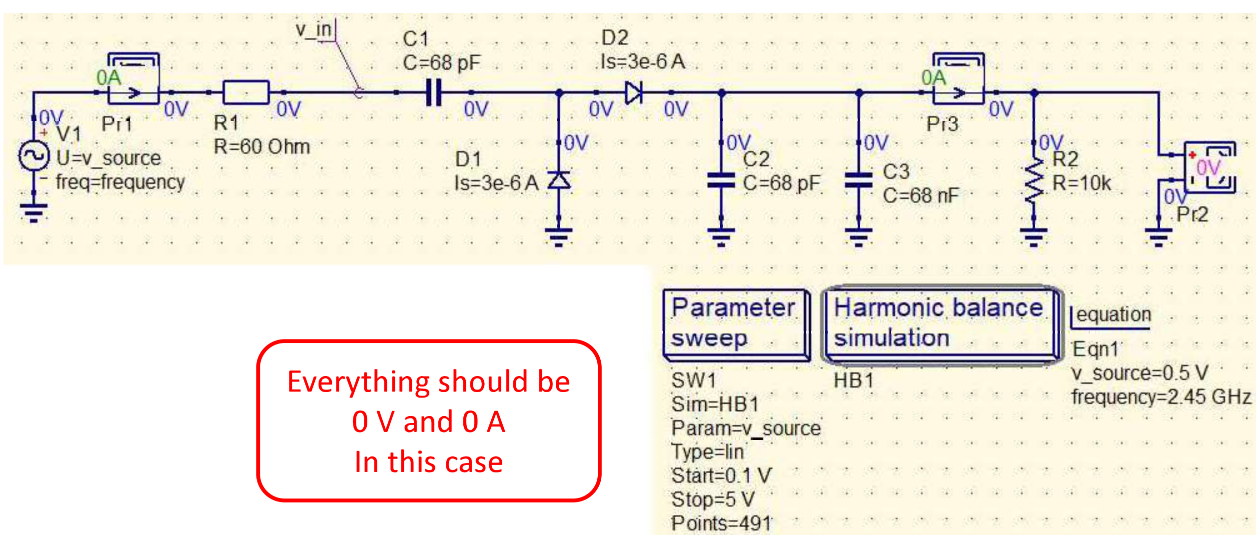

Everything should be
0 V and 0 A
In this case

WPW 2019

WPW SCHOOL

5. FREEWARE FULL-WAVE ANALYSIS - RECTIFIER

Run the Simulation

Now run the Harmonic Balance Simulation

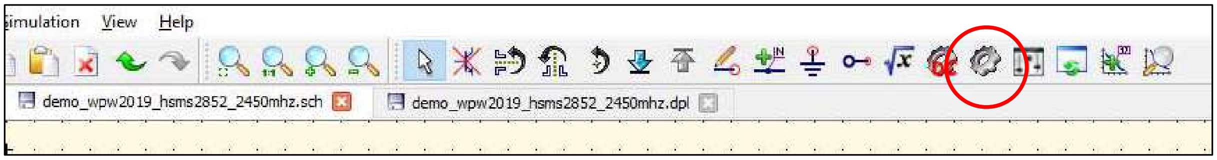

WPW 2019

WPW SCHOOL

5. FREEWARE FULL-WAVE ANALYSIS - RECTIFIER

Visualize the Results

Add:

- Diagrams/Tabular

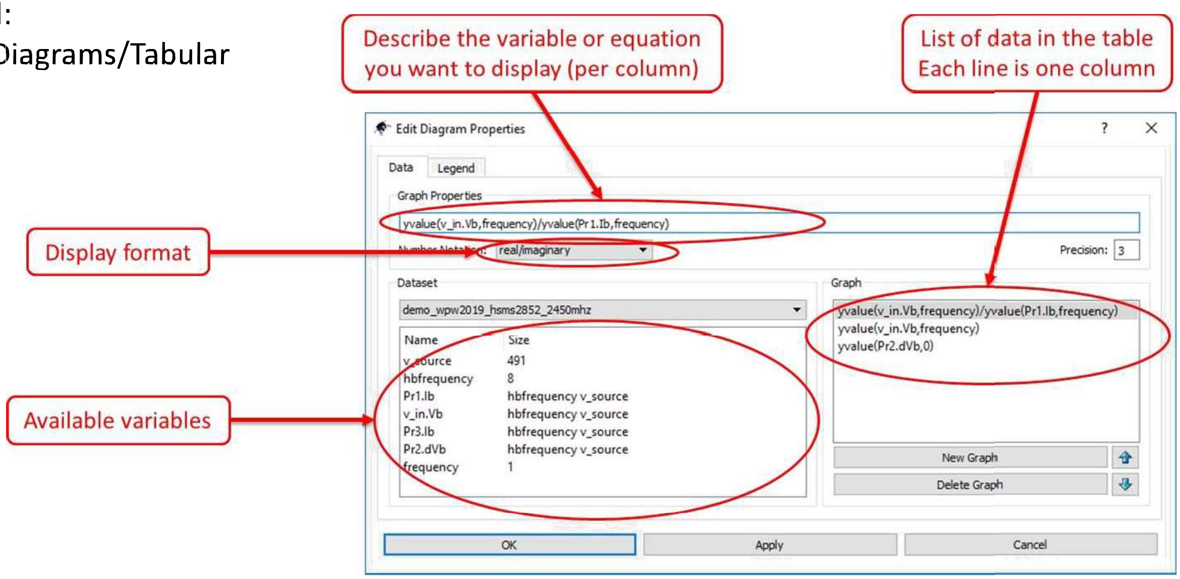

5. FREEWARE FULL-WAVE ANALYSIS - RECTIFIER

Visualize the Results

Add:

- Diagrams/Tabular
  - Z_{in}
  - V_{in}
  - V_{out}

The value of 'v_in' at 'frequency'(= 2.45 GHz)

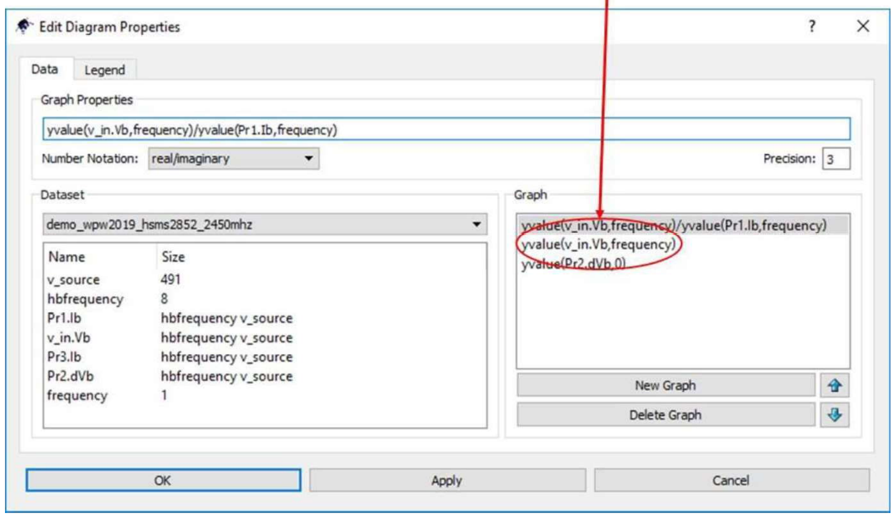

5. FREEWARE FULL-WAVE ANALYSIS - RECTIFIER

Visualize the Results

Add:

- Diagrams/Tabular
  - Z_{in}
  - V_{in}
  - V_{out}

The value of 'Pr2' (output voltage) at '0' Hz (DC)

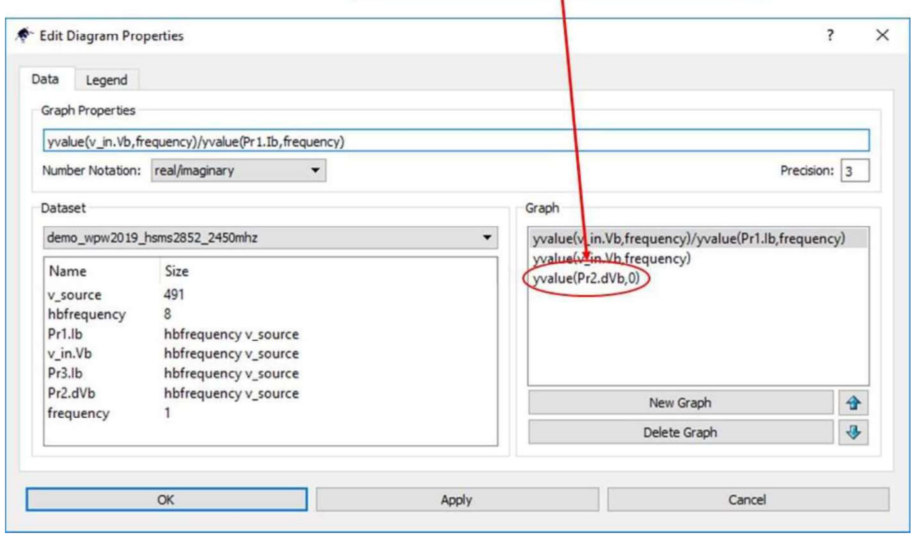

5. FREEWARE FULL-WAVE ANALYSIS - RECTIFIER

Visualize the Results

Add:

- Diagrams/Tabular
  - Z_{in}
  - V_{in}
  - V_{out}

The value of ‘v_in’ at ‘frequency’(= 2.45 GHz)

The value of ‘Pr1’ (input current) at ‘frequency’(= 2.45 GHz)

$Z_{in} = V_{in} / I_{in}$

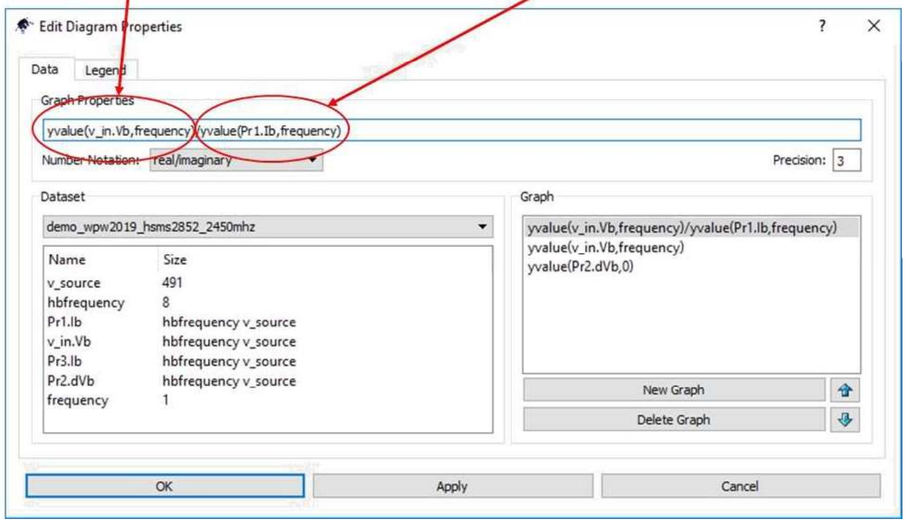

5. FREEWARE FULL-WAVE ANALYSIS - RECTIFIER

Visualize the Results

Your new title

Add:

- Diagrams/Tabular
  - Z_{in}
  - V_{in}
  - V_{out}
- Change column titles

Select which titles you want to change

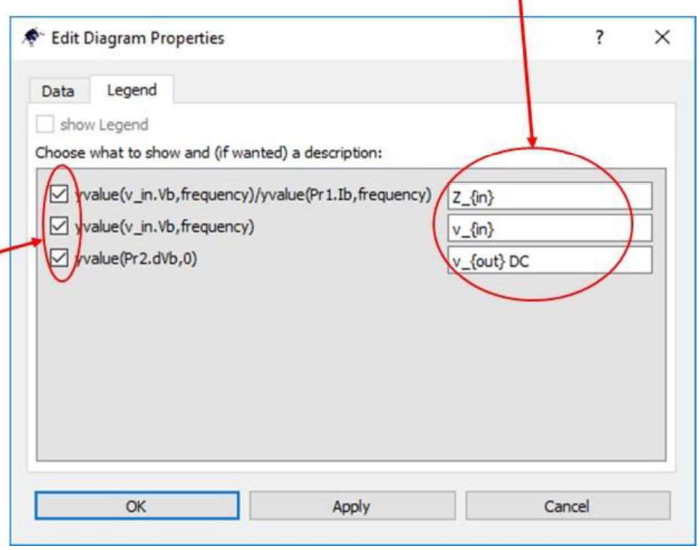

5. FREEWARE FULL-WAVE ANALYSIS - RECTIFIER

Visualize the Results

v_source	Z_{in}	v_{in}	v_{out} DC
1.54	33.2-j179	1.39 / -17°	2.2
1.55	33.3-j179	1.4 / -17°	2.22
1.56	33.3-j179	1.41 / -17°	2.24
1.57	33.4-j179	1.42 / -17°	2.25
1.58	33.4-j180	1.43 / -16.9°	2.27
1.59	33.5-j180	1.44 / -16.9°	2.29
1.6	33.6-j180	1.44 / -16.9°	2.3
1.61	33.6-j180	1.45 / -16.9°	2.32
1.62	33.7-j181	1.46 / -16.9°	2.33
1.63	33.8-j181	1.47 / -16.8°	2.35
1.64	33.8-j181	1.48 / -16.8°	2.37
1.65	33.9-j181	1.49 / -16.8°	2.38
1.66	34-j181	1.5 / -16.8°	2.4
1.67	34-j182	1.51 / -16.8°	2.42
1.68	34.1-j182	1.52 / -16.7°	2.43
1.69	34.1-j182	1.53 / -16.7°	2.45
1.7	34.2-j182	1.54 / -16.7°	2.47
1.71	34.3-j182	1.55 / -16.7°	2.48
1.72	34.3-j183	1.55 / -16.7°	2.5
1.73	34.4-j183	1.56 / -16.7°	2.51
1.74	34.5-j183	1.57 / -16.6°	2.53
1.75	34.5-j183	1.58 / -16.6°	2.55

Real / imag

Mag / phase

5. FREEWARE FULL-WAVE ANALYSIS - RECTIFIER

Visualize the Results

Choose the desired output voltage

For example:

- 2.5 V

Corresponds to input impedance

- 34.3 – j183 Ω

v_source	Z_{in}	v_{in}	v_{out} DC
1.54	33.2-j179	1.39 / -17°	2.2
1.55	33.3-j179	1.4 / -17°	2.22
1.56	33.3-j179	1.41 / -17°	2.24
1.57	33.4-j179	1.42 / -17°	2.25
1.58	33.4-j180	1.43 / -16.9°	2.27
1.59	33.5-j180	1.44 / -16.9°	2.29
1.6	33.6-j180	1.44 / -16.9°	2.3
1.61	33.6-j180	1.45 / -16.9°	2.32
1.62	33.7-j181	1.46 / -16.9°	2.33
1.63	33.8-j181	1.47 / -16.8°	2.35
1.64	33.8-j181	1.48 / -16.8°	2.37
1.65	33.9-j181	1.49 / -16.8°	2.38
1.66	34-j181	1.5 / -16.8°	2.4
1.67	34-j182	1.51 / -16.8°	2.42
1.68	34.1-j182	1.52 / -16.7°	2.43
1.69	34.1-j182	1.53 / -16.7°	2.45
1.7	34.2-j182	1.54 / -16.7°	2.47
1.71	34.3-j182	1.55 / -16.7°	2.48
1.72	34.3-j183	1.55 / -16.7°	2.5
1.73	34.4-j183	1.56 / -16.7°	2.51
1.74	34.5-j183	1.57 / -16.6°	2.53
1.75	34.5-j183	1.58 / -16.6°	2.55

5. FREEWARE FULL-WAVE ANALYSIS - RECTIFIER

Match the Rectifier

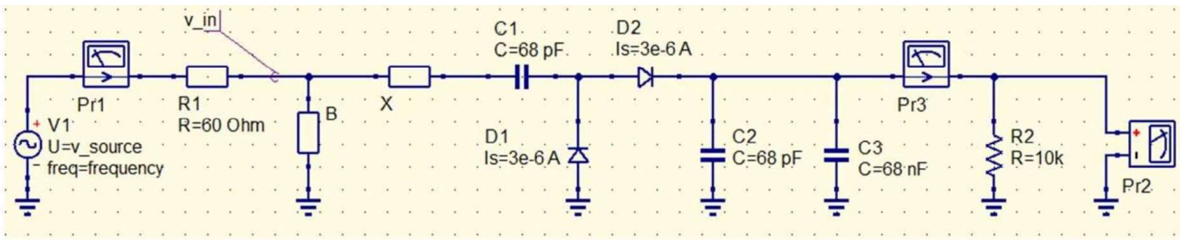

Input impedance = 34.3 – j183 Ω
Z_0 = 50 Ω

Re(Z_{in}) < Re(Z_0) [1]

[1] David M. Pozar, Microwave Engineering, 4th edition, Wiley, New York, NY, 2011

5. FREEWARE FULL-WAVE ANALYSIS - RECTIFIER

Match the Rectifier

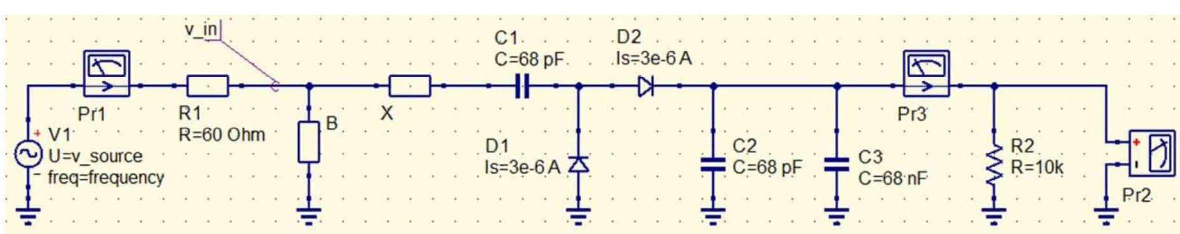

$$B = \pm \frac{\sqrt{(Z_0 - R_L)/R_L}}{Z_0} \ [\Omega^{-1}] \qquad X_L = j\omega L \ [\Omega]$$

$$X = \pm\sqrt{R_L(Z_0 - R_L)} - X_L \ [\Omega] \qquad X_C = \frac{1}{j\omega C} \ [\Omega]$$

Solution 1:	X = 13.4 nH	B = 0.88 pF
Solution 2:	X = 10.4 nH	B = 4.80 nH

[1] David M. Pozar, Microwave Engineering, 4th edition, Wiley, New York, NY, 2011

5. FREEWARE FULL-WAVE ANALYSIS - RECTIFIER
Match the Rectifier

Add columns to the table:

- Power Transfer Efficiency: P_{out}/P_{in} [%]
- 100 * (yvalue(Pr3.Ib,0)*yvalue(Pr2.dVb,0)) / (real(yvalue(v_in.Vb,frequency)*yvalue(Pr1.Ib,frequency))*0.5)

- P_{in} [dBm]
- 10 * log10(((yvalue(v_in.Vb,frequency))^2)/100) + 30

Give the columns appropriate titles

WPW 2019
WPW SCHOOL

5. FREEWARE FULL-WAVE ANALYSIS - RECTIFIER
Match the Rectifier

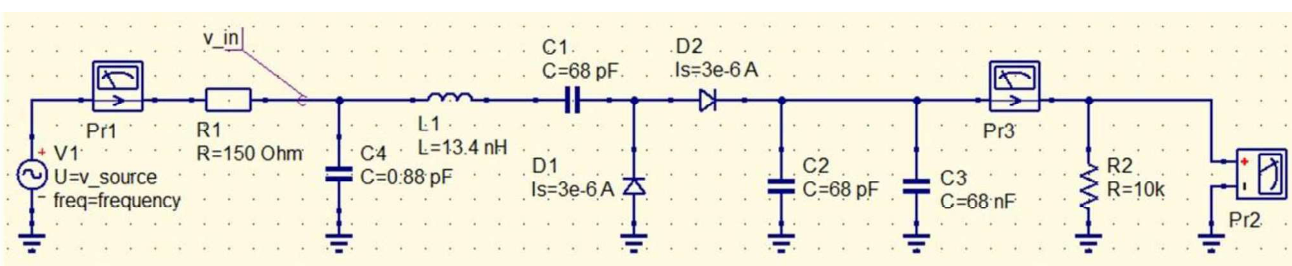

Solution 1: X = 13.4 nH B = 0.88 pF

5. FREEWARE FULL-WAVE ANALYSIS - RECTIFIER

Match the Rectifier

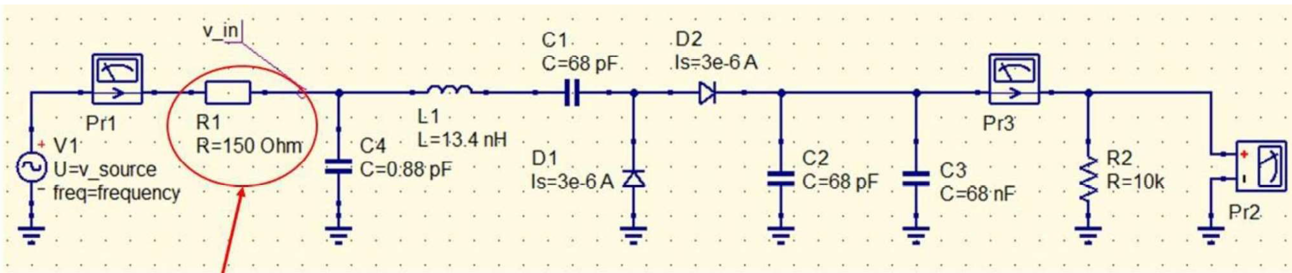

Solution 1: X = 13.4 nH B = 0.88 pF

I had to change the value to keep the simulation stable

5. FREEWARE FULL-WAVE ANALYSIS - RECTIFIER

Match the Rectifier

Solution 1: X = 13.4 nH B = 0.88 pF

V_{out} = 2.5 V
Z_{in} = 52.5 + j2.29 Ω
V_{in} = 354 mV
P_{in} ≈ +1 dBm
η = 52.3 %

QUCS uses V_{peak}, not V_{RMS}

v_source	Z_{in}	v_{in}	v_{out} DC	PCE	p_in [dBm]
1.34	53.1+j2.77	0.352 / 2.21°	2.46	52	0.922+j0.335
1.35	53+j2.65	0.352 / 2.12°	2.47	52.1	0.938+j0.321
1.35	52.8+j2.53	0.353 / 2.03°	2.48	52.2	0.953+j0.308
1.36	52.6+j2.41	0.354 / 1.94°	2.49	52.2	0.969+j0.294
1.37	52.5+j2.29	0.354 / 1.85°	2.5	52.3	0.984+j0.281
1.37	52.3+j2.17	0.355 / 1.76°	2.51	52.4	1+j0.267
1.38	52.1+j2.05	0.355 / 1.67°	2.52	52.4	1.02+j0.254
1.38	52+j1.93	0.356 / 1.58°	2.53	52.5	1.03+j0.24
1.39	51.8+j1.82	0.357 / 1.49°	2.54	52.6	1.05+j0.226
1.39	51.7+j1.7	0.357 / 1.4°	2.55	52.6	1.06+j0.213
1.4	51.5+j1.59	0.358 / 1.31°	2.56	52.7	1.08+j0.199
1.41	51.4+j1.47	0.359 / 1.22°	2.57	52.7	1.09+j0.186
1.41	51.2+j1.36	0.359 / 1.13°	2.58	52.8	1.11+j0.172
1.42	51+j1.25	0.36 / 1.04°	2.59	52.9	1.12+j0.158
1.42	50.9+j1.14	0.361 / 0.955°	2.6	52.9	1.14+j0.145
1.43	50.8+j1.03	0.361 / 0.865°	2.61	53	1.16+j0.131
1.43	50.6+j0.916	0.362 / 0.775°	2.62	53	1.17+j0.118
1.44	50.5+j0.807	0.363 / 0.685°	2.63	53.1	1.19+j0.104
1.45	50.3+j0.698	0.363 / 0.595°	2.64	53.2	1.2+j0.0903
1.45	50.2+j0.591	0.364 / 0.506°	2.65	53.2	1.22+j0.0766
1.46	50+j0.484	0.364 / 0.416°	2.66	53.3	1.23+j0.063

5. FREEWARE FULL-WAVE ANALYSIS - RECTIFIER

Match the Rectifier

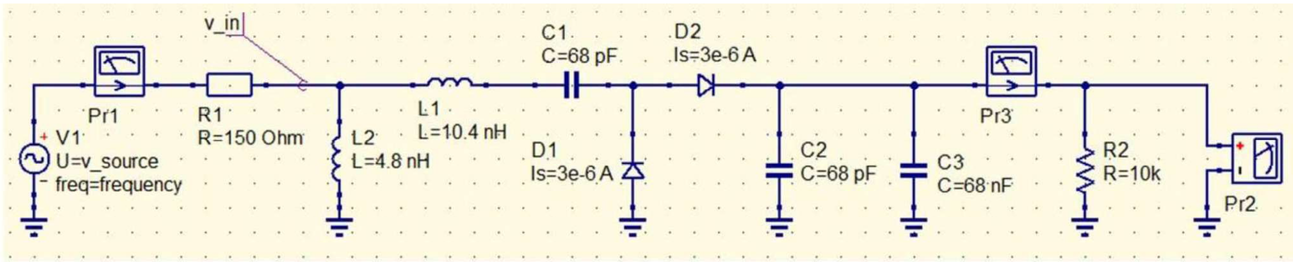

Solution 2: X = 10.4 nH B = 4.80 nH

WPW 2019
WPW SCHOOL

5. FREEWARE FULL-WAVE ANALYSIS - RECTIFIER

Match the Rectifier

Solution 2: X = 10.4 nH B = 4.80 nH

V_{out} = 2.5 V
Z_{in} = 46.4 + j0.254 Ω
V_{in} = 333 mV QUCS uses V_{peak}, not V_{RMS}
P_{in} ≈ +0.5 dBm
η = 52.3 %

v_source	Z_{in}	v_{in}	v_{out} DC	PCE	p_in [dBm]
1.34	42.9+j0.989	0.298 / 1.03°	2.3	51	-0.501+j0.156
1.35	43.2+j0.918	0.301 / 0.946°	2.32	51.1	-0.418+j0.143
1.35	43.5+j0.848	0.304 / 0.867°	2.34	51.3	-0.334+j0.131
1.36	43.8+j0.78	0.307 / 0.79°	2.35	51.4	-0.251+j0.12
1.37	44.1+j0.713	0.31 / 0.716°	2.37	51.5	-0.169+j0.109
1.37	44.4+j0.647	0.313 / 0.645°	2.39	51.6	-0.0868+j0.0978
1.38	44.7+j0.583	0.316 / 0.576°	2.4	51.7	-0.00523+j0.0873
1.38	45+j0.52	0.319 / 0.509°	2.42	51.8	0.0758+j0.0772
1.39	45.3+j0.458	0.322 / 0.445°	2.44	51.9	0.156+j0.0675
1.39	45.6+j0.398	0.325 / 0.384°	2.46	52	0.236+j0.0582
1.4	45.9+j0.339	0.328 / 0.324°	2.47	52.2	0.316+j0.0492
1.41	46.2+j0.282	0.331 / 0.267°	2.49	52.3	0.395+j0.0405
1.41	46.5+j0.226	0.334 / 0.213°	2.51	52.4	0.473+j0.0323
1.42	46.8+j0.172	0.337 / 0.161°	2.52	52.5	0.551+j0.0243
1.42	47.1+j0.119	0.34 / 0.11°	2.54	52.6	0.628+j0.0167
1.43	47.4+j0.068	0.343 / 0.0625°	2.56	52.7	0.704+j0.00947
1.43	47.7+j0.0182	0.346 / 0.0166°	2.57	52.8	0.78+j0.00252
1.44	48-j0.03	0.349 / -0.0271°	2.59	52.9	0.855-j0.00412
1.45	48.3-j0.0768	0.352 / -0.0689°	2.61	53	0.93-j0.0105
1.45	48.6-j0.122	0.355 / -0.109°	2.62	53.1	1-j0.0165
1.46	48.9-j0.166	0.358 / -0.147°	2.64	53.2	1.08-j0.0222

5. FREEWARE FULL-WAVE ANALYSIS - RECTIFIER

Match the Rectifier

Possible next steps:

- Verify whether you used enough orders in the Harmonic Balance
- Iterate to find different value of P_{in} (choose different V_{out})
- Change component values to standard values (10.4 nH → 10 nH, etc.)
- Add imperfections (ESR, ESL, etc.)
- Investigate bandwidth (use Parameter Sweep)
- Investigate susceptibility to component value tolerances (use Parameter Sweep)
- Usually one of the solutions has better tolerance and bandwidth

5. FREEWARE FULL-WAVE ANALYSIS - RECTIFIER

Export Data

Use the data in other programs

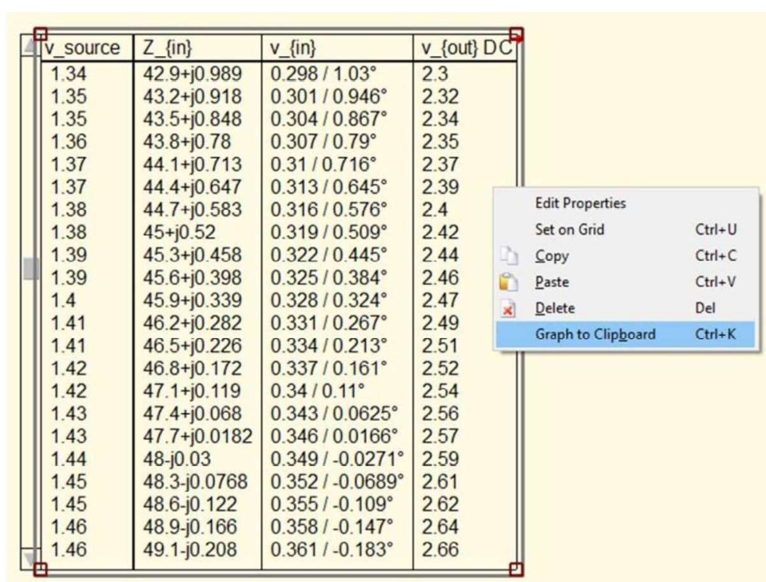

v_source	Z_{in}	v_{in}	v_{out} DC
1.34	42.9+j0.989	0.298 / 1.03°	2.3
1.35	43.2+j0.918	0.301 / 0.946°	2.32
1.35	43.5+j0.848	0.304 / 0.867°	2.34
1.36	43.8+j0.78	0.307 / 0.79°	2.35
1.37	44.1+j0.713	0.31 / 0.716°	2.37
1.37	44.4+j0.647	0.313 / 0.645°	2.39
1.38	44.7+j0.583	0.316 / 0.576°	2.4
1.38	45+j0.52	0.319 / 0.509°	2.42
1.39	45.3+j0.458	0.322 / 0.445°	2.44
1.39	45.6+j0.398	0.325 / 0.384°	2.46
1.4	45.9+j0.339	0.328 / 0.324°	2.47
1.41	46.2+j0.282	0.331 / 0.267°	2.49
1.41	46.5+j0.226	0.334 / 0.213°	2.51
1.42	46.8+j0.172	0.337 / 0.161°	2.52
1.42	47.1+j0.119	0.34 / 0.11°	2.54
1.43	47.4+j0.068	0.343 / 0.0625°	2.56
1.43	47.7+j0.0182	0.346 / 0.0166°	2.57
1.44	48-j0.03	0.349 / -0.0271°	2.59
1.45	48.3-j0.0768	0.352 / -0.0689°	2.61
1.45	48.6-j0.122	0.355 / -0.109°	2.62
1.46	48.9-j0.166	0.358 / -0.147°	2.64
1.46	49.1-j0.208	0.361 / -0.183°	2.66

5. FREEWARE FULL-WAVE ANALYSIS - RECTIFIER

Export Data

Use the data in other programs

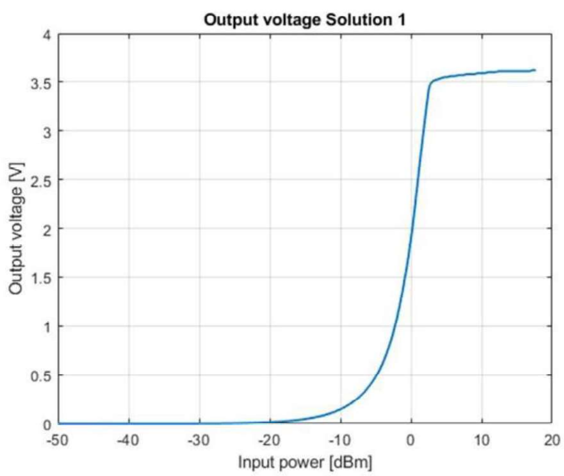

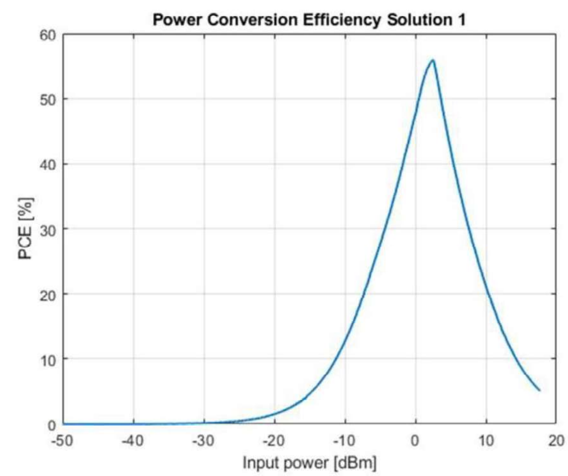

6. CONCLUSIONS

- For a rectenna design we need to predict the antenna resonance frequency and the rectifier input impedance accurately.
- Analytical methods can serve as an alternative to expensive full-wave COTS software.
- Analytical methods are not general purpose.
- Using Octave, OpenEMS and QucsStudio freeware can overcome this problem.
- The designer still needs to have a very good knowledge of the physics and theory involved.

Multi-band Rectenna Design for Radio Frequency Energy Harvesting

Jiafeng Zhou
University of Liverpool

Radio-frequency (RF) energy harvesting from ambient electromagnetic signals has a great potential to provide power for sensors and wireless communications. One great challenge of RF energy harvesting is that the power level of ambient electromagnetic signals is usually quite low. It is advantageous to harvest energy from different frequency band and convert the energy to DC with high efficiency. The core component of an RF energy harvesting system is the rectenna - a special type of receiving antenna that can convert electromagnetic energy into DC electricity. A simple rectenna consists of an antenna and a rectifying circuit. During this talk the challenges and potential solutions for harvesting RF energy from different frequency bands will be presented. It will be demonstrated how multi-band antennas suitable for energy harvesting can be designed and how rectifying circuits can be developed to operate with such antennas. Several impedance matching techniques will be introduced to simplify the design and to improve the efficiency of RF/DC conversion. This is crucial because the optimal impedance of a rectifier would vary significantly with frequency and the input power level. Recent development and results will be discussed in the talk.

Multi-band Rectenna Design for Radio Frequency Energy Harvesting

Chaoyun Song, Muayad Kod, Yi Huang and
Jiafeng Zhou

University of Liverpool, United Kingdom
Jiafeng.zhou@liverpool.ac.uk

WPW SCHOOL

CONTENTS

• WPT: at Liverpool

	RF energy harvesting	Inductive coupling	Resonance coupling
Field region	Far-field radiative	Near-field non-radiative	Near-field non-radiative
Method	Antennas	Coils	Resonators
Effective distance	m to km	mm to cm	cm
Efficiency	Low	Medium	High
Applications	energy harvesting wireless sensor networks, RFID etc.	Contactless cards, mobile phone charging pads etc.	Electric vehicles, medium range wireless charging etc.

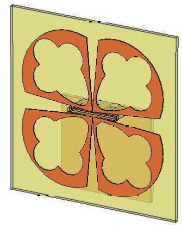

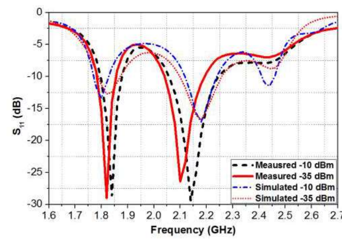

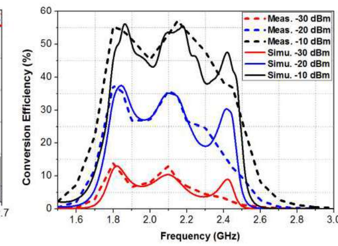

C. Song, Y. Huang, J. Zhou, J. Zhang, S. Yuan and P. Carter., "A high-efficiency broadband rectenna for ambient wireless energy harvesting," IEEE Trans. Antennas Propag., vol. 63, no. 8, pp. 3486–3495, May 2015.

• WPT: at Liverpool

	RF energy harvesting	Inductive coupling	Resonance coupling
Field region	Far-field radiative	Near-field non-radiative	Near-field non-radiative
Method	Antennas	Coils	Resonators
Effective distance	m to km	mm to cm	cm
Efficiency	Low	Medium	High
Applications	energy harvesting wireless sensor networks, RFID etc.	Contactless cards, mobile phone charging pads etc.	Electric vehicles, medium range wireless charging etc.

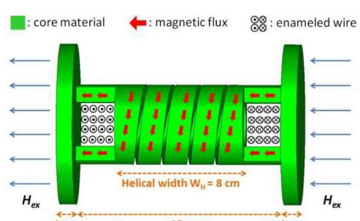

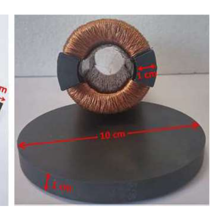

S. Yuan, Y. Huang, Q. Xu, J. Zhou, C. Song and G. Yuan, "A highly efficient helical core for magnetic field energy harvesting", IEEE Transactions on Power Electronics

• WPT: at Liverpool

	RF energy harvesting	Inductive coupling	Resonance coupling
Field region	Far-field radiative	Near-field non-radiative	Near-field non-radiative
Method	Antennas	Coils	Resonators
Effective distance	m to km	mm to cm	cm
Efficiency	Low	Medium	High
Applications	energy harvesting wireless sensor networks, RFID etc.	Contactless cards, mobile phone charging pads etc.	Electric vehicles, medium range wireless charging etc.

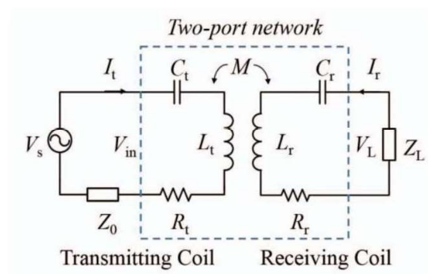

• Motivation

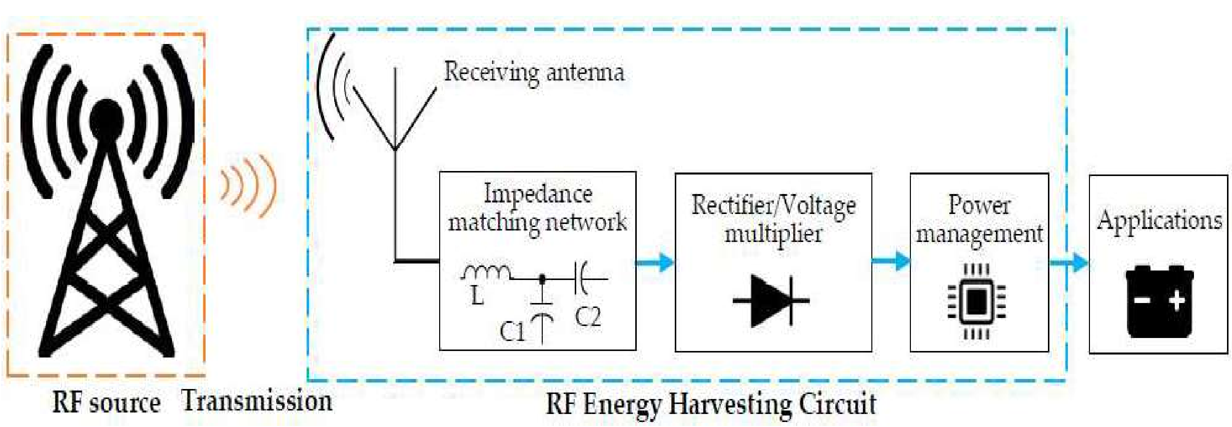

Ref: Tang et. al. Sensors 2018, 18, 4113; doi:10.3390/s18124113

- Challenges in Wireless Energy Harvesting
  - Low voltage, hence low efficiency
  - Low power, hence power combining needed
  - Variable working conditions
- How to develop rectennas to address these issues?
  - In its simplest form

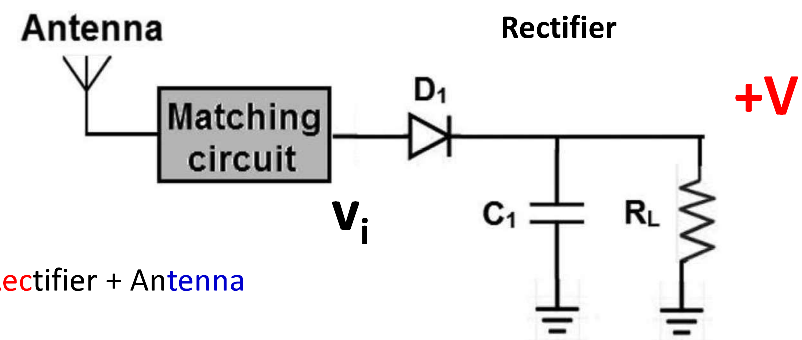

Rectenna = Rectifier + Antenna

- Rectifier Design: Voltage doubler

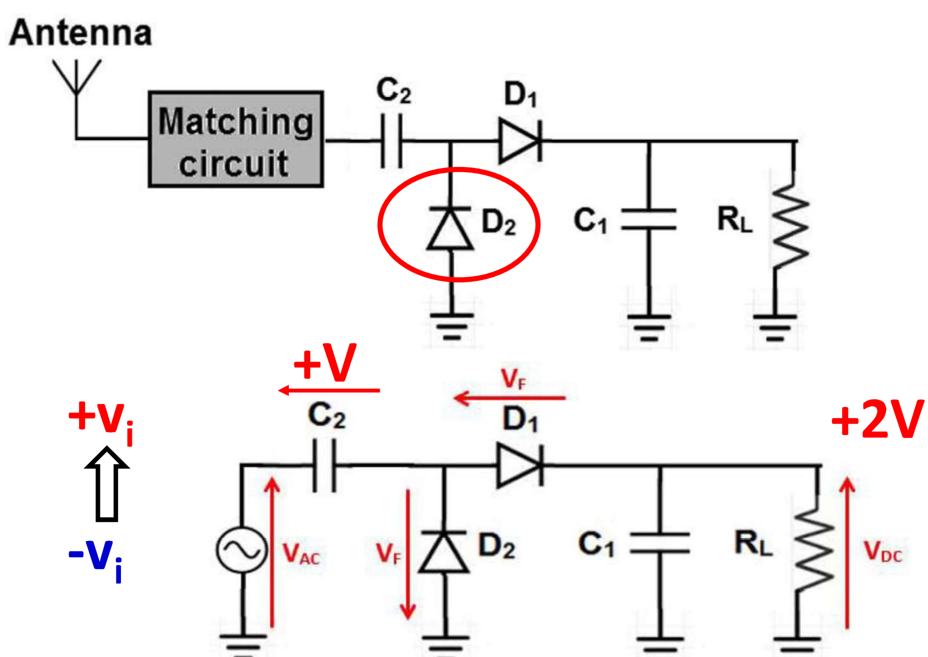

- Full-wave Greinacher rectifying circuit
  - The frequency could be different!

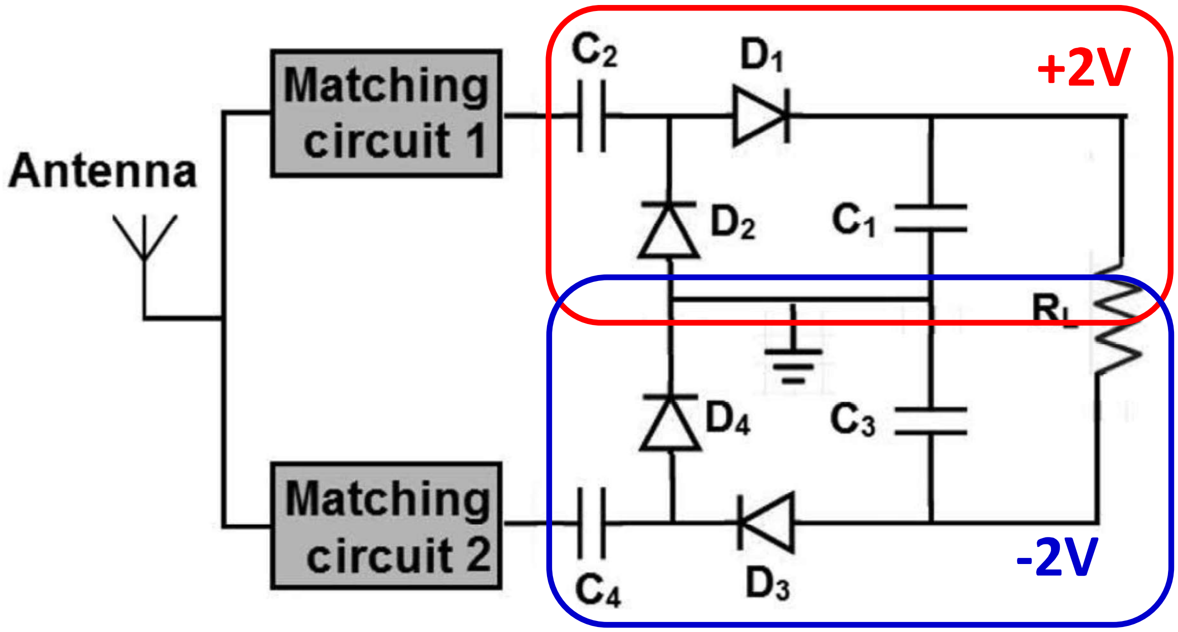

- Fabricated circuit
  - Two branches, three bands (1.8 GHz & 2.45 GHz for the upper branch, 2.1 GHz for the lower band).

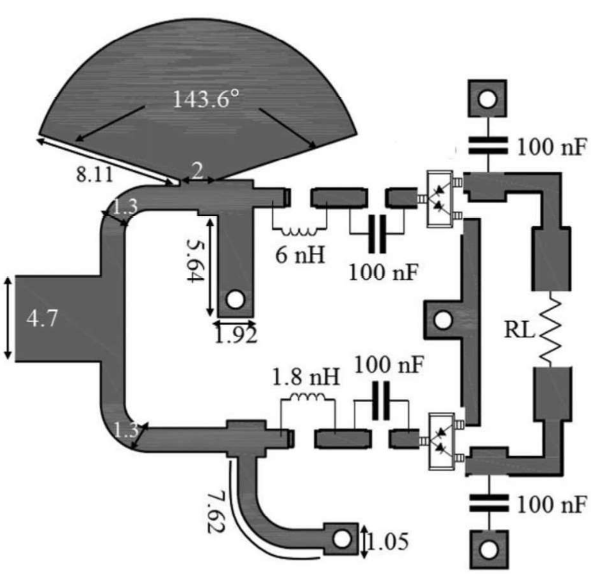

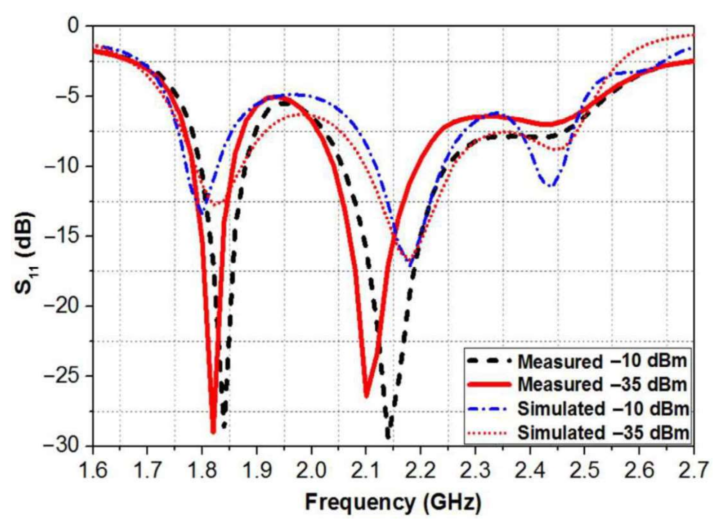

- Antenna Design: Flower shape dipole
  - A lowpass/bandpass filter is desired to reject the higher order harmonics

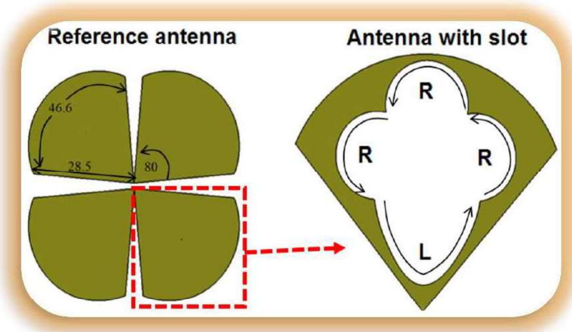

2nd harmonic rejection

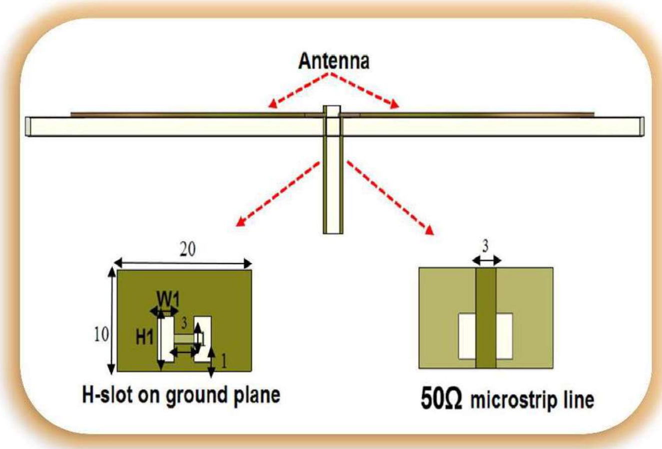

3rd harmonic rejection

- Fabricated circuit

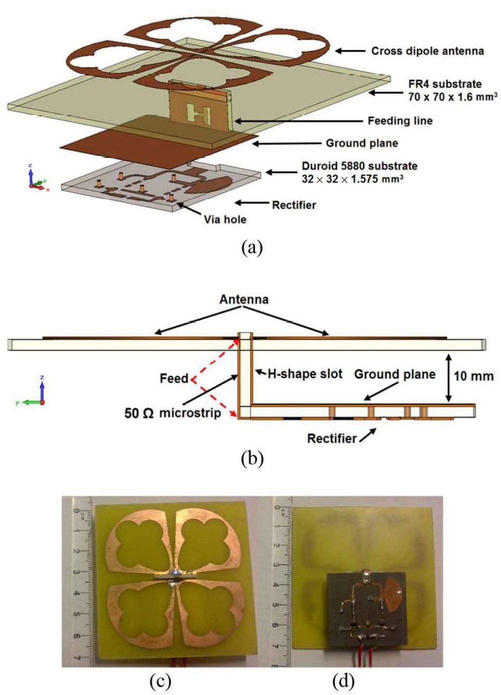

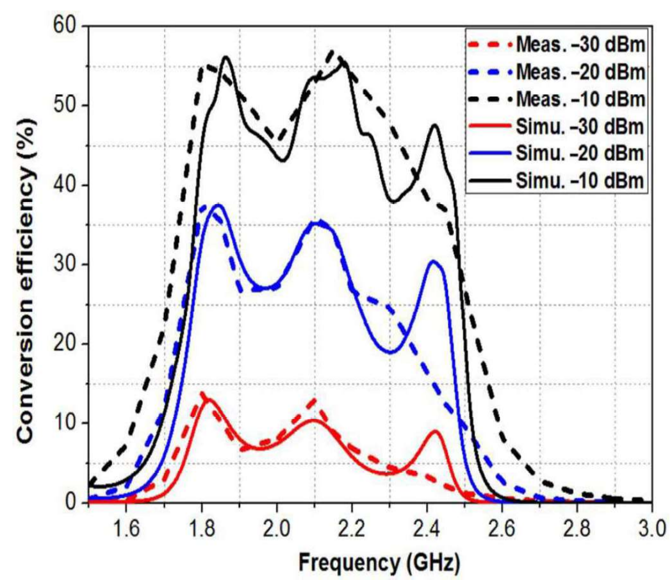

C Song, et al. IEEE TAP, 2015

- Three branches, each covering two bands

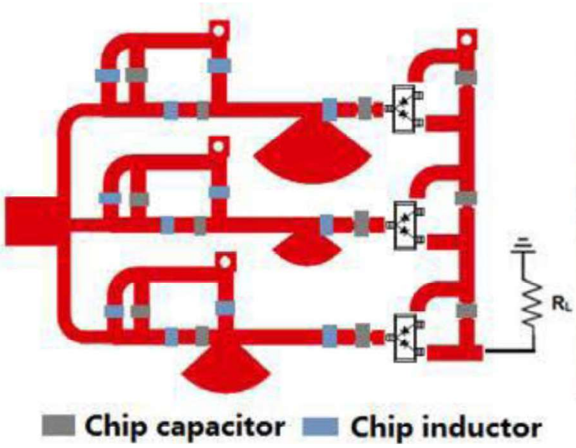

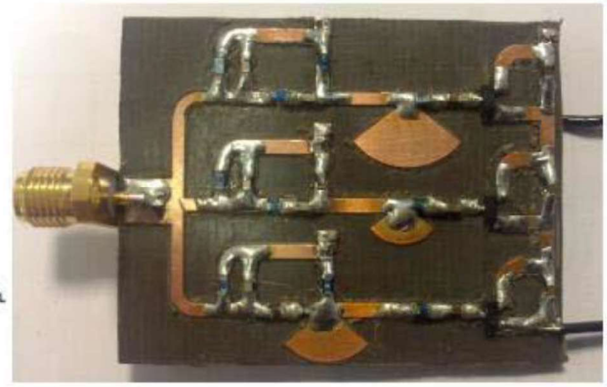

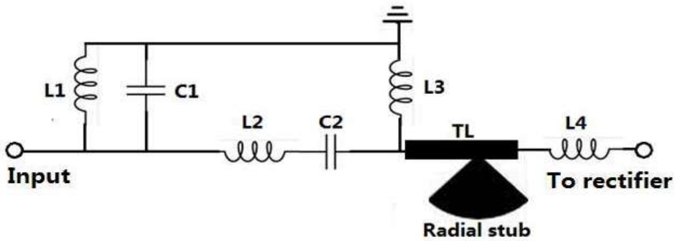

C Song et al. IEEE TAP, 2016

- Six bands

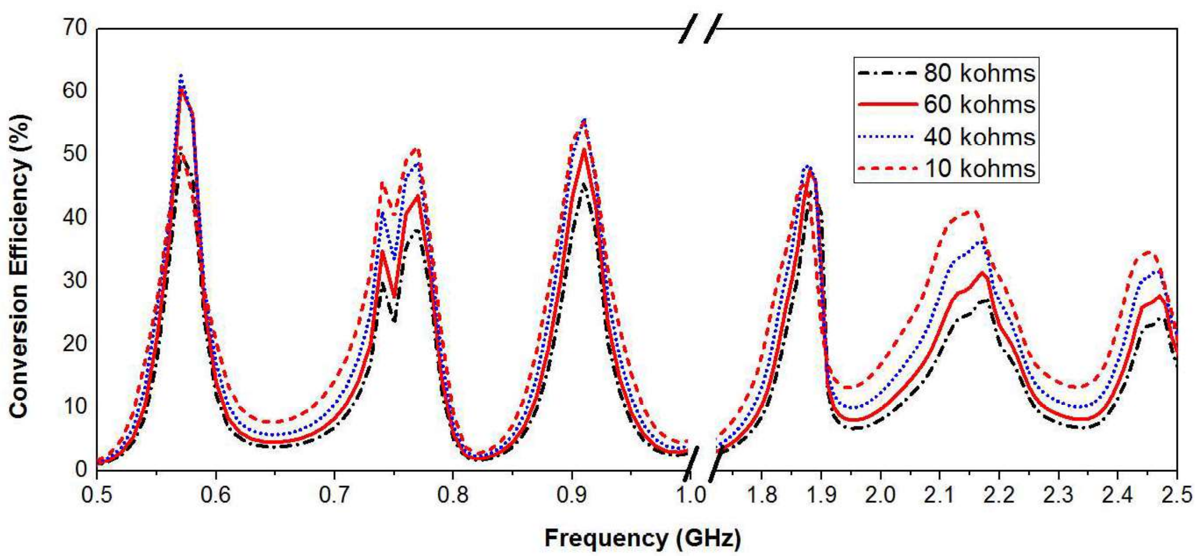

• Wideband circularly polarized antenna design

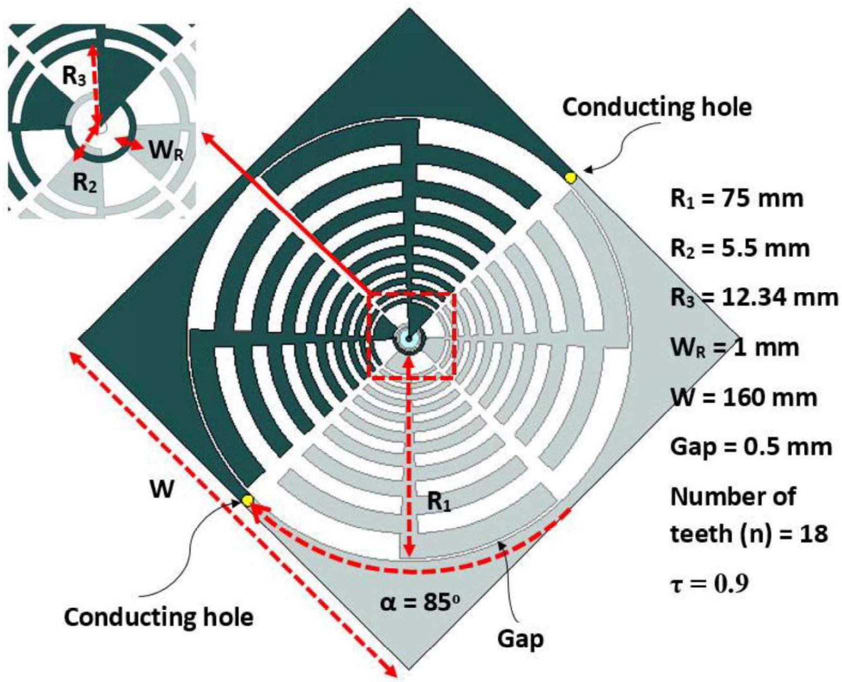

• Current distribution

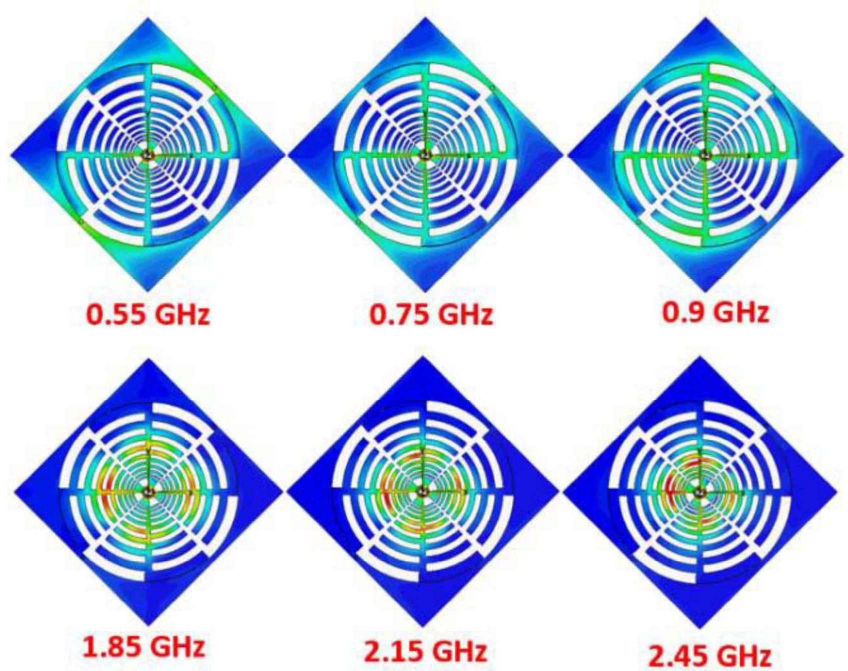

• Current distribution (animated)

CST

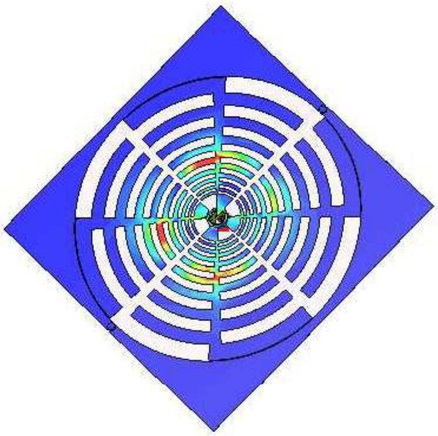

Low frequency mode

surface current (f=0.55) [1] (peak)

Component:	Abs
3D Maximum [A/m]:	68.73
Frequency:	0.55
Phase:	0

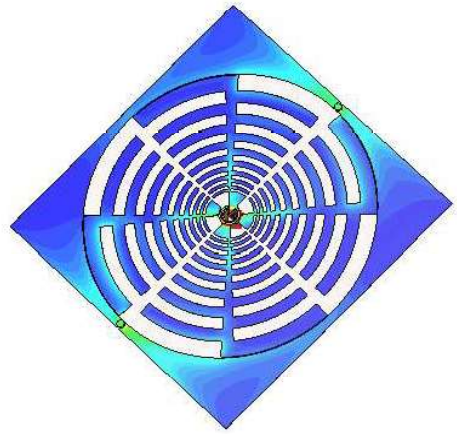

High frequency mode

• Measured performance

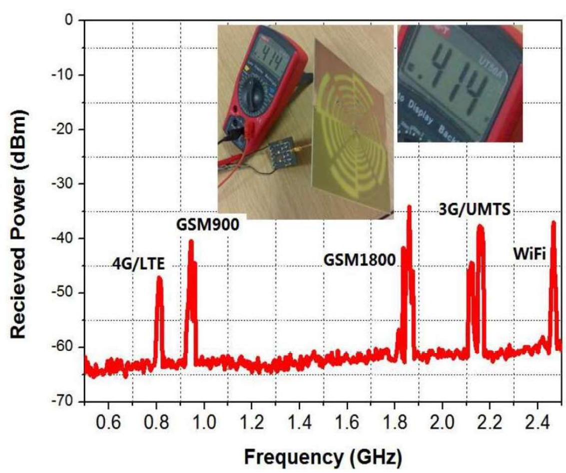

Indoor (8 uW harvested power)

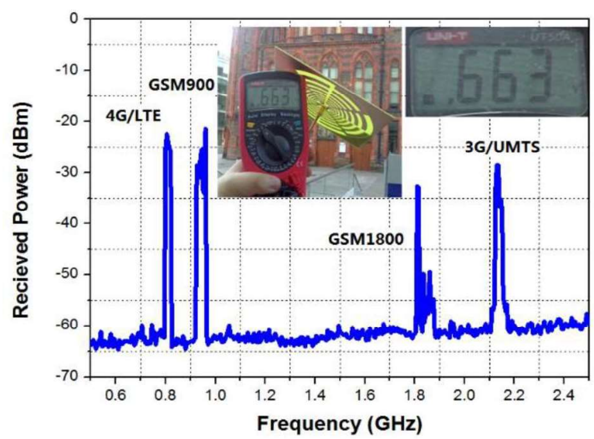

Outdoor (24 uW harvested power)

C Song et al. IEEE TAP, 2016

- Typical energy harvester → new configuration

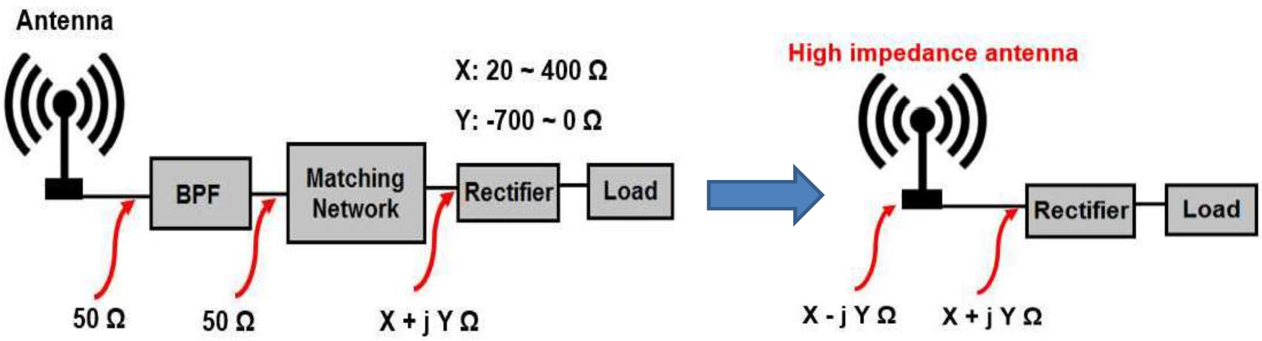

$$P = V/R^2$$

- Input impedance of a typical $\lambda/2$ dipole (~73 Ω)
  - Our case:

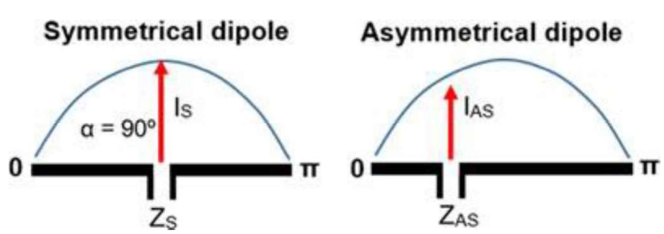

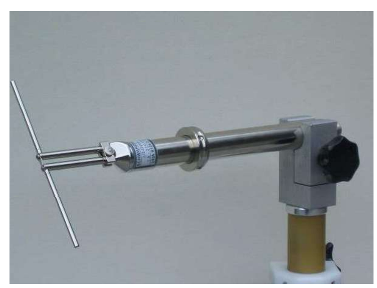

SIMULATED INPUT IMPEDANCE OF THE OFF-CENTER-FED DIPOLE

Long arm (mm)	Short arm (mm)	Real part at f_0 (Ω)	Imaginary part at f_0 (Ω)
90	10	320	–213
80	20	165	–30
70	30	102	–0.8
60	40	79	5.6
50	50	73	6.4

- Asymmetrical feed (design example)

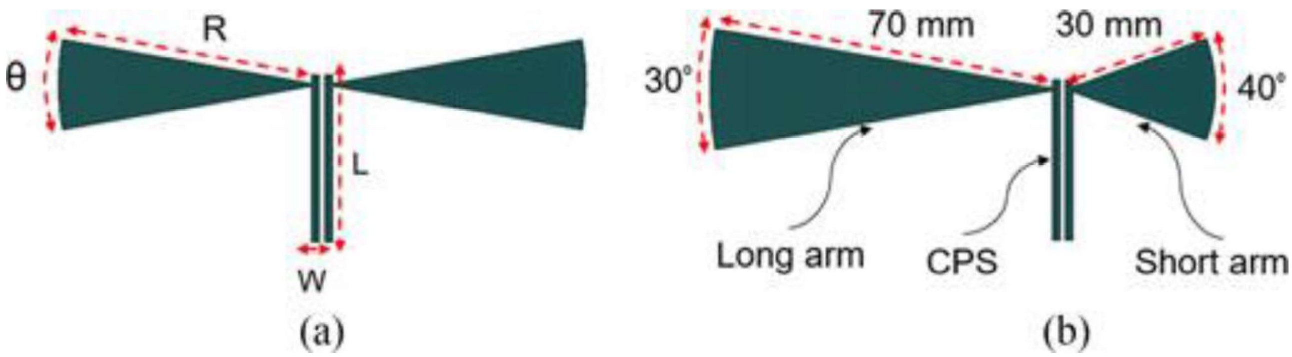

C Song et al. IEEE TIE, 2017

- Broadband high impedance antenna

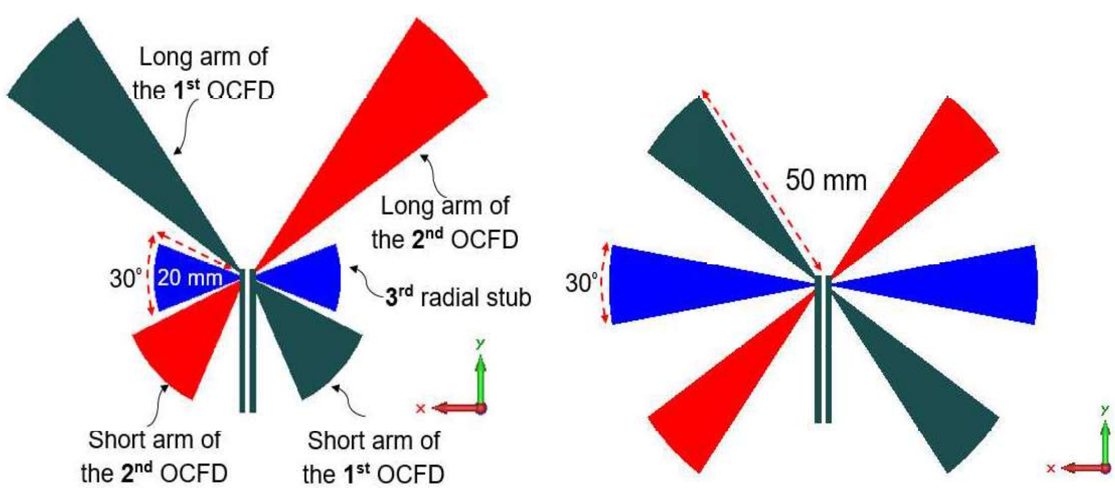

- Complex high impedance (non 50 Ω)

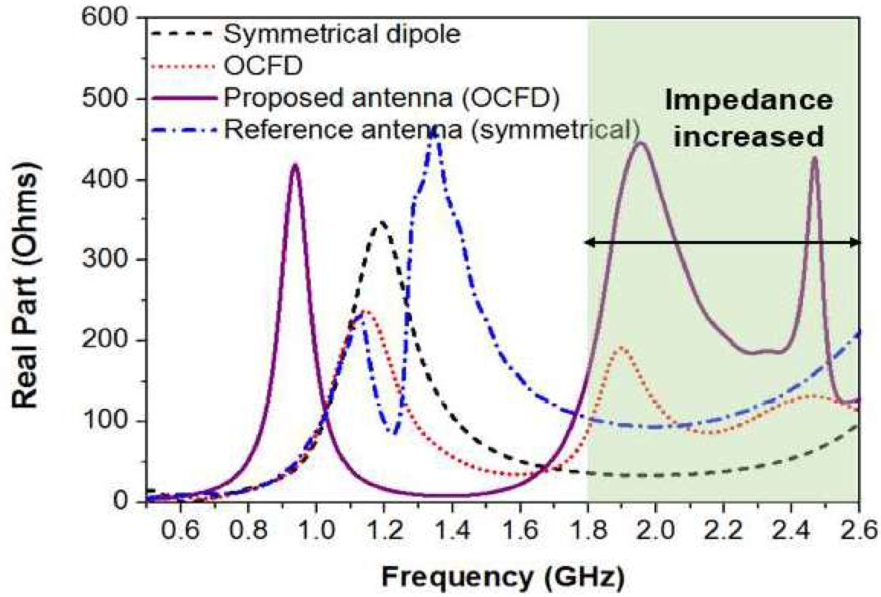

- Fabricated prototype

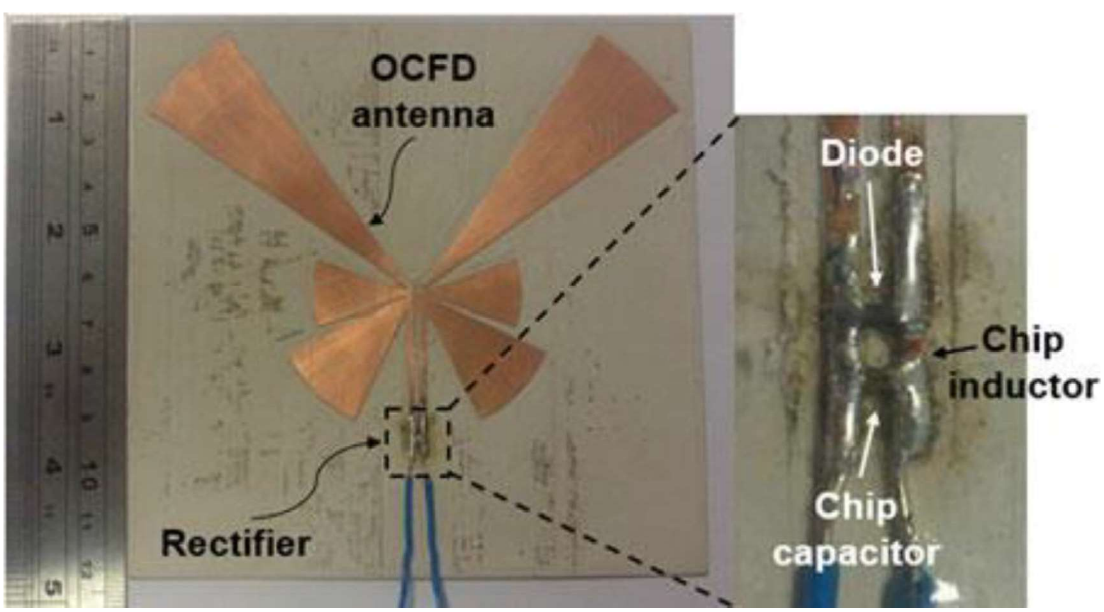

• Complete rectenna performance

- Asymmetrical feed
- No matching network!

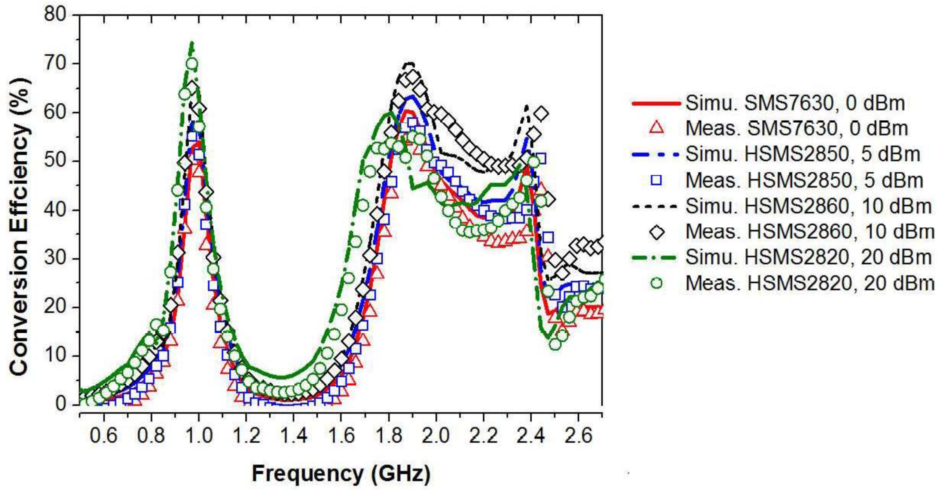

C Song et al. IEEE TIE, 2017

• Variable impedance

- Resistance Compression Network (RCN)

$$Zin = \frac{1}{\frac{1}{R+jX}+\frac{1}{R-jX}} = \frac{R^2+X^2}{2R} = \frac{1}{2}(R+\frac{X^2}{R})$$

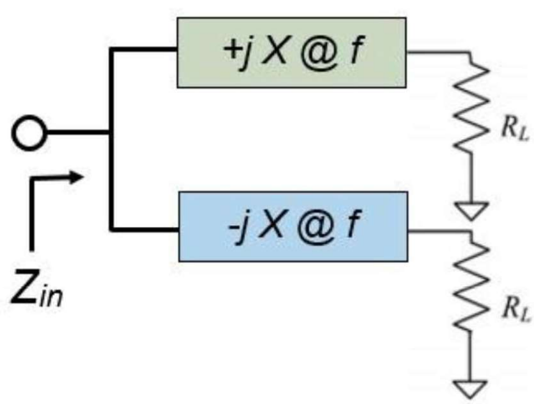

• Variable impedance

- Resistance Compression Network (RCN)

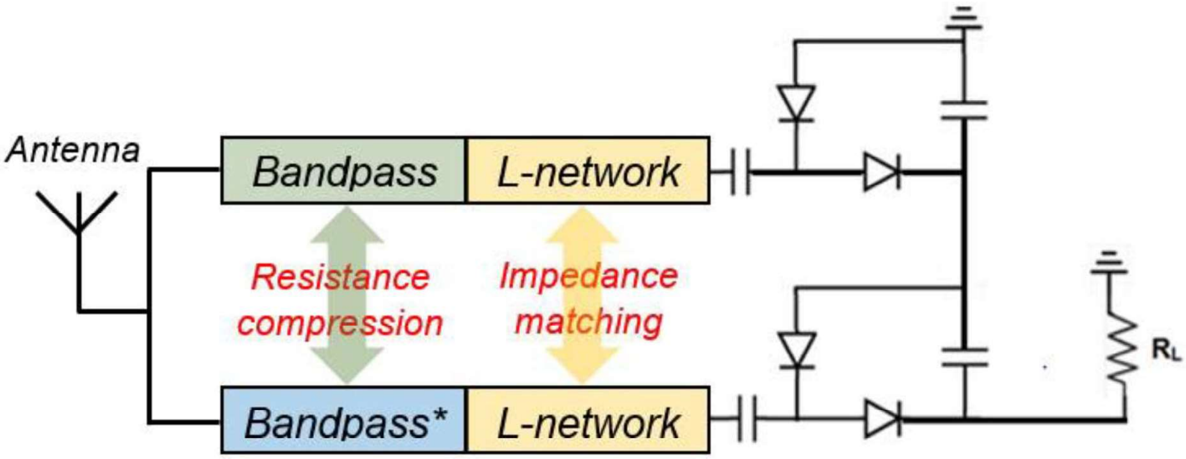

• Variable Impedance

- Resistance Compression Network (RCN)

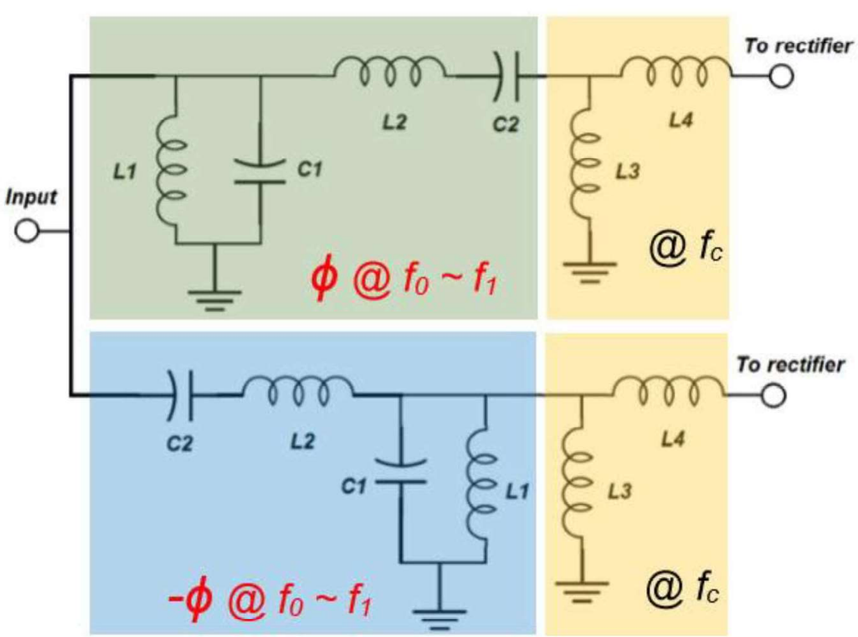

Variable Impedance

- Resistance Compression Network (RCN)

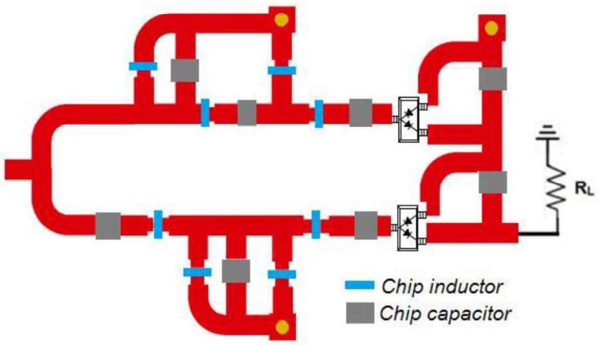

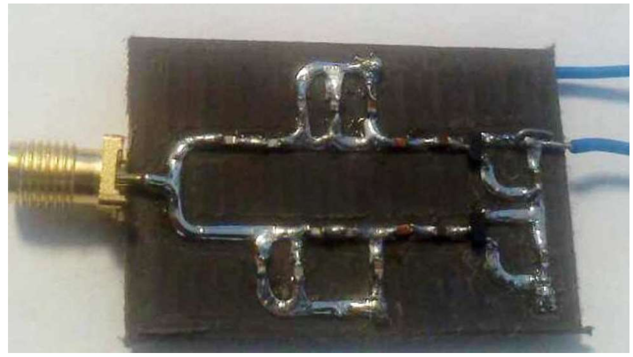

C Song et al. IEEE TAP, 2017

Variable Impedance

- Measured Performance

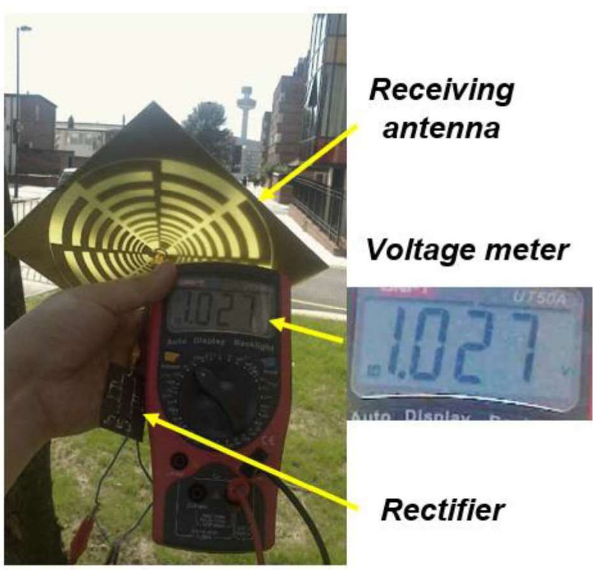

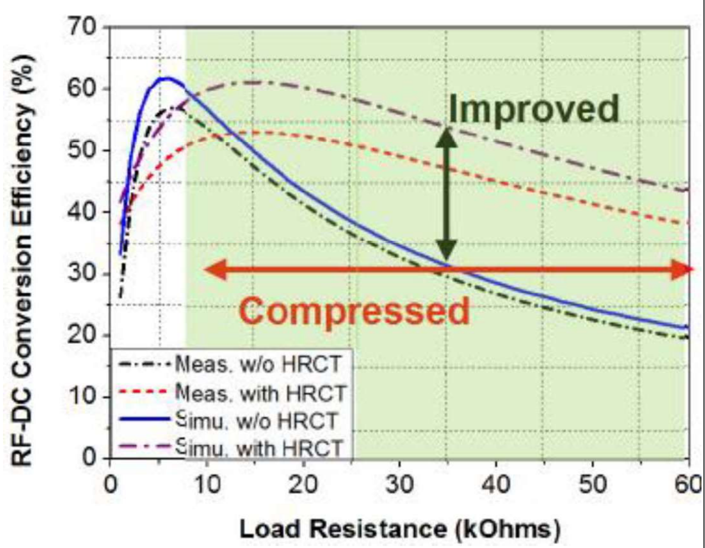

C Song et al. IEEE TAP, 2017

• Patch Antennas

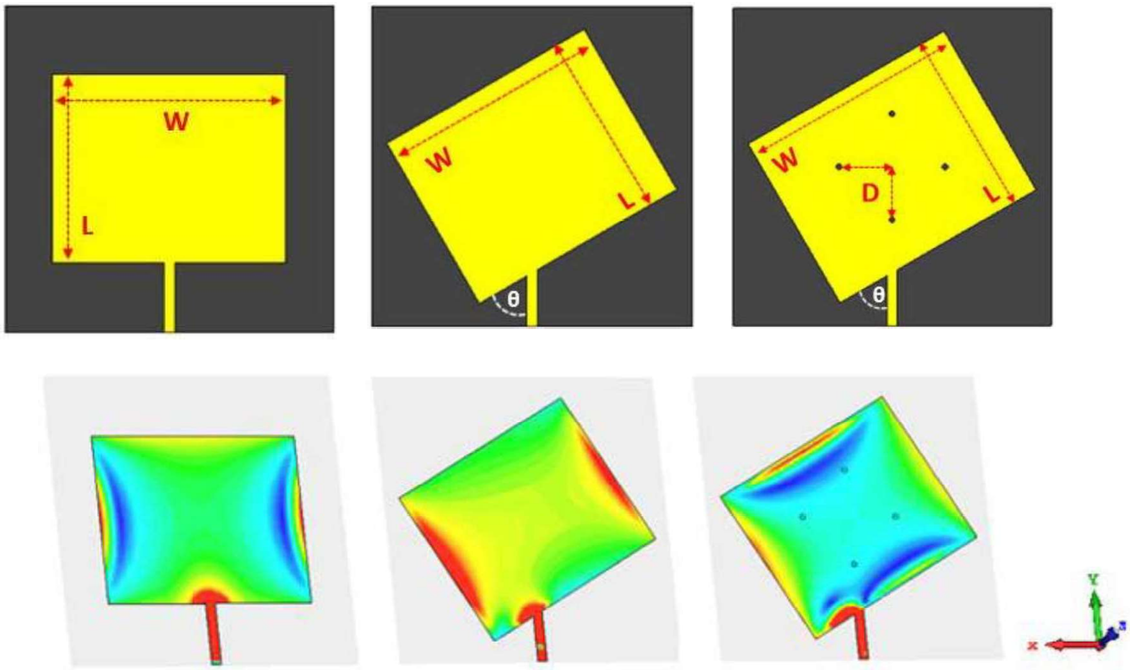

C Song et al. IEEE TAP, 2018

• Patch Antennas

- Center-Fed Patch (CFP)
- Off-Center-Fed Patch (OCFP)
- OCFP with shorting pins

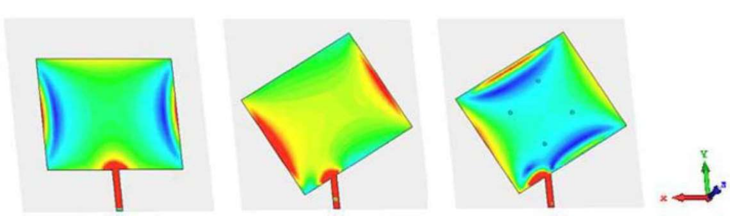

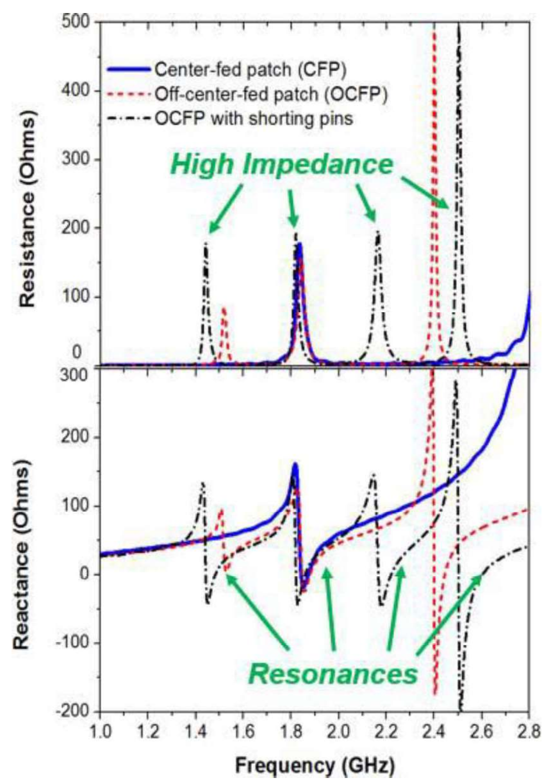

• Selectable frequency

- A function of D
- Selectable: 1 to 2.7 GHz

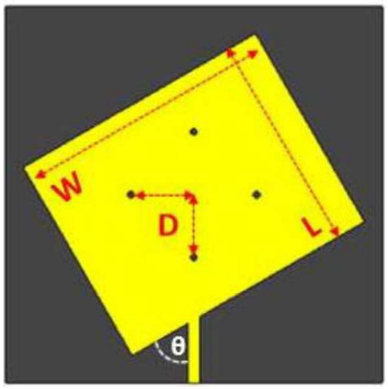

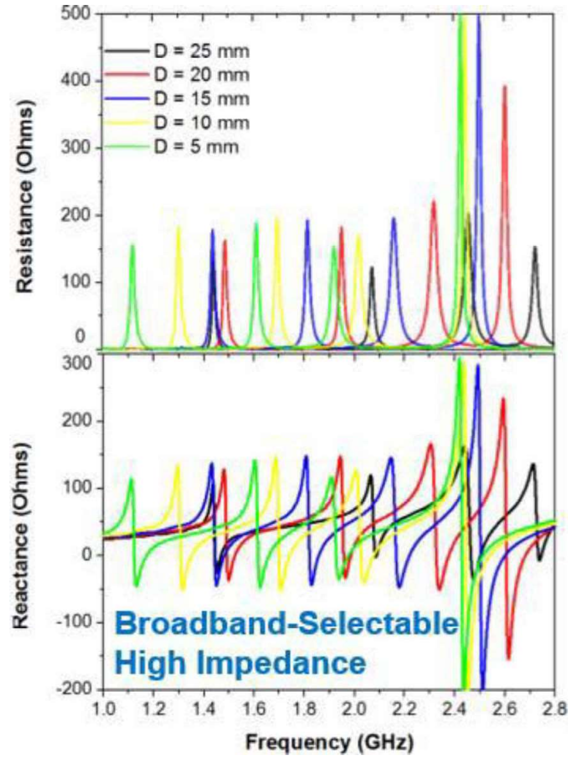

• Rectifier

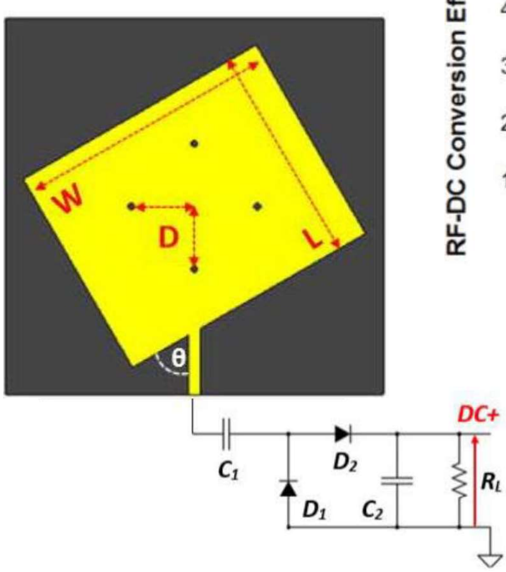

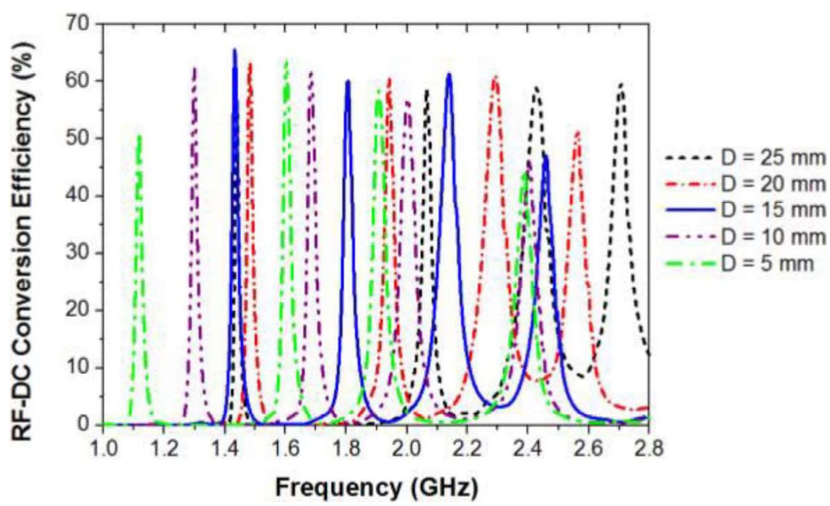

- Four Rectifiers
  - RC1 and RC2 same, orthogonal for polarization independency
  - RC3 and RC4 same, for different power level from RC1 and RC2

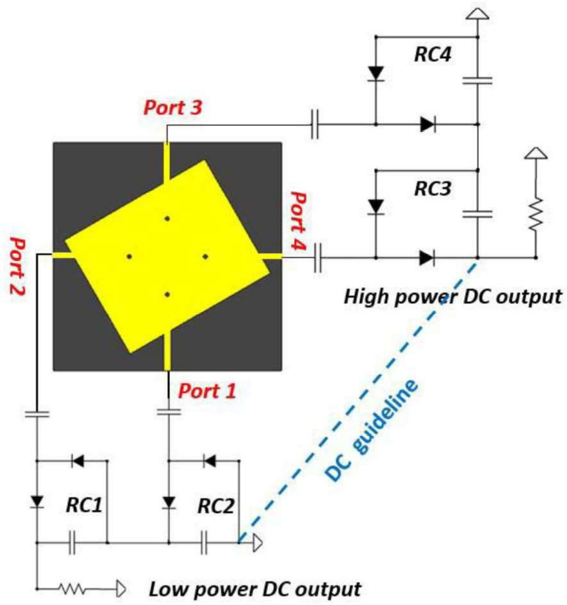

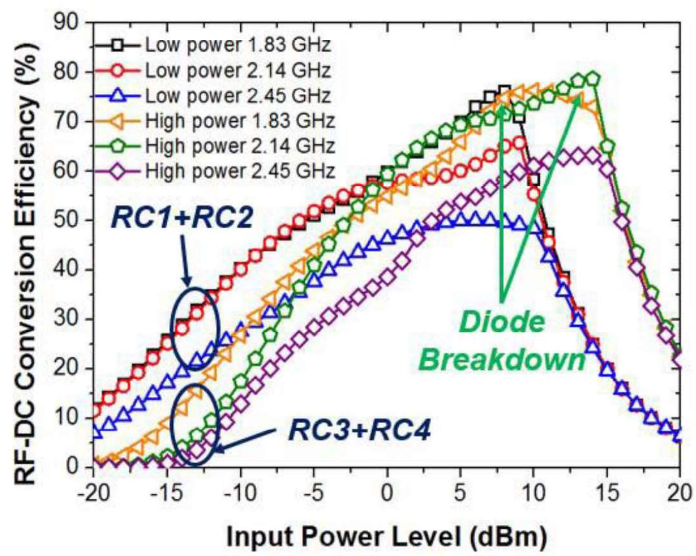

- Four Rectifiers
  - Radiation patterns
    - Left Port 1 and Port 3
    - Right Port 2 and Port 4
    - 1.83, 2.14, and 2.45 GHz

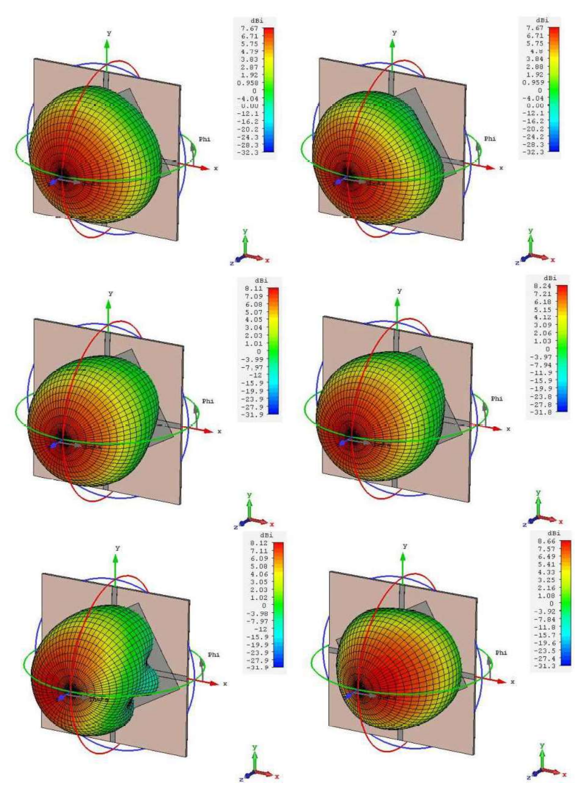

- Fabricated circuit

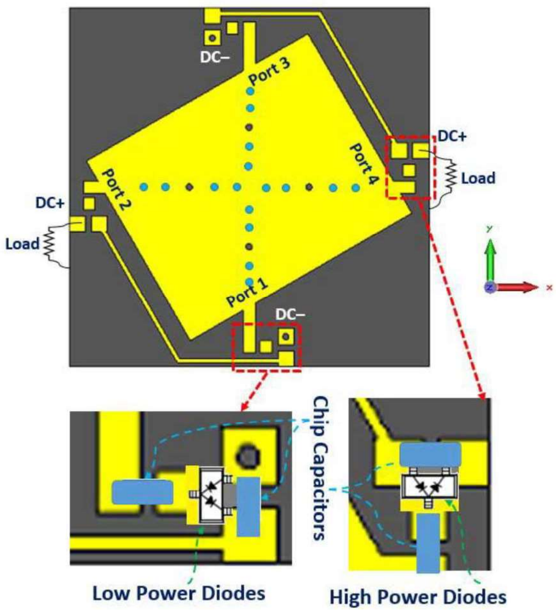

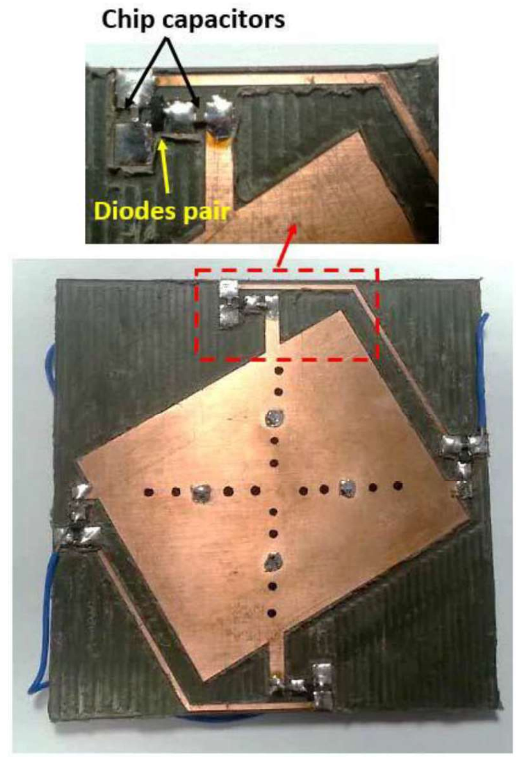

WPW 2019
WPW SCHOOL

- Measured Results

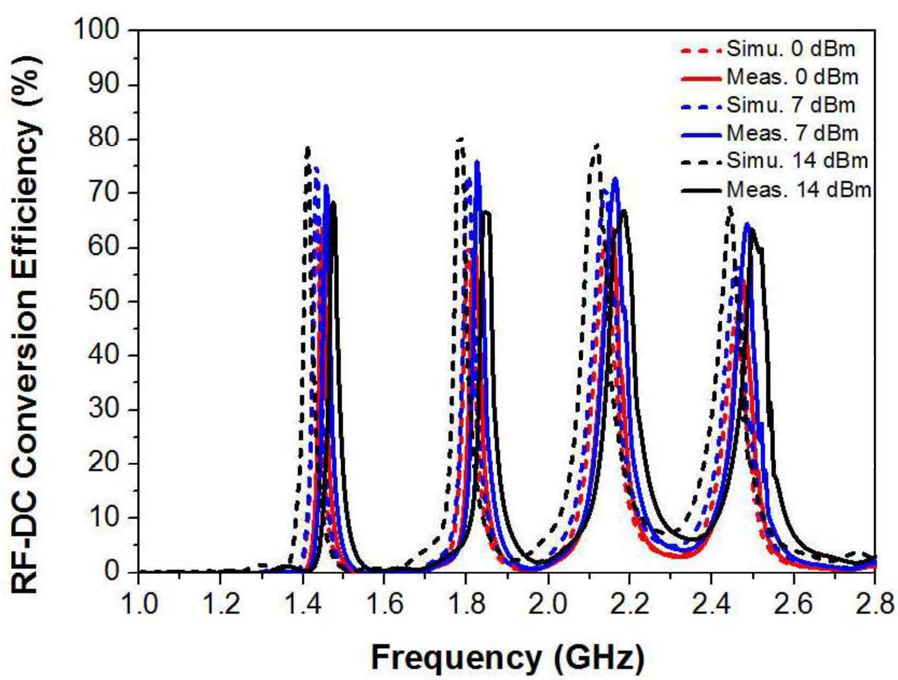

- Measured Results

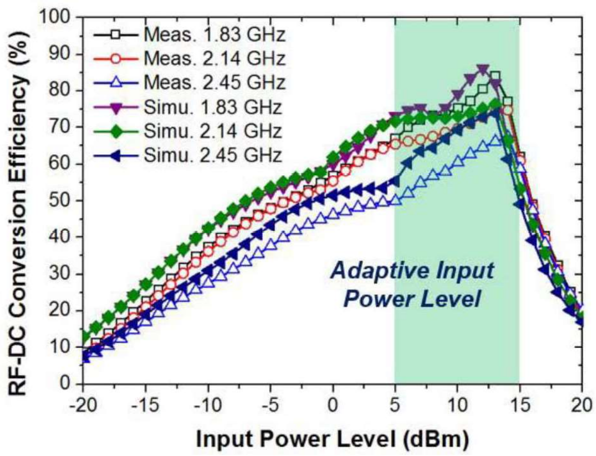

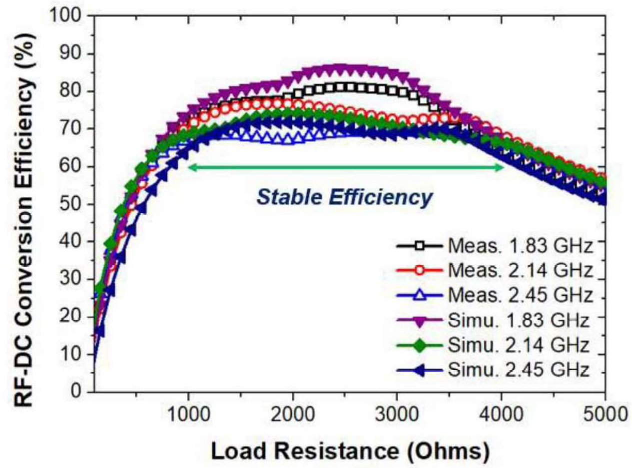

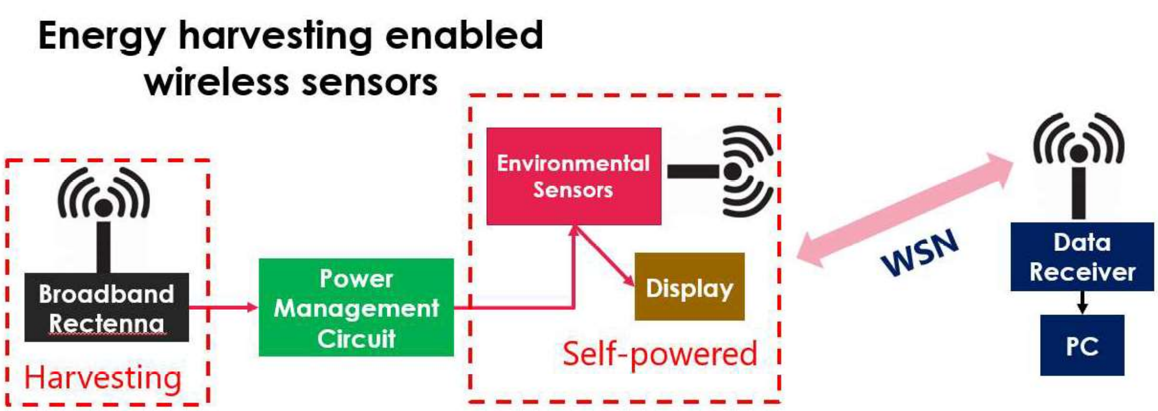

US patent filed

Battery-Free Quartz Clock With Wireless Sensing

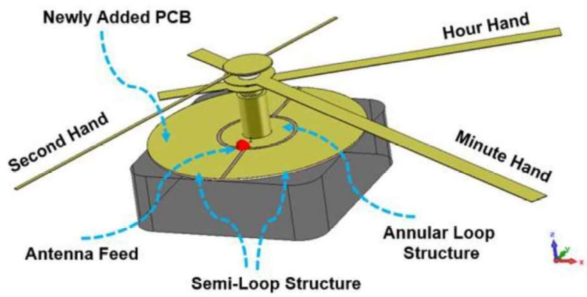

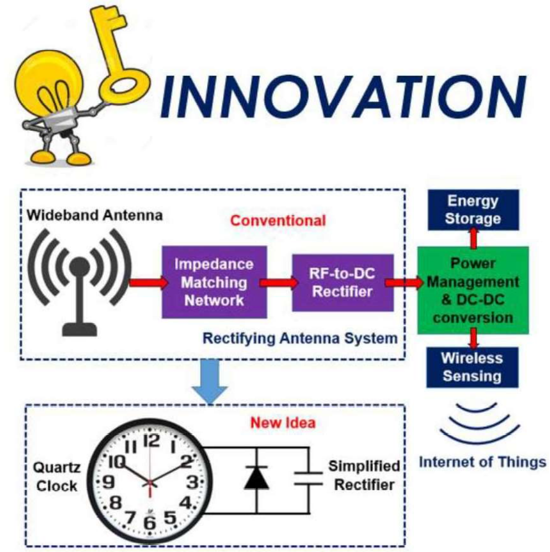

© **C. Song** et al., ""Novel Quartz Clock with Integrated Wireless Energy Harvesting and Sensing Functions" **IEEE Trans. Industrial Electronics, June 2018.**

- Improves patient's life by offering:
  - Regular Monitoring
  - Regular Stimulation or Treatment

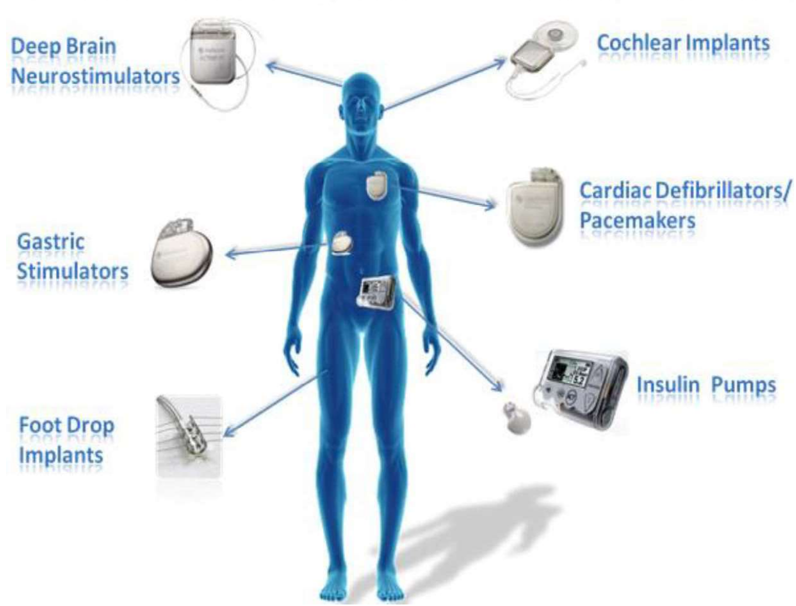

- Operation of pacemakers

- 600,000 pacemakers implanted every year
  (40,000 in the UK, 225,000 in the US)
  - ***Most successful*** implantable devices invented, in terms of lives saved or extended.
- Challenges
  - **Power: battery**
  - **Communication: monitoring**

- Pacemakers

- The Problem
  - Near-field, in-contact, short-range

- The reason?
  - **Casing**
  - **Loss of human tissues**

- Characteristic Modes on a 120mm x 60 mm PCB (www.feko.info)

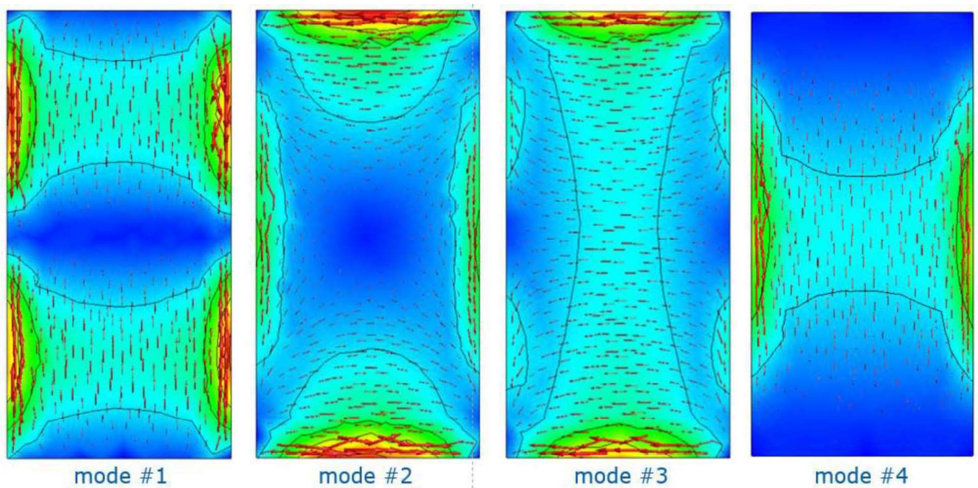

Instantaneous modal currents on the PCB, 2.6 GHz

- Lab adaption

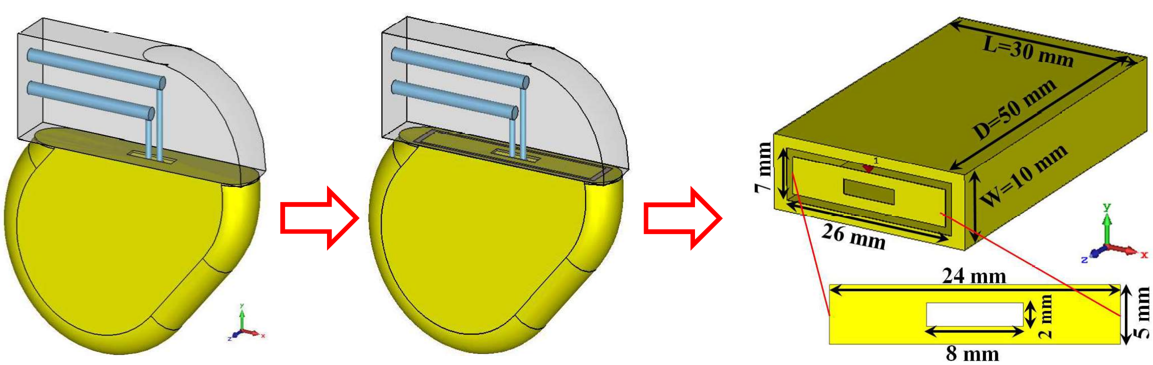

- Mode Analysis

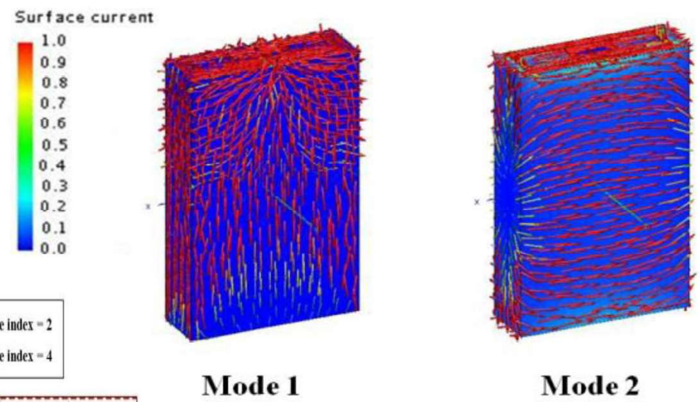

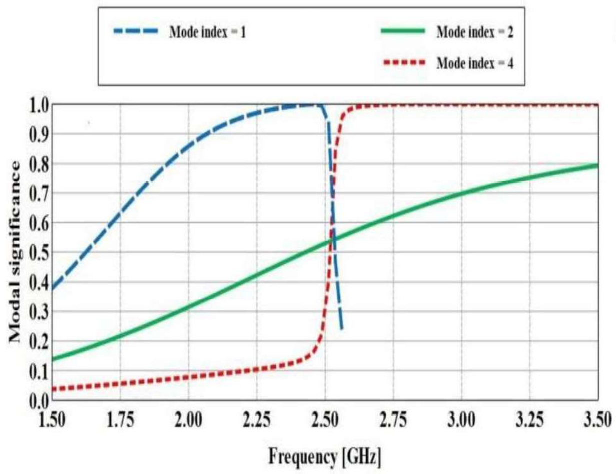

$$J = \sum_n \frac{V_n}{1 + j\lambda_n} J_n$$

Vn: the excitation coefficient

$\left|\frac{1}{1+j\lambda_n}\right|$: modal significance

WPW 2019

WPW SCHOOL

- Fabricated Circuit

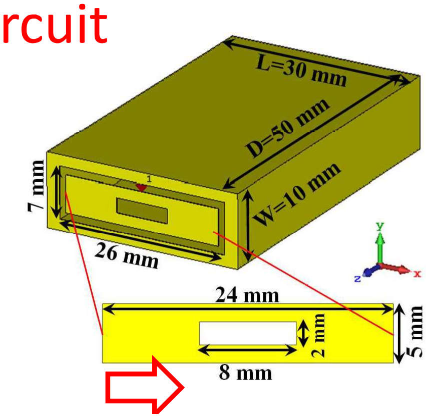

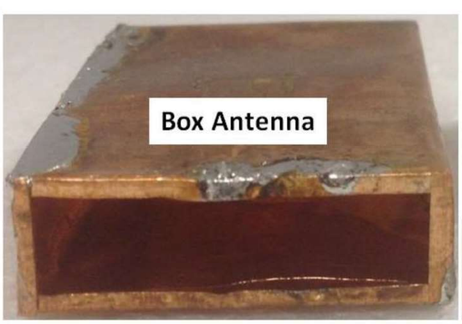

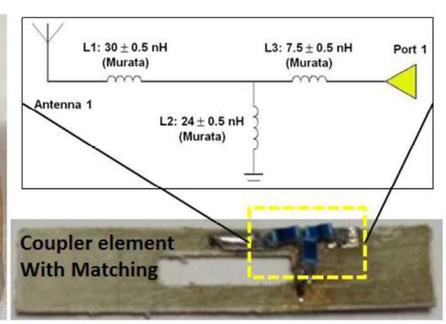

- Safety Limit
  - Exposure Limit
  - Specific Absorption Rate

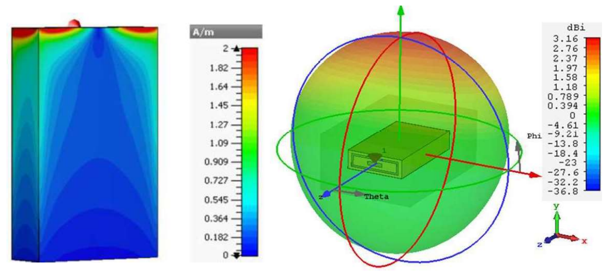

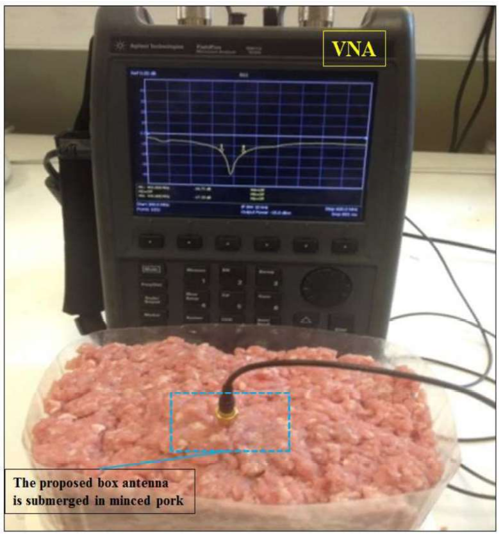

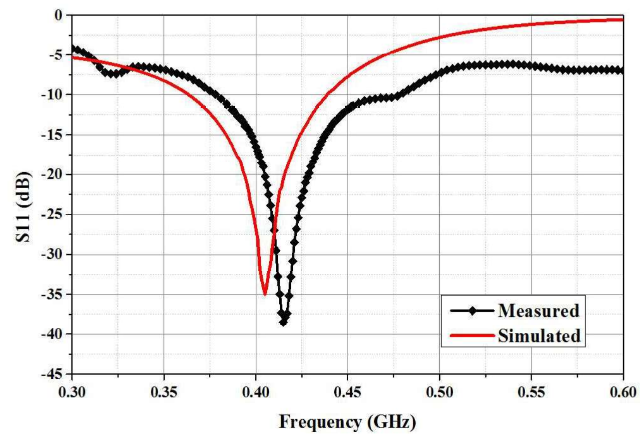

- Communications of implantable devices:

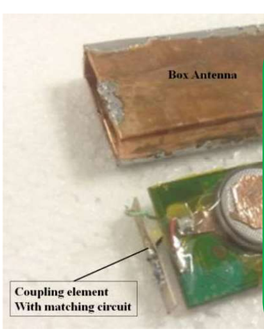

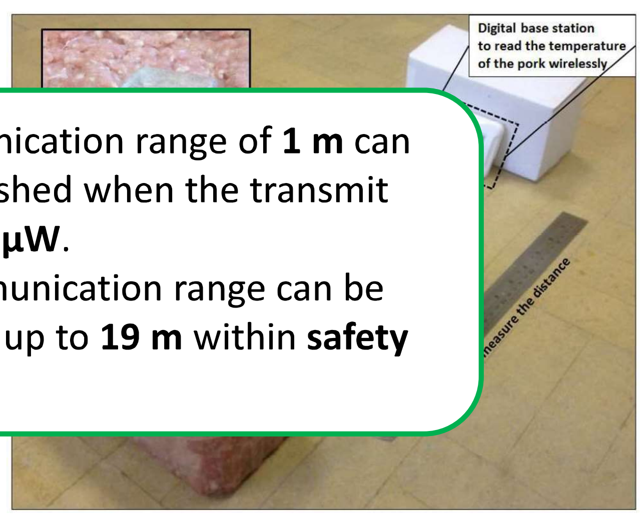

- A communication range of **1 m** can be established when the transmit power **25 µW**.
- The communication range can be increased up to **19 m** within **safety limits**.

- Wireless charging of implantable devices

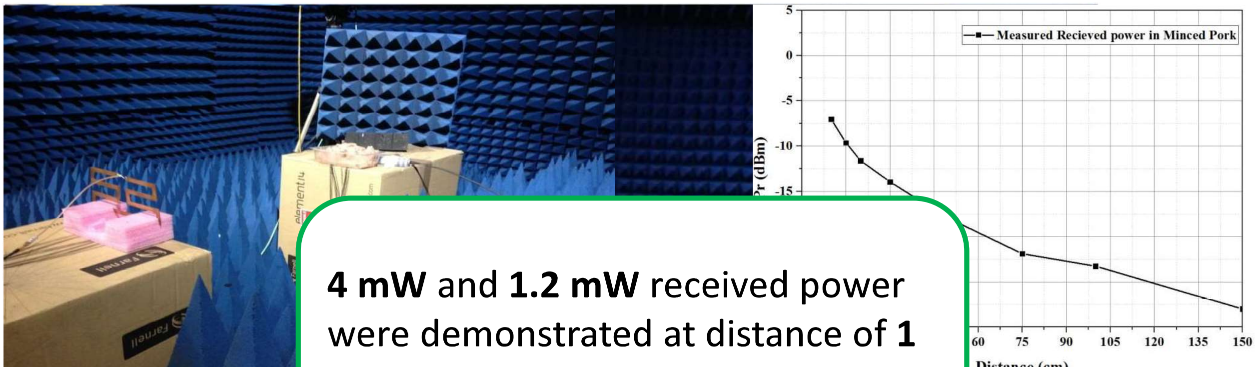

4 mW and **1.2 mW** received power were demonstrated at distance of **1 m** in a **rabbit** and **pork** respectively under public **safety limits.**

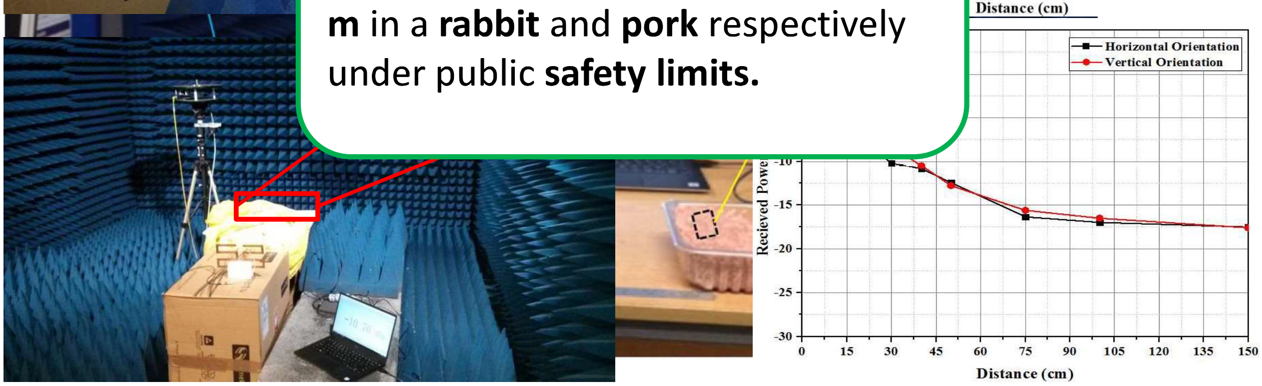

- Implantable devices: monitoring and charging

- Conclusions: Rectennas for RF Energy Harvesting
  - Low voltage
  - Low power
  - Impedance variation
  - Implantable devices
  - …

- Chaoyun Song, Kod Muayad, Yuan Zhuang, Wenzhang Zhang, Sheng Yuan, Yi Huang….

WPW SCHOOL

Environment aware battery-less IoT Frontend

Simon Hemour
University of Bordeaux

This presentation will first sketch the big picture of battery-less IoT frontend needs. Using analytical metrics, we will develop the concept of environment-aware IoT nonlinear circuits and describe a couple of example to demonstrate how those circuits can enhance their operational efficiencies by adapting to their radiofrequency, vibration, temperature, and location conditions.

WPW 2019

WPW SCHOOL

Environment-Aware Adaptive Energy Harvesters for IoT Applications

X. Gu[1], E. Vandelle[2], G. Ardila[2], T. P. Vuong[2], K. Wu[1], and S. Hemour[3]

[1] Poly-GRAMES Research Center, Polytechnique Montréal, Montréal, Canada

[2]IMEP-LaHC Laboratory, Grenoble INP, University of Grenoble Alpes, Grenoble, France

[3] IMS Laboratory, CNRS UMR 5218, University of Bordeaux, Talence, France

WPW 2019

Outline

WPW SCHOOL

- Introduction
- RF energy aware
- Vibration energy aware
- Communication direction aware
- Temperature aware
- Conclusions

Introduction

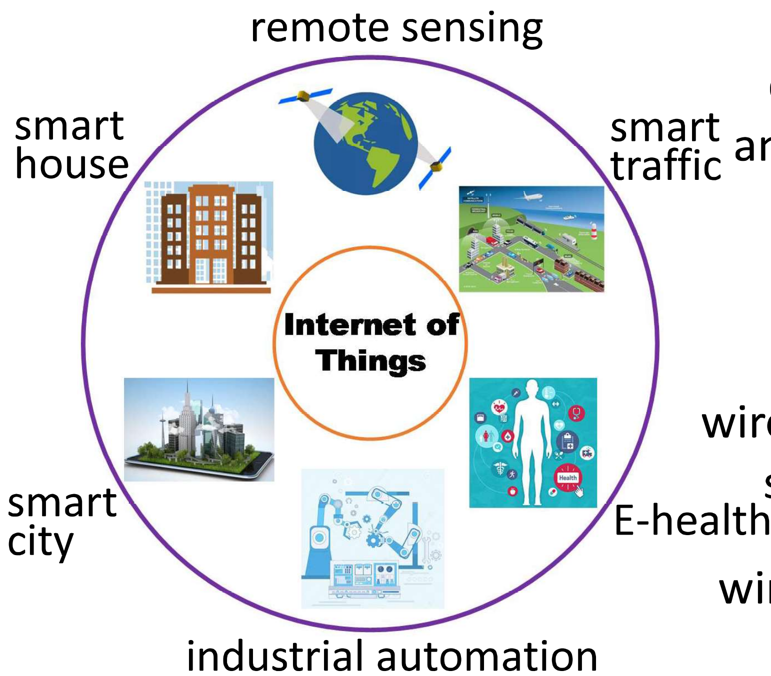

geographically distributed devices and/or mobile devices

power charging challenges

wired power supply

wireless power transfer (WPT)

Introduction

WPW SCHOOL

man-made electromagnetic radiation: RF base stations , mobile devices and others.

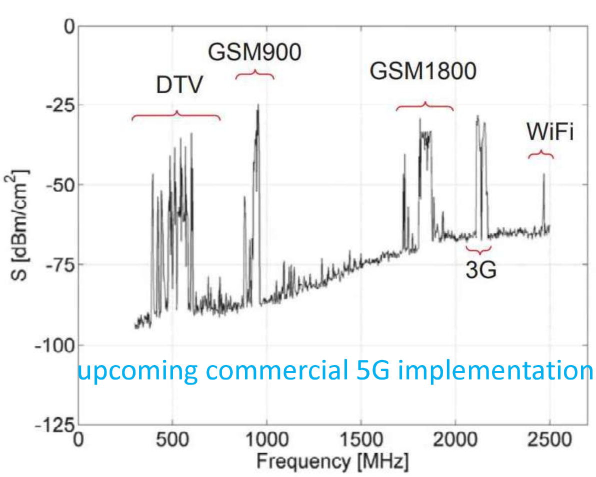

upcoming commercial 5G implementation

Million unit	Devices	Year
12	Cell phone base stations deployed: 5.9 million of macro-cells and 6 million of small-cells (lower power, shorter range).	2012
4000	Wi-Fi enabled consumer electronics devices.	2014
6800	Subscriber identification module (SIM) cards in use.	2013

recycle ***wasted*** RF energy if not used immediately by users

[M. Pinuela *et al.* (2013)]

Introduction

WPW SCHOOL

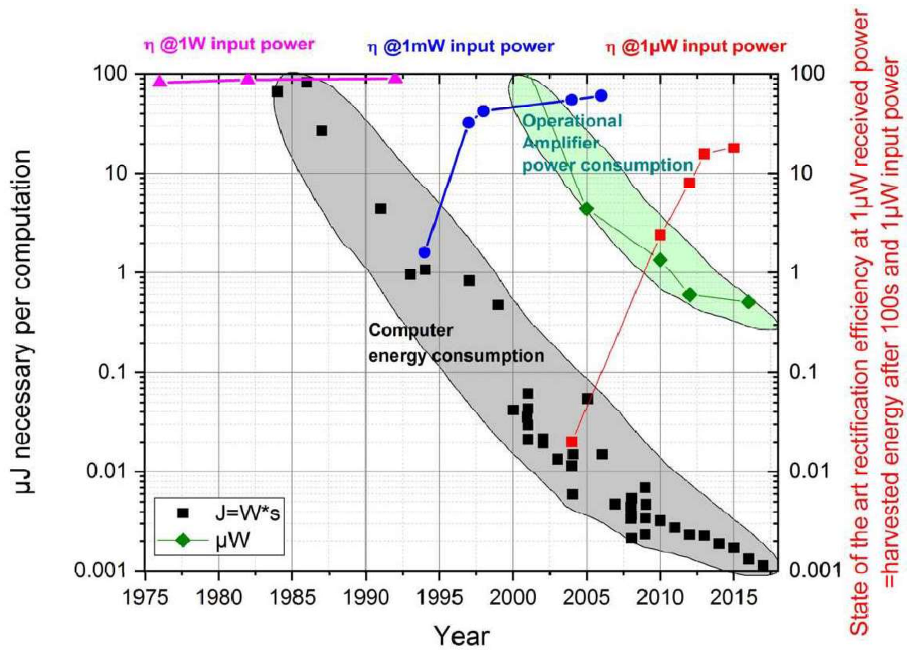

[S. Hemour *et al.*, 2018]

Introduction

WPW SCHOOL

Carnot Limitation

Efficiency of low-power harvester:

$$\eta = \frac{1}{2} \cdot \boxed{\Re_I^2} \cdot \boxed{P_{in}} \cdot \boxed{R_j} = \frac{q \cdot P_{in} \cdot R_j}{4 \cdot n \cdot k_B \cdot T}$$

$\Re_I$: current responsivity

P_{in}: input power

R_j: diode nonlinear junction resistance

q: electron charge

n: diode ideality factor

k_B: Boltzmann constant

T: operating temperature

- ❑ Increase junction resistance
  - higher Schottky barrier
  - high Q matching circuit (high impedance antenna)
- ❑ Increase the nonlinearity
  - tunnel diode
  - spin diode
  - lower temperature
- ❑ Increase the input power
  - High gain rectenna
  - Temporal energy multiplexing (multisine)
  - Hybrid harvesters

[S. Hemour *et al.*, 2014]

Introduction

WPW SCHOOL

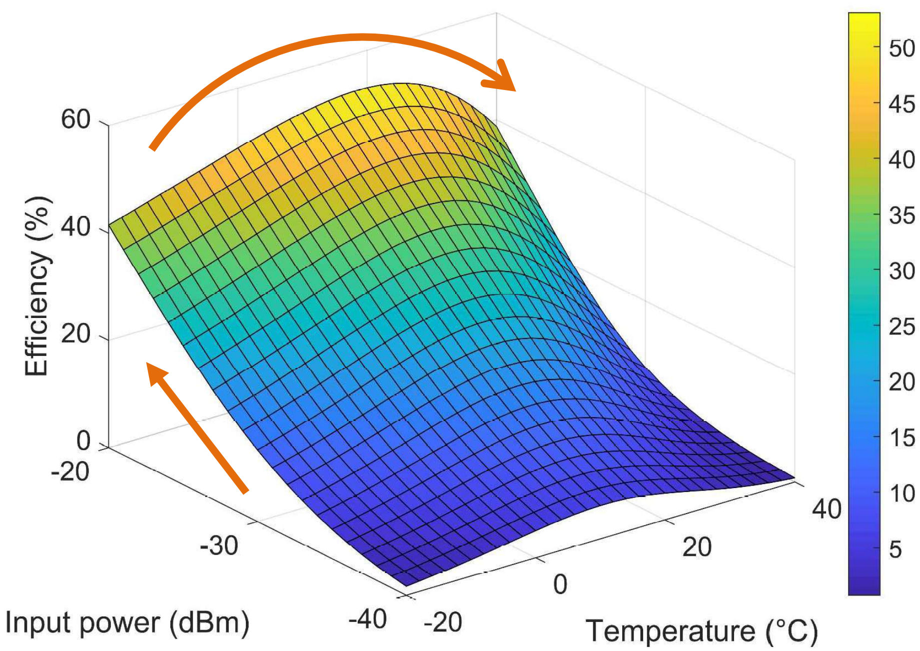

RF Energy Aware

WPW SCHOOL

Loss mechanisms of an RF harvester

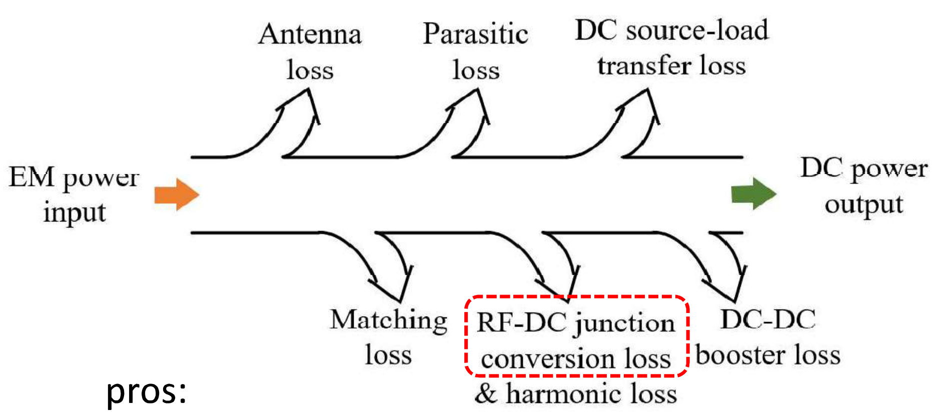

pros:

low cost

high reliability

easy fabrication

Schottky diodes

cons:

efficiency limitation

[S. Hemour *et al.*, 2018]

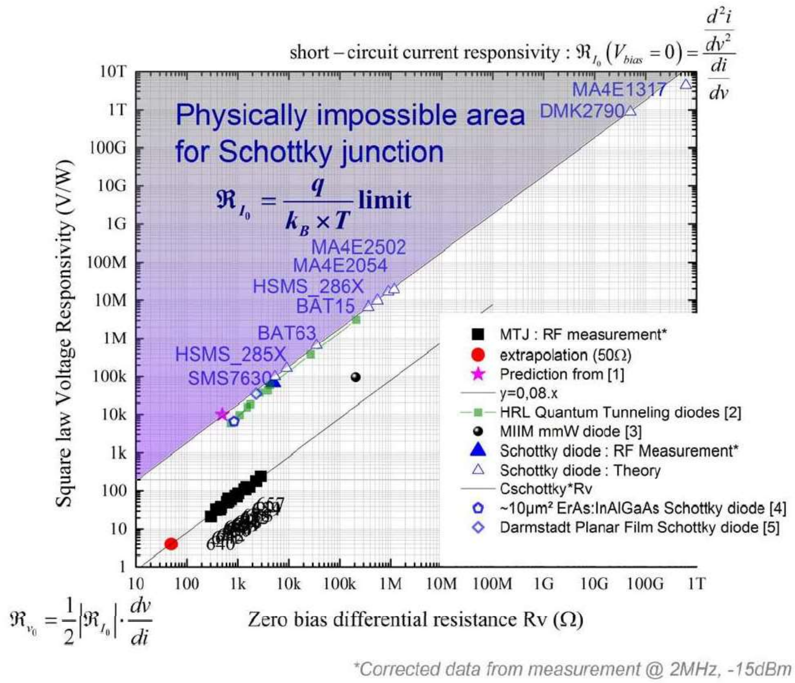

Schottky diodes
$\Re_{I0}$ = 19.34 A/W
(Max. at room temp.)

MIM diodes
spin diodes
tunnel diodes

[S. Hemour *et al.*, 2018]

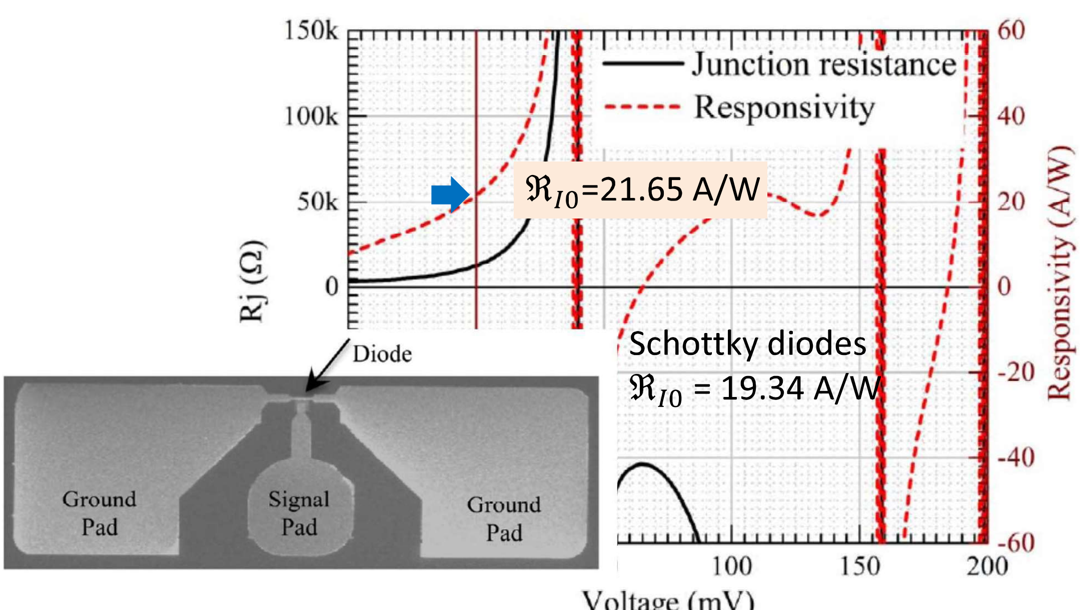

[C. Lorenz *et al.*, 2015]

RF Energy Aware

WPW SCHOOL

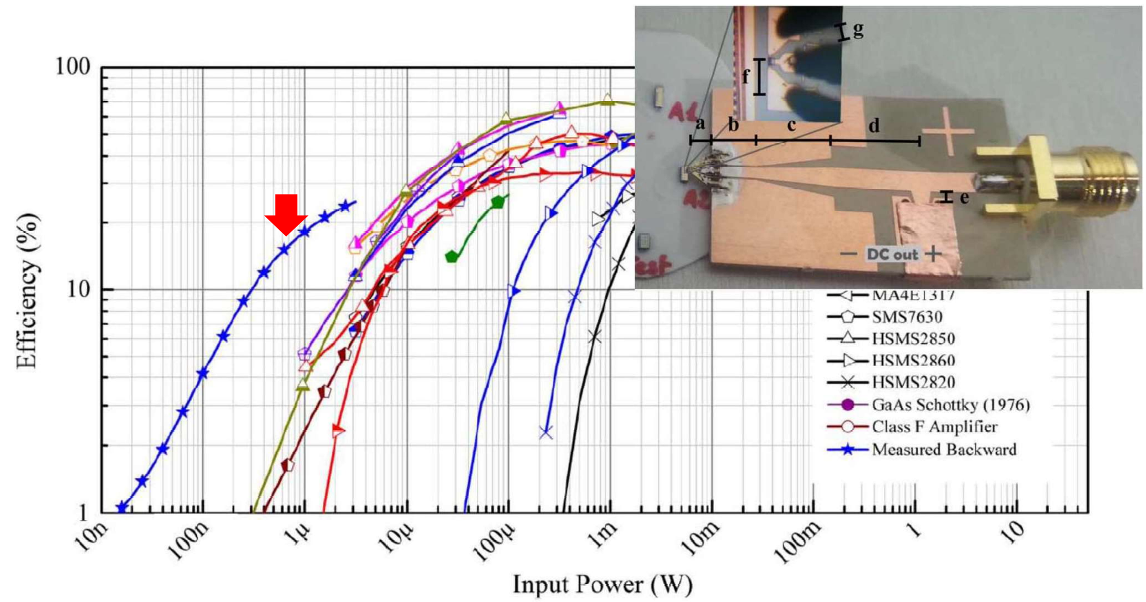

[C. Lorenz *et al.*, 2015]

RF Energy Aware

WPW SCHOOL

multiband rectenna

operating in all LTE bands

0.79-0.96, 1.71-2.17, 2.5-2.69 GHz

high impedance antenna

conjugate matching to diode

no matching network

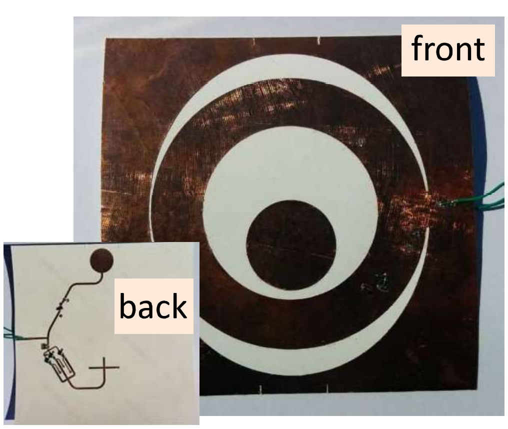

[V. Palazzi *et al.*, 2018]

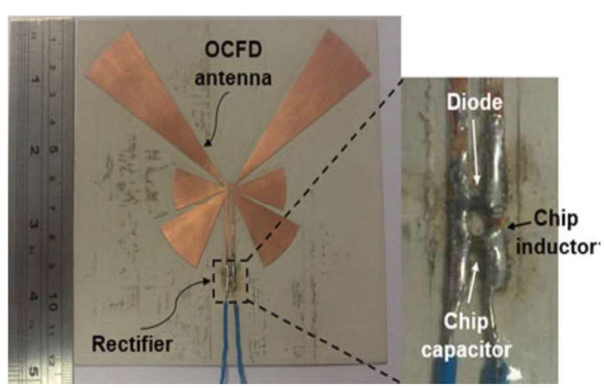

[C. Song *et al.*, 2017]

far-field ambient RF power WPT

+

vibration energy (high conversion efficiency)

- moving vehicles
- human motions
- household products vibrations
- ⋮

transduction mechanisms

- ➢ electromagnetic ★
- ➢ piezoelectric
- ➢ electrostatic

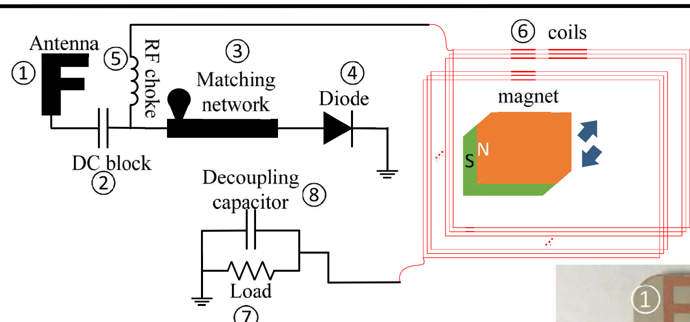

label marks are consistent

(Skyworks SMS7630-079LF)

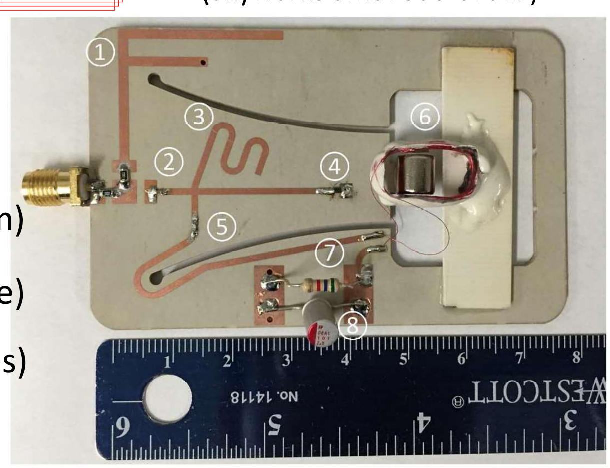

Strong Resilience

two harvesting modes (RF & vibration)

operating separately (only one source)

operating cooperatively (both sources)

[X. Gu *et al.*, 2018]

Vibration Energy Aware

WPW SCHOOL

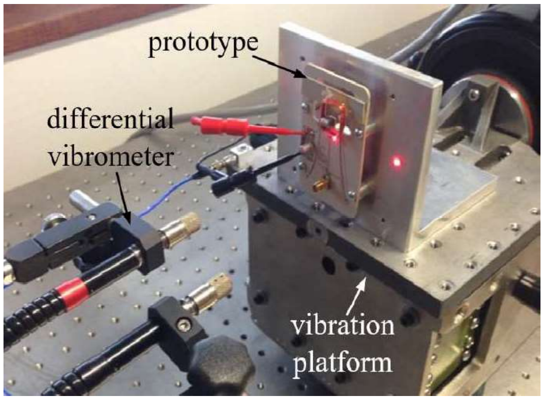

measurement setup

red line

efficiency gain of 150%

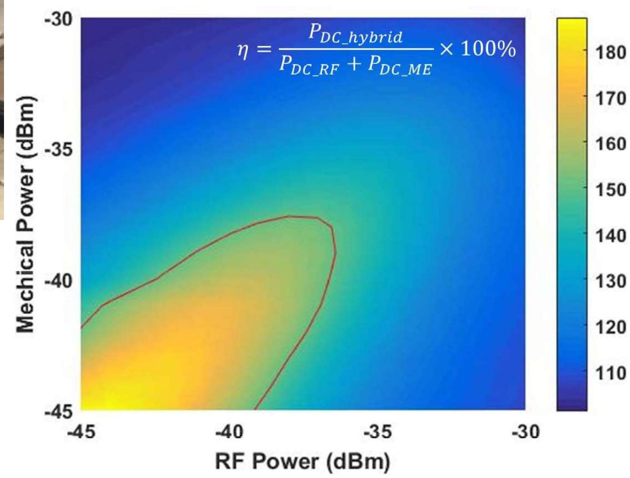

[X. Gu *et al.*, 2018]

Vibration Energy Aware

WPW SCHOOL

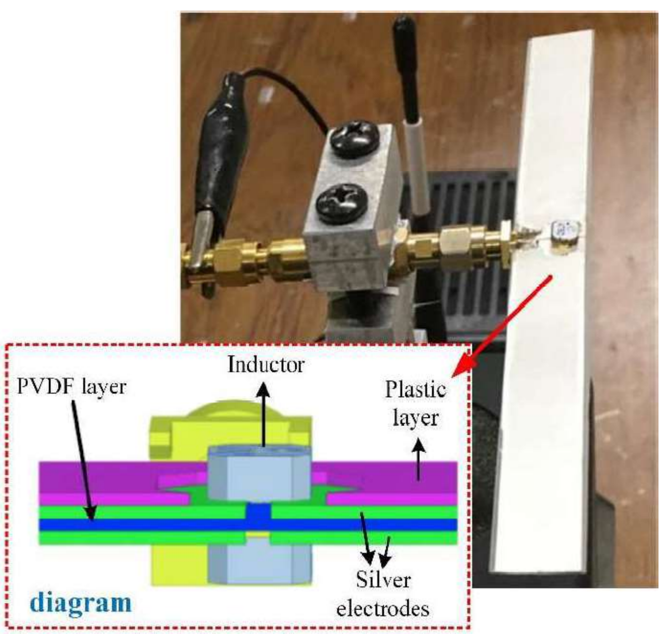

silver electrodes:
antenna working at 915 MHz

PVDF piezoelectric thin film sandwiched between electrodes:
kinetic energy scavenger working at 15 Hz

[S. Nguyen *et al.*, 2018]

Other possibilities

RF + solar energy

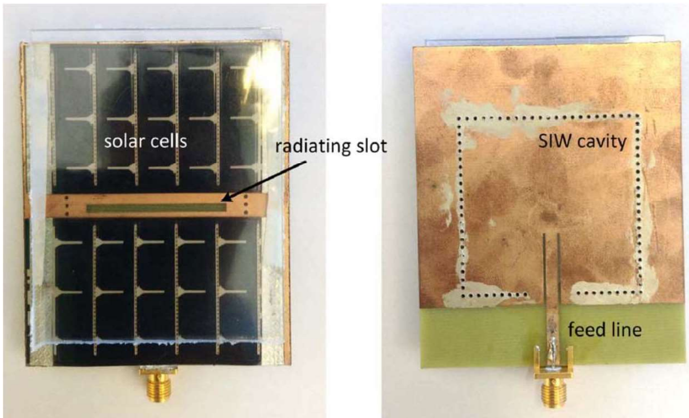

SIW solar cavity-backed slot antenna

[K. Niotaki *et al.*, 2014]

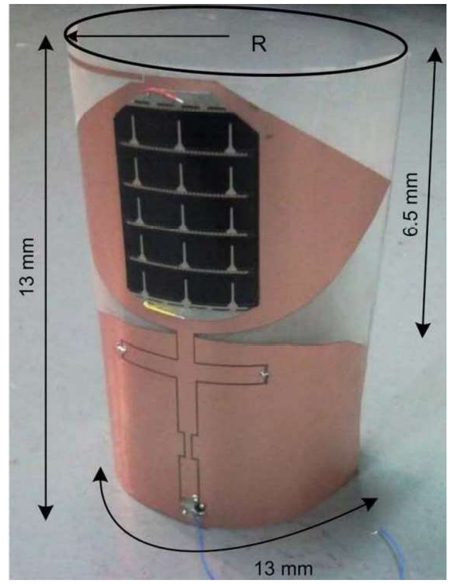

broadband solar printed monopole antenna

WPW 2019

Other possibilities

WPW SCHOOL

RF + thermal energy

potential application scenario

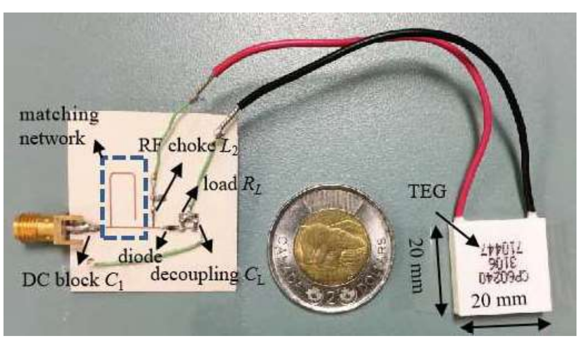

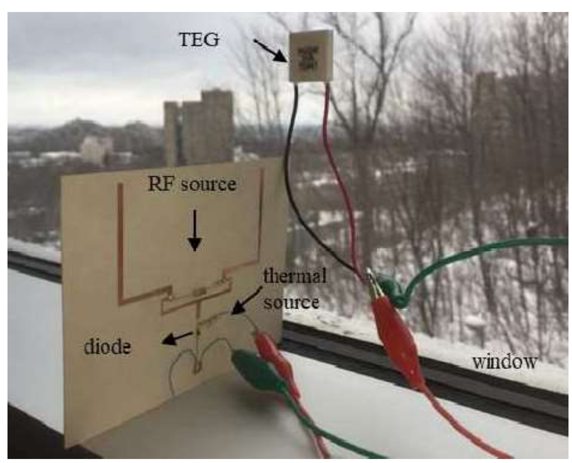

TEG converts thermal energy into dc

[L. Guo *et al.*, 2019]

Poly GRAMES ims

Communication Direction Aware

application scenario

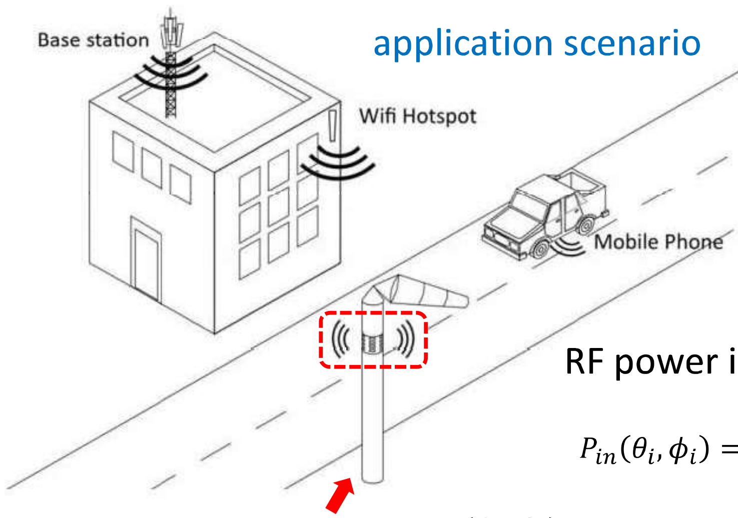

rectenna positioned on a windsock pole

RF power comes from:

- base station
- Wi-Fi hotspot
- mobile phone

RF power injecting into the rectifier:

$$P_{in}(\theta_i, \phi_i) = S(\theta_i, \phi_i).D(\theta_i, \phi_i).\eta_{rad}.\frac{\lambda_o^2}{4\pi}$$

$S(\theta_i, \phi_i)$: power density at the angle of the RF signal

$D(\theta_i, \phi_i)$: directivity of the antenna at the angle (θ_i, ϕ_i)

[E. Vandelle *et al.*, 2019]

WPW 2019 — WPW SCHOOL

Communication Direction Aware

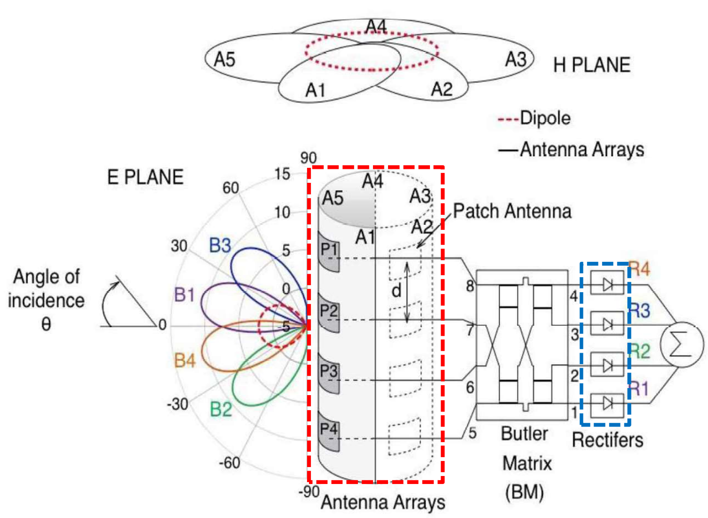

scheme of the multi-directional RF energy harvester

cylindrical antenna array

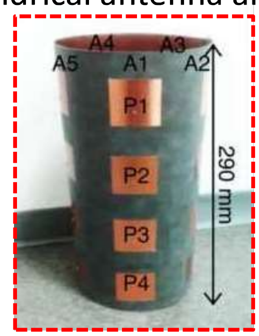

rectifier unit

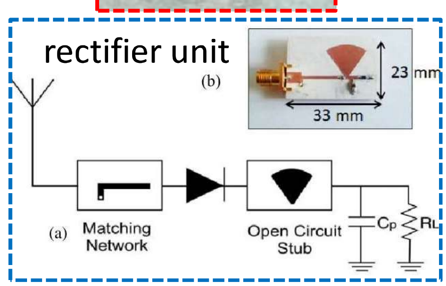

[E. Vandelle *et al.*, 2019]

Communication Direction Aware

WPW SCHOOL

experimental prototype of high gain rectenna with optimal angular coverage

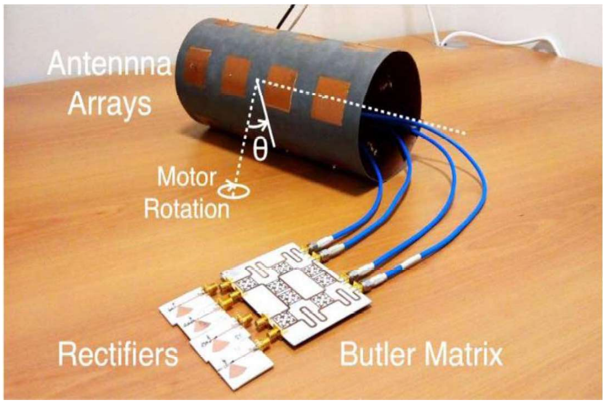

RF input power density

$S = 0.45\ \mu W \cdot cm^{-2}$

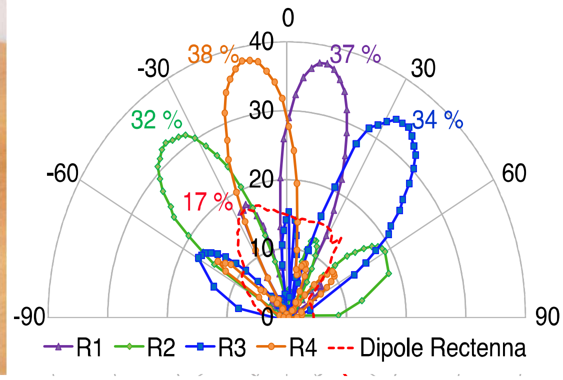

versus dipole rectenna

- higher efficiency
- larger coverage

[E. Vandelle *et al.*, 2019]

Temperature Aware

WPW SCHOOL

I-V relationship of diode HSMS285x

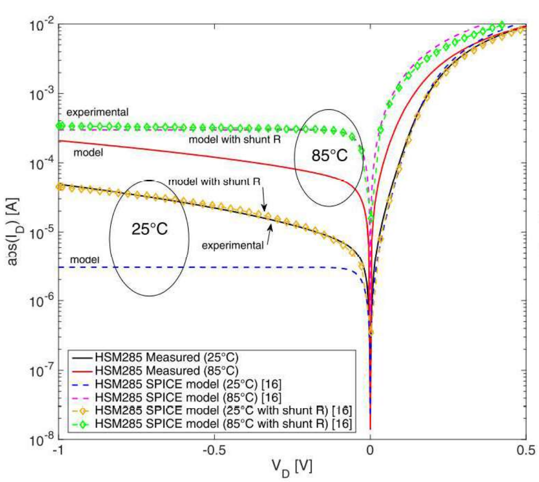

Rectifying efficiency

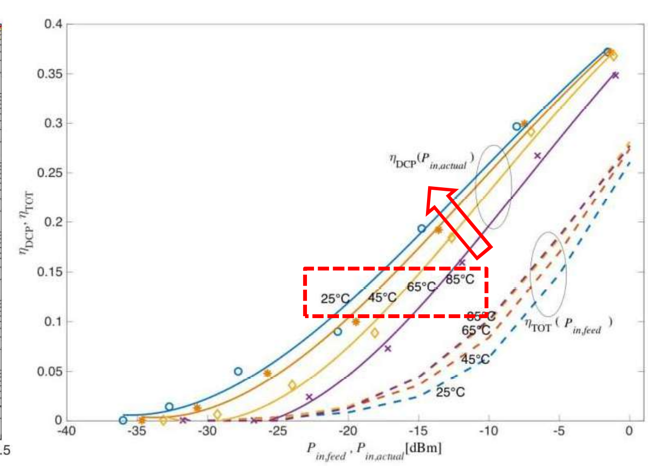

temperature decreases from 85°C to 25 °C, efficiency increases

[F. Della Corte *et al.*, 2018]

Temperature Aware

WPW SCHOOL

Efficiencies related to the Schottky diode:

- RF – dc conversion efficiency:

$$\eta_{RF-dc} = \frac{1}{2} \cdot \Re_I^2 \cdot P_{in} \cdot R_j$$

- Parasitic efficiency: T

$$\eta_p = \left(\frac{1}{1 + (\omega \cdot C_j)^2 \cdot R_s \cdot R_j}\right)^2$$

Optimum temperature?

I-V curve at different temperatures (HSMS-286x series)

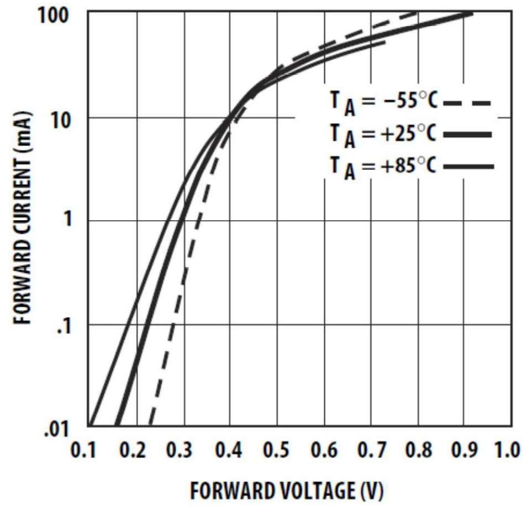

Temperature Aware

WPW SCHOOL

measurement setup

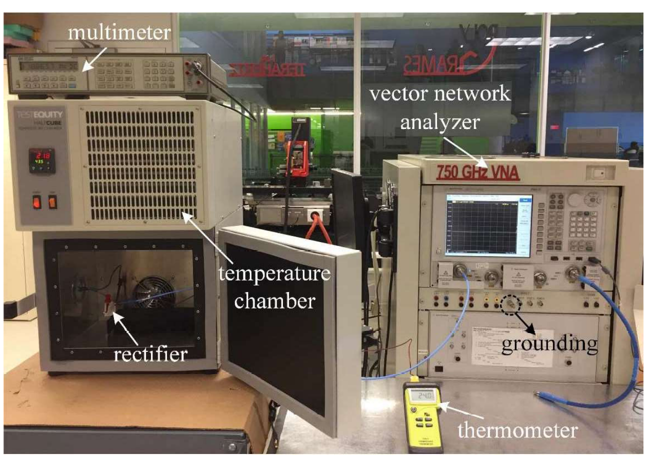

efficiency vs. temp. (−10 to +60 °C)

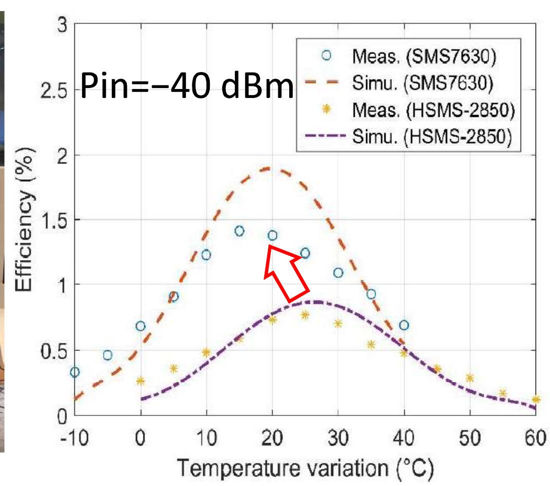

[X. Gu *et al.*, 2019]

Conclusion

Improvements in low-power RF energy harvesting are still possible!

- ❖ Use new diode technologies; (tunnel diode)
- ❖ Considering/harnessing other energy sources; (vibration, thermal, solar etc.)
- ❖ Maximizing the angle coverage of rectennas;
- ❖ Optimizing rectifiers according to the operating temperature.

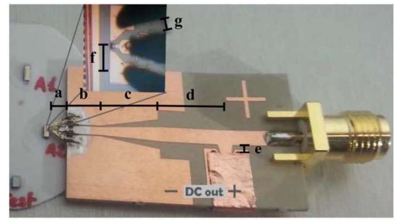

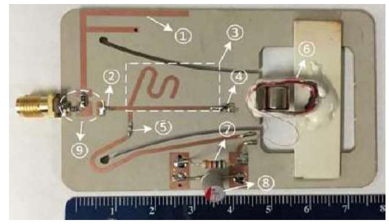

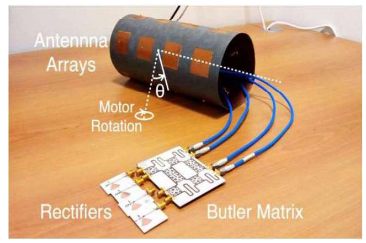

Thanks for your attention!

WPW SCHOOL

Battery-less UWB indoor location is the way forward for industry 4.0

Bruno Franciscatto
UWINLOC

Industry 4.0 refers to a new phase in the Industrial Revolution that focuses heavily on interconnectivity, automation, machine learning, and real-time data. Industry 4.0, also sometimes referred to as IIoT or smart manufacturing, marries physical production and operations with smart digital technology, machine learning, and big data to create a more holistic and better connected ecosystem for companies that focus on manufacturing and supply chain management. One of the critical building blocks of this ecosystem is reliable, accurate indoor location : in order to automate, you have to know where everything is, in most cases with sub-meter precision. In a reliable way, at ultra-low cost. Which means a communication system suited for an industrial environment. This is a tall order, and while there are a large number of technologies available, none of them fits the bill completely. Either the cost is low, but there is no location other than checking fixed points. Or the communication channel is not resilient enough for industrial, noisy environments. Or there is a battery involved, driving up the cost and complicating the management of the tracking devices. UWINLOC is the only company marrying the Ultra-Wide Band accurate industrial-grade communication system with energy harvesting for battery-less operation. This leads to low-cost, battery-less tags with a long reach, even in noisy environments, with the required precision.

WPW 2019

WPW SCHOOL

Battery-less UWB indoor location is the way forward for industry 4.0.

Dr Bruno Franciscatto

CTO at UWINLOC

bruno.franciscatto@uwinloc.com

UWINLOC™ INDOOR LOCATION SYSTEM

CONTENTS

1. Company Introduction
2. Technology overview
3. UWINLOC's Technology Breakthroughs
4. Conclusion

1. Company Introduction

UWINLOC presentation

FACTS & FIGURES

- Creation 2015
- 40 people
- Based in Blagnac
- 40 clients
- 9 countries

Eric CARIOU
CEO & co-founder
Extensive experience in the TMT sector and Co-founder of ARC Group / Informa Plc.

Jan MENNEKENS
CSO & co-founder
30+ years of innovation in embedded electronics and software

Cyril GUILBOT
COO

Dr. Bruno FRANCISCATTO
CTO

Cassandre LE CORRE
SALES DIRECTOR

FINANCE
LEGAL & IP
QUALITY

INDUSTRIALISATION
INSTALLATION
SUPPORT
PROCUREMENT

R&D PROJETS
DEV PRODUCT

SALES
PRODUCT
MARKETING

BOARD MEMBERS

Mathieu SIBRA
Investment Director at ACE Management
Aerospace - Partnership

André BENHAMOU
Ex-CEO of LIEBHERR Aerospace & Transportation
Governance – Aerospace – Request for Proposal

Marc ROUGIER
Partner at Elaia Partners
Deep Tech - Business & Marketing International

Antoine JOUIN
Ex-President of Continental France
Automotive - Governance

Claudia DAUGAN
Investment Director at Galia Gestion
Financial Engineering – IPO – Governance

Alexandre SCHERER
Managing Partner & Investment Director at MCapital Partners
International – Governance - IPO

1. Company Introduction

What problem are we trying to solve?

Impossibility of localising assets in quasi-real-time in the manufacturing process is detrimental to performance and productivity

- DELAYS IN PRODUCTION
  - > Inefficient picking operations
  - > Manual WIP tracking
- EXPENSIVE INVENTORY
  - > Low visibility Goods in / Goods out
  - > Time consuming inventory operations
- INEFFICIENT MAINTENANCE
  - > Searching for lost asset
  - > Quality/reliability

$ **8** Bn p.a.
worth of tools lost or stolen

$ **38** Bn p.a.
worth of logistics parcels lost

Global asset tracking market (1)

$ **14** Bn in 2018 — **15**% CAGR → $ **32** Bn in 2024

(1) Global Asset Tracking Market 2018-2023, Research and Markets, May 2018

1. Company Introduction

UWINLOC's market position

BATTERY-LESS SOLUTIONS

Good for identification
but not applicable to most real time
asset tracking (location) use cases

RFID

Annual volume sold:

20 billion passive RFID tags
2000 billion bar codes printed

UWINLOC
INDOOR LOCATION SYSTEM

BATTERY-POWERED SOLUTIONS

Economically limited
to some niche & low volumes
asset tracking use cases

WiFi LoRa UWB

Annual volume sold:

only 30 million battery-based UWB, RFID, BLE & WIFI tags

1. Company Introduction

Unique combination of UWB and Battery-less

		Power Source	Location Accuracy	Battery Lifetime	Tag & Maintenance Costs
	UWINLOC UWB	✓ Energy harvesting	30 cm	∞	€
Competing location technologies (*)	UWB Battery-Powered		30 cm		€€€
	BLE		8 m		€€
	LoRa		10 m		€€
	WiFi		15 m		€€€

Note (*): RFID solutions excluded from the competitive landscape – not relevant for asset location use cases

2. Technology overview

UWINLOC's solution

Battery-less tag Up to 30cm accuracy	RF Long Range 30-40m (UWB) & 10-15m (RFPT)	Visualization in 2D & 3D API available
EASY TO PLACE	EASY TO INSTALL	USER FRIENDLY

WPW 2019
WPW SCHOOL
UWINLOC™
INDOOR LOCATION SYSTEM

2. Technology overview

UWINLOC's Reference cell - deployment

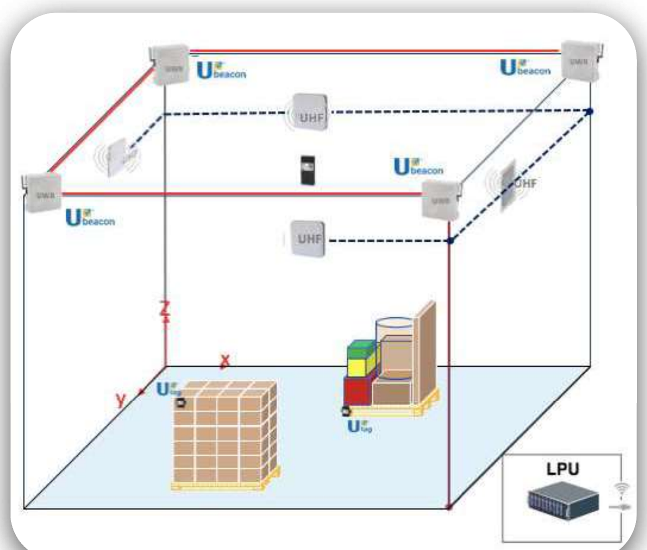

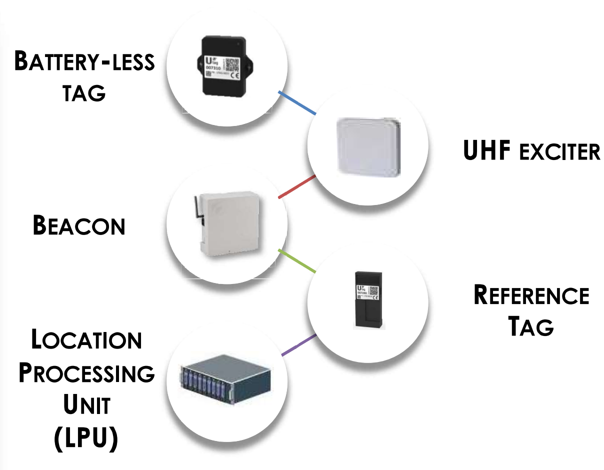

STATE-OF-THE-ART SOLUTION BASED ON RADIO-FREQUENCY ENERGY HARVESTING AND UWB

3. UWINLOC's Technology Breakthroughs

UWINLOC Tag – Power budget analysis

Technology	Active current (mA)	Pulse Duration (ms)	Sleep Current (uA)	Interval (min)	Electric charge Average (uAh)	factor
BLE	8.25	2.7	1	5	3867	1
Current UWL's version	20	1.5	0	5	360	11
Next UWL's version	11	0.3	0	5	39	98

WPW 2019
WPW SCHOOL
UWINLOC
INDOOR LOCATION SYSTEM

3. UWINLOC's Technology Breakthroughs

UWINLOC Tag – RF Link budget

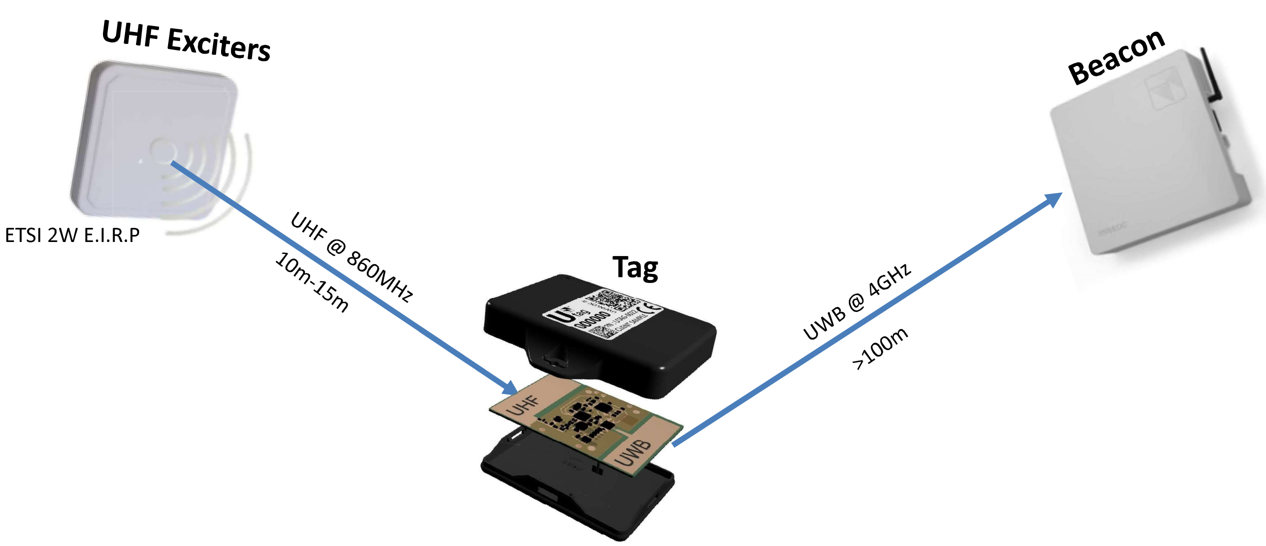

- Completely battery-less Tag
- RF harvester: minimum RF input power -18dBm
- Minimum necessary Energy for UWB signal transmission: 11uJ

This document is confidential. It cannot be communicated, transferred, reproduced, modified, adapted, published, disseminated, translated, either in full or in part, in any form, nor disclosed to any third party without the prior written consent of UWINLOC

3. UWINLOC's Technology Breakthroughs

Still some to come…

- Improvement of the RF harvester sensitivity
- Very-Small, flexible and low-cost antennas
- Ultra-large-band and/or Multiband antennas
- Innovative harvester topology
- Improvement of the RFPT link-budget (e.g. RFPT modulation)

WPW SCHOOL

How to detect position of user to keep high beam efficiency on wireless power transfer via radio waves

Naoki Shinohara
Kyoto University

Radio waves can carry an energy wirelessly to multi users by wide beam like RF-ID and also carry it to single user by narrow beam with high efficiency, which reaches theoretically 100%, instead of a wire. To keep the high beam efficiency for the narrow beam wireless power transfer (WPT) system and also to develop effective WPT system with the wide beam, we must detect the position of the user and must control a beam direction. In this talk, I show some method of a target position detecting via radio wave. A retrodirective target detecting method is often applied for the wireless power transfer system via radio wave. It is based on Van Atta reflector array and is mainly applied for a phased array antenna system. With the retrodirective method, we can not only detect the position of the target but also estimate an transmitting antenna plane. It is originally method for one target, but recently it is applied for multi target WPT system. I'll explain mainly the rectrodirective target detecting method for the WPT system and show the other methods of the target detecting.

WPW 2019

WPW SCHOOL

How to detect position of user to keep high beam efficiency on wireless power transfer via radio waves

Naoki Shinohara

Kyoto University

shino@rish.kyoto-u.ac.jp

WPW 2019

WPW SCHOOL

CONTENTS

1. INTRODUCTION

2. What happen when position is changed in WPT System?

Coupling WPT

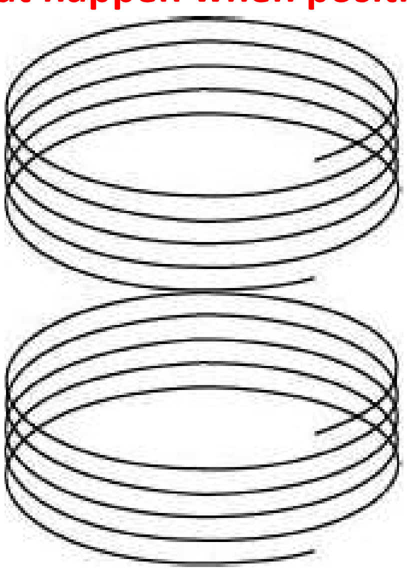

Resonance Frequency : Changed
Circuit Impedances : Un-Matched:
-> Efficiency : Decreased

Resonance Frequency : Matched
Circuit Impedances : Matched:
-> Efficiency : Max

In order to increase efficiency, circuit impedance and resonance frequency must be re-optimized.

2. What happen when position is changed in WPT System?

Uncoupled WPT
(WPT via Radio Waves)

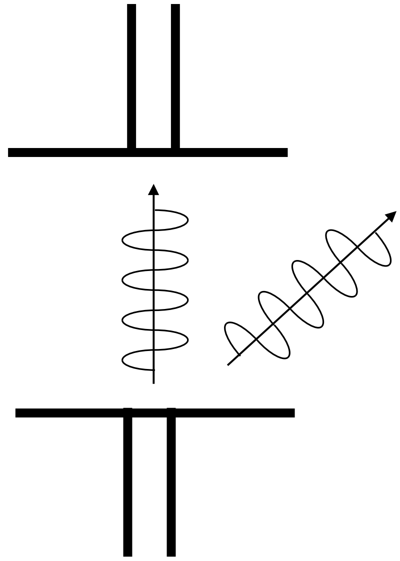

Resonance Frequency : Matched
Circuit Impedances : Matched:
-> Efficiency : Decreased

In order to increase efficiency, beam direction must be controlled and target position must be detected.

Resonance Frequency : Matched
Circuit Impedances : Matched:
-> Efficiency : Max

2. What happen when position is changed in WPT System?

Phased Array
for Beam Forming

(a) Same phases of radio waves from different antennas

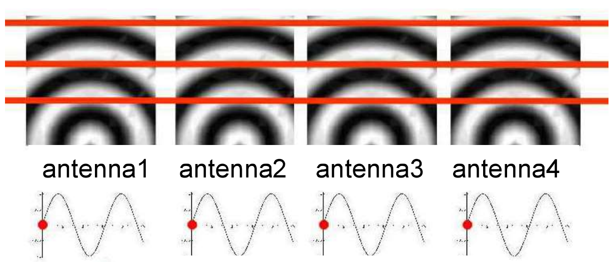

●: antenna, X-axis: distance from antenna

→ Equivalent phase plane is front
=Beam direction is to front

(b) Different phases of radio waves from different antennas

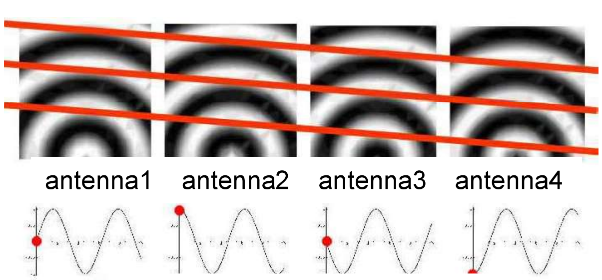

●: antenna, X-axis: distance from antenna

→ Equivalent phase plane is oblique
=Beam direction is to oblique

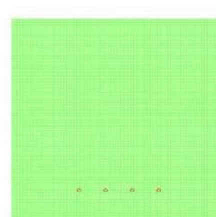

3. How to detect position of user

- Pilot Signal from User
  - Analog Phase Conjugation Circuits = Retrodirective
  - Direction of Arrival (DOA) + Beam Forming
    = Software Retrodirective
- GPS (Global Positioning System)
- Optical Method
- Supersonic Method
- Closed Loop

To keep high beam efficiency on WPT, accurate target detecting is not only required, but also is required recognize position of each antenna on phased array.

Retrodirective is recommended.

3.1 Retrodirective target detecting method

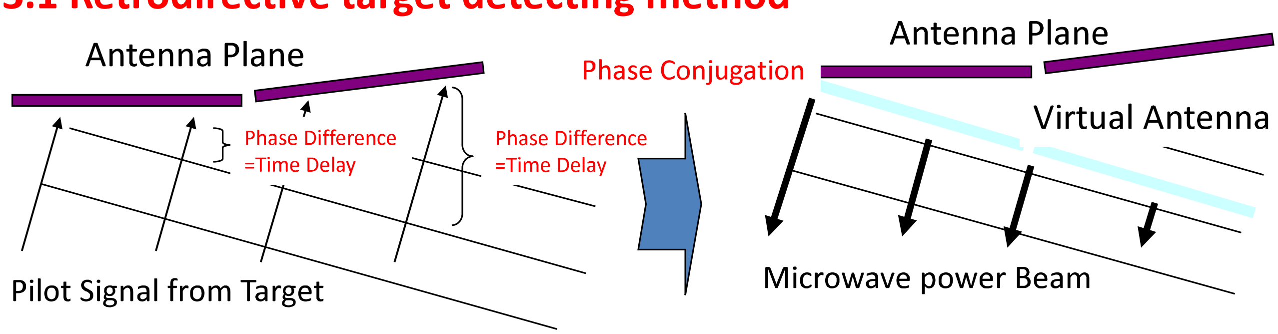

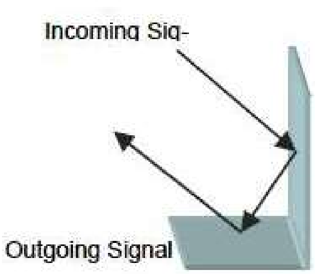

Corner Reflector
(Theoretical Retrodirective)

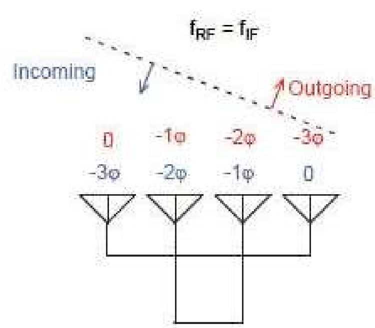

Van Atta Array
(Original Retrodirective)

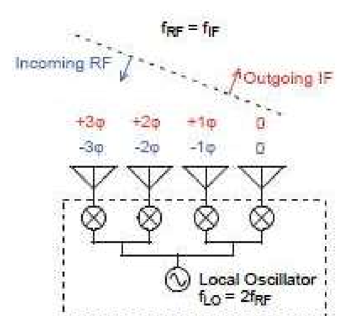

Retrodirective

3.1 Retrodirective target detecting method

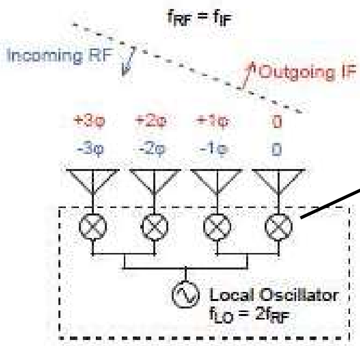

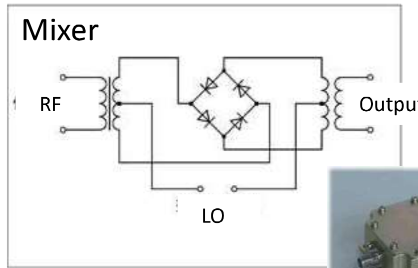

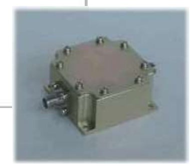

Phase conjugating circuit consists of only a mixer and a local oscillator.

$$(\varpi_{LO} = 2\varpi_{RF})$$

$$V_{IF} = V_{RF}\cos(\varpi_{RF}t + \theta_n)\cdot V_{LO}\cos(\varpi_{LO}t)$$

$$= \frac{1}{2}V_{RF}V_{LO}\begin{bmatrix}\cos((\varpi_{LO} - \varpi_{RF})t - \theta_n) + \\ \cancel{\cos((\varpi_{LO} + \varpi_{RF})t + \theta_n)}\end{bmatrix}$$

Elimination by LPF

$$= \frac{1}{2}V_{RF}V_{LO}\cos(\varpi_{RF}t - \theta_n) \qquad \because \varpi_{LO} = 2\varpi_{RF}$$

3.1 Retrodirective target detecting method

Queen's University (62-66GHz)

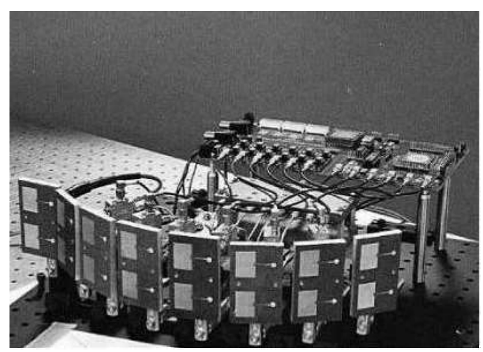

Jet Propulsion Laboratory and University of Michigan (2001) (5.9GHz)

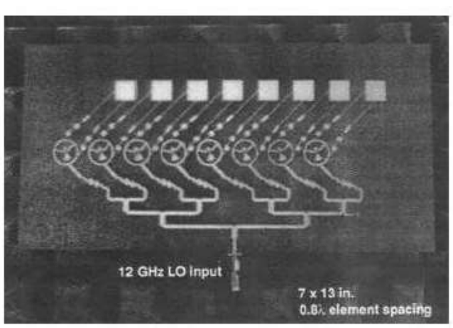

UCLA (1995) (6GHz)

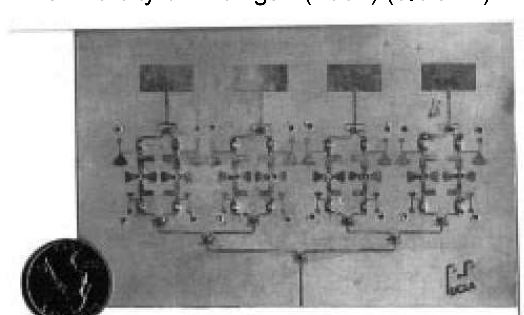

UCLA (2000) (6GHz)

3.1 Retrodirective target detecting method

Typical Beam Pattern of Retrodirective System

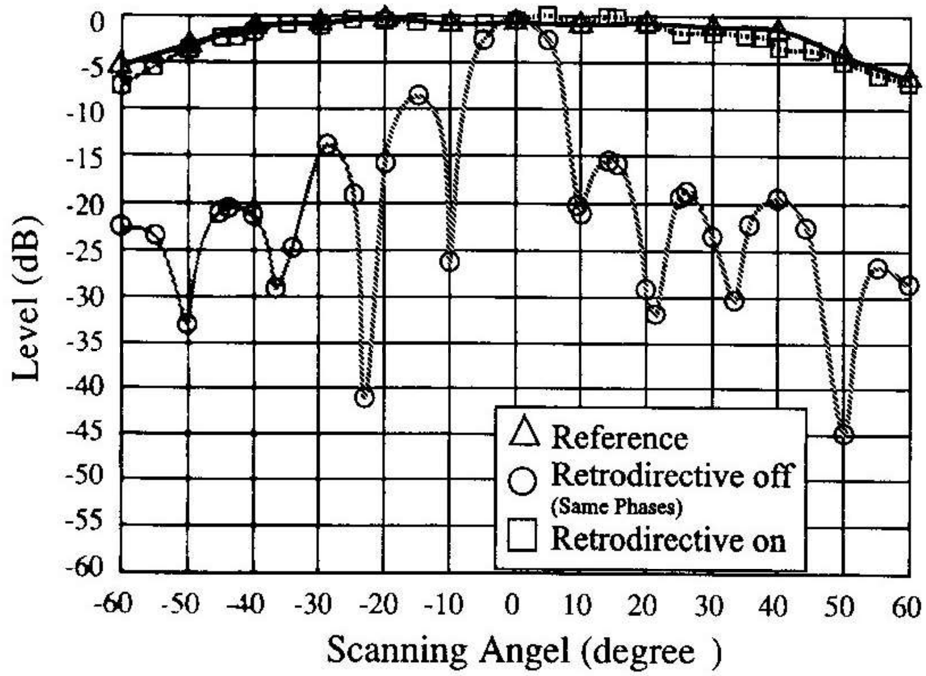

Element Pattern Only

Element Pattern x Array Factor

3.1 Retrodirective target detecting method

- Merits of Retrodirective System
  - Both target detecting and recognition of antenna position
  - Very high speed beam control
    <- Analog phase conjugation circuits only
  - Low Cost <- Without expensive phase shifters
- Demerits of Retrodirective System
  - Beam forming to user only
    <- Without phase shifters
  - Interference between pilot signal and WPT beam
    <- Theoretical requirement of the same frequency
  - Fluctuation of pilot signal source and WPT source
    <- Two indipendent sources

3.1 Retrodirective target detecting method

Avoidance of interference between pilot signal and WPT beam

- +Δω, +2Δω asymmetric 2 pilot signals

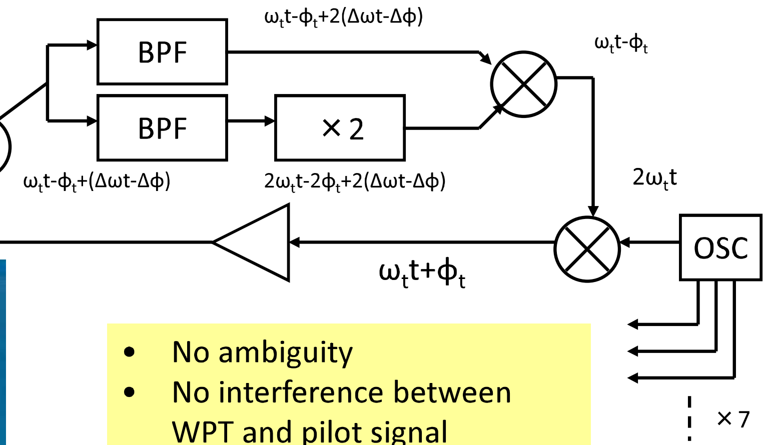

- No ambiguity
- No interference between WPT and pilot signal
- Tx and Rx shared antennas

H. Matsumoto, et al., "Activities of Study of Solar Power Satellite/Station in RASC of Kyoto University (in Japanese)", Technical Report of IEICE, SPS2002-07 (2002-11) pp.9-14, 2002

WPW 2019
WPW SCHOOL

3.1 Retrodirective target detecting method

Avoidance of fluctuation of pilot signal source and WPT source

- without local oscillator

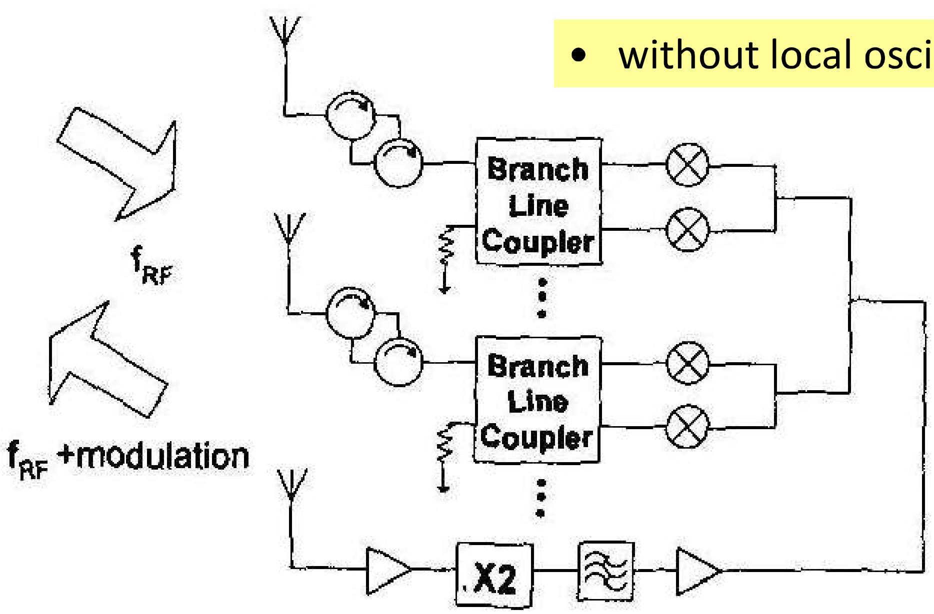

Leong, K. M. et al., "A Frequency Autonomous Retrodirective Array Transponder", 2002 IEEE MTT-S Digest, 2002, pp.1349-1352

3.1 Retrodirective target detecting method

- 1/3frequency pilot signal + reuse of pilot signal as source of WPT

Both Avoidances

- without local oscillator

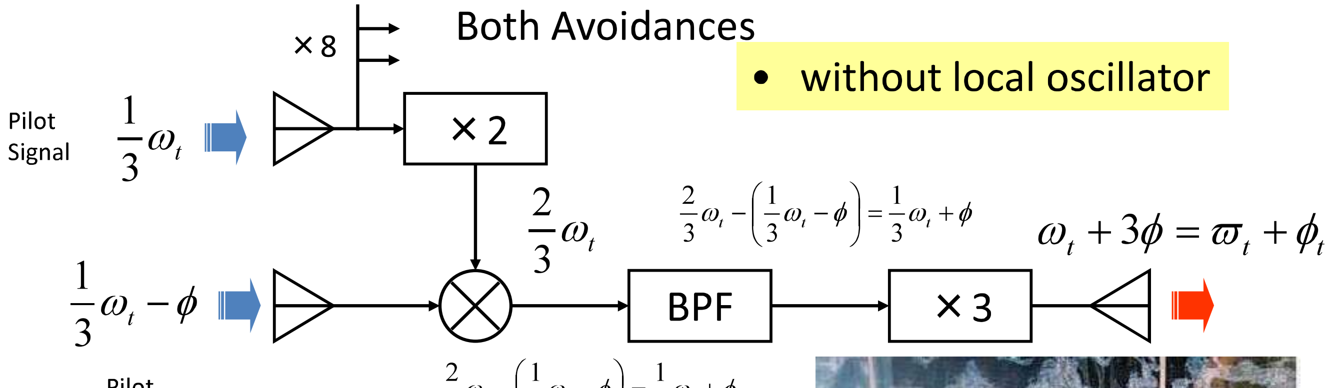

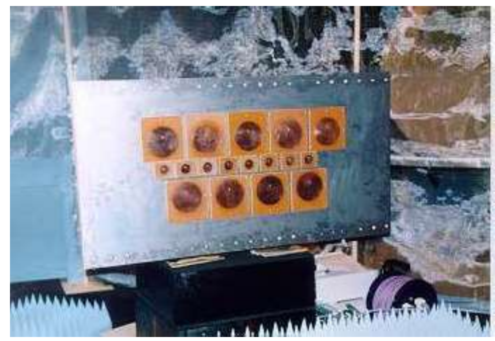

H. Matsumoto, et al., "Activities of Study of Solar Power Satellite/Station in RASC of Kyoto University (in Japanese)", Technical Report of IEICE, SPS2002-07 (2002-11) pp.9-14, 2002

3.2 Multi-pass retrodirective target detecting method

- Seamless delivery to simultaneous multiple devices in Cota (Ossia Corp.)

Retrodirective with Pulse in Multi-pass

Signal Replay

The transmitter establishes the signal shape from each device, and replays the signal to power the devices from memory.

Moving Devices

The transmitter would also refresh the signal shape for each device multiple times a second to be able to follow moving devices.

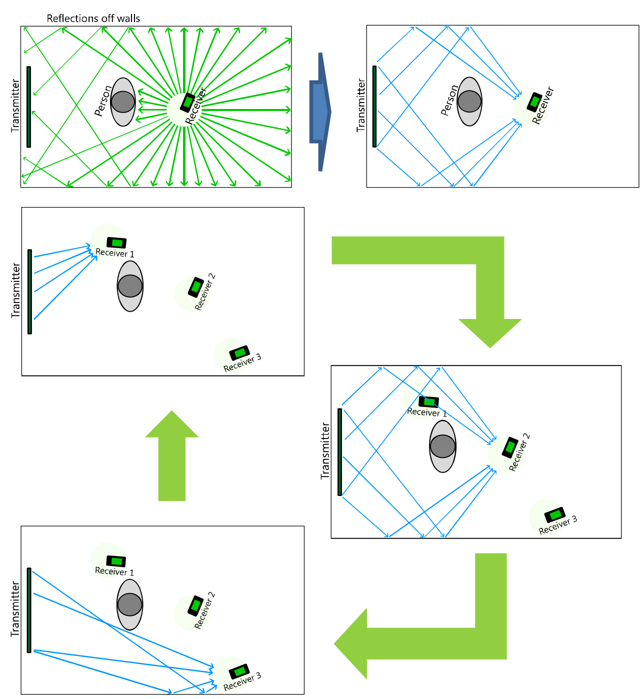

3.2 Multi-pass retrodirective target detecting method

1 Wall

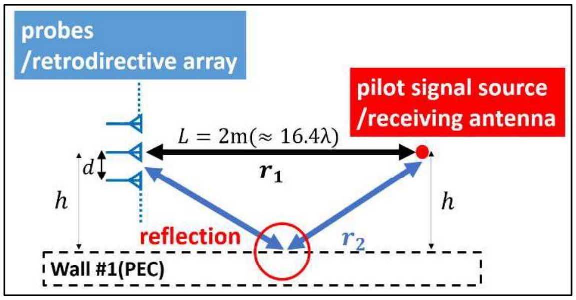

2 Walls

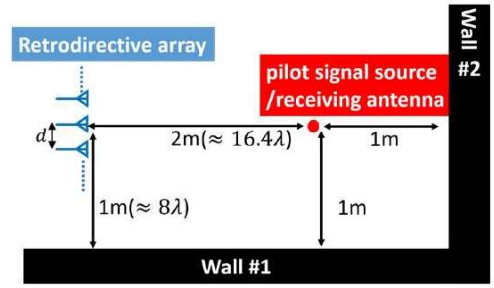

Frequency	2.45 GHz
Element	Half-wave dipole
Input power per port	0.5 W
L (line of sight distance)	2m
h (height from the wall)	1m or 2m
d (element interval)	$\lambda/4$ or $\lambda/2$
Definition of efficiency	$\frac{\text{received power}}{\text{input power}} \times 100$

T. Sasaki, et al., "Study on Multipath Retrodirective for Microwave Power Transmission", Proc. of IEEE WPTc2018

WPW 2019
WPW SCHOOL

3.2 Multi-pass retrodirective target detecting method

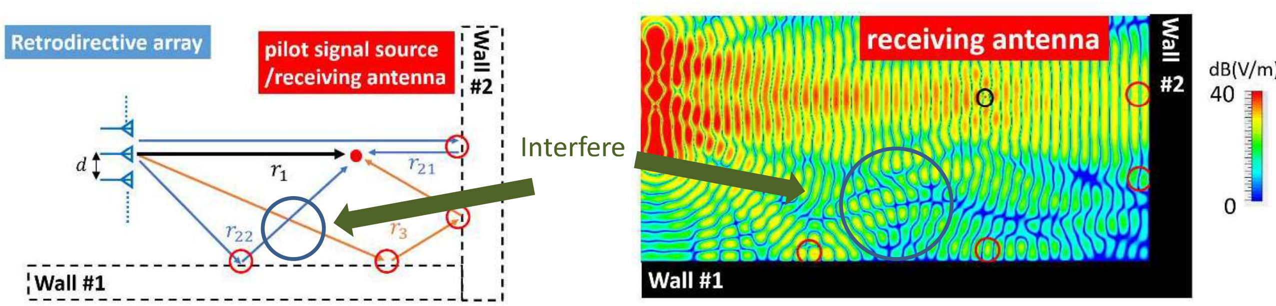

Theoretical Multipath

Simulated Power Signal
(13elements, $d = \lambda/2$)

- r_1 and r_{21} were mainly formed, and r_3 were weakly formed
- r_{22} and r_3 interfered and weakened each other

T. Sasaki, et al., "Study on Multipath Retrodirective for Microwave Power Transmission", Proc. of IEEE WPTc2018

3.2 Multi-pass retrodirective target detecting method

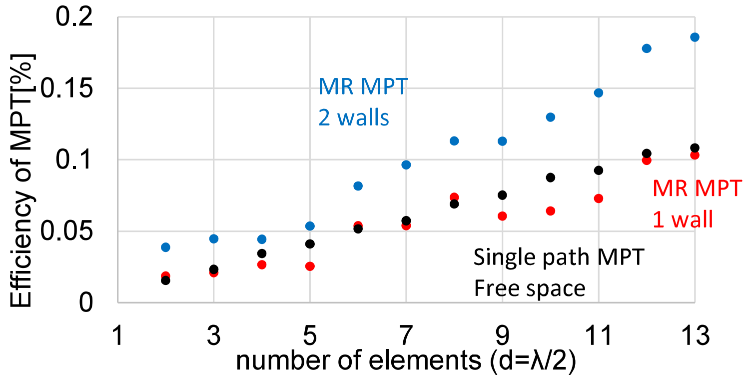

The case of 2 walls was better than other cases

With a number of multipath, higher power concentrated

Multipath Retrodirective possibly achieve higher efficiency than single path MPT

T. Sasaki, et al., "Study on Multipath Retrodirective for Microwave Power Transmission", Proc. of IEEE WPTc2018

4. Other Methods

Software Retrodirective

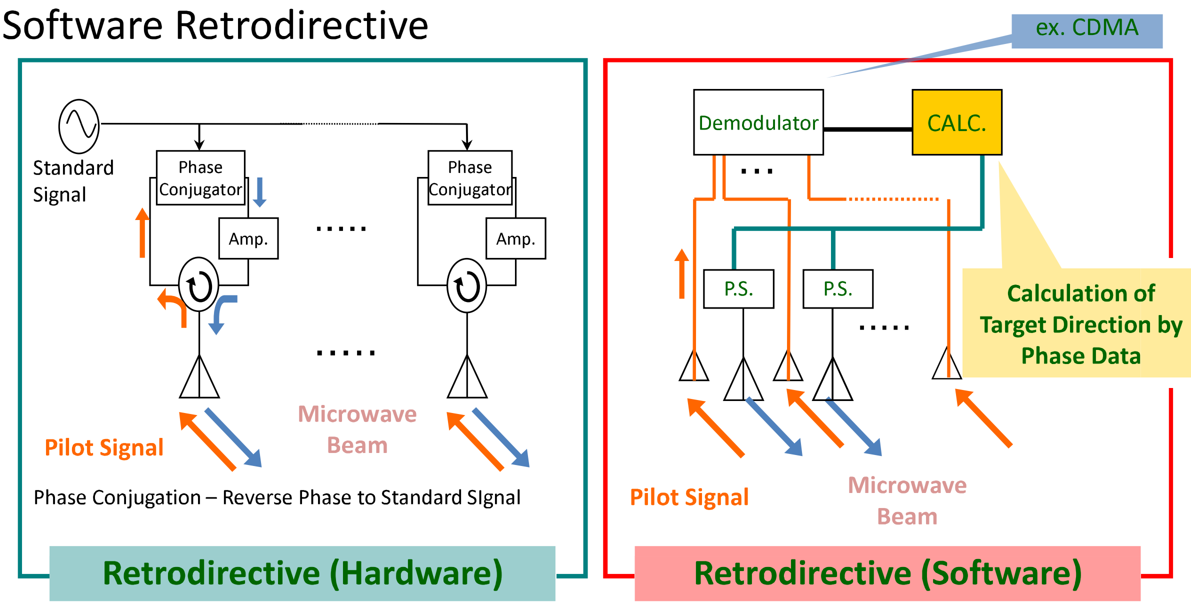

Retrodirective (Hardware) : with Phase Conjugators
Retrodirective (Software) : with Computer and Phase Shifters

4. Other Methods

DOA Algorisms

- Basic
  - Beamformer (by Beam Scanning)
  - Capon (by Beam Scanning)
  - Linear Prediction ; LP (by Null Scanning)

Basic DOA estimating error

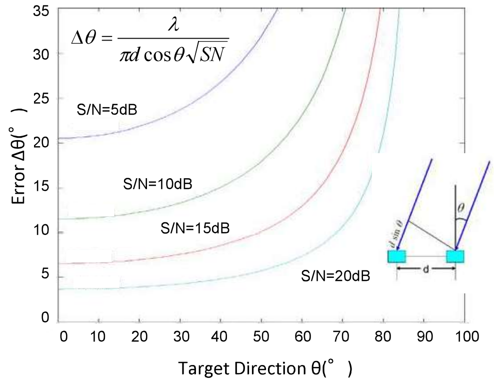

- High Resolution
  - Min-Norm
  - MUSIC(MUltiple SIgnal Classification) (for multi beam scanning)
  - ESPRIT(Estimation of Signal Parameters via Rotational Invariance Technique) (for multi beam scanning with more two sub array)
- etc
  - RBF(Radial Basis Function) by Neural Network

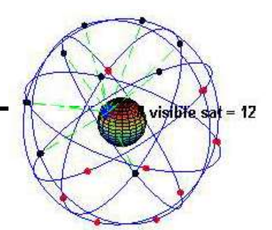

4. Other Methods

GPS

Measurement of Phase of GPS Signals

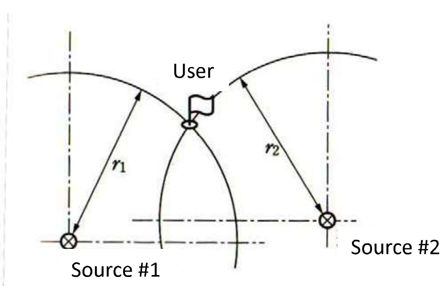

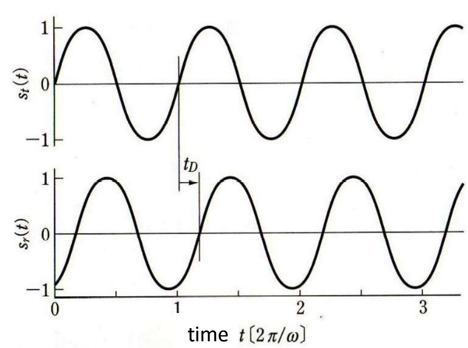

$$s_t(t) = \sin(\omega t + \phi_t)$$
$$s_r(t) = \sin(\omega(t - t_D) + \phi_t) = \sin(\omega t + \phi_r)$$
$$\phi_r = \phi_t - \omega t_D$$
$$t_D = \frac{\phi_t - \phi_r}{\omega}$$
$$d = c t_D$$

$$\begin{cases} r_1 = \sqrt{(x_1 - x)^2 + (y_1 - y)^2 + (z_1 - z)^2} + s \\ r_2 = \sqrt{(x_2 - x)^2 + (y_2 - y)^2 + (z_2 - z)^2} + s \\ \vdots \\ r_N = \sqrt{(x_N - x)^2 + (y_N - y)^2 + (z_N - z)^2} + s \end{cases}$$

From 4 signals (minimum),
we estimate x,y,z,s (error factor)

4. Other Methods

Optical Method

Experimental System in MILAX in Japan in 1992

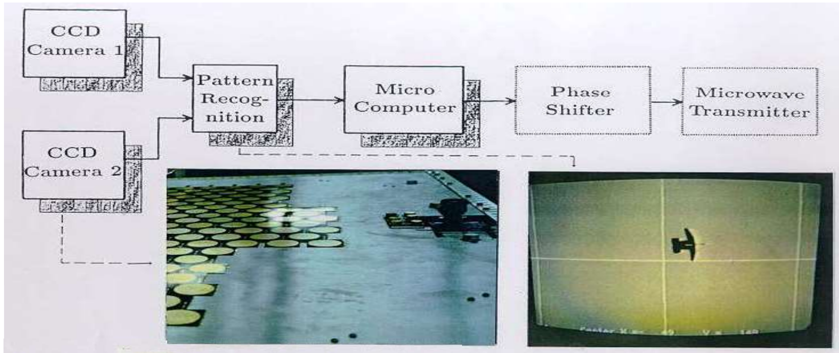

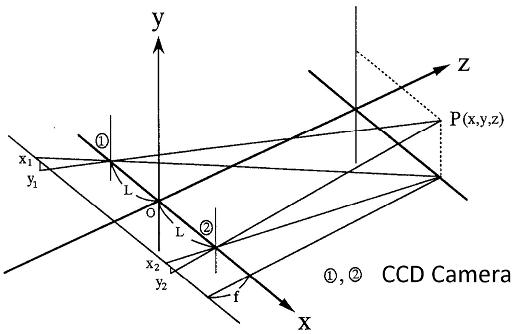

①, ② CCD Camera Position

Target Position (X,Y,Z)

$$X = Z\frac{x_1 + x_2}{2f}$$

$$Y = |y_1|\frac{Z}{f}$$

$$Z = \frac{2Lf}{|x_2 - x_1|}$$

4. Other Methods

REV : Rotating Electromagnetic Vector

Closed Loop (REV Method)

Rotation of Phase of One Element

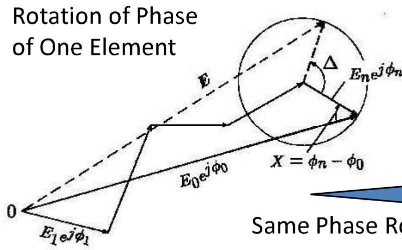

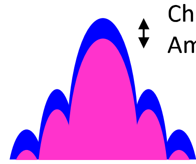

Change of Amplitude

Optimization of Vector to Get Maximum Amplitude

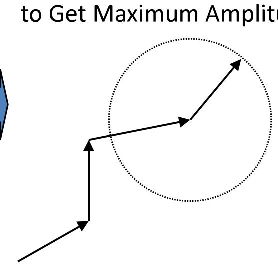

Same Phase Rotation at Each Antenna Element

Maximization

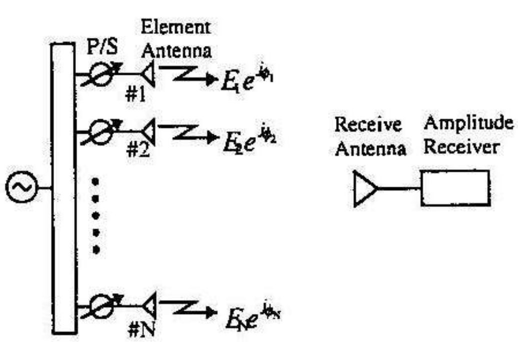

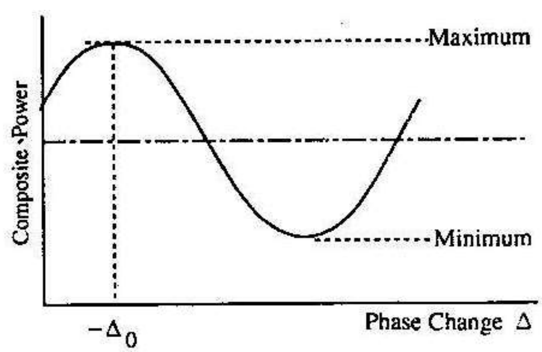

4. Other Methods

Experimental System in SHARP in Canada in 1987

Closed Loop (SHARP Method)

'Closed Loop' Method to estimate phase difference *p* from *sin p*
with correction of decrease of power with help of altimeter

$$A = Rke^{-jp}$$

$$A' = Rke^{-j(p-\frac{\pi}{2})}$$

$$A'' = Rke^{-j(p+\frac{\pi}{2})}$$

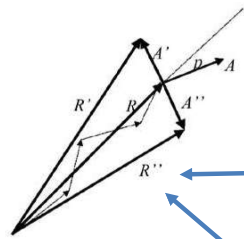

(2) Measure Change of Amplitude and Phase at Receiving Antenna

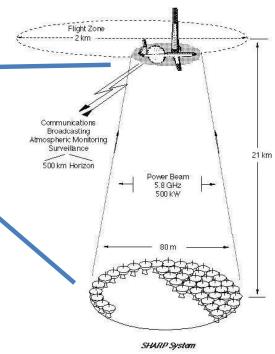

from ***R'=R+A'***、***R''=R+A''***

$$|R'| = |R|\sqrt{(1+2k\sin p)^2 + k^2\cos^2 p}$$

$$\approx |R|(1+k\sin p)$$

$$|R''| \approx |R|(1-k\sin p)$$

However k<<1
(when number of antennas is a lot)

$$|R'| - |R''| = 2|R|k\sin p = 2|A|\sin p$$

(1) Change of Phase at Transmitting Antenna Array by only 90° and -90°

East, T. W. R., "A Self-Steering Array for the SHARP Microwave-Powered Aircraft", IEEE-Trans. AP 40, No.12, 1992

5. CONCLUSIONS

- To keep high beam efficiency in WPT system, we must know a position of user and positions of each antenna on phased array
- There are various target detecting method, e.g. GPS, optical method, closed loop method, DOA (Direction of Arrival) Algorism, etc.
- Retrodirective target detecting method is one of best method to detect a user and to recognize positions of each antenna
- Retrodirective method can be applied in multi-pass circumstance.

WPW SCHOOL

Optimize, Learn and Prototype Wireless Communications and Power Transfer

Bruno Clerckx
Imperial College London

Wireless communication has shaped our society. Wireless is however not limited to communication. Far-field wireless power has recently become recognised as feasible for energising low-power devices due to reductions in power requirements of electronics. As wireless has disrupted communication, wireless will also disrupt the delivery of energy. Interestingly, radio waves carry both energy and information. Nevertheless, energy and information have traditionally been treated separately. Imagine instead a wireless network where information and energy flow together through the wireless medium. Wireless communication, or Wireless Information Transfer (WIT), and Wireless Power Transfer (WPT) would then refer to two extreme strategies respectively targeting communication-only and power-only. A unified Wireless Information and Power Transfer design would on the other hand have the ability to softly evolve in between those two extremes to make the best use of the RF spectrum and radiations and the network infrastructure to communicate and energize. In this talk, I will discuss recent progress on laying the foundations of the envisioned network by establishing a novel and unified signal theory for transmission and identifying the fundamental tradeoff between conveying information and power wirelessly. Recent results on the prototyping and experimentation of those new signals will also be discussed.

Optimize, Learn and Prototype Wireless Communications and Power Transfer

Bruno Clerckx

Department of Electrical and Electronic Engineering
Imperial College London

WPW 2019, London, UK

Wireless is More than just Communications

Radio waves carry both energy and information

Wireless Power Transmission (WPT)

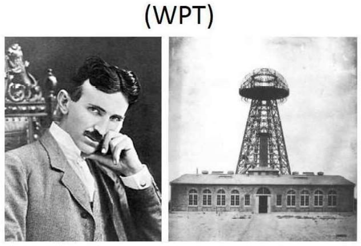

Tesla 1901

0G

Wireless Information Transmission (WIT)

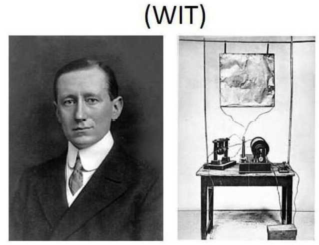

Marconi 1896

5G

Unified Wireless Information and Power Transmission (WIPT)

In 20 Years from Now ... **Trillions** of **Low-Power** Devices

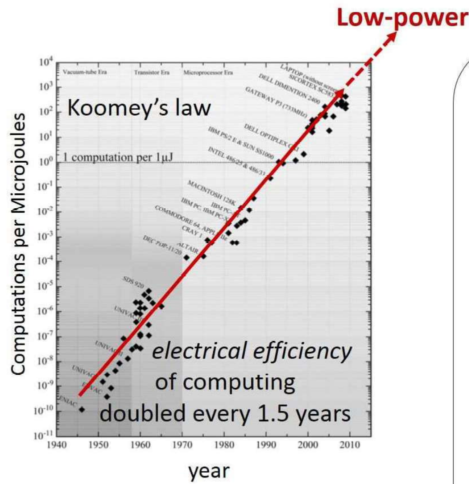

2017: 5 Billions phones

2035: **Trillions** IoT devices

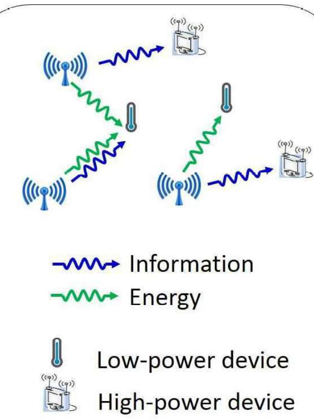

Future of Wireless:
Communicate and Energize

A **Missing** Signal Theory of Wireless Transmission

Wireless Power Transmission
- RF Theory ✓
- Signal Theory ✗

Wireless Information Transmission
- RF Theory ✓
- Signal Theory (Shannon, ...) ✓

Wireless Information and Power Transmission
- Unified Signal Theory ✗

WPT Architecture

A generic architecture

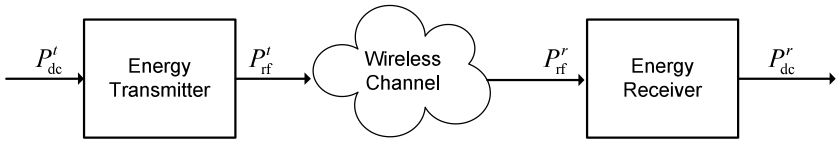

End-to-End Power Transfer Efficiency

$$e = \frac{P^r_{\text{dc}}}{P^t_{\text{dc}}} = \underbrace{\frac{P^t_{\text{rf}}}{P^t_{\text{dc}}}}_{e_1} \underbrace{\frac{P^r_{\text{rf}}}{P^t_{\text{rf}}}}_{e_2} \underbrace{\frac{P^r_{\text{dc}}}{P^r_{\text{rf}}}}_{e_3}$$

Careful! Maximizing e not achieved by maximizing e_1, e_2, e_3 independently from each other

- e_1, e_2, e_3 coupled due to **nonlinearity**, especially at $1\mu W$-$1mW$
- e_2, e_3 are both functions of the Tx signal and wireless channel state

Nonlinear Energy Harvester Model

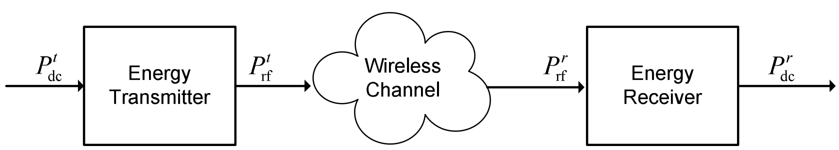

Nonlinear Model: P^r_{dc} proportional to

$$\underbrace{k_2 R_{ant} \underbrace{\mathcal{E}\left\{y(t)^2\right\}}_{P^r_{\text{rf}}}}_{\text{Linear term/model}} + \underbrace{k_4 R_{ant}^2 \mathcal{E}\left\{y(t)^4\right\} + \ldots}_{\text{Nonlinear term}}$$

- $\max e_2 e_3 \neq \max e_2$
- Maximizing P^r_{rf} is **not** the same as maximizing P^r_{dc}
- Typical values given by $k_2 = 0.0034$, $k_4 = 0.3829$, $R_{ant} = 50$

Waveform Design for WPT

Multi-sine multi-antenna transmit signal (antenna $m = 1, ..., M$ and sinewave $n = 0, ..., N-1$)

$$x_m(t) = \sum_{n=0}^{N-1} s_{n,m} \cos(2\pi f_n t + \phi_{n,m})$$

Received signal after multipath

$$y(t) = \sum_{m=1}^{M} \sum_{n=0}^{N-1} s_{n,m} A_{n,m} \cos(2\pi f_n t + \underbrace{\phi_{n,m} + \bar{\psi}_{n,m}}_{\psi_{n,m}})$$

Frequency response of the channel of antenna m at w_n

$$h_{n,m} = A_{n,m} e^{j\bar{\psi}_{n,m}}$$

Goal: Design amplitudes and phases $\{s_{n,m}, \phi_{n,m}\}_{\forall n,m}$ to maximize the DC output power subject to average transmit power constraint

Systematic Waveform Design

Assume an **adaptive closed-loop WPT** system with **channel known to the Tx**

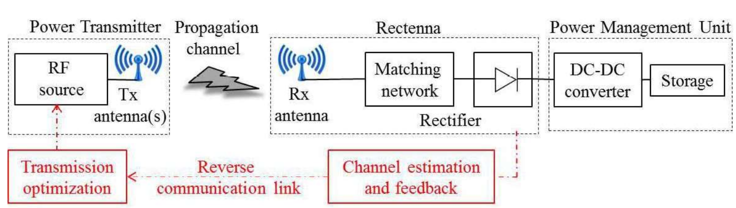

Problem: Maximize the quantity z_{DC}

$$\max_{\mathbf{S},\mathbf{\Phi}} \quad z_{DC}(\mathbf{S},\mathbf{\Phi}) = \underbrace{k_2 R_{ant} \mathcal{E}\{y(t)^2\}}_{\text{Linear term}} + \underbrace{k_4 R_{ant}^2 \mathcal{E}\{y(t)^4\} + ...}_{\text{Nonlinear terms}}$$

$$\text{subject to} \quad \frac{1}{2}\|\mathbf{S}\|_F^2 \leq P$$

Systematic design? Yes, for any M, N, n_o.

Waveform Illustration

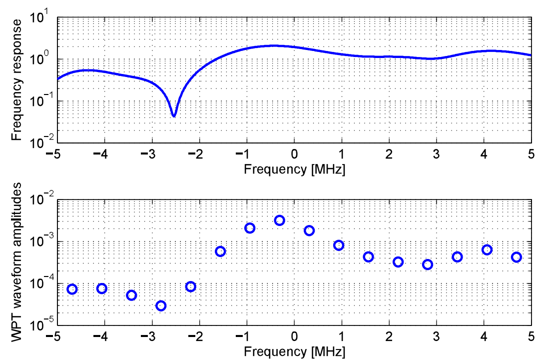

Observation

1. *Allocate power over multiple sinewaves with more power to frequencies exhibiting larger channel gains*
2. *Optimally exploits **frequency-diversity gain**, spatial **beamforming gain** and **rectifier nonlinearity***

Circuit Evaluations

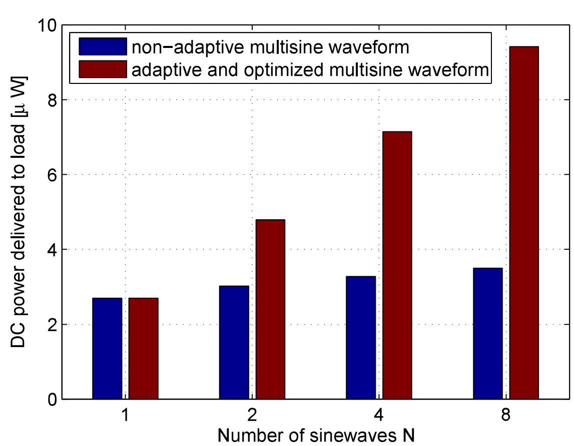

Observation

1. *Significant performance gains with systematic and optimized waveforms.*

Low-Complexity Waveform Design

So far, not implementation friendly.

Low-Complexity Adaptive Multisine Waveform

- Idea: allocate more power to frequencies exhibiting larger channel gains
- Scaled Matched Filter (SMF): $s_n = cA_n^{\beta}$ with c a constant
- A_n^{β}: amplify strong frequency components and attenuate weak ones

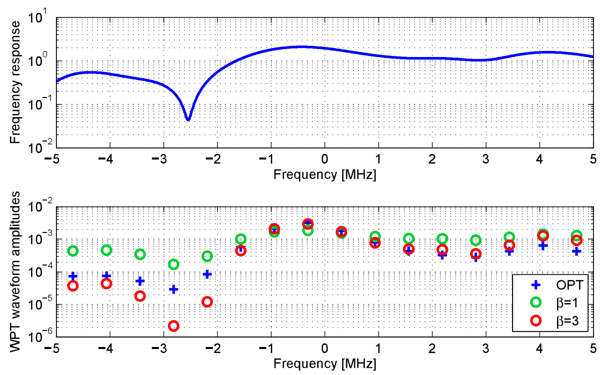

Circuit Evaluations

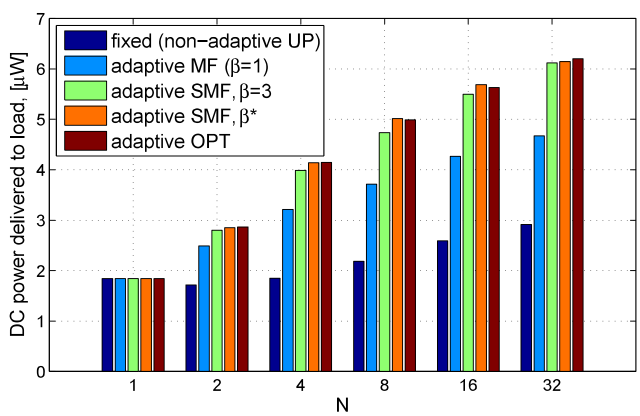

Observation

1. *SMF very close to OPT despite much lower design complexity*
2. *Waveform design holds for single and multiple-diode rectennas*

Large-Scale WPT Architecture

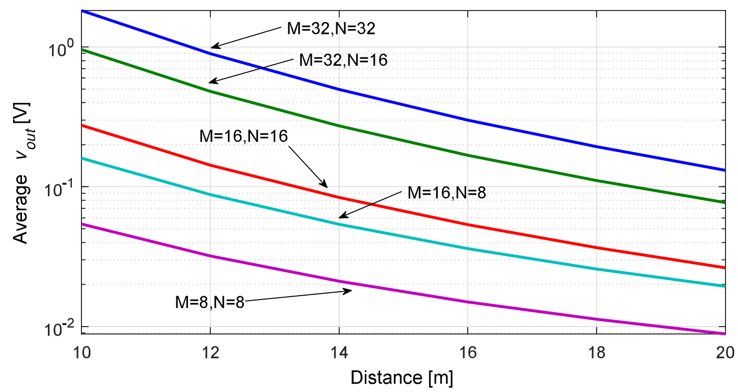

Observation

1. *Significant benefits of the architecture to* ***boost the end to end power transfer efficiency*** *and the* ***transmission range***

Modulation Design for WPT

Energy modulation in single-carrier/sinewave transmission to **boost** e_3?

Induce random fluctuations of the transmit signal

Recall $z_{DC} = k_2 R_{ant} \mathcal{E}\left\{y(t)^2\right\} + k_4 R_{ant}^2 \mathcal{E}\left\{y(t)^4\right\}$

Design modulation/**input distribution** with **large fourth order moment**!

Flash signaling distribution with following probability mass function (with $l \geq 1$)

$$p_r(r) = \begin{cases} 1 - \frac{1}{l^2}, & r = 0, \\ \frac{1}{l^2}, & r = l\sqrt{P}. \end{cases}$$

Low probability of high amplitude signals

- Average power constant $\mathcal{E}\left\{r^2\right\} = P$
- ... but $\mathbb{E}\left[r^4\right] = l^2 P^2$, i.e. the larger l, the larger the fourth order moment.

Circuit Evaluations

Received DC power as a function of modulation (CW continuous wave, CN CSCG input, N real Gaussian input, l for flash signaling)

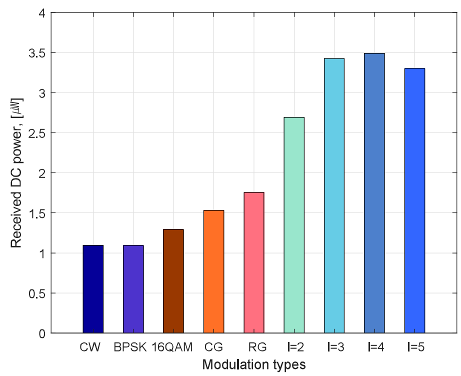

Observation

1. *Energy modulation gives a 250% gain over CW*
2. *Rectenna **nonlinearity favors distributions with a large fourth moment**!*

Transmit Diversity for WPT

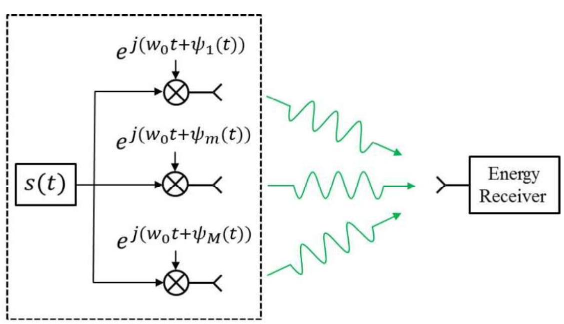

Energy transmitter with transmit diversity

Multiple **dumb antennas** to **induce fast fluctuations of the wireless channel**

Fluctuations **boost** e_3 thanks to EH nonlinearity

Multiple antenna but **no CSIT** (in contrast to beamforming)

Multiple transmit antennas be useful to WPT in the absence of CSIT!

Circuit Evaluations

Increase in RF-to-DC conversion efficiency

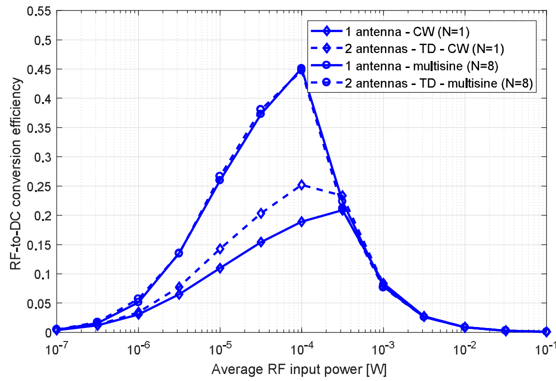

35% **gain with two antennas over one antenna**

Very **low** implementation **complexity**

Well suited for **massive IoT** for which CSIT acquisition is unpractical

Multi-User WPT Signal Design

Multi-User WPT: WPT to K single-antenna users/rectennas

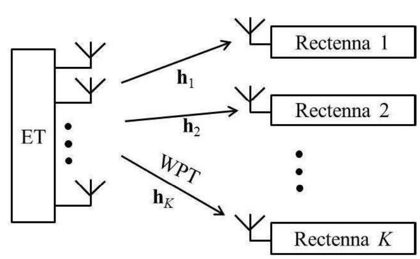

Trade-off: $z_{DC,q}$ in general depends on $z_{DC,p}$, $p \neq q$

Energy Region $\mathcal{Z}_{DC}$: set of all rectenna harvested energy $(z_{DC,1}, \ldots, z_{DC,K})$ that are simultaneously achievable

Boundary of $\mathcal{Z}_{DC}$: **weighted sum** of $z_{DC,k}$ with weights v_k, $k = 1, \ldots, K$

$$\max_{\mathbf{S},\mathbf{\Phi}} Z_{DC}(\mathbf{S}, \mathbf{\Phi}) = \sum_{k=1}^{K} v_k z_{DC,k}(\mathbf{S}, \mathbf{\Phi}) \text{ s.t. } \frac{1}{2} \|\mathbf{S}\|_F^2 \leq P$$

Energy region

Energy region: Achievable v_{out} region, with $M = 20$ and $N = 10$

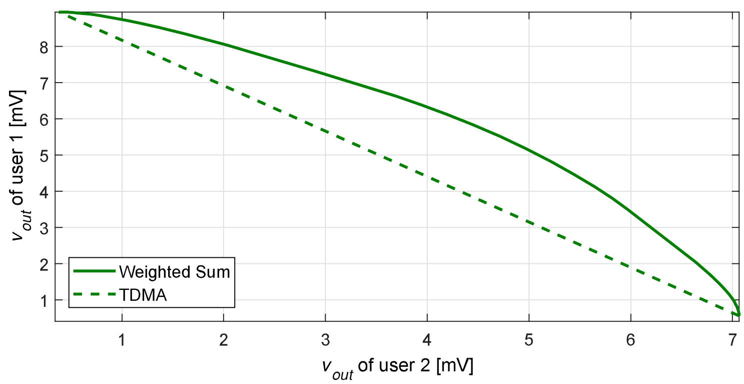

Observation

1. *Multi-user waveform design outperforms TDMA*

Channel Acquisition for WPT

Waveform/beamforming requires **Channel State Information** (CSI) at Tx

Unique considerations

- **CSI at (energy) receiver**: not required for WPT
- **Net energy maximization**: to balance the energy overhead for CSI acquisition and the energy harvested with CSI-based signal design
- **Hardware constraint**: no/low signal processing capability for low-cost ERs

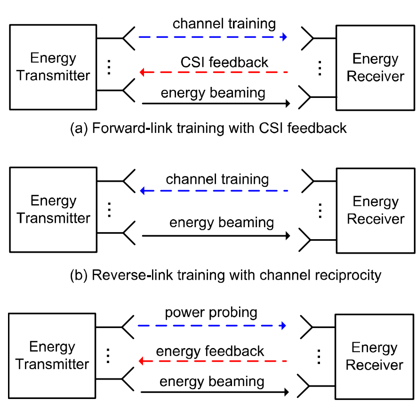

(a) Forward-link training with CSI feedback

(b) Reverse-link training with channel reciprocity

(c) Power probing with energy feedback

Wireless Information and Power Transmission

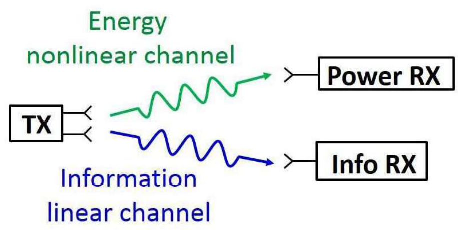

Fundamental tradeoff between rate and harvested DC power?

Unified signal theory and design for WIPT?

Rate-Energy Tradeoff

Average Rx power of -20dBm. 20dB SNR. $B = 1$MHz. $N = 16$, $M = 1$.

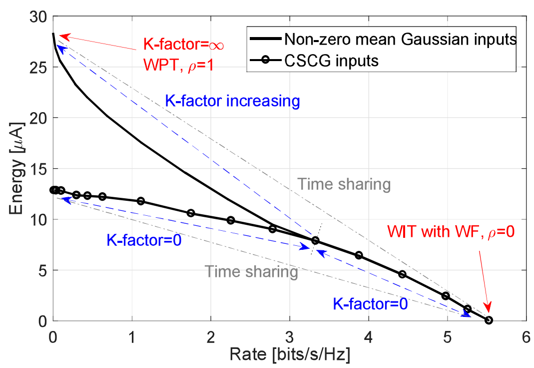

Observation

1. ***Non-trivial tradeoff*** *between rate and energy*
2. *Superposition of power and communication waveforms beneficial*
3. ***Need for new WIPT signals****: conventional communication signals/modulation/waveform suboptimal for WIPT*

Machine Learning to design WIPT modulation

Representation of 16-symbols modulation for different values of energy

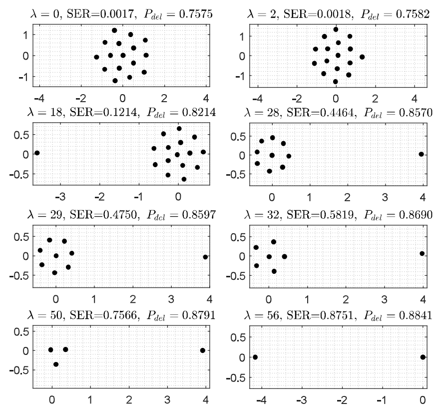

Observation

1. *Reminiscent of QAM for low power delivery and flash signaling for high power delivery*

Prototyping and Experimentation of Closed-Loop WPT

Establish an **experimental environment for closed-loop and open-loop WPT**

- Design optimized WPT signals
- Implement CSI acquisition/channel estimator
- Design efficient rectenna

Verify advantages of systematic signal designs for WPT

- waveform, beamforming, modulation, transmit diversity

Measurements confirm theory: gains very promising

Prototype Architecture

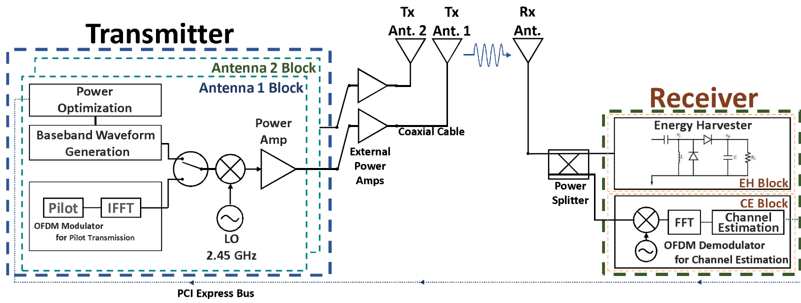

- The system operates in 2.4 GHz ISM band
- Software Defined Radio (SDR) used for transmitter and channel estimator. NI FlexRIO (PXI-7966R) and transceiver module (NI 5791R)
- Channel estimation and waveform design implemented in LabVIEW

Actual Prototype

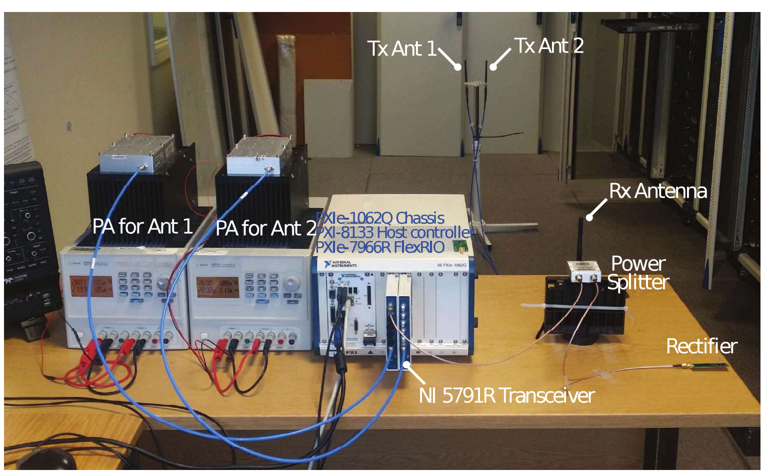

Measurement Results: Waveform

Received DC power as a function of N with 10 MHz bandwidth in NLoS

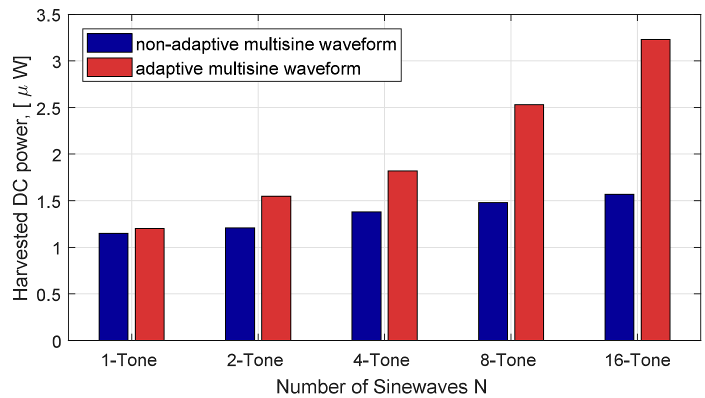

Measurement Results: Joint Beamforming and Waveform

Received DC power as a function of N with 10 MHz bandwidth in NLoS

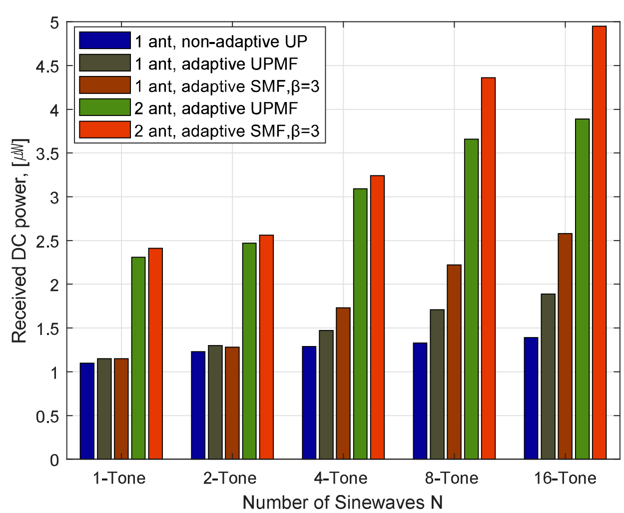

Measurement Results: Modulation

Received DC power as a function of modulation (CW continuous wave, CN CSCG input, N real Gaussian input, l for flash signaling)

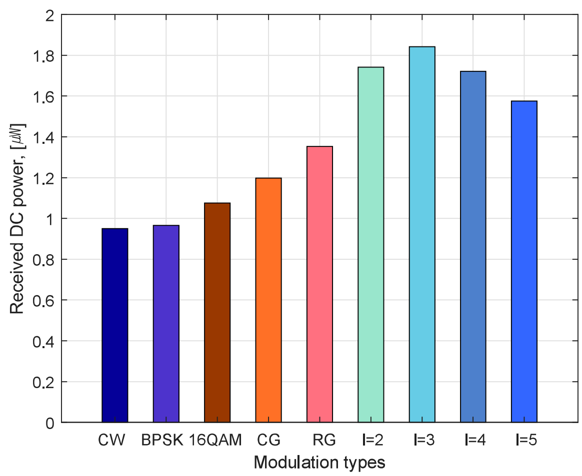

Measurement Results: Transmit Diversity

Received DC power with a continuous wave (CW), transmit diversity ($M = 2$) with continuous wave, multisine ($N = 8$) and transmit diversity with multisine ($N = 8$)

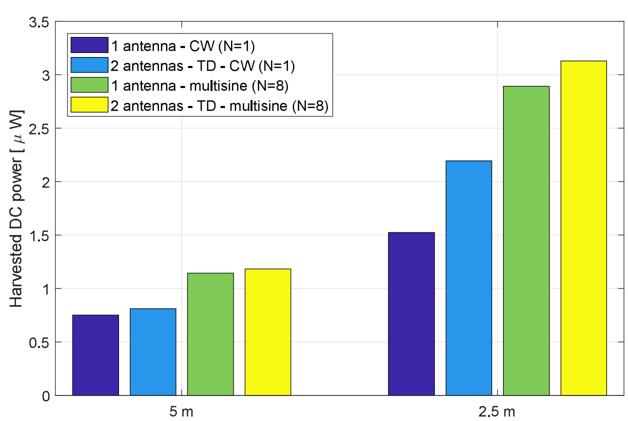

WIPT Prototype Architecture

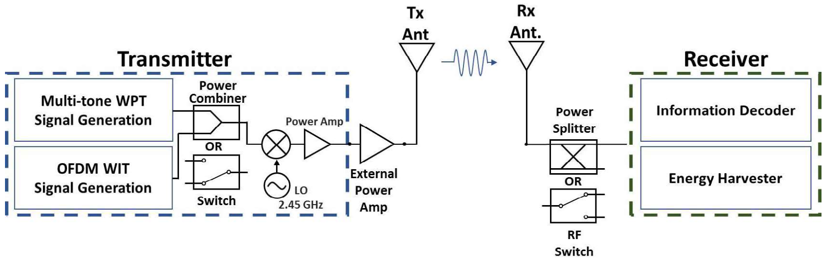

- Evaluate **harvested energy-throughput** (E-T) performance with different transmission signal designs, modulation schemes, and receiver architectures
- Validate theory and signal designs

WPTC 2019 - Session 1 - Tuesday 09:45-11:15

Conclusions

Communications and signals for WPT/WIPT systems

- Lay the foundations and tackle the challenges of the envisioned network
- Develop a signal theory for transmission over the nonlinear wireless power channel and the linear wireless communication channel
- Two complementary approaches: Optimize and Learn
- Identify the fundamental tradeoff between conveying information and power wirelessly
- Validated by circuit simulations, prototyping and experiments

Nonlinearity is a fundamental property of the rectifier and is beneficial

- The wireless power channel is nonlinear
- Do not compensate the nonlinearity but exploit it
- Importance of accounting for the nonlinearity in any design involving wireless power
- Leads to fundamental changes to WIPT design (PHY and MAC layers)

Need for **bridging RF and comms/signal processing**

References

Communications and Signals Design for WPT
Y. Zeng, B. Clerckx and R. Zhang, "Communications and Signals Design for Wireless Power Transmission," IEEE Trans. on Comm, invited paper, Vol 65, No 5, pp 2264 - 2290, May 2017.

Systematic waveform designs for WPT
B. Clerckx and E. Bayguzina, "Waveform Design for Wireless Power Transfer," IEEE Trans on Sig Proc, Vol. 64, No. 23, pp. 6313-6328, Dec 2016.

Low-complexity design of WPT waveform
B. Clerckx and E. Bayguzina, "A Low-Complexity Multisine Waveform Design for Wireless Power Transfer," IEEE Antennas and Wireless Propagation Letters, vol 16, pp 2207 2210, 2017.

Large scale and multi-user designs for WPT waveforms
Y. Huang and B. Clerckx, "Large-Scale Multi-Antenna Multi-Sine Wireless Power Transfer," IEEE Trans. on Sig Proc., vol. 65, no. 21, pp 5812-5827, Nov 2017.

CSI feedback/acquisition in WPT
Y. Huang and B. Clerckx, "Waveform Design for Wireless Power Transfer with Limited Feedback," IEEE Trans. on Wireless Commun., vol 17, no 1, pp 415 429, Jan. 2018.

Transmit Diversity for WPT
B. Clerckx and J. Kim, "On the Beneficial Roles of Fading and Transmit Diversity in Wireless Power Transfer with Nonlinear Energy Harvesting," IEEE Trans. on Wireless Commun, vol. 17, no. 11, pp. 7731 7743, Nov. 2018.

References

Prototyping and Experimentation of WPT
J. Kim, B. Clerckx, and P.D. Mitcheson, "Prototyping and Experimentation of a Closed-Loop Wireless Power Transmission with Channel Acquisition and Waveform Optimization," IEEE WPTC 2017.
J. Kim, B. Clerckx, and P.D. Mitcheson, "Signal and System Design for Wireless Power Transfer : Prototype, Experiment and Validation," in submission.

Fundamentals of WIPT
B. Clerckx, R. Zhang, R. Schober, D. W. K. Ng, D. I. Kim, and H. V. Poor, "Fundamentals of Wireless Information and Power Transfer: From RF Energy Harvester Models to Signal and System Designs," IEEE Journal on Selected Areas in Communications, vol. 37, no. 1, pp. 4-33, Jan 2019.

Closer to characterizing the fundamental limits of WIPT: waveform, input distribution
B. Clerckx, "Wireless Information and Power Transfer: Nonlinearity, Waveform Design and Rate-Energy Tradeoff," IEEE Trans. on Sig Proc, vol 66, no 4, pp 847-862, Feb 2018.
M. Varasteh, B. Rassouli and B. Clerckx, "Wireless Information and Power Transfer over an AWGN channel: Nonlinearity and Asymmetric Gaussian Signaling," IEEE ITW 2017.
M. Varasteh, B. Rassouli and B. Clerckx, "SWIPT Signalling over Frequency-Selective Channels with a Nonlinear Energy Harvester: Non-Zero Mean and Asymmetric Inputs," in submission, arXiv:1901.01740.

References

Practical Modulation of WIPT

E. Bayguzina and B. Clerckx, "Modulation Design for Wireless Information and Power Transfer with Nonlinear Energy Harvester Modeling," IEEE SPAWC 2018.

Fundamental limits of WIPT: optimal signal, modulation, input distribution

M. Varasteh, B. Rassouli and B. Clerckx, "On Capacity-Achieving Distributions for Complex AWGN Channels Under Nonlinear Power Constraints and their Applications to SWIPT," in submission, arXiv:1712.01226

Deep Learning for WIPT

M. Varasteh, E. Piovano and B. Clerckx, "A Learning Approach to Wireless Information and Power Transfer Signal and System Design," IEEE ICASSP 2019.

M. Varasteh, J. Hoydis, and B. Clerckx, "Learning Modulation Design for SWIPT with Nonlinear Energy Harvester: Large and Small Signal Power Regimes," IEEE SPAWC 2019.

Prototyping and Experimentation of WIPT

J. Kim, B. Clerckx, and P.D. Mitcheson, "Experimental Analysis of Harvested Energy and Throughput Trade-off in a Realistic SWIPT System," IEEE WPTC 2019.

Bridging RF, Signal and System Designs

B. Clerckx, A. Costanzo, A. Georgiadis, and N.B. Carvalho, "Toward 1G Mobile Power Networks: RF, Signal and System Designs to Make Smart Objects Autonomous" IEEE Microwave Magazine, Sept/Oct 2018.

WPW SCHOOL

Combining backscatter communications with WPT, the new Wireless Power Communication Paradigm

Nuno Carvalho
University of Aveiro

The Internet-of-Things (IoT) vision calls for thousands interconnected devices in wearables, vehicles, buildings, using a multitude of sensors to provide us with useful information. Backscatter communication provides an enabling technology to address the needs of IoT, due to the simplicity of the tag circuit and the ability to minimize the usage of batteries or even completely eliminate them taking advantage of wireless power transmission as well as energy harvesting. This talk presents the latest advances in backscatter communication technology, covering a wide range of topics, focusing on the combination of modulation constellation diagrams with the smith chart.

WPW 2019

WPW SCHOOL

WIRELESS POWER COMMUNICATIONS BASED ON BACKSCATTER

Nuno Borges Carvalho,
Ricardo Correia, Daniel Belo and Felisberto Pereira
Instituto de Telecomunicações
Universidade de Aveiro, Portugal

radio systems

instituto de telecomunicações

DETI.UA.PT universidade de aveiro

Motivation

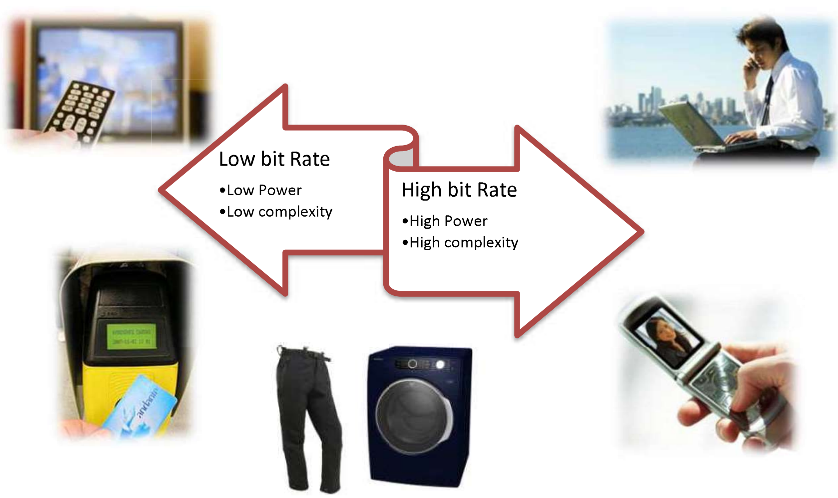

Motivation

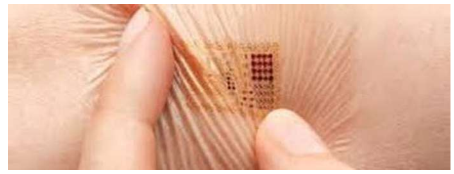

Motivation

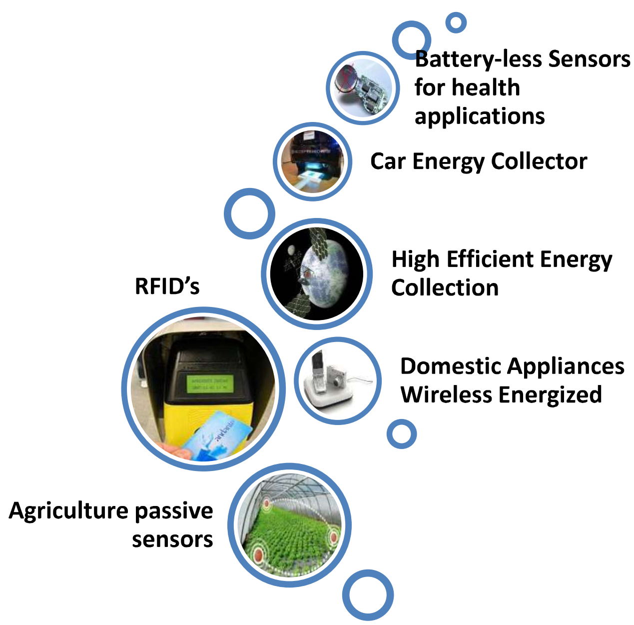

IoT

Internet of Things is a network of physical objects “things” embedded with electronics, software, sensors and network connectivity, which enable these objects to collect and exchange data.

RFID → Sensor → Smart Tech → Nano Tech

RFID: To identify and track the data of things.
Real-time item traceability and addressability by RFIDs.
Tagging things

Sensor: To collect and process the data to detect the changes in the physical status of things.
Sensors act as primary devices to collect data from environment.
Feeling things

Smart Tech: To enhance the power of the network by devolving processing capabilities to different part of the network.
Embedded intelligence in devices through sensors has formed the network connection to the Internet.
Thinking things

Nano Tech: Nanotechnology has provoked the ability of smaller things to interact and connect within the things or smart devices.
Shrinking things

Radio System Drawbacks

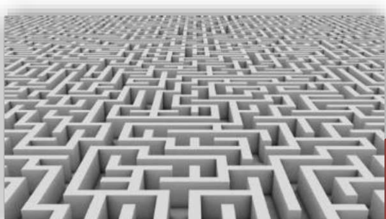

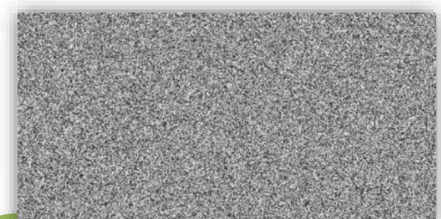

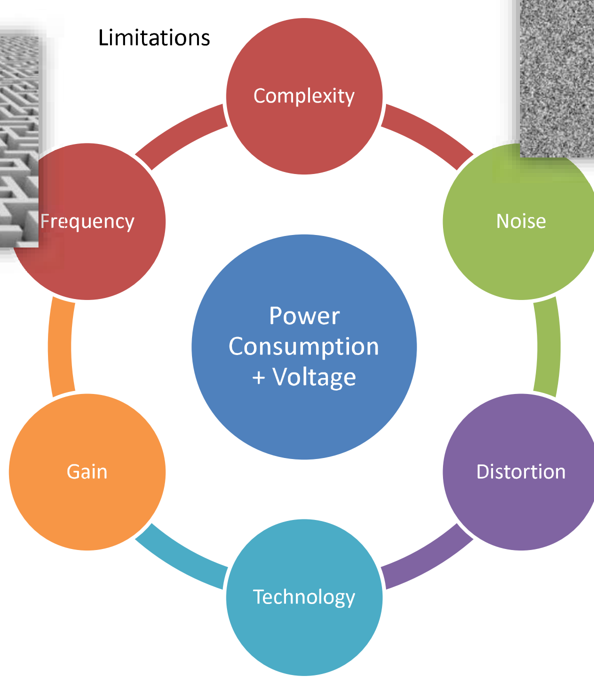

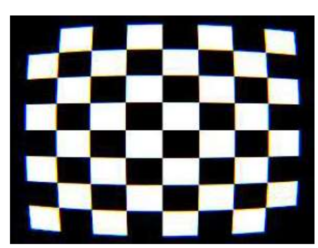

RF Receivers

Super-heterodyne

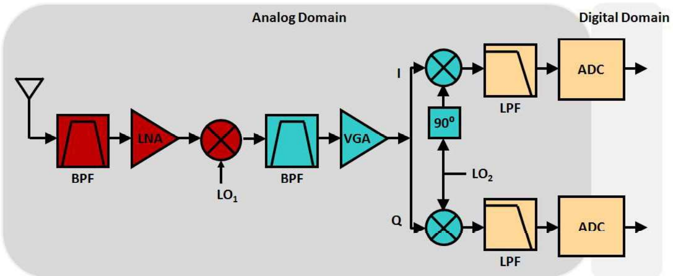

- Conversion to the digital domain at baseband where it can be processed
- Currently adopted in most radio receivers due to low cost components
- Full on-chip integration is concerned and its design to a specific channel → prevents the expansion of receiving band

Zero-IF

- Signal is selected at RF by BPF, amplified and directly translated to DC
- Evident reduction in number of components → high level integration
- Components much more difficult to design DC offset, 2nd order IMD products generated around DC

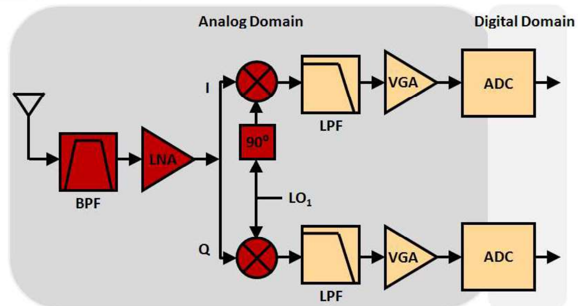

Transmitter

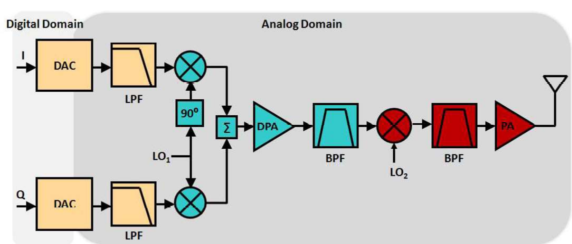

Super-Heterodyne Transmitter

- Signal created in digital domain, modulated at IF, and up-converted
- I/Q modulator working at IF; Output spectrum is far away from LO
- Suffers from similar problems of the receiver case
- Multi-mode implementation is difficult

Direct-Conversion Transmitter

- Digital baseband signals are converted and directly modulated to RF
- Reduced amount of circuitry that allows high level integration
- Carrier leakage, phase gain mismatch, and requires highly linear PA
- With careful design can be employed in SDR TX's

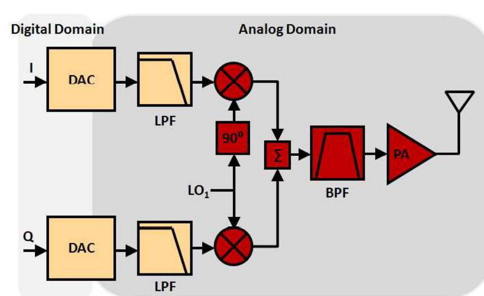

Energy

These radio architectures are responsible for a large amount of energy consumption….

Energy

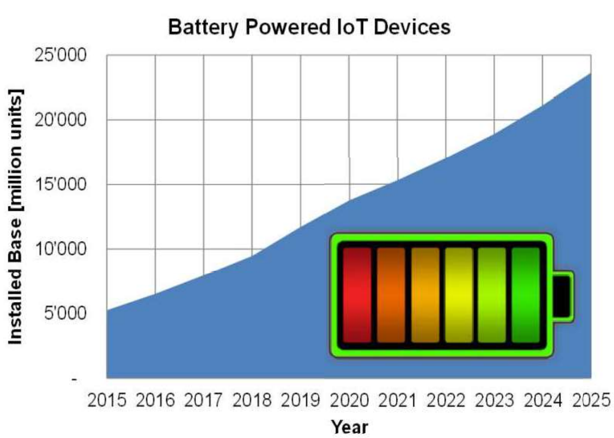

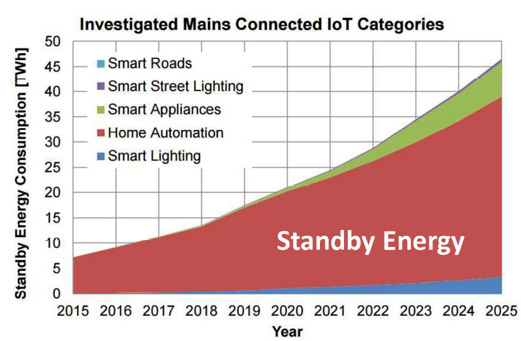

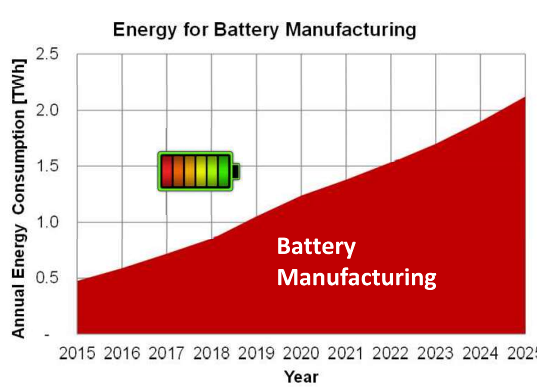

Source: 2016 data http://edna.iea-4e.org

Batteries

Batteries take **hundreds of years to decompose**, posing a serious threat to the public health and to the environment.

- Considering 4 Million habitual residences in Portugal (INE – Censos 2011) and assuming that:
  - ✓ 75% of them have a TV equipment
  - ✓ 40% have a cable TV Box
  - ✓ 30% have a Sound System

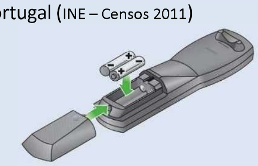

- We end up with an average of **5.8 Millions of remotes in Portugal**
- Assuming two batteries per remote and two battery changes per year we have a …

total of 23.2 Millions batteries being wasted every year !!

Case study

Energy Consumption

Solutions for IoT

How much power is low power?

Market Solutions

Typical example from one of the top sellers of IoT Sensors

Parameter	Value	Unit
Minimum supply voltage	1.9	V
Temperature range	-40 to +85	°C
Supply current in transmit @ -10dBm output power	9	mA
Supply current in receive mode	12.5	mA
Supply current for µ-controller 4MHz @ 3volt	1	mA
Supply current for ADC	0.9	mA
Maximum transmit output power	10	dBm
Data rate	50	kbps
Sensitivity	-100	dBm
Supply current in power down mode	2.5	µA

SoC 1 - Sub <1GHz

Transmit – 17mW
Receive – 24mW

- 2.4 GHz transceiver
  - -96 dBm sensitivity in *Bluetooth*® low energy mode
  - 1 Mbps, 2 Mbps supported data rates
  - TX power -20 to +4 dBm in 4 dB steps
  - Single-pin antenna interface
  - 5.3 mA peak current in TX (0 dBm)
  - 5.4 mA peak current in RX
  - RSSI (1 dB resolution)

SoC 2 – UltraLow Power Bluetooth

Supply Voltage 1,7 to 3,6 V
Transmit/Receive – 9mW

Market Solutions

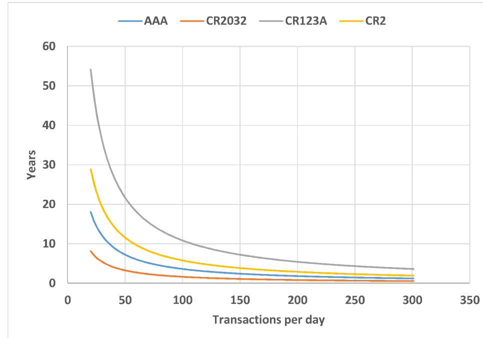

Type	AAA	CR2032	CR123A	CR2
Material	Alkaline	LiMn02*	Lithium	Lithium
Voltage	3V	3V	3V	3V
Capacity	500 mAh	225 mAh	1500 mAh	800 mAh

Sensor Transmit, 1s duration per transaction
Transmit – 17mW
Receive – 24mW

"Guilty as charged."

IoT Alternatives

Can we remove the need of power for transmit receive?

Can we eliminate batteries?

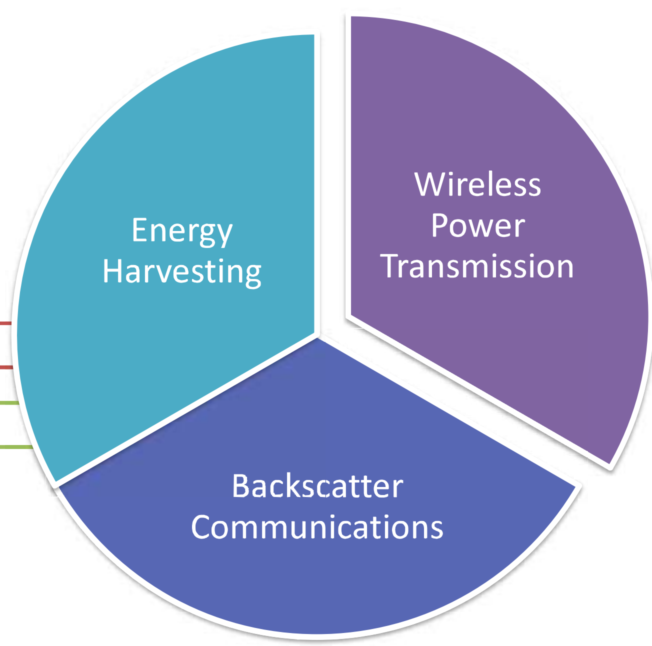

Energy Harvesting vs Wireless Power Transmission

Comparison of Power Density of Energy Harvesting Methods		
Energy Source	Power Density & Performance	Source of Information
Acoustic Noise	0.003 μW/cm3 @ 75Db 0.96 μW/cm3 @ 100Db	(Rabaey, Ammer, Da Silva Jr, Patel, & Roundy, 2000)
Temperature Variation	10 μW/cm3	(Roundy, Steingart, Fréchette,Wright, Rabaey, 2004)
Ambient RF	1 μW/cm2	(Yeatman, 2004)
Ambient Light	100 mW/cm2 (direct sun) 100 _W/cm2 (illuminated office)	Not Cited
Thermoelectric	60 _W/cm2	(Stevens, 1999)
Vibration (micro generator)	4 _W/cm3 (human motion - Hz) 800 _W/cm3 (machines – kHz)	(Mitcheson, Green, Yeatman, & Holmes, 2004)
Vibrations (Piezoelectric)	200 μW/cm3	(Roundy, Wright, & Pister, 2002)
Airflow	1 μW/cm2	(Holmes, 2004)
Push Buttons	50 _J/N	(Paradiso & Feldmeier, 2001)
Shoe Inserts	330 μW/cm2	(Shenck & Paradiso, 2001)
Hand Generators	30 W/kg	(Starner & Paradiso, 2004)
Heel Strike	7 W/cm2	(Yaglioglu, 2002) (Shenck & Paradiso, 2001)

Wi-Fi

GSM/Cellular

Radio and TV broadcast

Source: The Journal of Technology Studies

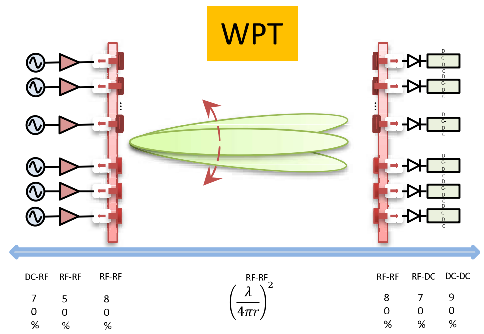

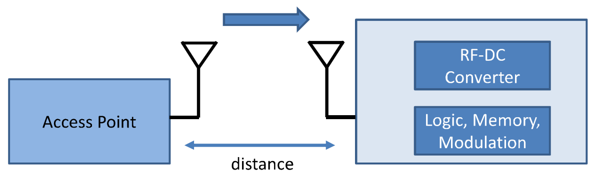

Sensor RF-DC Converter

WPT Receiver

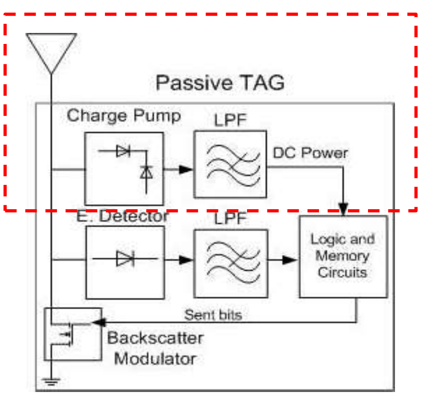

$$y_{out} = NL[x_{in}(f_0)] = \boxed{Y(DC)} + Y(f_0) + Y(2f_0) + Y(3f_0) + _{...} + Y(nf_0)$$

Desired component

RF-DC conversion process in a diode detector

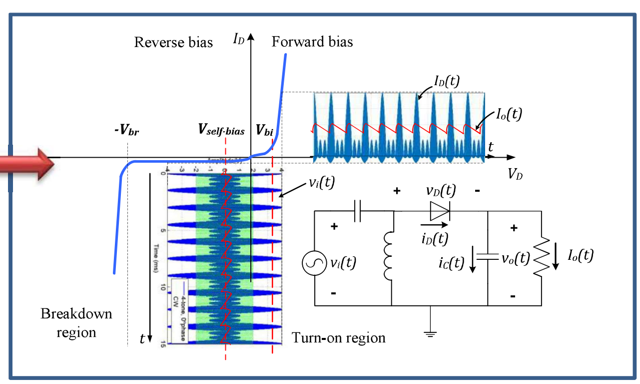

$$I_D = I_S(e^{\frac{qV_j}{\eta kT}} - 1) = I_S(e^{\frac{V_j}{\eta V_t}} - 1) = I_S(e^{\frac{V_D - R_S I_D}{\eta V_t}} - 1)$$

A. Boaventura, D. Belo, R. Fernandes, A. Collado, A. Georgiadis and N. B. Carvallo, "Boosting the Efficiency: Unconventional Waveform Design for Efficient Wireless Power Transfer," in *IEEE Microwave Magazine*, vol. 16, no. 3, pp. 87-96, April 2015.

Rectifying devices exhibit a NON-ZERO turn-on voltage → a certain amount of energy is needed to overcome the turn-on voltage → low power level efficiency is degraded

Backscatter

Backscatter

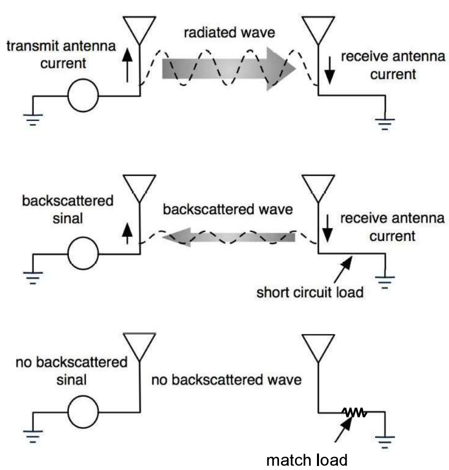

- Backscatter communications has its roots in radars type approach
- The RF-front end reflects part of an incoming electromagnetic wave back to the reader based on the information pattern
- The backscatter reflection efficiency is maximized for antennas that are resonating with the incoming signal frequency.

Backscatter

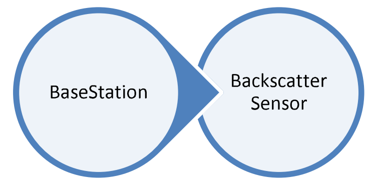

- RF Transmitter
- RF Receiver

- Voltage Harvester
- Signal Processor

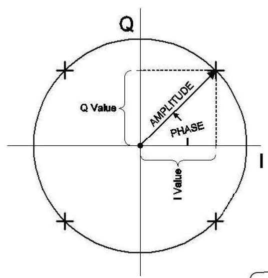

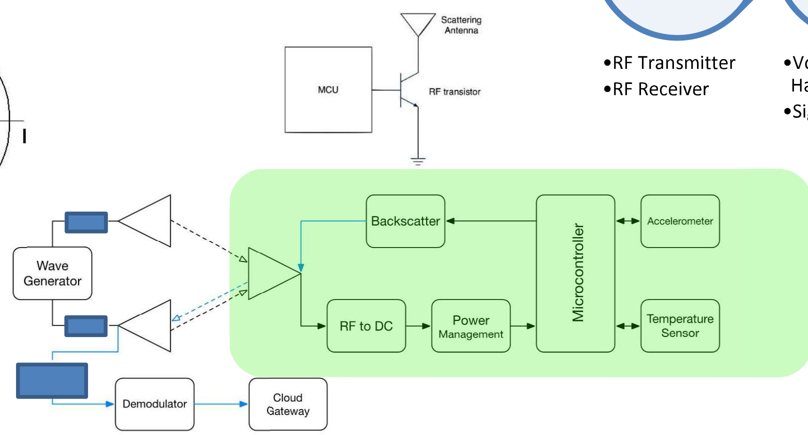

Backscatter

Access Point-to-sensor link has two goals

- Communication
- Energy transfer

Data communication and Energy transfer can take place simultaneously

- In such cases the Modulation and Codification must be carefully designed, otherwise the Energy transfer will be degraded
- An inappropriate combination of Codification-Modulation with long dead periods (signal off) would lead the tag to fail

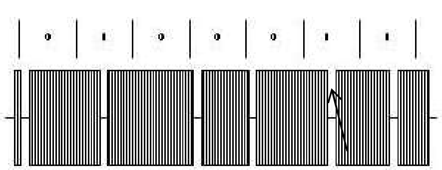

Good choice: signal is off for short periods of time

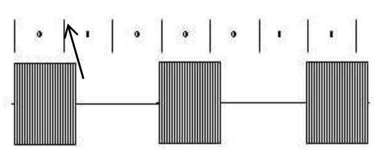

Bad choice: signal is off for long periods of time → At those periods tag has no available energy to operate

Backscatter with WPT

Combining WPT and Backscatter using dual band sensors

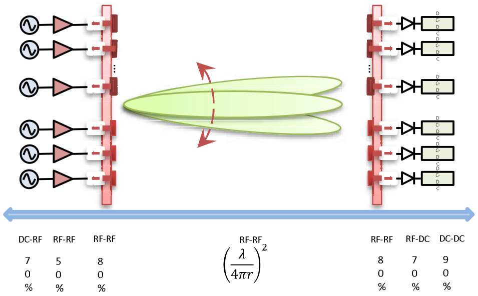

ONE frequency for WPT and OTHER for backscatter

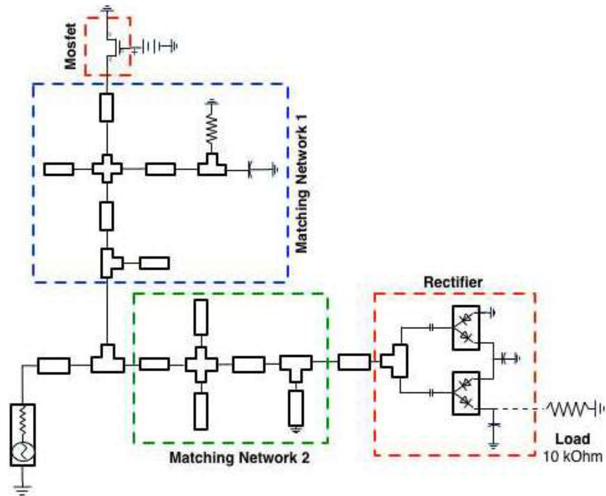

R. Correia, N. Borges Carvalho and S. Kawasaki, "Continuously Power Delivering for Passive Backscatter Wireless Sensor Networks," in *IEEE Transactions on Microwave Theory and Techniques*, vol. 64, no. 11, pp. 3723-3731, Nov. 2016.

Backscatter with WPT

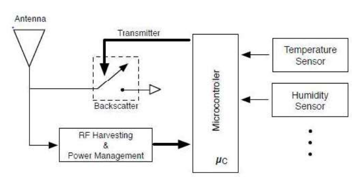

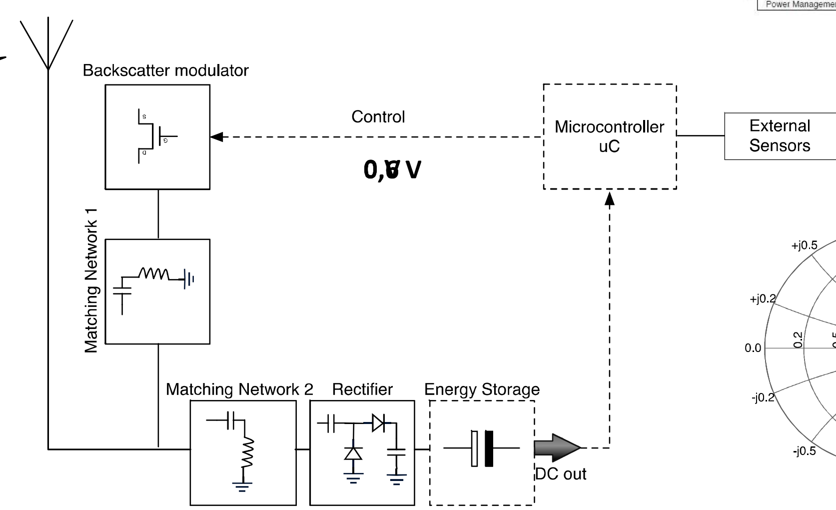

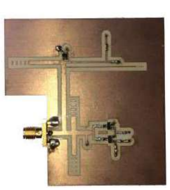

F1 = 1.8 GHz
F2 = 2.45 GHz

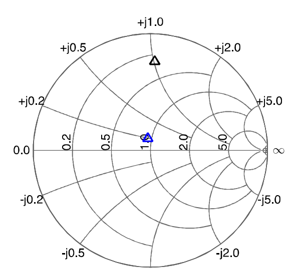

R. Correia, N. Borges Carvalho and S. Kawasaki, "Continuously Power Delivering for Passive Backscatter Wireless Sensor Networks," in *IEEE Transactions on Microwave Theory and Techniques*, vol. 64, no. 11, pp. 3723-3731, Nov. 2016.

Backscatter Higher Order Modulation

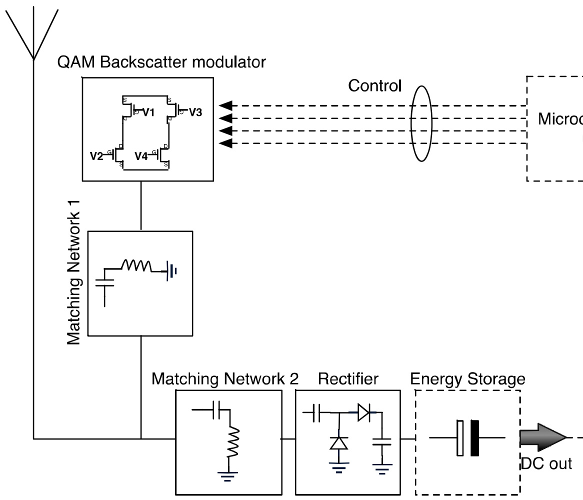

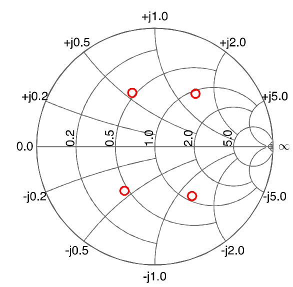

R. Correia and N. B. Carvalho, "Design of high order modulation backscatter wireless sensor for passive IoT solutions," *2016 IEEE Wireless Power Transfer Conference (WPTC)*, Aveiro, 2016, pp. 1-3.

Backscatter Higher Order Modulation

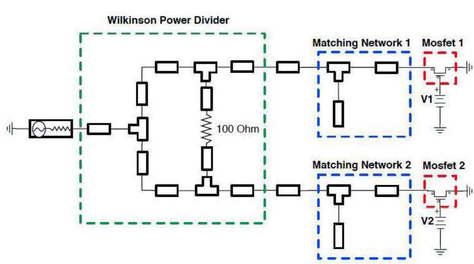

(a)

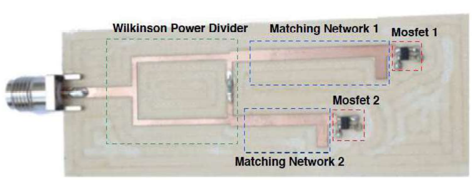

(b)

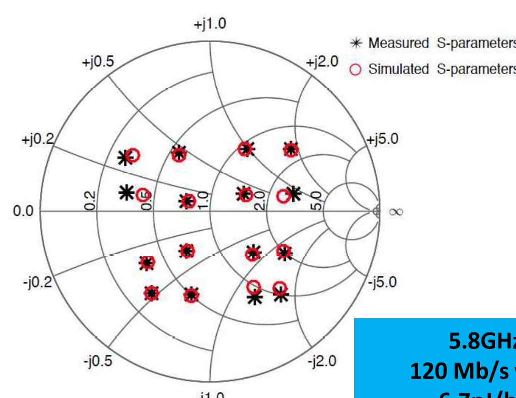

5.8GHz
120 Mb/s with
6.7pJ/bit

R. Correia; A. Boaventura; N. B. Carvalho, "Quadrature Amplitude Backscatter Modulator for Passive Wireless Sensors in IoT Applications," in *IEEE Transactions on Microwave Theory and Techniques* , vol.PP, no.99, pp.1-8

Backscatter Higher Order Modulation

960Mbps

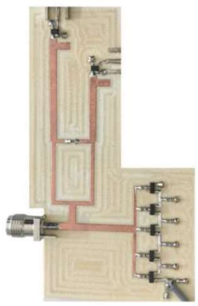

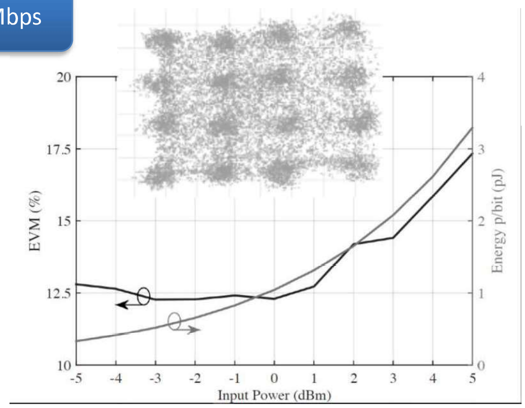

5.8GHz
960 Mb/s with
0,9 pJ/bit

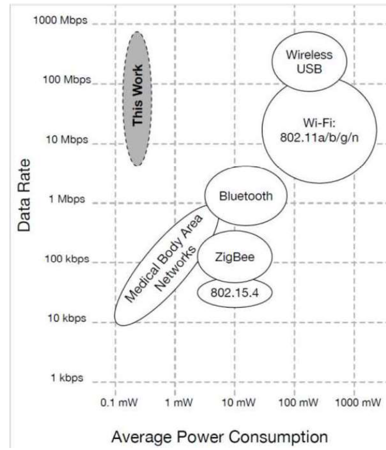

Ambient Backscatter

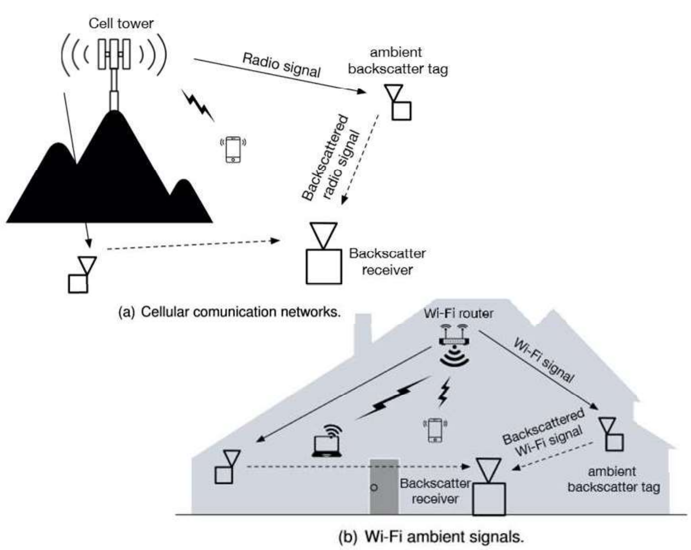

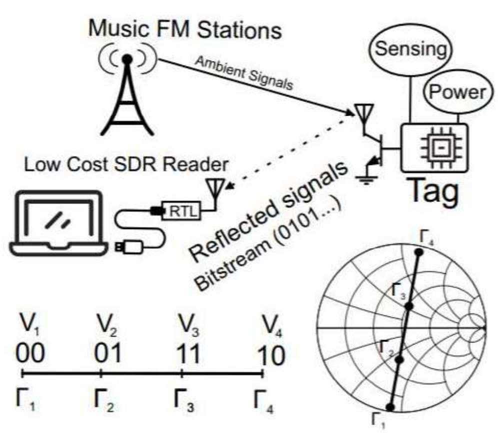

Spyridon N Daskalakis et all, "Spectrally Efficient 4-PAM Ambient FM Backscattering for Wireless Sensing and RFID Applications", to be presents in the next IMS2018 in Philadelphia

Millimeterwave Backscatter

Design an MMIC chip for higher frequencies based on high order backscatter modulation.

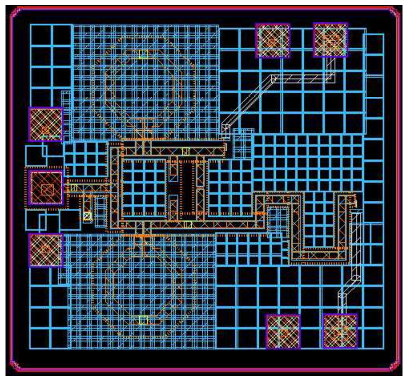

SiGe BICMOS
SG13S technology
0.92 mm^2

WPC Network

Cloud RAN Access Point

Real Implementation

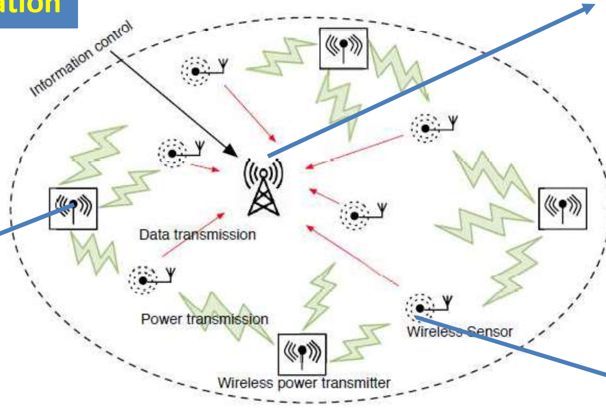

Wireless Transmitters

Battery-less Sensors

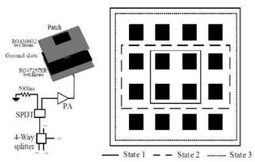

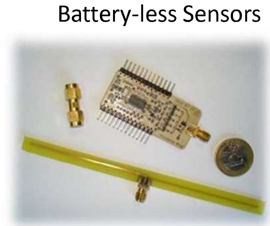

R. Correia and N. B. Carvalho, "Design of high order modulation backscatter wireless sensor for passive IoT solutions," *2016 IEEE Wireless Power Transfer Conference (WPTC)*, Aveiro, 2016, pp. 1-3.

Applications: Passive Remote Control

Batteryless Remote Control

A battery-free **Remote Control System** is proposed:

- The Remote requires no battery, based on passive backscatter technology
- Device to be Controlled wirelessly powers the remote control using radio waves
- The remote control send back information using Backscattering (Power reflection)

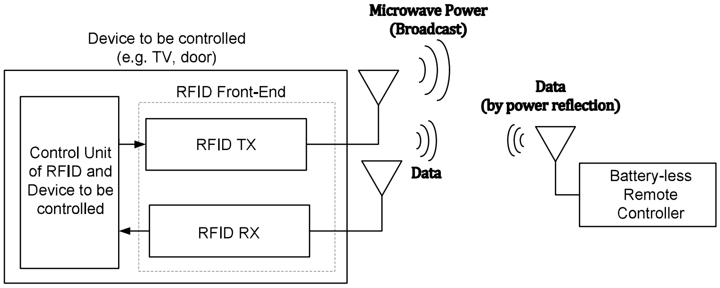

Advantages compared to conventional IR technology:

- ✓ **Elimination of costs** associated to battery maintenance and treatment of toxic waste
- ✓ **Long range and no line of sight communication** thanks to the use of radio waves
- ✓ **Cost-effective solution**, thanks to the use of a low-cost RFID technology (UHF EPC)

Batteryless Remote Control Multi RFID

Operating principle:

- N passive RFID tags associated to N keys/switchs
  - By default, no tag responds to reader (silent mode)
  - Once a key is pressed the respective tag is allowed to respond
  - Inactive tags must not interfere with the active one
- Two challenges: Antenna sharing, Tag activation/deactivation

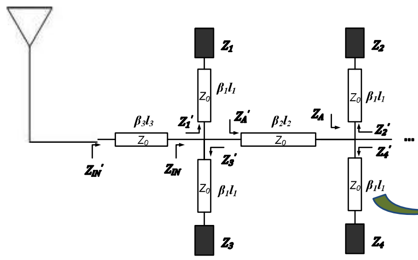

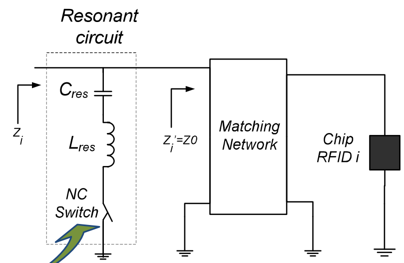

Port termination
= 0 Ohms by default
= 50 Ohms if user presses the key

Tags interconnection (N-port Network)

Batteryless Remote Control Multi RFID

Remote control prototypes: 3, 4 and 5 keys

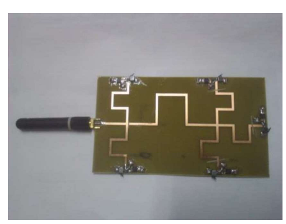

Return loss (S11) of 4-key prototype when each key is presses by the user

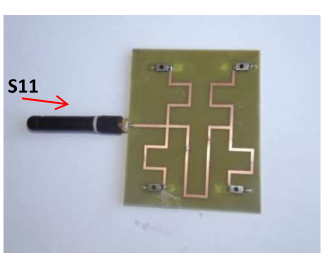

S11 - Return Loss (dB)

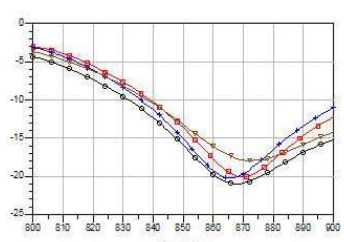

o – key 1 pressed
x – key 2 pressed
▪ – key 3 pressed
< – key 4 pressed

Batteryless Remote Control Multi RFID

- ✓ The complete system has been successfully tested and validated
- ✓ The remote control system has been integrated in a TV device
- ✓ **CH +**, **CH -**, **Vol +** and **Vol –** functions were implemented.

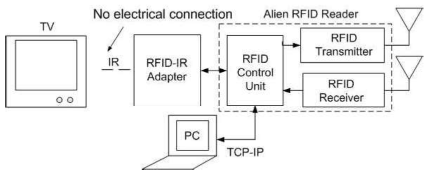

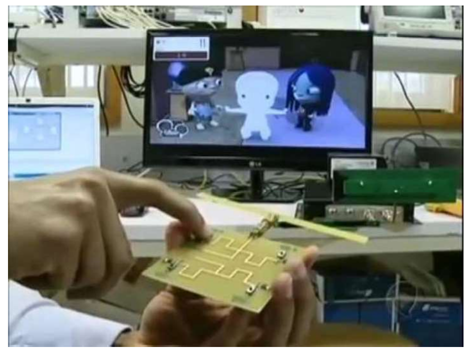

The prototype is composed by:

1) TV
2) RFID reader and Computer
3) RFID-IR adapter

WPW 2019
WPW SCHOOL

Questions?

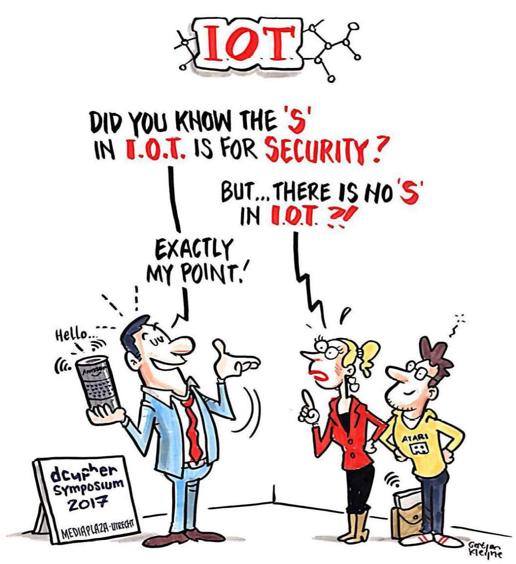

universidade de aveiro

Acknowledgments

Aveiro Group
Arnaldo Oliveira
Pedro Pinho
José Neto Vieira
João Nuno Matos
Pedro Cruz
Ricardo Correia
Daniel Belo
Diogo Ribeiro
André Prata
Daniel Dinis
Ricardo Gonçalves
Daniel Malafaia
Felisberto Pereira

Alumni
Alírio Boaventura
Nelson Silva
Luis Brás
Ricardo Fernandes
Eduardo Bolas
José Borrego
Wonhoon Jang
Rui Fiel
Jorge Santos
João Santos

R&D Colleagues
Alessandra Costanzo
Ana Collado
Apostolos Georgiadis
Christopher Fager
Dominique Schreurs
José Carlos Pedro
Luca Roselli
Kate Remley
Kevin Gard
Manos Tentzeris
Marc Vanden Bossche
Michael Steer
Naoki Shinohara
Roberto Gomez-Garcia
Shigeo Kawasaki

NATIONAL INSTRUMENTS
altice labs
EVOLEO
wavecom wireless experts

Bibliography

- N.B.C. Carvalho, RGG Gomez-Garcia, AC Cidronali, White Space Communication Technologies, Cambridge University Press, London, 2014,
  N.B.C. Carvalho, D. Schreurs, Microwave and Wireless Measurement Techniques, Cambridge University Press, London, 2013,
- R. Correia; A. Boaventura; N. B. Carvalho, "Quadrature Amplitude Backscatter Modulator for Passive Wireless Sensors in IoT Applications," in *IEEE Transactions on Microwave Theory and Techniques* , vol.PP, no.99, pp.1-8
- A.P. Prata, D. Ribeiro, P.M. Cruz, A. Oliveira, N.B.C. Carvalho, RF Subsampling Feedback Loop Technique for Concurrent Dual-Band PA Linearization, IEEE Trans. on Microwave Theory and Tech., Vol. 64, No. 12, pp. 1 - 9, December, 2016
- N.B.C. Carvalho, J. Santos, A. Oliveira, A. Boaventura, Perfect Isolation: Dealing with Self-Jamming in Passive RFID Systems, IEEE Microwave Magazine, Vol. 17, No. 11, pp. 20 - 39, November, 2016,
- R. Correia, N.B.C. Carvalho, S. Kawasaki, Continuously Power Delivering for Passive Backscatter Wireless Sensor Networks, IEEE Trans. on Microwave Theory and Tech., Vol. PP, No. 99, pp. 1 - 9, September, 2016
- W. Jang, R. Cordeiro, A. Oliveira, N.B.C. Carvalho, A Broadband Almost-Digital Radio Frequency Transmitter with an Efficient Power Amplifier, IEEE Trans. on Microwave Theory and Tech., Vol. 64, No. 5, pp. 1526 - 1534, May, 2016,
- P. Pinho, N.B.C. Carvalho, T.M. Moura, High-efficiency D-TV energy harvesting system for low-input power, Wireless Power Transfer, Vol. 3, No. 1, pp. 34 - 42, March, 2016,
- R. Gonçalves, S.R. Rima, R. M. Magueta, P. Pinho, A.C. Collado, A. G. Georgiadis, JH Hester, N.B.C. Carvalho, MT Tentzeris, RFID-Based Wireless Passive Sensors Utilizing Cork Materials, IEEE Sensors Journal, Vol. 15, No. 12, pp. 7242 - 7251, December, 2015,
- D. Ribeiro, A.P. Prata, P.M. Cruz, N.B.C. Carvalho, D-Parameters: A Novel Framework for Characterization and Behavioral Modeling of Mixed-Signal Systems, IEEE Trans. on Microwave Theory and Tech., Vol. PP, No. 99, pp. 1 - 11, September, 2015,
- R. D. Fernandes, J. N. Matos, N.B.C. Carvalho, Low-power ultra-wide band pulse generator based on a PIN diode, IET Microwaves Antennas & Propagation, Vol. 9, No. 11, pp. 1230 - 1232, August, 2015
- P.M. Cruz, N.B.C. Carvalho, Improving dynamic range of software-defined radio receivers for multi-carrier wireless systems, IET Microwaves Antennas & Propagation, Vol. 9, No. 1, pp. 16 - 23, January, 2015,
- D. Ribeiro, P.M. Cruz, N.B.C. Carvalho, Synchronous Oversampled Measurements for the Extraction of Mixed-Signal Behavioral Models in Digital to Analog Integrated Transmitters, IEEE Trans. on Microwave Theory and Tech., Vol. 62, No. 12, pp. 3183 - 3192, December, 2014,
- L.R. Roselli, N.B.C. Carvalho, F.A. Alimenti, P. M. Mezzanotte, G.O. Orecchini, M. V. Virili, C. M. Mariotti, R. Gonçalves, P. Pinho, Smart Surfaces: Large Area Electronics Systems for Internet of Things Enabled by Energy Harvesting, Proceedings of the IEEE, Vol. 102, No. 11, pp. 1723 - 1746, November, 2014
- W. Jang, N.V.S. Silva, A. Oliveira, N.B.C. Carvalho, Analysis on in-band distortion caused by switching amplifiers, IET Microwaves Antennas & Propagation, Vol. 8, No. 5, pp. 351 - 357, April, 2014,
- A. Boaventura, A.C. Collado, N.B.C. Carvalho, A. G. Georgiadis, Spatial Power Combining of Multi-Sine Signals for Wireless Power Transmission applications, IEEE Trans. on Microwave Theory and Tech., Vol. 62, No. 4, pp. 1022 - 1030, April, 2014
- N.B.C. Carvalho, A. Boaventura, Wireless Power Transmission: R&D Activities Within Europe, IEEE Trans. on Microwave Theory and Tech., Vol. 62, No. 4, pp. 1031 - 1045, April, 2014
- R. Emrick, P.M. Cruz, N.B.C. Carvalho, S. Gao, R. Quay, P. Waltereit, The Sky´s the Limit: Key Technologies and Market Trends in Satellite, IEEE Microwave Magazine, Vol. 15, No. 2, pp. 65 - 78, March, 2014,
- J. Vieira, RGG Gomez-Garcia, JPM Magalhães, N.B.C. Carvalho, Filling the Spectral Holes: Novel/Future Wireless Communications and Radar Receiver Architectures, IEEE Microwave Magazine, Vol. 15, No. 2, pp. 45 - 56, March, 2014
- A.P. Prata, N.B.C. Carvalho, A. Oliveira, An Agile Digital Radio System for UHF White Spaces, IEEE Microwave Magazine, Vol. 15, No. 1, pp. 92 - 97, January, 2014
- P.M. Cruz, N.B.C. Carvalho, M.E. Valkama, Multi-Stage Mixed Frequency-Time Simulator for Bandpass Sampling Receiver Front-Ends, i-ETC : ISEL Academic Journal of Electronics, Telecomunications and Computers, Vol. 2, No. 1, pp. 1 - 8, June, 2013,
- W. Jang, N.V.S. Silva, A. Oliveira, N.B.C. Carvalho, Designing Harmonic-Controlled Drivers for Switching Power Amplifiers, IEEE Trans. on Circuits and Systems - II: Express Briefs, Vol. 60, No. 5, pp. 247 - 251, May, 2013
- J. Vieira, JPM Magalhães, N.B.C. Carvalho, RGG Gomez-Garcia, Bio-Inspired Hybrid Filter Bank for Software-Defined Radio Receivers, IEEE Trans. on Microwave Theory and Tech., Vol. 61, No. 4, pp. 1455 - 1466, April, 2013,
- A. Boaventura, A.C. Collado, N.B.C. Carvalho, A. G. Georgiadis, Optimum Behavior: Wireless power transmission system design through behavioral models and efficient synthesis techniques, IEEE Microwave Magazine, Vol. 14, No. 2, pp. 26 - 35, March, 2013
- N.V.S. Silva, A. Oliveira, N.B.C. Carvalho, Design and Optimization of Flexible and Coding Efficient All-Digital RF Transmitters, IEEE Trans. on Microwave Theory and Tech., Vol. 61, No. 1, pp. 625 - 632, January, 2013,
- A. Boaventura, N.B.C. Carvalho, Extending Reading Range of Commercial RFID Readers, IEEE Trans. on Microwave Theory and Tech., Vol. 61, No. 1, pp. 48 - 57, January, 2013,

WPW SCHOOL

Inductive Resonant WPT: design equations for different operative regimes

Giuseppina Monti
University of Salento

This contribution will focus on inductive resonant wireless power transfer. The link will be modelled as a two-port network and the performance will be described by using the three power gains usually adopted in the context of active networks. The design equations for achieving different operative regimes will be illustrated and discussed. In particular, two different regimes will be analysed. The first operative regime which will be illustrated aims at maximizing the performance of the link in terms of power gains. In this regard, possible approaches for achieving the best operating conditions will be presented. The second operative regime which will be presented adopts a frequency agile scheme and is well-suited for applications requiring a performance independent of the coupling coefficient. Some experimental data will be also reported for validation.

WPW SCHOOL

Inductive Resonant WPT: Design Equations for Different Operative Regimes

Giuseppina Monti

Department of Engineering for Innovation

University of Salento (Lecce, Italy)

giuseppina.monti@unisalento.it

Faculty of Engineering, University of Salento, Lecce, Italy

Outline

- Introduction:
    - Two-port network representation
    - Variables of interest and figures of merit
- Non-radiative WPT based on inductive coupling, possible operative regimes:
    - Maximizing the performance with a fixed load
    - Operating with a variable load: the load-independent regime
    - How to provide performance independent of the coupling coefficient

WPT – Goal and strategies

***WPT** - transmission* of electrical energy from a *power* source to an electrical load without a physical connection

Far-field coupling

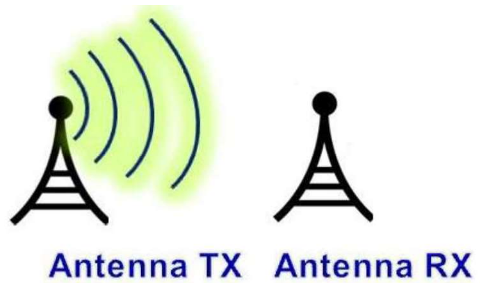

Features: Long transfer distance, High mobility
Key devices: Electromagnetically coupled Antennas

Near-field coupling

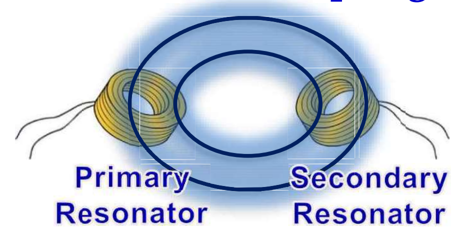

Electric coupling: Sensitive to distance variations, High interaction with the surrounding environment

Magnetic coupling: Low interaction with the surrounding environment, Short transfer distance

Inductive Resonant WPT

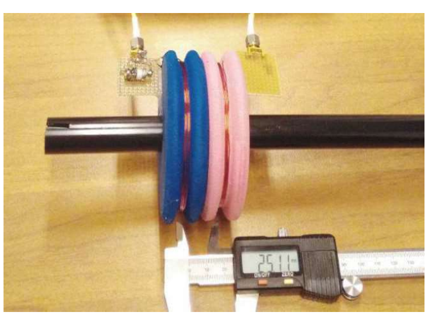

Equivalent circuit

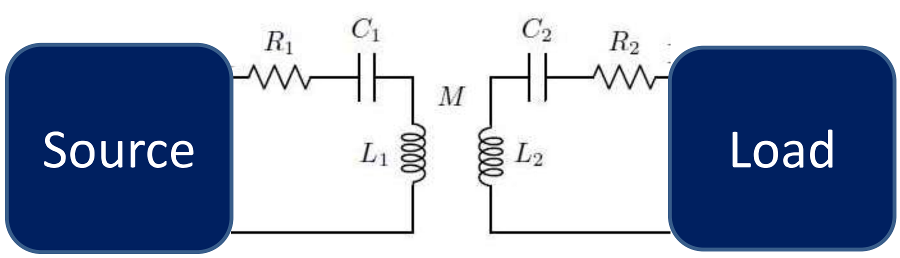

$\omega_0 = \frac{1}{\sqrt{L_i C_i}}$	$M = k\sqrt{L_1 L_2}$	$Q_i = \frac{\omega_0 L_i}{R_i}$
$u = \frac{\omega}{\omega_0}$	$X_0 = \sqrt{\frac{L_1}{C_1}}$	$n = \sqrt{\frac{L_1}{L_2}}$

WPT based on inductive resonant coupling

$$\mathbf{V} = \mathbf{ZI}$$

$$\mathbf{Z} = \begin{pmatrix} z_{11} & z_{12} \\ z_{21} & z_{22} \end{pmatrix}$$

$$z_{ij} = r_{ij} + jx_{ij}, (i, j = 1,2)$$

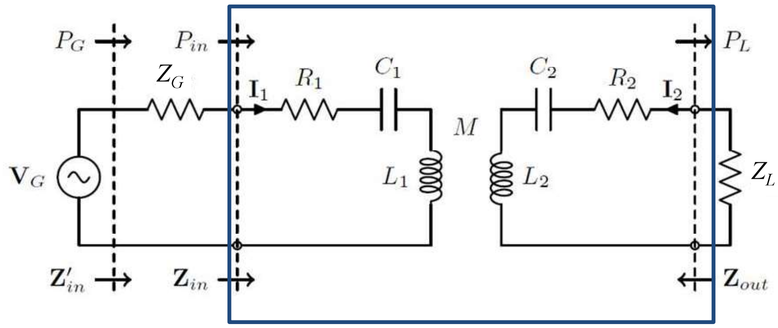

In order to introduce the variables of interest, it is assumed that a voltage generator is on port 1 and that a load Z_L is on port 2.

$$\boxed{Z_{in} = \frac{V_1}{I_1} = z_{11} - \frac{z_{12}z_{21}}{z_{22} + Z_L}}$$

$$\boxed{Z_{out} = \frac{V_2}{I_2}\bigg|_{V_G=0} = z_{22} - \frac{z_{12}z_{21}}{z_{11} + Z_G}}$$

$\omega_0 = \frac{1}{\sqrt{L_i C_i}}$	$M = k\sqrt{L_1 L_2}$	$Q_i = \frac{\omega_0 L_i}{R_i}$
$u = \frac{\omega}{\omega_0}$	$X_0 = \sqrt{\frac{L_1}{C_1}}$	$n = \sqrt{\frac{L_1}{L_2}}$

Dionigi, M., Mongiardo, M., Perfetti, R.: Rigorous network and full-wave electromagnetic modeling of wireless power transfer links. Microwave Theory and Techniques, IEEE Transactions on 63(1), 65–75 (2015). DOI 10.1109/TMTT.2014.2376555

IR WPT link: figures of merit

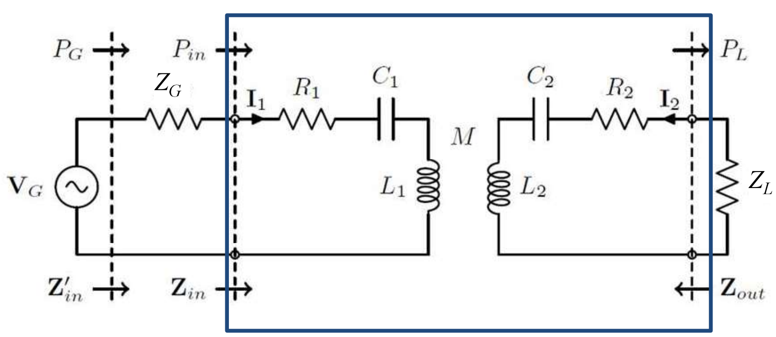

$$\omega_0 = \frac{1}{\sqrt{L_i C_i}} \; (i = 1,2)$$

With regard to the use of the two-port network for WPT applications, two are the main figures of merit:

➔ the active power delivered to the load **(PDL)**;

➔ the power transfer efficiency **(PTE)**, η, defined as:

$$\eta = \frac{P_L}{P_{in}}$$

IR WPT link: figures of merit

WPW 2019 — WPW SCHOOL

	Definition	$\overline{\overline{Z}}$	$\overline{\overline{S}}$
G_P	$\frac{P_L}{P_{in}}$	$\frac{R_L}{R_{in}}\left\|\frac{z_{21}}{z_{22}+Z_L}\right\|^2$	$\frac{\|\mathcal{S}_{21}\|^2}{1-\|\mathcal{S}_{11}\|^2}$
G_A	$\frac{P_A}{P_{AG}}$	$\frac{R_G}{R_{out}}\left\|\frac{z_{21}}{z_{11}+Z_G}\right\|^2$	$\frac{\|\mathcal{S}_{21}\|^2}{1-\|\mathcal{S}_{22}\|^2}$
G_T	$\frac{P_L}{P_{AG}}$	$\frac{4\|z_{21}\|^2 R_G R_L}{\|(z_{11}+Z_G)(z_{22}+Z_L)-z_{12}z_{21}\|^2}$	$\|\mathcal{S}_{21}\|^2$

Active input power delivered from the generator to the network	$P_{in} = \frac{1}{2}R_{in}\|I_1\|^2$
Active power on the load	$P_L = \frac{1}{2}R_L\|I_2\|^2$
Available input power	$P_{AG} = \frac{\|V_G\|^2}{8R_G}$
Maximum available load power	$P_A = \frac{\|V_{th}\|^2}{8R_{out}}$

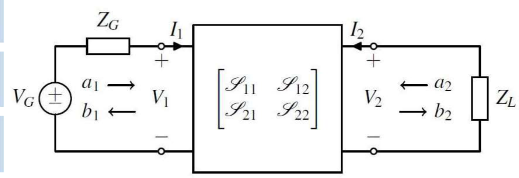

IR WPT link: possible operative regimes

WPW 2019 — WPW SCHOOL

Charging of electronic devices

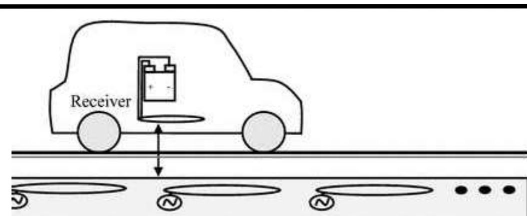

Electric vehicles charging

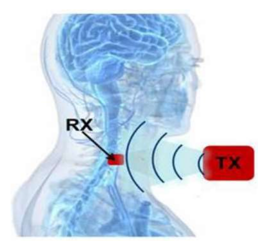

Medical implants

Medical and military devices

For a given resonant-inductive WPT link different design goals lead to different optimal operative schemes

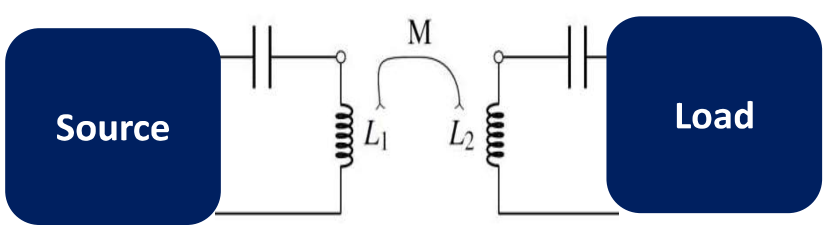

IR WPT link: possible operative regimes

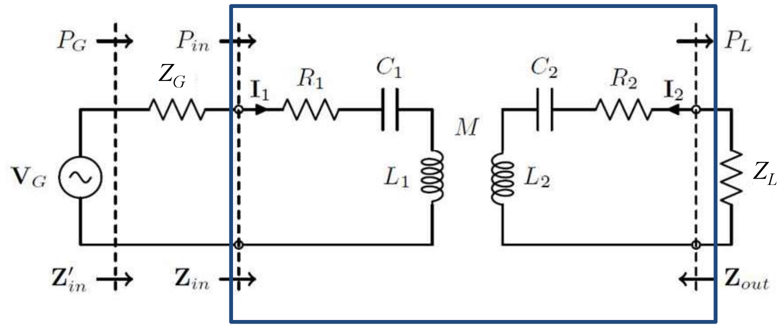

$$M = k\sqrt{L_1 L_2}$$

$$\omega_0 = \frac{1}{\sqrt{L_i C_i}} \quad (i = 1,2)$$

CASE 1: the link is given and the goal is to find the optimal terminating impedances for maximizing the performance

CASE 2: the load is variable and it is necessary to guarantee a constant output voltage (consider the case where the link is used to recharge a battery)

CASE 3: the load is given and the goal is to find the operating conditions for realizing performance independent of the coupling coefficient

IR WPT: how to maximize the performance

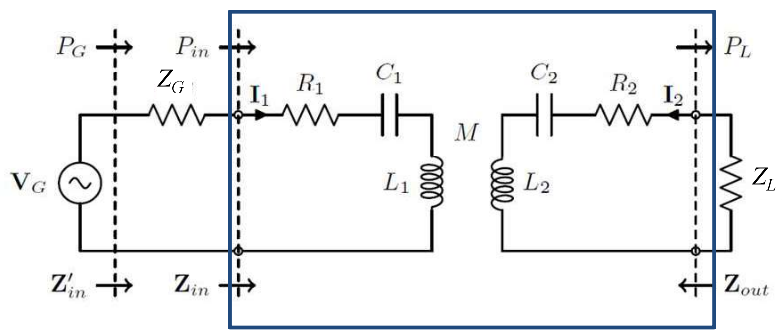

$$M = k\sqrt{L_1 L_2}$$

$$\omega_0 = \frac{1}{\sqrt{L_i C_i}} \quad (i = 1,2)$$

CASE 1: the link is given and the goal is to find the optimal terminating impedances for maximizing the performance

CASE 2: the load is variable and it is necessary to guarantee a constant output voltage (consider the case where the link is used to recharge a battery)

CASE 3: the load is given and the goal is to find the operating conditions for realizing performance independent of the coupling coefficient

IR WPT: how to maximize the performance

WPW 2019

WPW SCHOOL

Definition		General expression
G_P	$\frac{P_L}{P_{in}}$	$\frac{R_L}{R_{in}}\left\lvert\frac{z_{21}}{z_{22}+Z_L}\right\rvert^2$
G_A	$\frac{P_A}{P_{AG}}$	$\frac{R_G}{R_{out}}\left\lvert\frac{z_{21}}{z_{11}+Z_G}\right\rvert^2$
G_T	$\frac{P_L}{P_{AG}}$	$\frac{4\lvert z_{21}\rvert^2 R_G R_L}{\lvert(z_{11}+Z_G)(z_{22}+Z_L)-z_{12}z_{21}\rvert^2}$

➔ Power Gain: it is independent of Z_G

➔ Available Gain: it is independent of Z_L

➔ Transducer Gain: it depends on both Z_G and Z_L and it is maximized for $Z_G=Z_{in}^*$ and $Z_L=Z_{out}^*$.

The biconjugate match has to be realized for maximizing all the three gains:

Z_G should be complex conjugate to Z_{in} when port 2 is terminated on Z_L

Z_L should be complex conjugate to Z_{out} when port 1 is terminated on Z_G

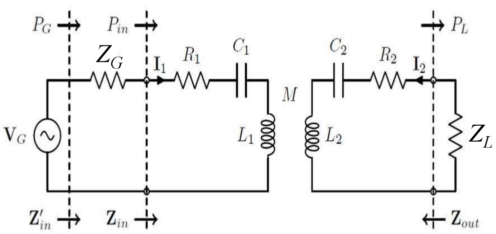

IR WPT: how to maximize the performance

WPW 2019

WPW SCHOOL

The ultimate gain is realized by the conjugate image impedances of the network

$$Z_{c1} = R_{c1} + jX_{c1}$$
$$Z_{c2} = R_{c2} + jX_{c2}$$

The conjugate image impedances are an intrinsic property of the network

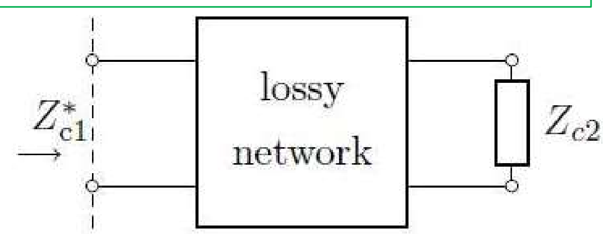

When port 2 is terminated on Z_{c2} the input impedance seen from port 1 is Z_{c1}*. Similarly, when port 1 is terminated on Zc1 the input impedance seen from port 2 is Z_{c2}.*

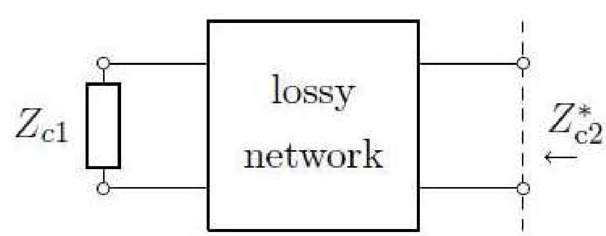

Roberts, S.: Conjugate-image impedances, in Proc. of the IRE, 1946, 198–204.

IR WPT: how to maximize the performance

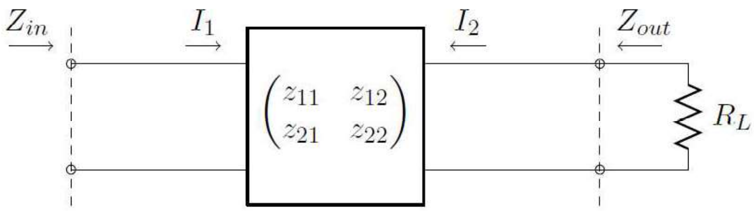

$$z_{ij} = r_{ij} + jx_{ij}, (i, j = 1{,}2)$$

$$\begin{aligned} \chi^2 &= \frac{x_{12}^2}{r_{11} r_{22}} \\ \xi^2 &= \frac{r_{12}^2}{r_{11} r_{22}} \end{aligned}$$

$$\begin{aligned} \theta_r &= \sqrt{1+\chi^2}\sqrt{1-\xi^2} \\ \theta_x &= \chi\xi\,. \end{aligned}$$

$$\begin{aligned} Z_{c1} &= R_{c1} + jX_{c1} = r_{11}(\theta_r + j\theta_x) - jx_{11} \\ Z_{c2} &= R_{c2} + jX_{c2} = r_{22}(\theta_r + j\theta_x) - jx_{22} \end{aligned}$$

Roberts, S.: Conjugate-image impedances, in Proc. of the IRE, 1946, 198–204.

IR WPT: how to maximize the performance

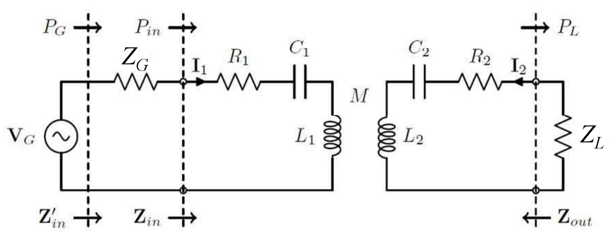

$M = k\sqrt{L_1 L_2}$	$Q_1 = \frac{\omega_0 L_1}{R_1}$	$Q_2 = \frac{\omega_0 L_2}{R_2}$
$u = \frac{\omega}{\omega_0}$	$X_0 = \sqrt{\frac{L_1}{C_1}}$	$n = \sqrt{\frac{L_1}{L_2}}$

$$\mathbf{Z}_{\boldsymbol{norm}} = \frac{\mathbf{Z}}{X_0} = \begin{pmatrix} \frac{1}{Q_1} + ju\left(1 - \frac{1}{u^2}\right) & ju\frac{k}{n} \\ ju\frac{k}{n} & \frac{1}{n^2\,Q_2} + j\frac{u}{n^2}\left(1 - \frac{1}{u^2}\right) \end{pmatrix}$$

$$\xi = \theta_x = 0; \chi^2 = \frac{k^2}{\left[\frac{1}{Q_1} + ju\left(1 - \frac{1}{u^2}\right)\right]\left[\frac{1}{Q_2} + ju\left(1 - \frac{1}{u^2}\right)\right]}; \theta_r = \sqrt{1+\chi^2}$$

IR WPT: how to maximize the performance

$$z_{11} = \frac{1}{Q_1} + ju\left(1 - \frac{1}{u^2}\right)$$
$$z_{21} = z_{12} = ju\frac{k}{n}$$
$$z_{22} = \frac{1}{n^2\,Q_2} + j\frac{u}{n^2}\left(1 - \frac{1}{u^2}\right)$$

$$Z_{c1} = R_{c1} + jX_{c1} = r_{11}(\theta_r + j\theta_x) - jx_{11}$$
$$Z_{c2} = R_{c2} + jX_{c2} = r_{22}(\theta_r + j\theta_x) - jx_{22}$$

$$\xi = \theta_x = 0;\ \chi^2 = \frac{k^2}{\left[\frac{1}{Q_1} + ju\left(1 - \frac{1}{u^2}\right)\right]\left[\frac{1}{Q_2} + ju\left(1 - \frac{1}{u^2}\right)\right]};\ \theta_r = \sqrt{1 + \chi^2}$$

$$x_{11} = u\left(1 - \frac{1}{u^2}\right)$$
$$x_{22} = \frac{u}{n^2}\left(1 - \frac{1}{u^2}\right)$$

when u=1 (i.e., at the frequency of resonance) the conjugate image impedances are real quantities: **resistive values of Z_G and Z_L are necessary for maximizing all the three gains**

When u≠1 the imaginary parts of the optimal values of Z_G and Z_L are the ones necessary for compensating the reactive parts of z_{11} and z_{22} : **the link has to be resonant for maximizing all the gains!**

IR WPT: how to maximize the performance

Optimal terminating impedances for u=1

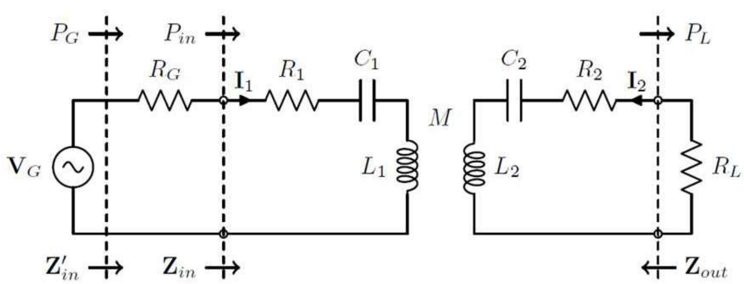

$$Z_G = R_G = Z_{c1} = \frac{X_0}{Q_1}\sqrt{1 + k^2Q_1Q_2}$$

$$Z_L = R_L = Z_{c2} = \frac{X_0}{n^2\,Q_2}\sqrt{1 + k^2Q_1Q_2}$$

All the gains are maximized and assume the same value

$$G_P = G_A = G_T = G_M = \frac{k^2Q_1Q_2}{\left|1 + \sqrt{1 + k^2Q_1Q_2}\right|^2} = \frac{\sqrt{1 + k^2Q_1Q_2} - 1}{\sqrt{1 + k^2Q_1Q_2} + 1}$$

Gain maximization: experimental validation

The primary coil has N_1 = 6 turns and an inner diameter of about 18.3 mm, the secondary coil has N_2 =2 turns and an inner diameter of about 18 mm.

The two coils are at a distance of 9.7 mm

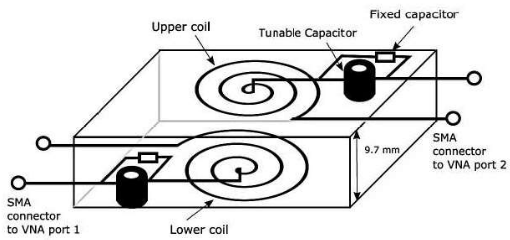

Resonant frequency f_0 (MHz)	13.65
R_G (mΩ)	0
V_G (V)	1
R_P (Ω)	2.05
R_S (Ω)	1.14
L_P (μH)	1.1
L_S (μH)	0.43
M (nH)	61.9
k	0.09
n	1.6
Q_P	46
Q_S	32.4
C_1 (pF)	123.59
C_2 (pF)	316.16

From analytical formulas

$$Z_{c1} = 7.37\Omega, Z_{c2} = 4.09\Omega, G_M = 0.567$$

Gain maximization: experimental validation

From analytical formulas

$$Z_{c1} = 7.37\Omega, Z_{c2} = 4.09\Omega, G_M = 0.567$$

Circuital simulations

$$R_G = Z_{c1} = 7.37\Omega$$
$$R_L = Z_{c2} = 4.09\ \Omega$$

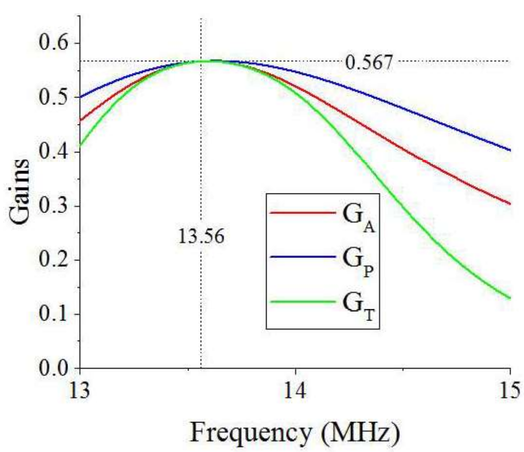

Results obtained from the measured scattering parameters

Gains realized for

$$R_G = Z_{c1} = 7.37\Omega$$
$$R_L = Z_{c2} = 4.09\Omega$$

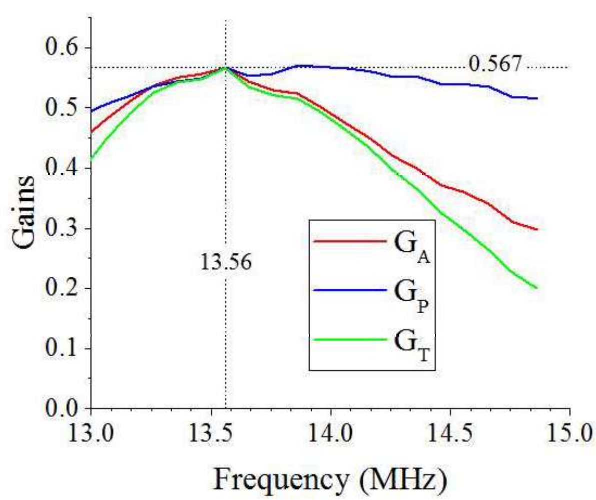

IR WPT link: possible operative regimes

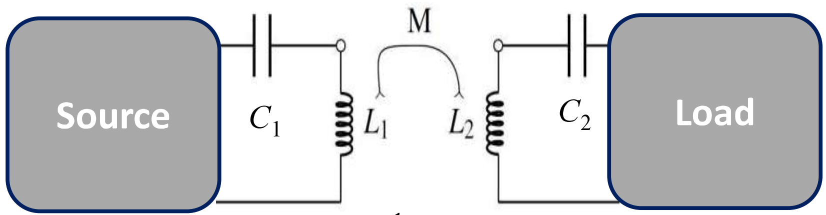

$$\omega_0 = \frac{1}{\sqrt{L_i C_i}} \quad (i = 1,2)$$

CASE 1: the link is given and the goal is to find the optimal terminating impedances for maximizing the performance

CASE 2: the load is variable and it is necessary to guarantee a constant output voltage (consider the case where the link is used to recharge a battery)

CASE 3: the load is given and the goal is to find the operating conditions for realizing performance independent of the coupling coefficient

IR WPT: load-independent regime

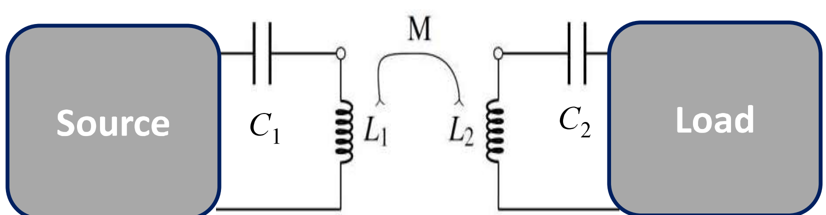

$$\omega_0 = \frac{1}{\sqrt{L_i C_i}} \quad (i = 1,2)$$

CASE 2: How to realize a load-independent voltage gain

Goal: find the optimal operating frequency to guarantee a load-independent voltage gain

IR WPT: load-independent regime

WPW 2019 — WPW SCHOOL

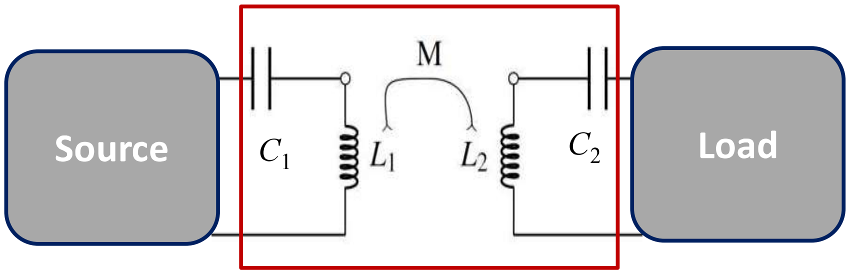

The ABCD matrix is used to represent the link

$$V_1 = AV_2 - BI_2$$
$$I_1 = CV_2 - DI_2$$

Depending on the source (voltage or current source), two different voltage gains can be introduced

$$Voltage\ source:\ G_{VV} = \frac{V_2}{V_1} = \frac{R_L}{AR_L + B}$$

$$Current\ source:\ G_{VI} = \frac{V_2}{I_1} = \frac{R_L}{CR_L + D}$$

IR WPT: load-independent regime

WPW 2019 — WPW SCHOOL

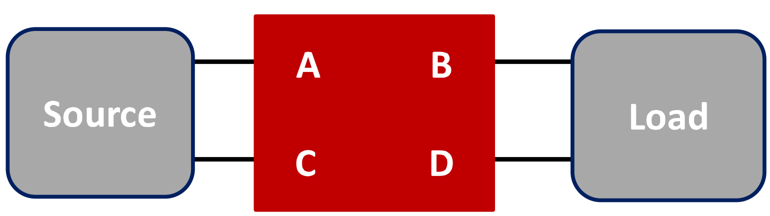

Conditions for a generic two-port network

$$V_1 = AV_2 - BI_2$$
$$I_1 = CV_2 - DI_2$$

Condition for a load-independent Voltage Controlled Voltage Gain (VCVG)

$$Voltage\ source:\ G_{VV} = \frac{V_2}{V_1} = \frac{R_L}{AR_L + B} \quad \Rightarrow \quad G_{VV} = \frac{1}{A} \text{ for } \boldsymbol{B = 0}$$

Condition for a load-independent Current Controlled Voltage Gain (CCVG)

$$Current\ source:\ G_{VI} = \frac{V_2}{I_1} = \frac{R_L}{CR_L + D} \quad \Rightarrow \quad G_{VI} = \frac{1}{C} \text{ for } \boldsymbol{D = 0}$$

WPW 2019

IR WPT: load-independent regime

WPW SCHOOL

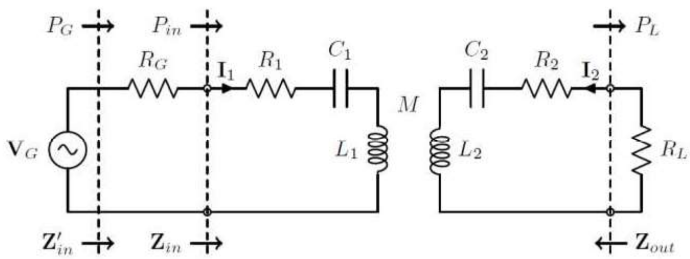

STEP 1: calculation of the frequency/ies for nullifying the ABCD parameters in the lossless case (otherwise complex frequency/ies may be obtained)

Step 2: Feasibility check for the lossy case by inspection of the variables of interest in the lossy case

WPW 2019

Load-independent regime: lossless case

WPW SCHOOL

$$M = k\sqrt{L_1 L_2}$$

$$\omega_0 = \frac{1}{\sqrt{L_i C_i}} \quad (i = 1{,}2)$$

$$u = \frac{\omega}{\omega_0}$$

Lossless case: $R_1 = R_2 = 0$

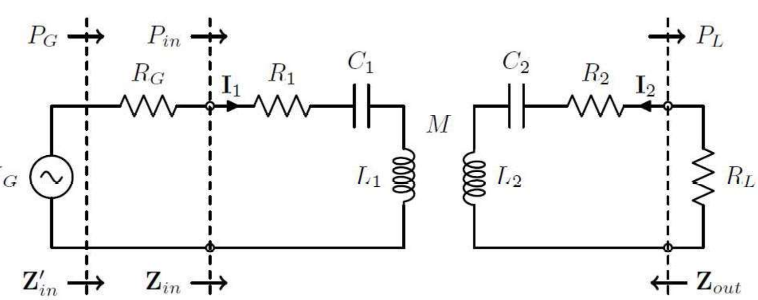

In the lossless case the ABCD parameters are

$$ABCD = \begin{pmatrix} \frac{n\,(u^2-1)}{k\,u^2} & \boxed{-\frac{j\,(k\,u^2-u^2+1)\,(k\,u^2+u^2-1)}{k\,n\,u^3}} \\ -\frac{j\,n}{k\,u} & \boxed{\frac{(u-1)\,(u+1)}{k\,n\,u^2}} \end{pmatrix}$$

Load-independent regime: lossless case

WPW 2019 WPW SCHOOL

Condition for a load-independent Voltage Controlled Voltage Gain (VCVG)

$$B = -\frac{j(ku^2 - u^2 + 1)(ku^2 + u^2 - 1)}{knu^3} = 0 \Rightarrow \boldsymbol{u_{L,H}} = \frac{\boldsymbol{\omega}}{\boldsymbol{\omega_0}} = \frac{\mathbf{1}}{\sqrt{\mathbf{1} \pm \boldsymbol{k}}}$$

$$\boxed{V_2(u = u_L) = -\frac{V_1}{n}} \qquad \boxed{V_2(u = u_H) = \frac{V_1}{n}}$$

Condition for a load-independent Current Controlled Voltage Gain (CCVG)

$$D = \frac{(u-1)(u+1)}{knu^2} = 0 \Rightarrow \boldsymbol{u} = \frac{\boldsymbol{\omega}}{\boldsymbol{\omega_0}} = 1$$

$$\boxed{V_2(u = 1) = -jkI_1\sqrt{\frac{L_2}{C_1}} = -j\frac{k}{n\omega_0}I_1}$$

Load-independent regime: lossy case

WPW 2019 WPW SCHOOL

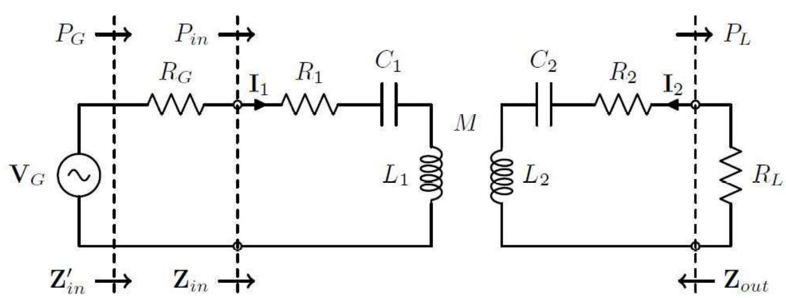

$$M = k\sqrt{L_1 L_2}$$

$$\omega_0 = \frac{1}{\sqrt{L_i C_i}} \quad (i = 1,2)$$

$$u = \frac{\omega}{\omega_0}, \quad n = \sqrt{\frac{L_1}{L_2}}, \quad X_0 = \sqrt{\frac{L_1}{C_1}}$$

Lossy case: $(R_1, R_2) \neq 0$

$$\begin{aligned}
A &= \frac{n\,(u^2-1)}{k\,u^2} - j\,\frac{n}{k\,u\,Q_P} \\
B &= \frac{c\,(u^2-1)}{k\,n\,u^2\,d} + j\,\frac{d\,[(1-k^2)\,u^4 - 2\,u^2 + 1] - u^2}{k\,n\,u^3\,d} \\
C &= -\frac{j\,n}{k\,u} \\
D &= \frac{(u^2-1)}{k\,n\,u^2} - j\,\frac{1}{k\,n\,u\,Q_S},
\end{aligned}$$

$$\boxed{Q_p = \frac{X_0}{R_1}}$$ *Quality factor of the primary resonator*

$$\boxed{Q_S = n^2\frac{X_0}{R_2}}$$ *Quality factor of the secondary resonator*

$$\boxed{Q_L = n^2\frac{X_0}{R_L}}$$ *Quality factor of the load*

Load-independent regime: lossy case

In the lossless case it has been shown that

A VCVG scheme is obtained at

$$\boldsymbol{u_{L,H} = \frac{1}{\sqrt{1 \pm k}}}$$

In the lossy case the expressions of the output voltage at these frequencies are

$$V_2(u = u_L) = -\frac{(knQ_1Q_2)/Q_L}{k(Q_1 + Q_2) + \frac{n^2}{Q_L}\left(kQ_1Q_2 + jQ_1\sqrt{1+k}\right) - j\sqrt{1+k}} V_1$$

$$V_2(u = u_H) = \frac{(knQ_1Q_2)/Q_L}{k(Q_1 + Q_2) + \frac{n^2}{Q_L}\left(kQ_1Q_2 - jQ_1\sqrt{1-k}\right) - j\sqrt{1-k}} V_1$$

$$Q_L = n^2 \frac{L_1\omega_0}{R_L}$$

WPW 2019

Load-independent regime: lossy case

WPW SCHOOL

In the lossless case it has been shown that

A CCVG scheme is obtained at

$$\boldsymbol{u_0 = 1}$$

In the lossy case the expressions of the output voltage at this frequency is

$$V_2(u = 1) = j\frac{kL_1\omega_0}{n\left(1 + \frac{1}{n^2Q_1R_L}\right)} I_1$$

In the general case the output voltage depends on R_L!

Load-independent regime: lossy case

If the quality factors satisfy the condition

$$n^2 \frac{Q_i}{Q_L} \gg 1, \qquad i = 1{,}2 \quad \Rightarrow \quad R_L \gg R_1, \qquad R_L \gg \frac{R_2}{n^2}$$

the output voltage assumes the following asymptotic expressions:

$$V_2(u = u_L) = -\frac{1}{n\left(1 + j\dfrac{\sqrt{1+k}}{kQ_1}\right)} V_1$$

$$V_2(u = u_H) = \frac{1}{n\left(1 - j\dfrac{\sqrt{1-k}}{kQ_1}\right)} V_1$$

$$V_2(u = 1) = j\frac{kL_1\omega_0}{n} I_1$$

In this case a load-independent output voltage is obtained: both the VCVG and the CCVG schemes are feasible if the load is above a threshold value which depends on the quality factors of the link

Load-independent regime: summary

For a realistic link a load-independent voltage gain can be realized only for values of the load satisfying the condition

$$n \frac{Q_i}{Q_L} \gg 1, \qquad i = 1{,}2$$

In most WPT links the inductances L_1 and L_2 assume the same value (n=1) and the resistances modelling the inductor losses are of the order of a few ohms or smaller

$\Downarrow$

values of R_L of the order of a few tens of ohms are sufficient to make feasible the VCVG and CCVG schemes.

V_1	$u_H = \frac{1}{\sqrt{1-k}}$ $u_L = \frac{1}{\sqrt{1+k}}$ $V_{2L} = -\frac{1}{n\,(1+j\,\frac{\sqrt{1+k}}{k\,Q_P})} V_1$ $V_{2H} = \frac{1}{n\,(1-j\,\frac{\sqrt{1-k}}{k\,Q_P})} V_1$ VCVG for $\frac{n\, r_L}{r_i} \gg 1$
I_1	$u = 1$ $V_2 = j\frac{k\,X_P}{n} I_1$ CCVG for $\frac{n\, r_L}{r_i} \gg 1$

Alessandra Costanzo, Marco Dionigi, Franco Mastri, Mauro Mongiardo, Giuseppina Monti, Johannes A. Russer, Peter Russer, and Luciano Tarricone, "Conditions for a Load–independent Operating Regime in Resonant Inductive WPT," *IEEE Transactions on Microwave Theory and Techniques,* Volume 65, Issue 4, April 2017, pp. 1066-1076.

Load-independent regime: measurements

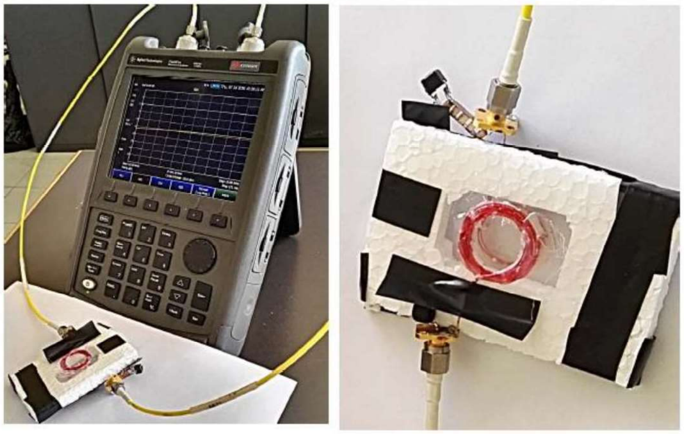

Parameter	experiment in Fig. 7
Resonant frequency f_0 (MHz)	13.65
R_G (mΩ)	0
V_G (V)	1
R_P (Ω)	2.05
R_S (Ω)	1.14
L_P (μH)	1.1
L_S (μH)	0.43
M (nH)	61.9
k	0.09
n	1.6
Q_P	46
Q_S	32.4
C_1 (pF)	123.59
C_2 (pF)	316.16

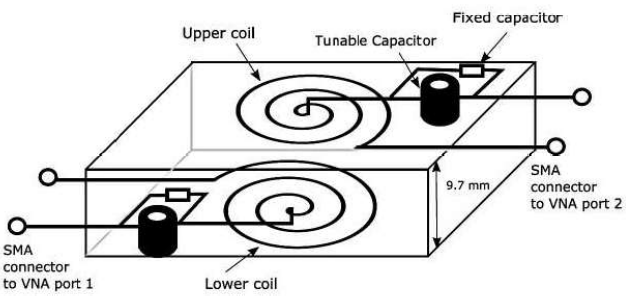

Load-independent regime: measurements

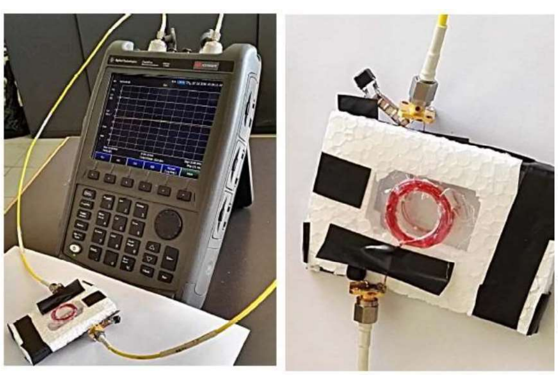

$$R_L \gg nR_1 = 3.3\Omega, \quad R_L \gg \frac{R_2}{n} = 0.7\Omega$$

$$f_0 = 13.65\ MHz, f_L = 13.07\ MHz, f_H = 14.31\ MHz$$

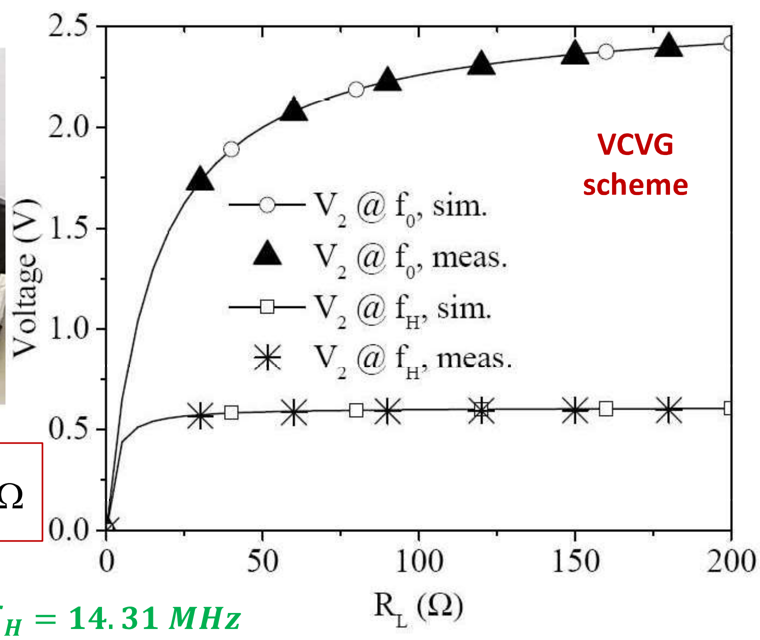

IR WPT link: possible operative regimes

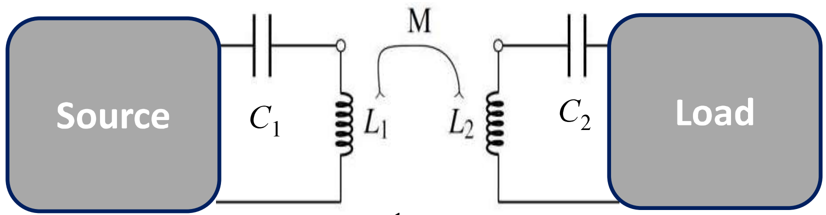

$$\omega_0 = \frac{1}{\sqrt{L_i C_i}} \; (i = 1{,}2)$$

CASE 1: the link is given and the goal is to find the optimal terminating impedances for maximizing the performance

CASE 2: the load is variable and it is necessary to guarantee a constant output voltage (consider the case where the link is used to recharge a battery)

CASE 3: the load is given and the goal is to find the operating conditions for realizing performance independent of the coupling coefficient

Fixed frequency schemes

Fixed frequency schemes

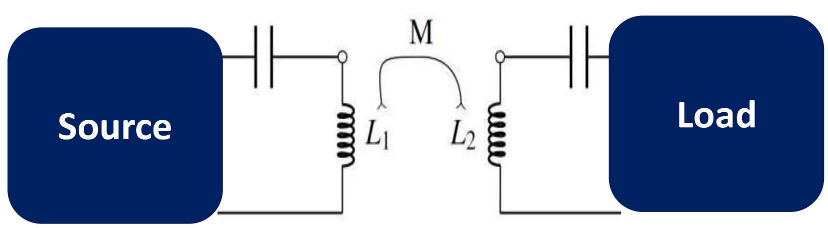

Power output is maximized by using:
TX and RX ***syncronous*** resonators.
The resonant frequency is the WPT operating frequency.

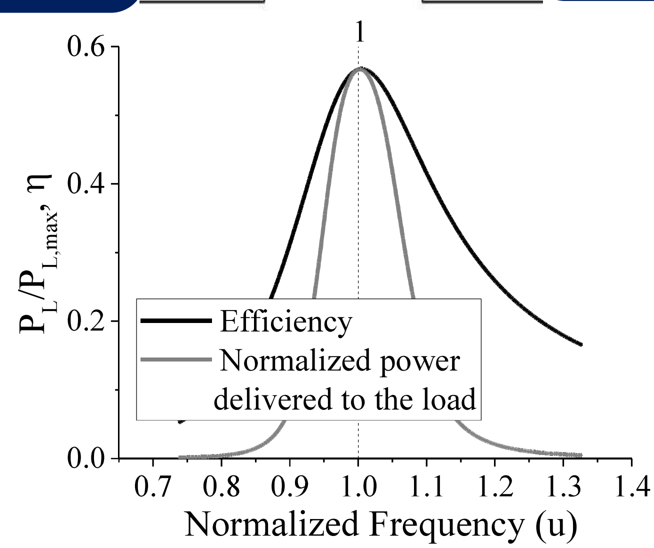

Fixed frequency schemes

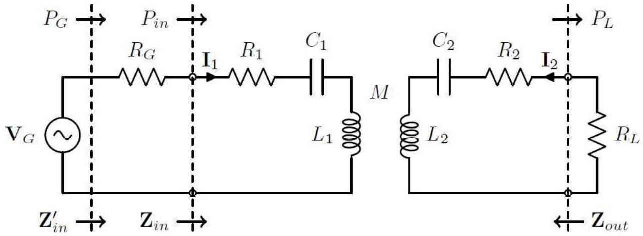

$$\omega_0 = \frac{1}{\sqrt{L_i C_i}} \; (i = 1,2) \qquad M = k\sqrt{L_1 L_2}$$

At ω_0 (main resonance) the input impedance is purely resistive

$$Z_{in}(\omega = \omega_0) = R_1 + \frac{k^2 \omega_0{}^2 L_1 L_2}{R_L}$$

main resonant frequency: the coupled resonators behave as an immittance inverter whose inversion constant is proportional to k^2.

Operating at ω_0 leads to a coupling-dependent performance!

Goal: Find the conditions for additional resonances (secondary resonances)

$$Z_{in}(\omega) = R_{in} + jX_{in}$$

Solve for $X_{in} = 0$

IR WPT link: coupling-independent regime

Goal

Find new possible operating resonant frequencies for achieving a **coupling-independent regime**

$$\Downarrow$$

Performance in terms of power on the load (PL) and efficiency ($\eta = \frac{P_L}{P_{in}}$) inpendent of k

It is necessary to study the frequency behaviour of the link

IR WPT: frequency splitting

WPW 2019

WPW SCHOOL

f_0 (kHz)	R_G (Ω)	R_i (Ω)	Q_1	Q_2	R_L (Ω)	$L_1 = L_2$ (μH)	$C_1 = C_2$ (nF)
24.48	0.98	0.83	23.7	20.8	1.33	128	330

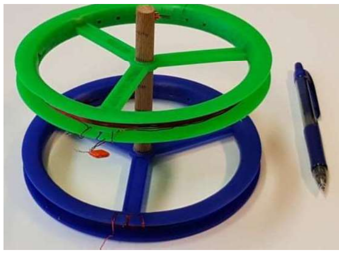

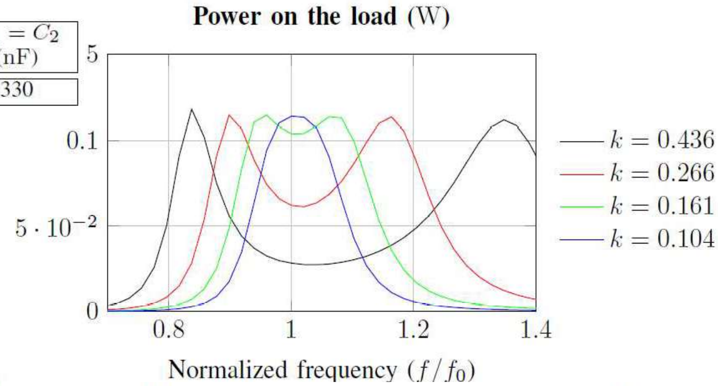

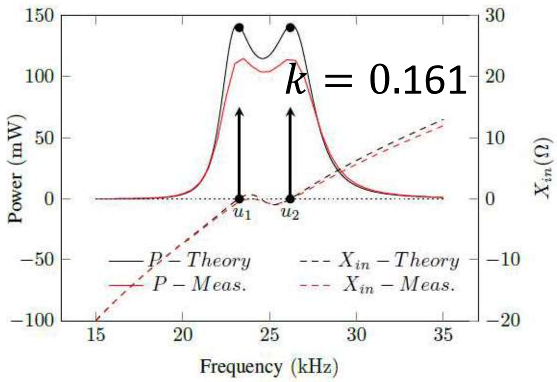

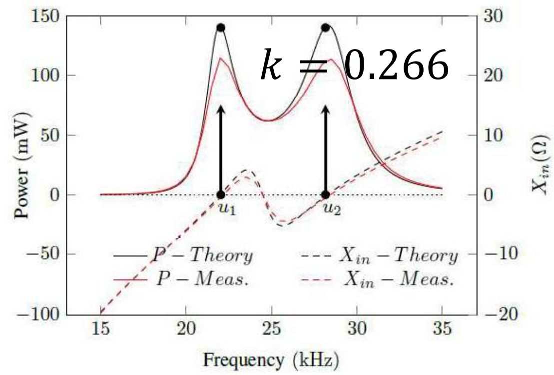

Wang-Qiang Niu, Jian-Xin Chu, Wei Gu, and Ai-Di Shen, "Exact Analysis of Frequency Splitting Phenomena of Contactless Power Transfer Systems," IEEE TRANSACTIONS ON CIRCUITS AND SYSTEMS—I: REGULAR PAPERS, VOL. 60, NO. 6, JUNE 2013.

IR WPT link: secondary resonances

WPW 2019

WPW SCHOOL

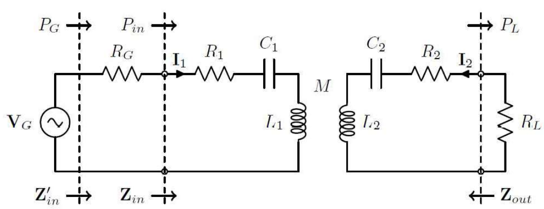

$$R_{in} = X_0 r_1 + X_0 \frac{k^2 u^4 r_{2T}}{u^4 - (2 - r_{2T}^2) u^2 + 1},$$

$$X_{in} = X_0 \frac{(u^2 - 1)\left[(1 - k^2)u^4 - (2 - r_{2T}^2)u^2 + 1\right]}{u\left[u^4 - (2 - r_{2T}^2)u^2 + 1\right]}$$

Two secondary resonances, u_1 and u_2, exist if the following conditions are satisfied

Condition on the load

$$r_{2T} = \left(\frac{1}{Q_2} + \frac{1}{Q_L}\right) < \sqrt{2}$$

Condition on the coupling

$$k \geq k_b = r_{2T}\sqrt{1 - \frac{r_{2T}{}^2}{4}}$$

X_{in} = 0 for: $u_1, u_2 = \sqrt{\dfrac{2 - r_{2T}^2 \pm \sqrt{4k^2 + r_{2T}^4 - 4r_{2T}^2}}{2(1 - k^2)}}$

Input reactance map with respect to k and u

frequency bifurcation takes place where the zero-reactance curves converge

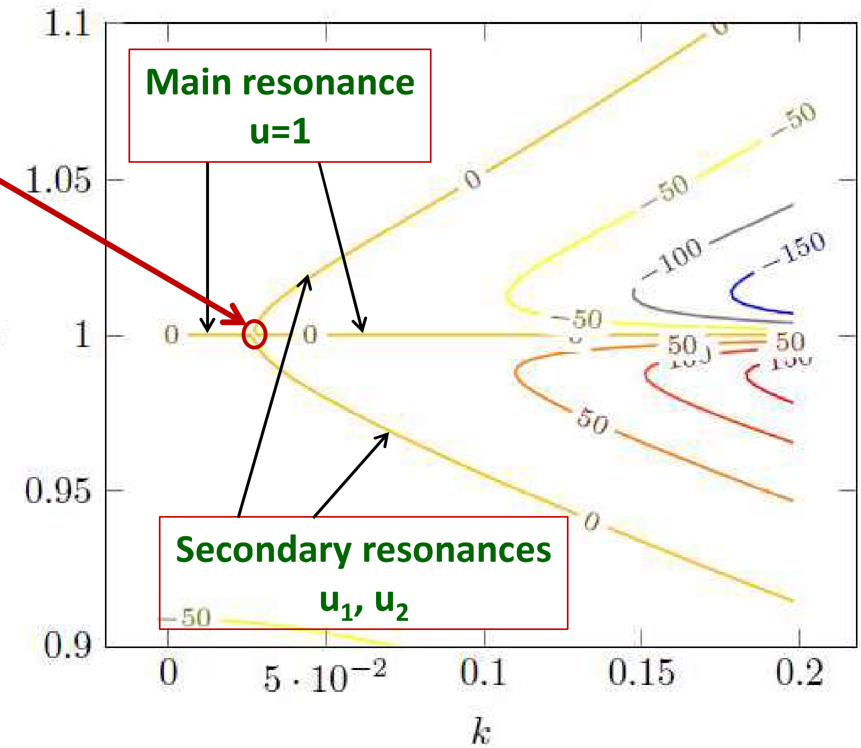

F. Mastri, A. Costanzo, M. Mongiardo, "Coupling-Independent Wireless Power Transfer," IEEE Microwave and Wireless Components Letters, Volume: 26, Issue: 3, March 2016).

Frequency-agile operating scheme

A Coupling-independent performance can be realized by adopting a frequency-agile scheme: the operating frequency is varied so to operate at the secondary resonances

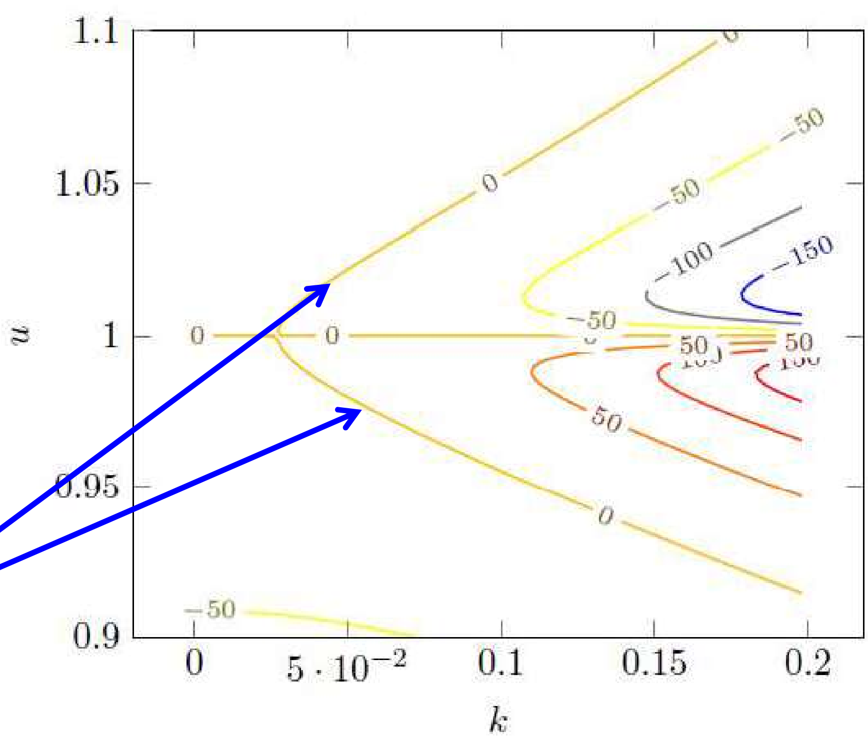

Input impedance at the secondary resonances

WPW 2019 — WPW SCHOOL

main resonant frequency: the coupled resonators behave as an immittance inverter whose inversion constant is proportional to k^2.

$$Z_{in}(\omega = \omega_0) = R_1 + \frac{k^2 {\omega_0}^2 L_1 L_2}{R_L}$$

At the secondary resonances ω_1 and ω_2 the input impedance is

$$Z_{in}(\omega = \omega_{1,2}) = R_1 + \frac{L_1}{L_2}(R_2 + R_L)$$

At the secondary resonances the coupled resonators behave as an **ideal transformer** with transform ratio $n = \sqrt{\frac{L_1}{L_2}}$

Alessandra Costanzo, Wenquan Che, Marco Dionigi, Franco Mastri, Mauro Mongiardo, Giuseppina Monti Qinghua Wang, Luciano Tarricone, “Matched Resonant Inductive WPT Using the Coupling–Independent Regime: Theory and Experiments,” to be presented at EuMC 2017.

Coupling-independent regime: experimental Validation

WPW 2019 — WPW SCHOOL

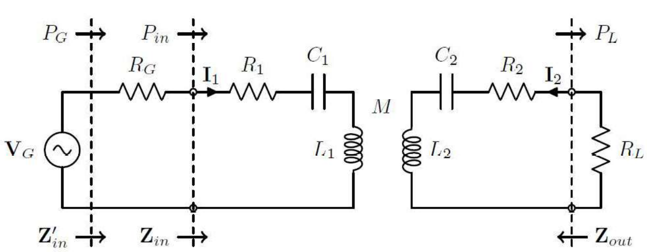

Experiment

The inductors are 20-turn air-core copper wire coils of diameter 140mm realizing an inductance of 128 μH. The capacitors are 330 nF nominal-value lumped capacitors realizing the resonance condition at f_0 =24.48 kHz.

f_0 (kHz)	R_G (Ω)	R_i (Ω)	Q_1	Q_2	R_L (Ω)	r_{2T}	k_b	$L_1 = L_2$ (μH)	$C_1 = C_2$ (nF)
24.48	0.98	0.83	23.7	20.8	1.33	0.11	0.11	128	330

Alessio De Angelis; Marco Dionigi; Paolo Carbone; Mauro Mongiardo; Qinghua Wang; Wenquan Che; Franco Mastri; Alessandra Costanzo; Giuseppina Monti; Luciano Tarricone, “Resonant inductive WPT link operating in a coupling-independent regime,” 2017 International Applied Computational Electromagnetics Society Symposium - Italy (ACES).

Experimental validation

WPW 2019 | WPW SCHOOL

f_0 (kHz)	R_G (Ω)	R_i (Ω)	Q_1	Q_2	R_L (Ω)	r_{2T}	k_b	$L_1 = L_2$ (μH)	$C_1 = C_2$ (nF)
24.48	0.98	0.83	23.7	20.8	1.33	0.11	0.11	128	330

Mutual inductance and corresponding coupling coefficient measured at different distances

case	a	b	c	d
distance (mm)	16	33	54	75
M (μH)	55.8	34.1	20.6	13.3
k	0.436	0.266	0.161	0.104

Conditions for secondary resonances:

$r_{2T} < \sqrt{2}$ **is always met** $(for\ the\ analyzed\ case\ r_{2T} = 0.11)$

$$k \geq k_b = r_{2T}\sqrt{1 - \frac{{r_{2T}}^2}{4}} \approx r_{2T}$$ **Satisfied by the cases a, b, c**

Experimental validation

WPW 2019 | WPW SCHOOL

f_0 (kHz)	R_G (Ω)	R_i (Ω)	Q_1	Q_2	R_L (Ω)	r_{2T}	k_b	$L_1 = L_2$ (μH)	$C_1 = C_2$ (nF)
24.48	0.98	0.83	23.7	20.8	1.33	0.11	0.11	128	330

Mutual inductance and corresponding coupling coefficient measured at different distances

case	a	b	c	d
distance (mm)	16	33	54	75
M (μH)	55.8	34.1	20.6	13.3
k	0.436	0.266	0.161	0.104

Conditions for secondary resonances:

$r_{2T} < \sqrt{2}$ **is always met** $(for\ the\ analyzed\ case\ r_{2T} = 0.11)$

$$k \geq k_b = r_{2T}\sqrt{1 - \frac{{r_{2T}}^2}{4}} \approx r_{2T}$$ **Satisfied by the cases a, b, c**

Z_{in} variations with distance

WPW 2019

WPW SCHOOL

It is evident that for

$k \geq k_b = 0.11$

The link exhibits three resonances: the main resonance and two secondary resonances

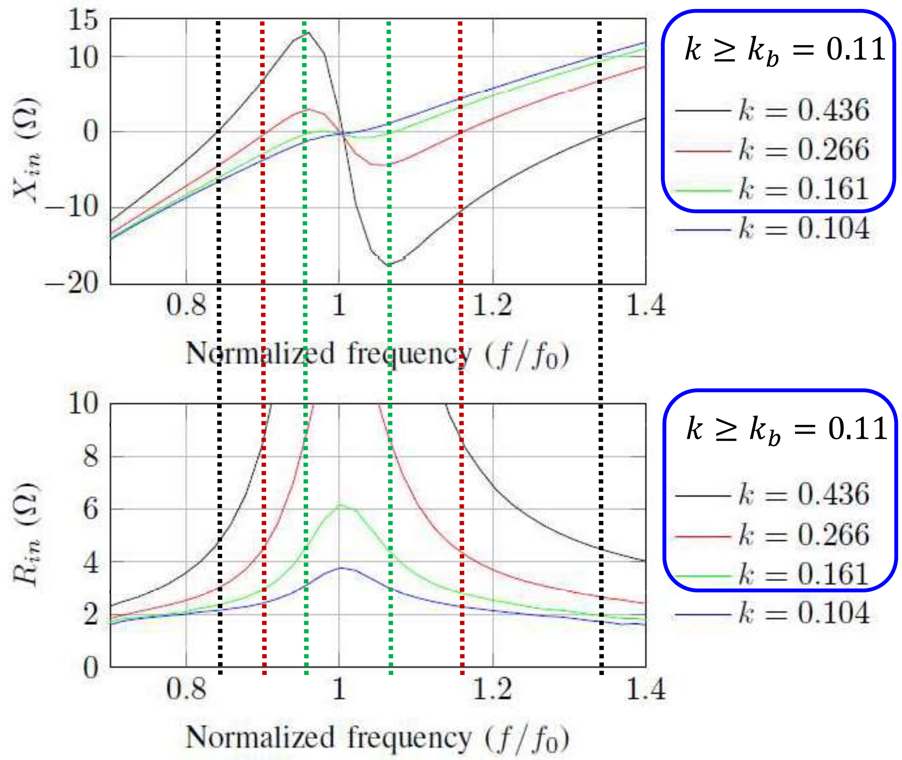

Z_{in} variations with distance

WPW 2019

WPW SCHOOL

It is evident that for

$k \geq k_b = 0.11$

The link exhibits three resonances: the main resonance and two secondary resonances

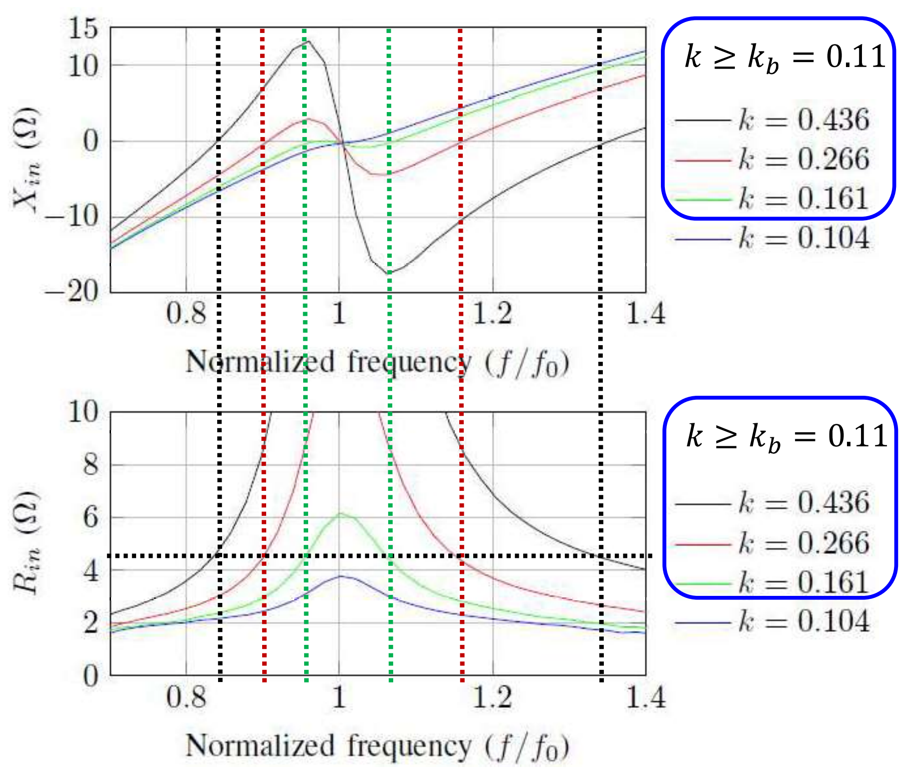

WPW 2019

Measured performance

WPW SCHOOL

Operating at the secondary resonances (see the vertical dashed lines) leads to a performance (power delivered to the load and efficiency) independent of the coupling coefficient.

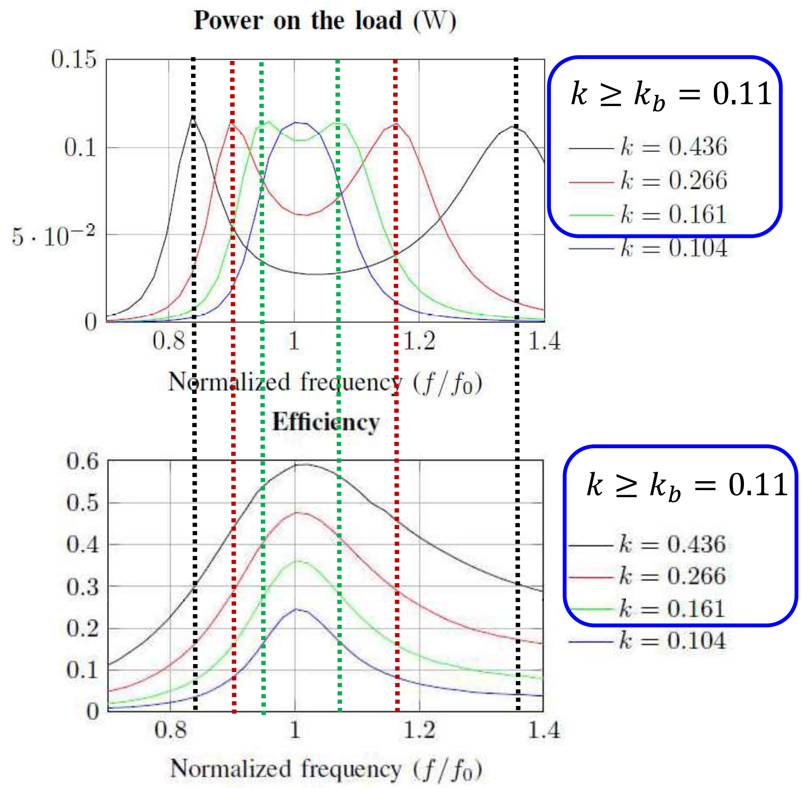

WPW 2019

Measured performance

WPW SCHOOL

Operating at the secondary resonances (see the vertical dashed lines) leads to a performance (power delivered to the load and efficiency) independent of the coupling coefficient

At the secondary resonances the measured values of P_L and η for different couplings are nearly coincident

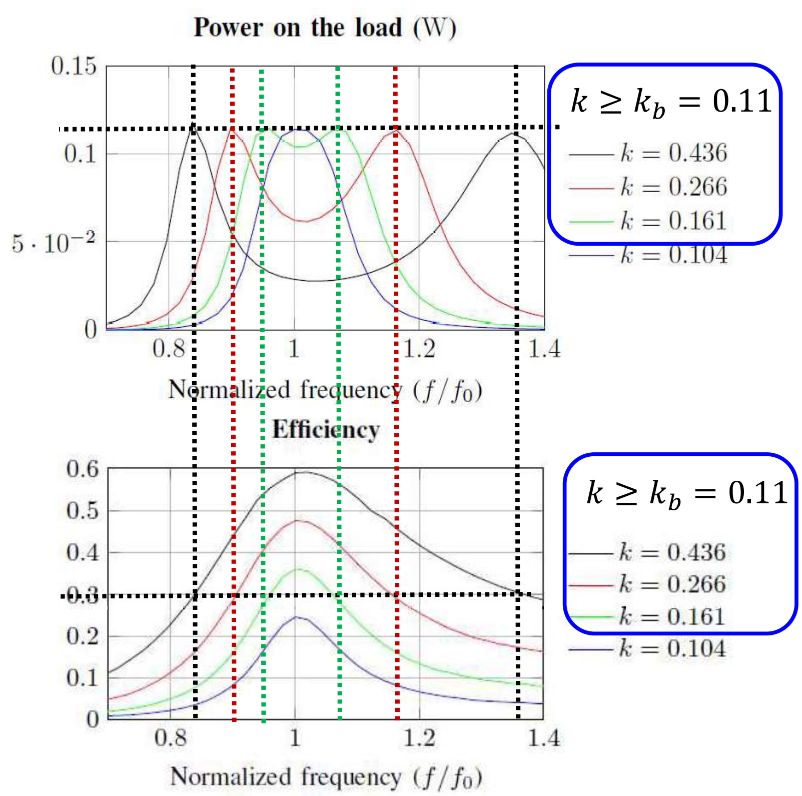

Conclusions

WPW SCHOOL

	Load	Coupling	Goal	Frequency
CASE 1	constant	constant	**MAXIMIZE THE PERFORMANCE** for **maximizing the performance** it is necessary to operate at the **main resonance** of the link.	Constant Main resonance
CASE 2	variable	constant	**ACHIEVE A LOAD INDEPENDENT OUTPUT VOLTAGE** provided that the load impedance is above a threshold value, a **load-independent output voltage** can be realized by operating at the main resonance when the source is a current generator, a different operating frequency is necessary in the case where the generator is a voltage generator	Constant CCVG (main resonance) VCVG (alternative frequencies)
CASE 3	constant	variable	**ACHIEVE A CONSTANT PERFORMANCE** for a link in an over-coupled regime **performance independent of the coupling coefficient** can be realized by adopting a frequency agile scheme where the frequency is varied so to operate at the secondary resonances.	Variable (secondary resonances)

Suggested readings

WPW SCHOOL

1. Wireless Power Transfer Algorithms, Technologies and Applications in Ad Hoc Communication Networks, Editors: Sotiris Nikoletseas; Yuanyuan Yang; Apostolos Georgiadis; Springer International Publishing, 10.1007/978-3-319-46810-5.
2. A. Costanzo, M. Dionigi, D. Masotti, M. Mongiardo, G. Monti, L. Tarricone, R. Sorrentino, "Electromagnetic Energy Harvesting and Wireless Power Transmission: A Unified Approach," *Proceedings of the IEEE*, Vol. 102, Issue 11, pp. 1692–1711, DOI: 10.1109/JPROC.2014.2355261, INSPEC Accession Number: 14682530, ISSN: 0018-9219, Oct. 2014
3. Dionigi, M., Mongiardo, M., Perfetti, R.: Rigorous network and full-wave electromagnetic modeling of wireless power transfer links. Microwave Theory and Techniques, IEEE Transactions on 63(1), 65–75 (2015). DOI 10.1109/TMTT.2014.2376555.
4. *Roberts, S.: Conjugate-image impedances, in Proc. of the IRE, 1946, 198–204.*
5. Alessandra Costanzo, Marco Dionigi, Franco Mastri, Mauro Mongiardo, Giuseppina Monti, Johannes A. Russer, Peter Russer, and Luciano Tarricone, "Conditions for a Load–independent Operating Regime in Resonant Inductive WPT," *IEEE Transactions on Microwave Theory and Techniques,* Volume 65, Issue 4, April 2017, pp. 1066-1076.
6. Wang-Qiang Niu, Jian-Xin Chu, Wei Gu, and Ai-Di Shen, "Exact Analysis of Frequency Splitting Phenomena of Contactless Power Transfer Systems," IEEE TRANSACTIONS ON CIRCUITS AND SYSTEMS—I: REGULAR PAPERS, VOL. 60, NO. 6, JUNE 2013.
7. F. Mastri, A. Costanzo, M. Mongiardo, "Coupling-Independent Wireless Power Transfer," *IEEE Microwave and Wireless Components Letters*, Volume: 26, Issue: 3, March 2016.
8. Alessandra Costanzo, Wenquan Che, Marco Dionigi, Franco Mastri, Mauro Mongiardo, Giuseppina Monti Qinghua Wang, Luciano Tarricone, "Matched Resonant Inductive WPT Using the Coupling–Independent Regime: Theory and Experiments," *EuMC 2017*.
9. Qinghua Wang, Wenquan Che , Marco Dionigi, Franco Mastri, Mauro Mongiardo, Giuseppina Monti, "Gains Maximization via Impedance Matching Networks for Wireless Power Transfer," *Progress In Electromagnetics Research*, vol. 164, 2018, pp. 135-153.
10. F. Mastri, M. Mongiardo, G. Monti, M. Dionigi, L. Tarricone, "Gain expressions for resonant inductive wireless power transfer links with one relay element," *Wireless Power Transfer*, https://doi.org/10.1017/wpt.2017.13, Published online: 12 October 2017.
11. G. Monti, P. Arcuti, L. Tarricone, "Resonant Inductive Link for Remote Powering of Pacemakers," *IEEE Transactions on Microwave Theory and Techniques*, Vol. 63, Issue 11, pp. 3814 – 3822, DOI: 10.1109/TMTT.2015.2481387, ISSN: 00189480, Nov. 2015.
12. G. Monti, L. Corchia, E. De Benedetto and L. Tarricone, "A Wearable Wireless Energy Link for Thin-Film Batteries Charging," *International Journal of Antennas and Propagation*, Vol. 2016, 9 pages, DOI: 10.1155/2016/9365756, ISSN: 16875869, 2016.

Suggested readings

12. G. Monti, W. Che, Q. Wang, M. Dionigi, M. Mongiardo, R. Perfetti, and Y. Chang, "Wireless Power Transfer Between One Transmitter and Two Receivers: Optimal Analytical Solution," *Wireless Power Transfer*, Vol. 3, Issue 1, pp. 63-73, DOI: 10.1017/wpt.2016.3, April 2016.
13. G. Monti, G., A. Costanzo, F. Mastri, M. Mongiardo and L. Tarricone, "Rigorous Design of Matched Wireless Power Transfer Links Based on Inductive Coupling," Radio Science, Vol. 51, pp. 858 – 867, DOI: 10.1002/2016RS006043, ISSN: 00486604, 2016.
14. M. Dionigi, M. Mongiardo, G. Monti, R. Perfetti, "Modeling of Wireless Power Transfer Links based on Capacitive Coupling," *International Journal of Numerical Modelling: Electronic Networks, Devices and Fields*, DOI: 10.1002/jnm.2187, ISSN: 08943370, July 2016.
15. G. Monti, A. Costanzo, F. Mastri, M. Mongiardo, "Optimal design of a Wireless Power Transfer Link using Parallel and Series Resonators," *Wireless Power Transfer*, 2016. DOI: 10.1017/wpt.2016.7 (About DOI), Vol. 3, Issue 2, 2016, pp. 105-116.
16. G. Monti, L. Corchia, L. Tarricone, M. Mongiardo "A Network Approach for Wireless Resonant Energy Link Using Magneto–inductive Guides," *IEEE Transactions on Microwave Theory and Techniques*, Vol. 64 , Issue 10, pp. 3271-3279, DOI: 10.1109/TMTT.2016.2601092, ISSN: 00189480, October 2016.
17. Giuseppina Monti, Wenquan Che, Qinghua Wang, Alessandra Costanzo, Franco Mastri, Mauro Mongiardo, Renzo Perfetti, Luciano Tarricone, and Yumei Chang, "Wireless Power Transfer with Three-Ports Networks: Optimal Analytical Solutions," *IEEE Transactions on Circuits and Systems-I: Regular Papers*, Vol. 64, Issue 2, August 2016, pp. 494-503, DOI: 10.1109/TCSI.2016.2603187, Feb. 2017.
18. Giuseppina Monti, Marco Dionigi, Mauro Mongiardo, Renzo Perfetti, "Optimal Design of Wireless Energy Transfer to Multiple Receivers: Power Maximization," *IEEE Transactions on Microwave Theory and Techniques*, Vol. 65, Issue: 1, DOI: 10.1109/TMTT.2016.2614511, ISSN: 00189480, Jan. 2017.
19. Giuseppina Monti, Luciano Tarricone, Mauro Mongiardo, "Two-port network approach for a Wireless Power Transfer Link Using a Cascade of Inductively Coupled Resonators," in *International Journal of Numerical Modelling: Electronic Networks*, *Devices and Fields*, January 2017.
20. Alessandra Costanzo, Marco Dionigi, Franco Mastri, Mauro Mongiardo, Giuseppina Monti, Johannes A. Russer, Peter Russer, and Luciano Tarricone, "Conditions for a Load–independent Operating Regime in Resonant Inductive WPT," *IEEE Transactions on Microwave Theory and Techniques*, Volume 65, Issue 4, April 2017, pp. 1066-1076.
21. Nuno Borges Carvalho, et al., "Europe and the Future for WPT: European Contributions to Wireless Power Transfer Technology," *IEEE Microwave Magazine*, 18(4): 56 – 87, May 2017, DOI: 10.1109/MMM.2017.2680078.
22. G. Monti, M. V. De Paolis, L. Corchia, M. Mongiardo, L. Tarricone, "Inductive Link for Power and Data Transfer to a Medical Implant," *Wireless Power Transfer*, DOI: 10.1017/wpt.2016.7.

Analytical and numerical design of non-static WPT systems

Alessandra Costanzo
University of Bologna

In this lecture the analytical characterization of an inductive resonant link is presented and the system figures of merit are parametrically represented as a function of a set of circuital parameters. The lecture demonstrates the need for a system-as-whole design at the circuit level, with the actual RF link terminations, consisting of the nonlinear power source and the RF-dc converter. Design solutions for industrial applications, such as the wireless powering of rotating or sliding tools are studied and the achievable performance in dynamic conditions are discussed.

WPW 2019

WPW SCHOOL

Analytical and numerical design of non-static WPT systems

Alessandra Costanzo

University of Bologna (Italy)

alessandra.costanzo@unibo.it

Imperial College, LONDON June 17, 2019

WPW 2019

WPW SCHOOL

CONTENTS

- ❑ Introduction to Wireless Power Transfer (WPT)
- ❑ The circuit-level description of an entire WPT link
- ❑ WPT inductive resonant (IR) link
- ❑ IR-WPT link performance at variable distance and load
- ❑ The transmitter and receiver design
- ❑ TWO EXAMPLES:
  - ❑ A rotating tool combining data and power transfer
  - ❑ A sliding chart
- ❑ DC-to-DC IR-WPT system design
- ❑ Conclusion

WPT BASICS

- Power transmitted <u>without conductors</u> using time-varying electromagnetic fields

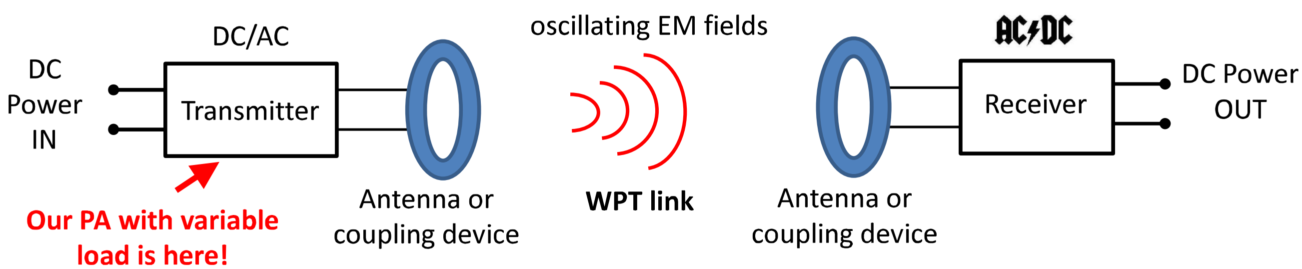

- Many advantages in “cutting the cord”: free positioning, simultaneous charging of multiple devices of different type, powering electrical devices not accessible by cables (e.g. hazardous sites, implantable medical devices etc. ...), remote powering ....

Transmission of POWER rather than information → How much power? Is it safe? → Regulations for environmental and public safety

Transmission of POWER rather than information → Efficiency? Distance? Direction? Frequency? Technology? → **Different types of WPT**

WPT CLASSIFICATION

- **Near field** - non radiative techniques
- **Far field** – radiative techniques

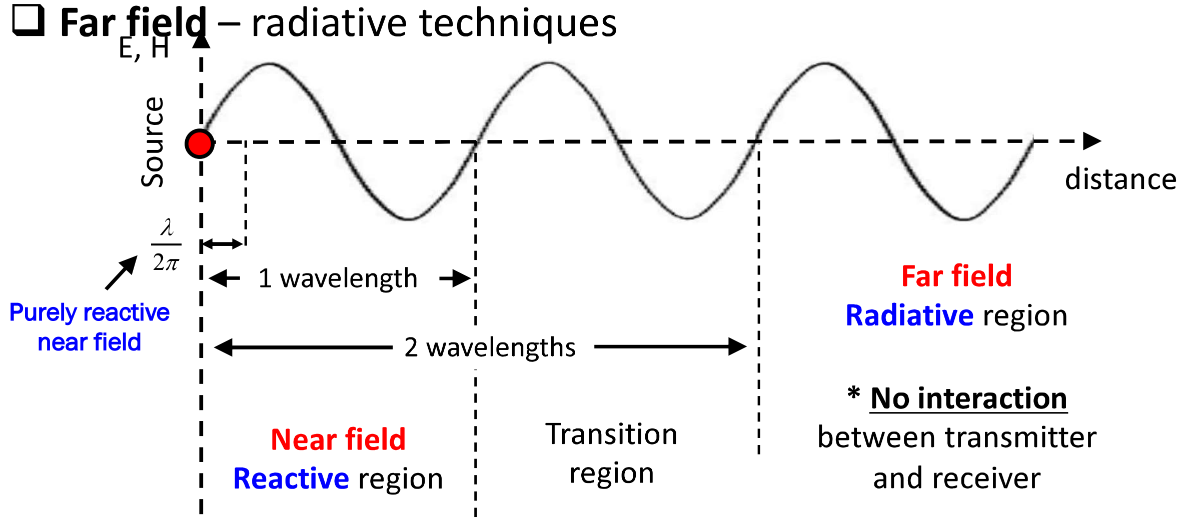

* **Interaction** between transmitter and receiver

* This makes a difference for the Power Amplifier (PA) in the transmitter: **fixed/variable load regime**

NEAR-FIELD NON-RADIATIVE WPT

- The oscillating EM fields stay very close to the coupling device (**almost no radiation**)
- **Power** is non directive and **vanishes very rapidly** with distance ($1/r^3$)
- **Interaction** between TX and RX: with no receiver coupled in the immediate vicinity, the power delivered to the field is sent back to the receiver, **purely reactive region**

How can I transfer Power?

- **Inductive coupling** (magnetic induction, MI): power is transmitted by an oscillating **magnetic** field **between coils of wire**
- **Capacitive coupling** (electrostatic induction): power is transmitted by an oscillating **electric** field between **electrodes** (e.g. metal plates).

  - Pros and cons for both techniques
  - Both used in commercial applications and investigated by research
  - Inductive coupling more successful

WPT SYSTEM EFFICIENCY

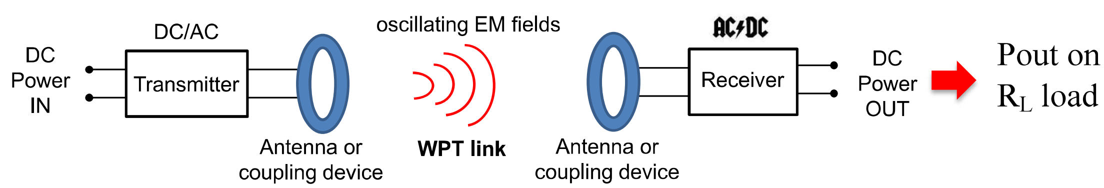

$$\eta_{WREL} = \eta_{DC-RF} \cdot \eta_{RF-RF} \cdot \eta_{RF-DC}$$

PA efficiency | **IR-link efficiency** | **rectifier efficiency**

WPT link configurations can vary [2]:

- Variable link distance
- Link misalignment
- Orientation angle

→ Coupling factor (k) variations →

- Variable equivalent loading resistance R_L

→ Variations of η_{RF-RF}, Pout, η_{DC-RF} and η_{WREL}

[2] A. Costanzo et al., "Electromagnetic Energy Harvesting and Wireless Power Transmission: A Unified Approach," in Proceedings of the IEEE, vol. 102, no. 11, pp. 1692-1711, Nov. 2014.

RF-RF EFFICIENCY AND QULITY FACTORS

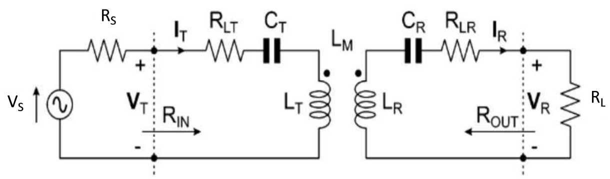

$$P_T = \mathrm{Real}\left\{\frac{1}{2}\mathbf{V}_T\mathbf{I}_T^*\right\}$$ Power delivered to TX coil

$$P_R = \mathrm{Real}\left\{\frac{1}{2}\mathbf{V}_R\mathbf{I}_R^*\right\} = 4P_R^{AV}\frac{R_{OUT}R_L}{(R_{OUT}+R_L)^2}$$

Power delivered to R_L

@ resonance ω_0

$$\omega_0 = \frac{1}{\sqrt{L_T C_T}} = \frac{1}{\sqrt{L_R C_R}}$$ Resonant frequency

$$L_M = k\sqrt{L_T L_R} = \frac{\chi_T k}{n\omega_0}$$ Mutual inductance

$$\chi_i = \frac{V_{Li}}{I_i} = \frac{V_{Ci}}{I_i} = \sqrt{\frac{L_i}{C_i}}$$ Resonator slope parameter

$$n = \sqrt{\frac{L_T}{L_R}} = \sqrt{\frac{\chi_T}{\chi_R}}$$ Transform ratio

$$\eta_{RF-RF} = \frac{P_R}{P_T} = \frac{\chi_T^2 k^2 R_L}{(R_{LR}+R_L)\left[n^2 R_{LT}(R_{LR}+R_L)+\chi_T^2 k^2\right]}$$

$$= \frac{\omega_0^2 {L_M}^2 R_L}{(R_{LR}+R_L)\left[R_{LT}(R_{LR}+R_L)+\omega_0^2 {L_M}^2\right]}$$

WPW 2019

WPW SCHOOL

RF-RF EFFICIENCY IS DEIFINED BY THE PRODUCT OF KQ

$$\eta_{RF-RF} = \frac{P_R}{P_T} = \frac{k^2 \cdot Q_T Q_{R-LOADED}}{1+k^2 \cdot Q_T Q_{R-LOADED}} \cdot \frac{Q_{R-LOADED}}{Q_{LOAD}}$$

Increases with *k* →

Maximized for :

For $Q_T Q_{R-LOADED} >> 1/k^2$ →

$$\eta_{MAX} = Q_{R-LOADED}/Q_{LOAD}$$

$$Q_T Q_{R-LOADED} >> 1/k^2$$

$$\eta_{RF-RF} = \eta_{MAX}/2$$

$$R_{IN} = \frac{V_T}{I_T} = R_{LT} + \frac{\omega_0^2 {L_M}^2}{(R_{LR}+R_L)} = R_{LT} + \frac{\chi_T^2 k^2}{n^2(R_{LR}+R_L)}$$ @ ω_0 depends on ***k***

- ❑ η_{RFRF} depends on load (R_L) and coupling factor (k)
- ❑ Different WPT optimum system *LOAD* for:
  - *maximum* power delivered to the load (MPDL)
  - *maximum* RF-to-RF efficiency (MPTE)

Quality factors

$$Q_{R-LOADED} = \frac{\chi_R}{R_{LR}+R_L} = \frac{\omega_0 L_R}{R_{LR}+R_L}$$

$$Q_{T-LOADED} = \frac{\chi_T}{R_{LT}+R_S} = \frac{\omega_0 L_T}{R_{LT}+R_S}$$

$$Q_T = \frac{\chi_T}{R_{LT}} = \frac{\omega_0 L_T}{R_{LT}} \qquad Q_R = \frac{\chi_R}{R_{LR}} = \frac{\omega_0 L_R}{R_{LR}}$$

$$Q_{LOAD} = \frac{\chi_R}{R_L} = \frac{\omega_0 L_R}{R_L}$$

C. Florian; F. Mastri; R. P. Paganelli; D. Masotti; A. Costanzo, "Theoretical and Numerical Design of a Wireless Power Transmission Link With GaN-Based Transmitter and Adaptive Receiver," IEEE Transactions on Microwave Theory and Techniques, Year: 2014, Volume: 62, Issue: 4

A. Costanzo, M. Dionigi, F. Mastri, M. Mongiardo, J. Russer, P. Russer, "Design of magnetic-resonant wireless power transfer links realized with two coils: a comparison of solutions, Int. Jour. of Microwave and Wireless Technologies, 2015, pp: 349–359

MAXIMIZING kQ

- k depends only on the geometries (distance included)
  - There is an optimum size and shape to maximize k for a certain distance
  - Use specially shaped coils (i.e. conformal to the magnetic field)
- $Q_{\mathrm{x}} = \omega \mathrm{L_x}/\mathrm{R_x}$
  - Generally, maximize the coil area ($\mathrm{L_x} \uparrow$) in the space available, but minimize the conductor length ($\mathrm{R_x} \downarrow$)
  - Maximize the number of turns $\mathrm{N_x}$: $\mathrm{L_x} \propto \mathrm{N_x}^2$, but $\mathrm{R_x} \propto \mathrm{N_x}$ and $k(\mathrm{N_x}) \sim \mathrm{const}$
  - Choose an optimal frequency
  - Q is maximized when radiation begins to dominate losses for a certain size, but then the coil impedance is affected by parasitics
  - It is usually advised to use the highest frequency with a linear reactance
  - This push the need of MHz power electronics
- One bigger coil at a fixed distance can lower k but still increase kQ
- k and Q are not mutually independent and an EM optimization of the inductive link should be performed

ROTATING TOOLS IN AN AUTOMATIC MACHINE

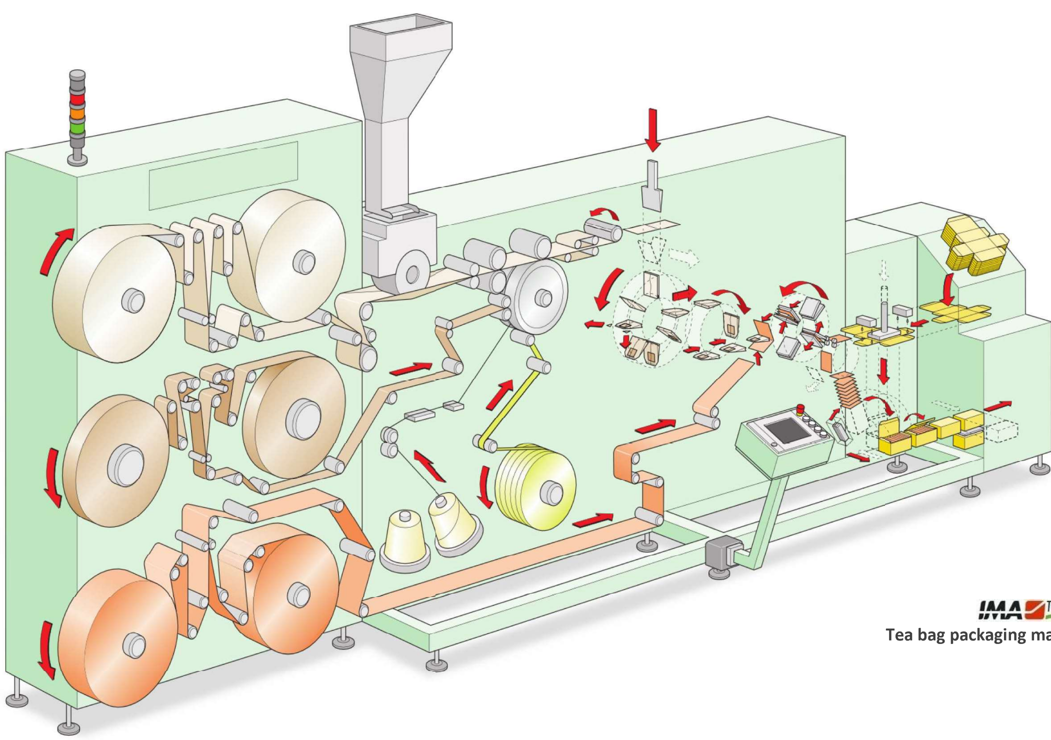

IMA TEA&COFFEE
Tea bag packaging machine

OTHER INDUSTRIAL WPT APPLICATIONS

Linear-track CET unit
The movable core is free to move along the primary loop (multiple cores can also be included)

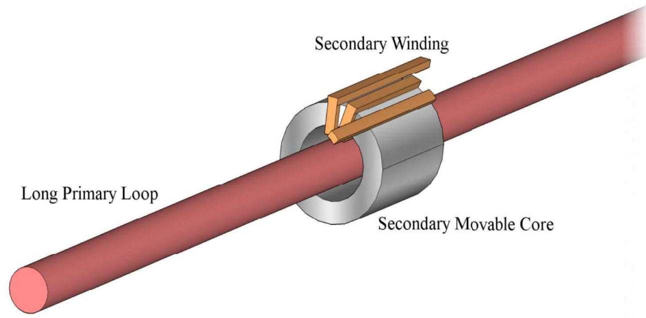

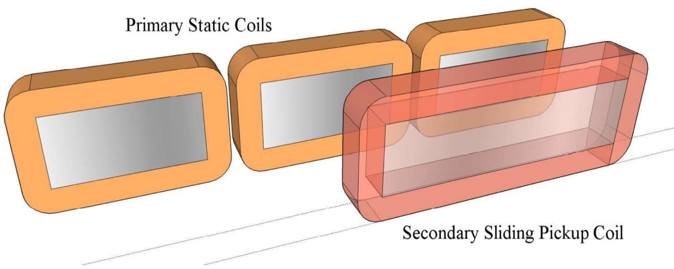

Sliding CET unit
The pickup coil always faces two or more static coils (multiple pickup coils can also be included)

WPW 2019
WPW SCHOOL

ROTATING SEALER

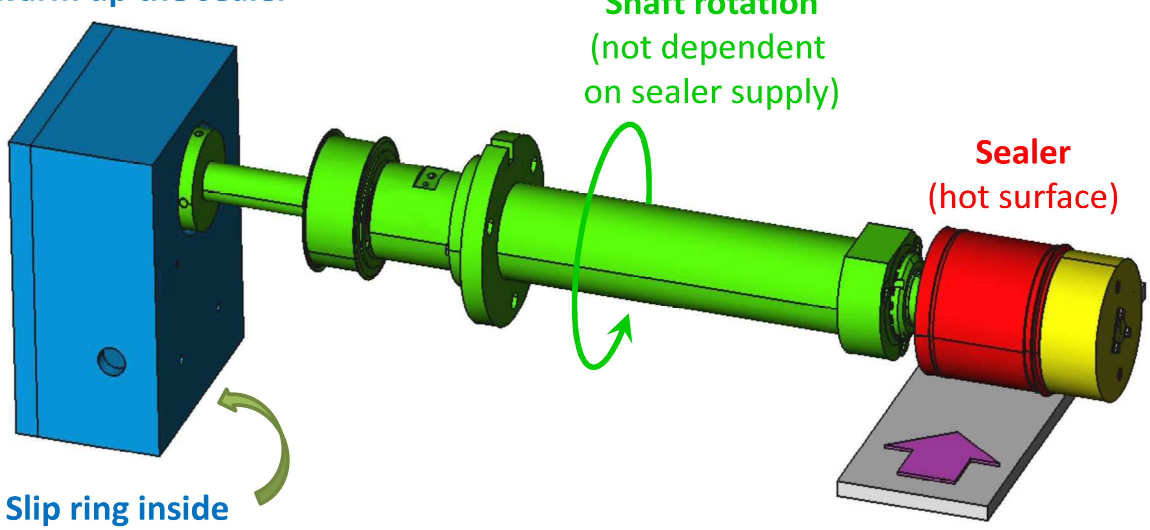

SLIP RING

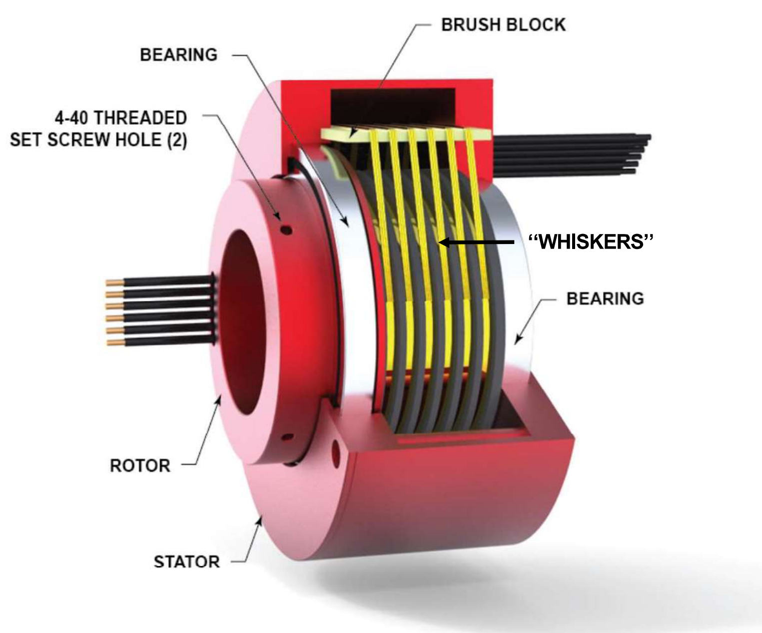

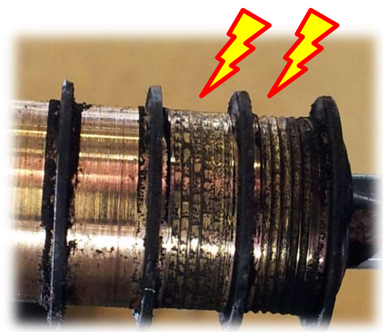

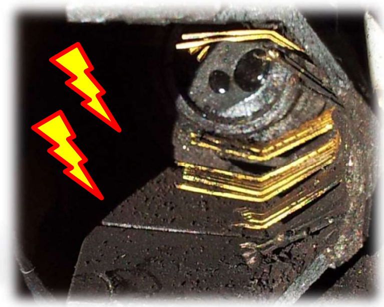

1,3kW CET UNIT CONSTRAINTS

- Requirements:
  - Output voltage = 230 Vac
  - Power rating = 1.3 kW
  - Air gap = 0.6 mm
  - Temperature = [20 – 80] °C
  - Efficiency > 90 %

- Limitations:
  - Frequency (~ 50 kHz)
  - Winding and core losses (~ 30 W)
  - Core's saturation (~ 0,5 T)
  - Temperature (~ 100 °C)
  - Electro-magnetic compatibility (EMC)
  - Available radial space (35 mm)

- Trade-offs:
  - Wire (section, strands)
  - Turns
  - Frequency tuning
  - Ferrite type
  - Compensation schemes
  - Core size

STATE-OF-THE-ART WPT CHANNEL

- Contactless energy transfer (**CET**) units are now used to supply the **rotating sealers** of a packaging machine (1.3 kW)
- CET units are based on **rotary transformers**
- Each CET system requires a temperature **feedback signal** to operate in a closed-loop condition

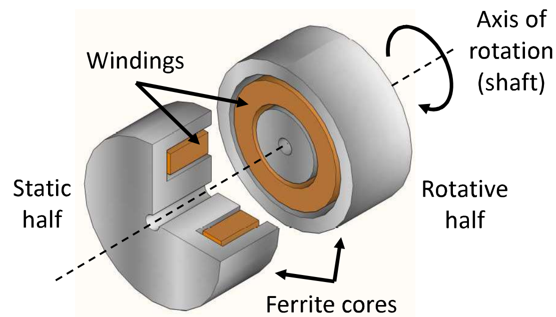

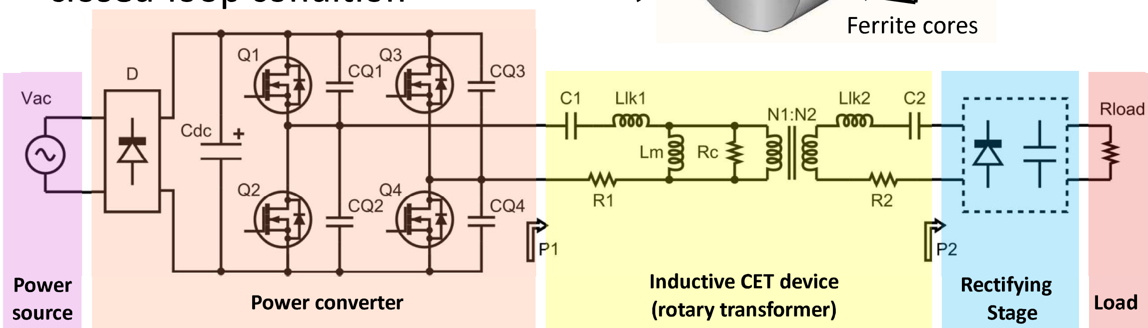

Trevisan, Costanzo, "A 1-kW contactless energy transfer system based on a rotary transformer for sealing rollers," *IEEE Trans. Ind. Electron.*, 2014

WPW 2019
WPW SCHOOL

THE COMPACT ROTATING WPT

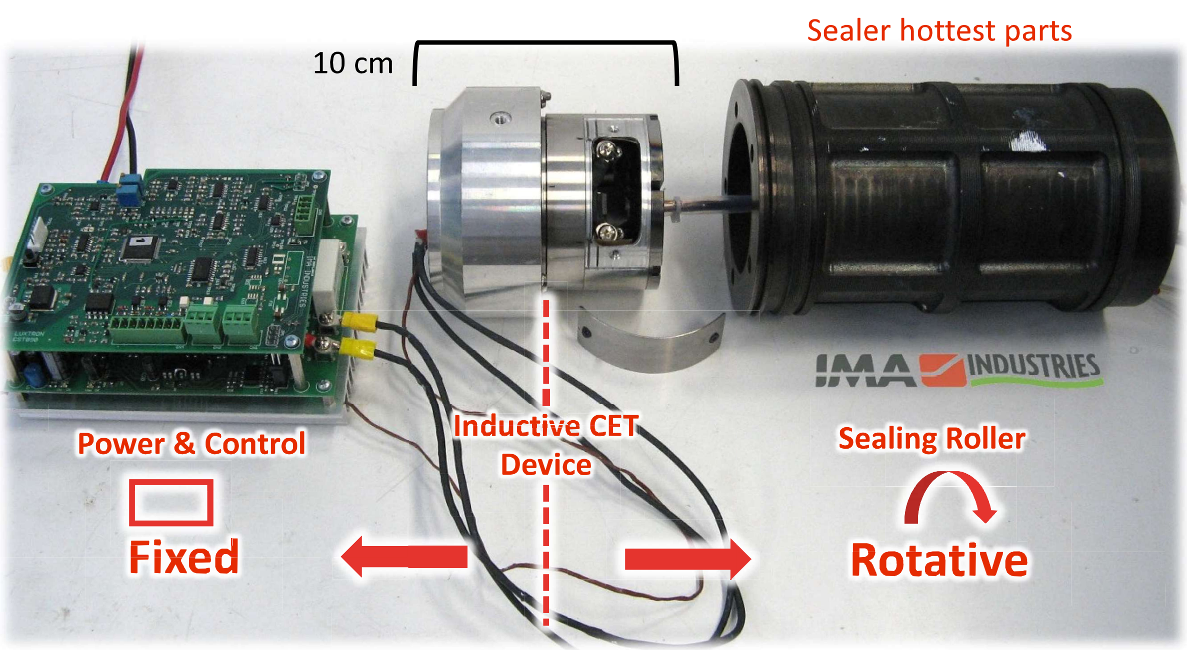

POWER SUPPLY

- Full-bridge MOSFET ac/ac converter
  - Soft-switching reduces commutation losses and increases lifetime
- Pseudo (quasi) –resonance topology
  - Zero-voltage turn on and turn off
- $L_{in,CET}$ resonates with $C_{Q1\text{-}4}$ to ease soft-switching

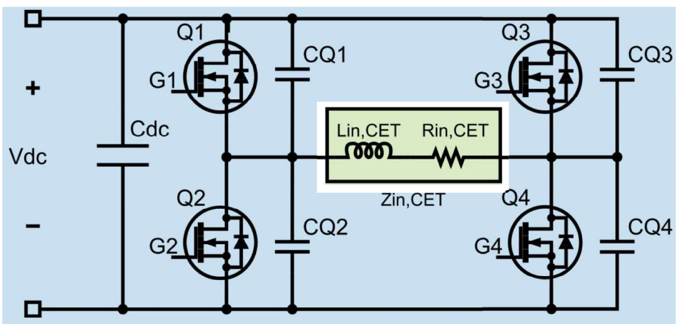

SPICE simulations (Q2), P_{CET} = 1.7 kW

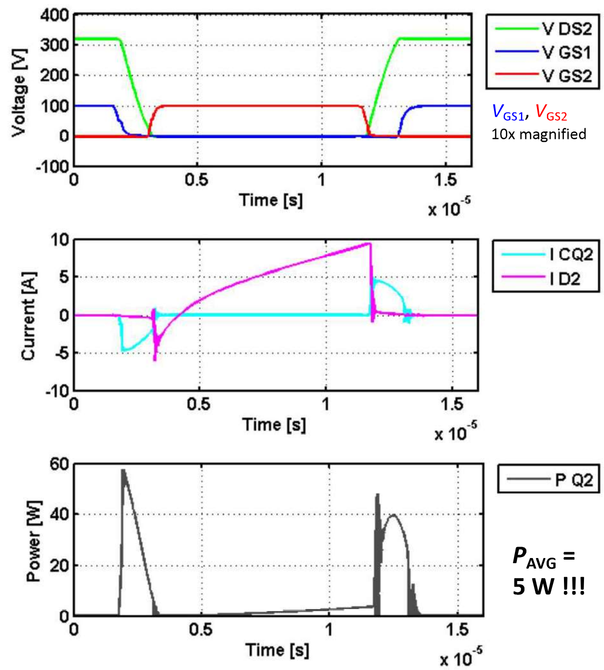

EXPERIMENTAL RESULTS WITH TWO CHOICED OF THE RF-RF LINK

	Setup 18	Setup 27	Units
Litz wire	0,10 mm x 500	0,18 mm x 84	
N_1, N_2	18, 17	27, 24	turns
R_1, R_2 (est.)	55, 47	255, 174	mΩ
Winding losses	**4**	**21**	**W**
L_{lk1}, L_{lk2}, L_m (est.)	28, 25, 303	63, 50, 682	µH
L_{lk1}, L_{lk2}, L_m (meas.)	48, 10, 269	65, 49, 670	µH
Core losses	**13**	**8**	**W**
C_1, C_2	-, -	100, -	nF
Resonance	**-**	**37**	**kHz**
η (est.)	99	97	%
η (meas.)	**98**	**96**	**%**

WIRELESSLY-POWERED CONTROLLED SYSTEMS

- Every controlled system requires a feedback signal to “close the loop”
- The data channel can be paired to the IPT device by several wireless means (secondary inductive channel, capacitive coupling, optical coupling, etc.)

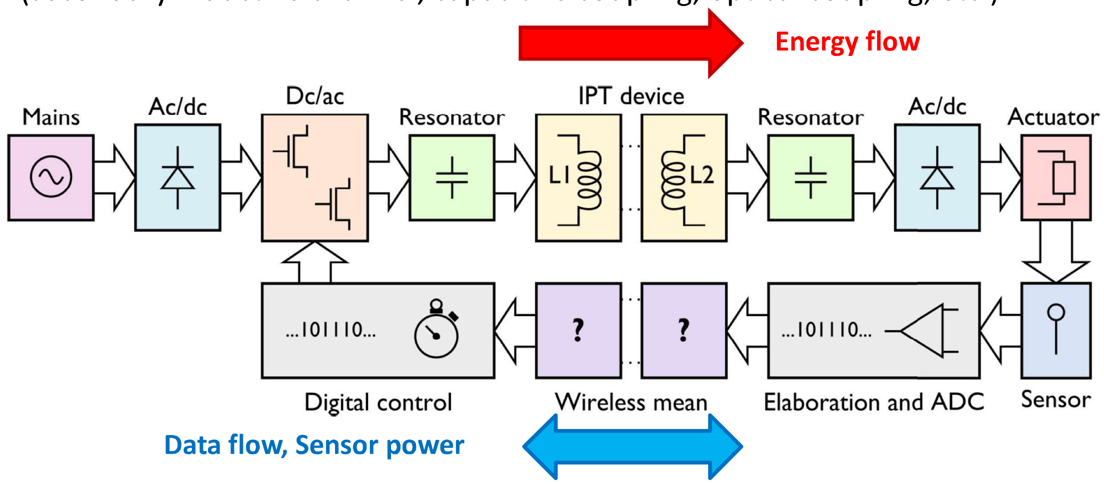

- The sensing circuitry cannot be supplied by the main energy flow (discontinuous)
- A secondary energy source available at the remote side is desired, or
- A channel that combines sensor power + sensor data

PASSIVE SENSING

Exploit power or voltage curves at the input port where the sensitivity is maximum with respect to load variations

- Rload has a **range of variation** [Rmin, Rmax], Rmean is the average
- **Mismatch** is helpful to maximise such quantity variations

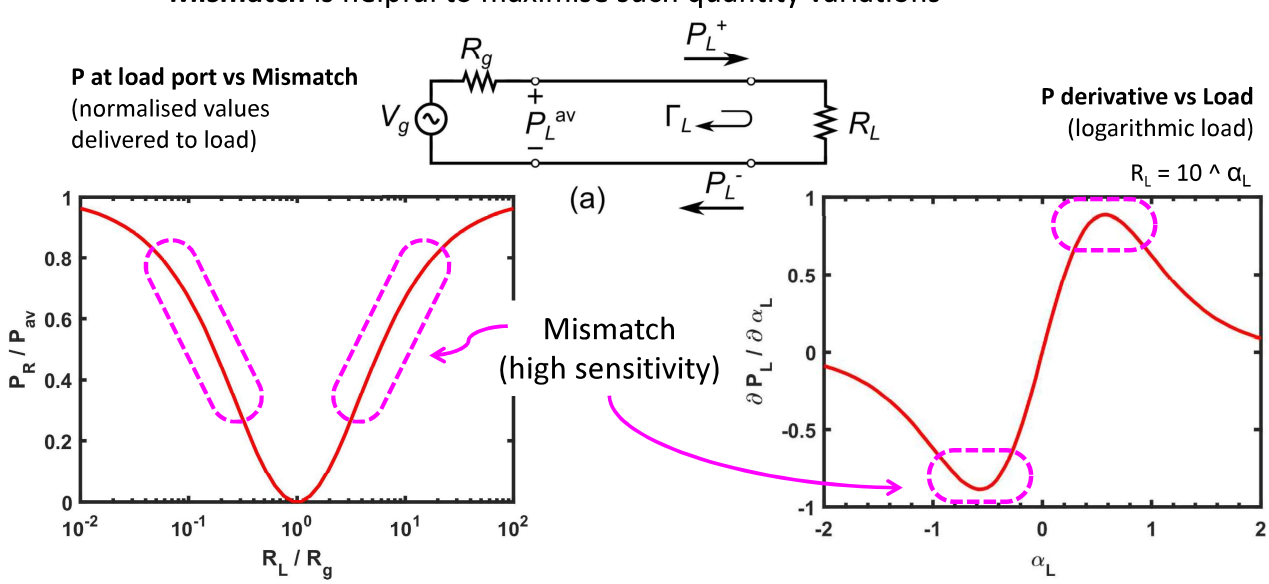

WIRELESS POWER AND INFORMATION TRANSFER (prior art)

- **WPIT**: Transfer of (high) power and information through the same contactless energy transfer (CET) device
- Examples in literature:
  - A. Capacitive plates (Esser1993)
  - B. Overlapped data (Kawamura1996)
  - C. Decoupled coils (Bieler2002)

(C)

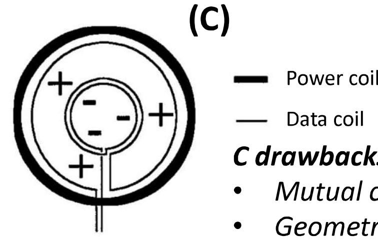

C drawbacks:
- *Mutual coupling*
- *Geometry*

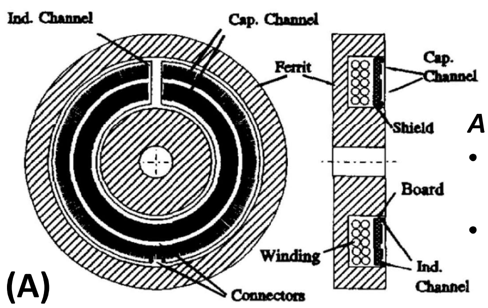

(A)

A drawbacks:
- *Capacitive cross-coupling*
- *Channel performance*

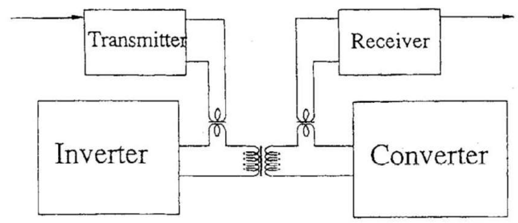

B drawbacks:
- *Bandwidth*
- *EMI / filtering*

(B)

A. Esser, Nagel, "Contactless high speed signal transmission integrated in a compact rotatable power transformer," *Proc. 1993 IEEE 5th European Conf. Power Electronics and Applications.*, 1993, pp. 409-414 vol.4.
B. Kawamura, Member, Ishioka, Hirai, "Wireless transmission of power and information through one high-frequency resonant ac link inverter for robot manipulator applications," *IEEE Trans. Ind. Appl.*, vol. 32, 1996, pp. 503-508.
C. Bieler, Perrottet, Nguyen, Perriard, "Contactless power and information transmission," *IEEE Trans. Ind. Appl.*, vol. 38, 2002, pp. 1266-1272

INTEGRATION OF THE COMMUNICATION LINK WITH THE WPT LINK

SPLIT RING RESONATOR
AT 868 MHz

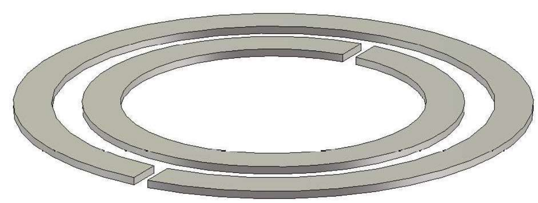

Split Ring Resonator (SRR)
- Often employed in metamaterial studies
- Usually coupled to an external transmission line, or waveguide
- Each SRR can be modelled as two different microstrip lines (internal, external) coupled together

Our case:
- Two faced SRRs
- FR4 substrate
- **Ground backplane**

Model representation of a SSR with slots on opposite sides
Zhurbenko, *et al.*, "**Analytical model of planar double split ring resonator**," *Microwave and Optoelectronics Conf., 2007*
→

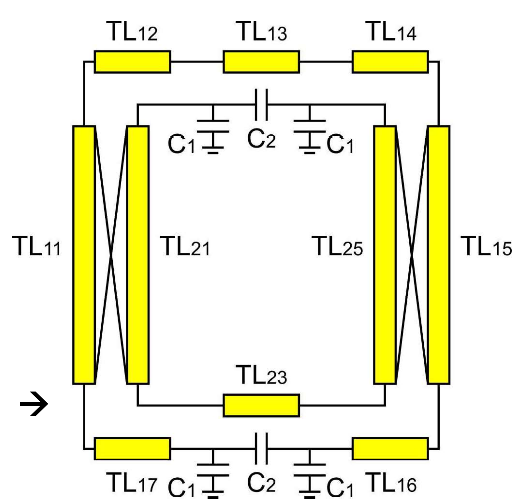

CHARACTERIZATION OF THE SRR COMMUNICATION LINK

- Multiple (self-)resonance frequencies
- Resonant frequencies depend on several factors, including:
  - Clearance between rings
  - Ring slot size and position
  - Ground plane slot size and position

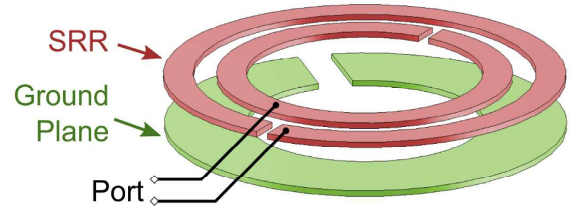

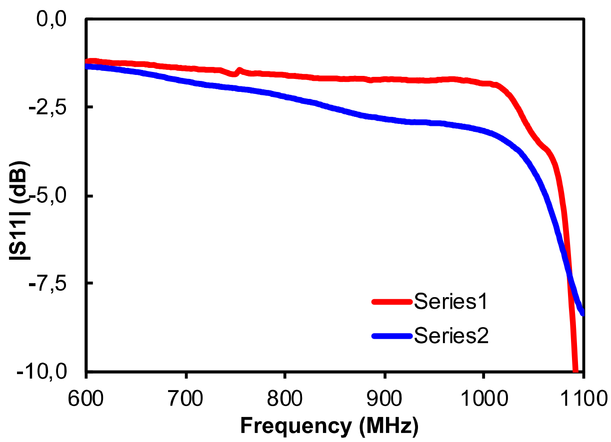

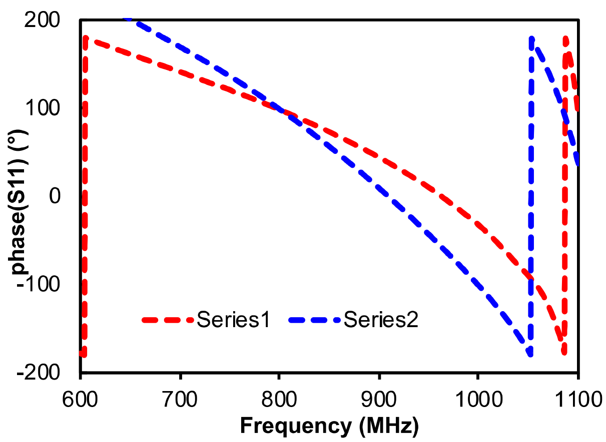

WPW 2019
WPW SCHOOL

COMMUNICATION LINK

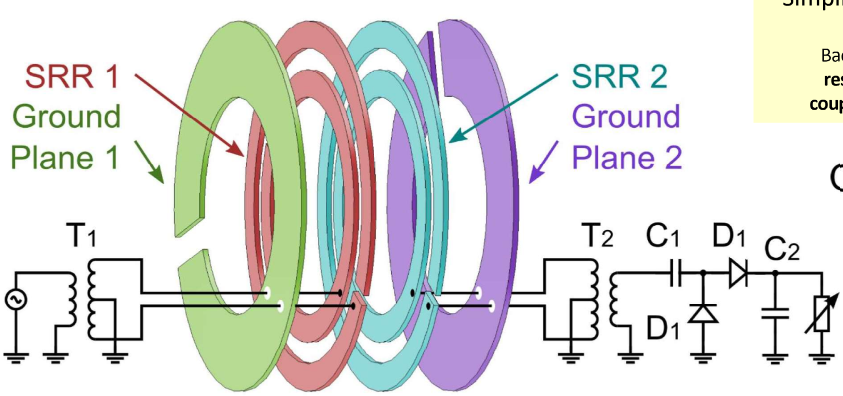

Simplified circuit of a single SRR w/o ground plane. The structure self-resonates.
Baena, et al., "**Equivalent-circuit models for split-ring resonators and complementary split-ring resonators coupled to planar transmission lines**," *IEEE Trans. MTT*

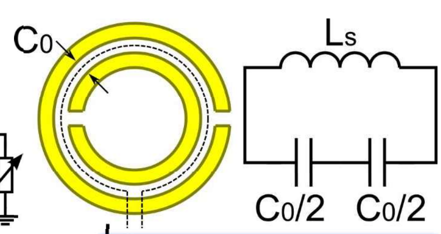

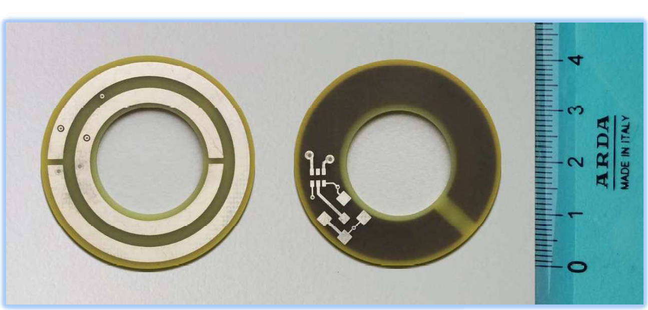

← Prototyped SRRs

Test board → used for design verification

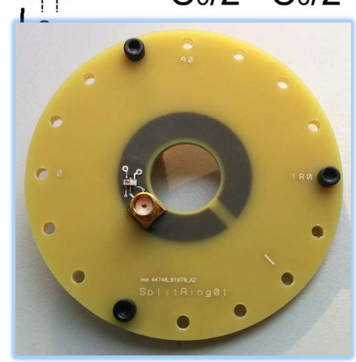

WPW SCHOOL

COMMUNICATION LINK BEHAVIOR INSENSITIVE TO ROTATION

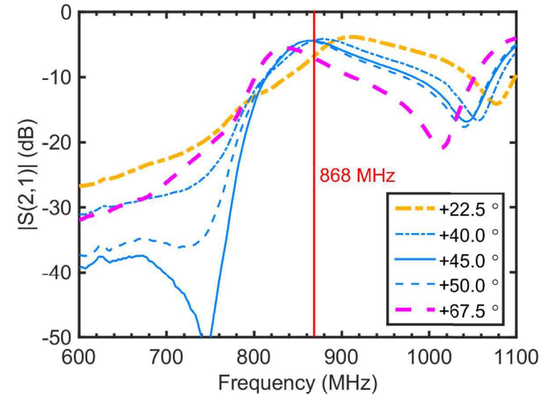

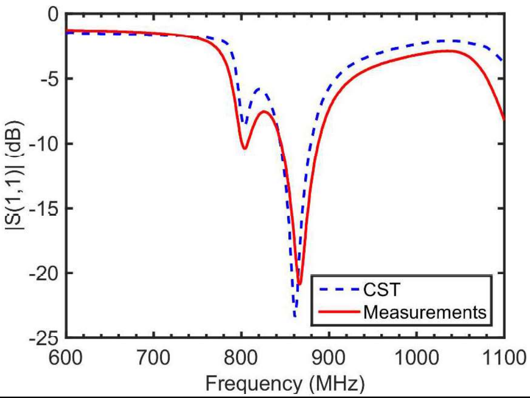

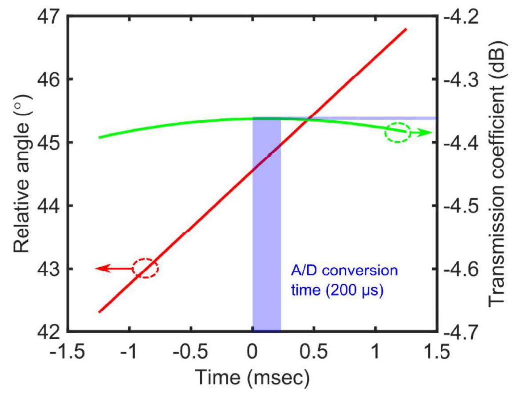

WPW SCHOOL

THE COMMUNICATION LINK

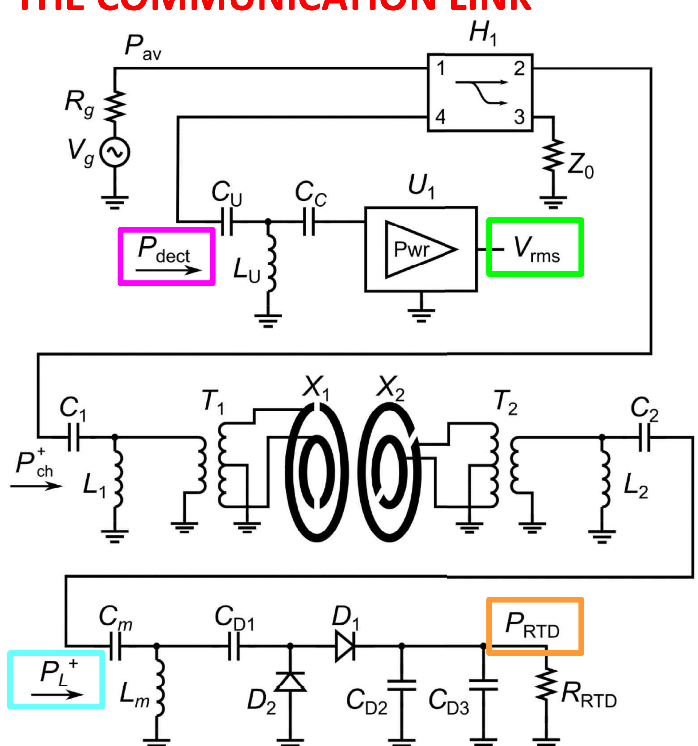

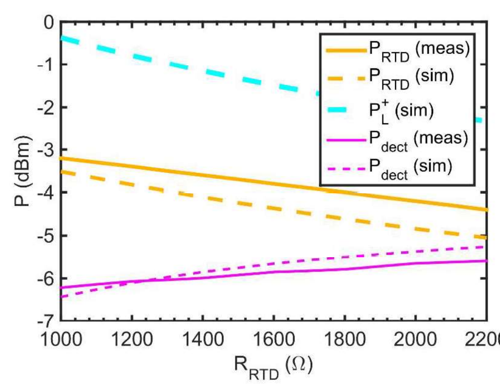

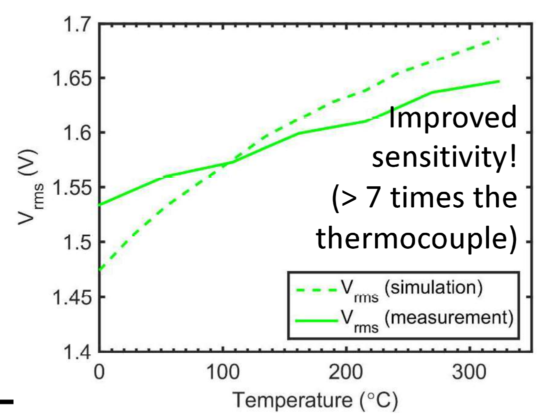

SLIDING CHARTS IN INDUSTRIAL PLANTS

Distributed reconfigurable TX coils instead of a unique one

- The goal is to maintain a constant output voltage independently from position and load
- Can a coupled inductive system be position independent just by some geometrical optimizations and multiple transmitters?
- Can a complete link be load independent without any feedback control?

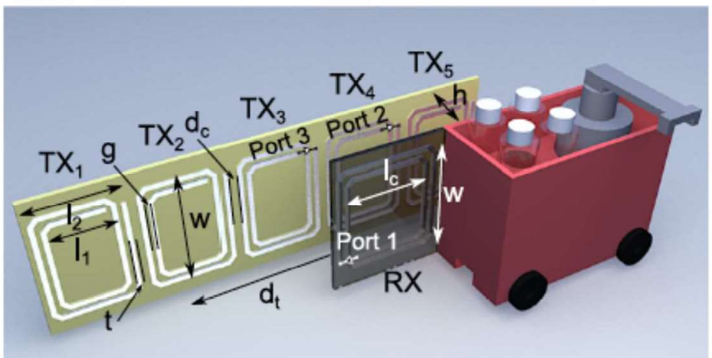

[Final] Dimensions (cm):
$l_c = 17.2,\ l_1 = 12$
$l_2 = 18,\ d_c = 2$
$w = 24,\ g = 1,$
$t = 1,\ h = 6$

WPW 2019
WPW SCHOOL

CONCURRENT TX AND RX COILS OPTIMIZATION

RX slides from a) to b) at a distance of 6 cm, facing two TX coils: EM based optimization of the three-port network: P_1: (RX) P_2 : (TX_1) P_3 : (TX_2).

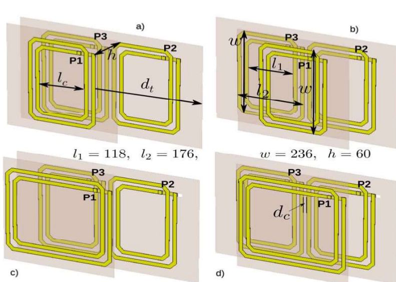

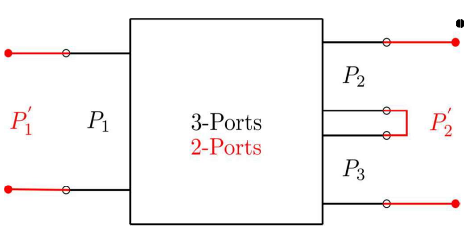

- EM-based optimization of the RX length l_c *wrt* the TX ones (l_1). $l_c \approx l_1 + \frac{l_2 - l_1}{2} + d_c$
- Coupling factor: $k_{i,j} = \frac{X_{i,j}}{\sqrt{X_{i,i} \cdot X_{j,j}}}$
- Series of two TX: $k_{TX-RX} = \frac{\sqrt{2}}{2} \frac{k_{1,2} + k_{1,3}}{\sqrt{1 + k_{1,3}}}$
- $k_{TX\text{-}RX}$ is constant if $k_{1,2}$ and $k_{1,3}$
  - $Z'_{11} = Z_{11}$;
  - $Z'_{12} = Z_{12} + Z_{13}$;
  - $Z'_{22} = Z_{22} + Z_{33} + Z_{23}$
  - $L'_2 = L_2 + L_3 + M_{23}$

[1] Pacini, Mastri, Trevisan, Masotti, Costanzo, "Geometry optimization of sliding inductive links for position-independent wireless power transfer," IMS 2016.

SLIDING POSITIONS

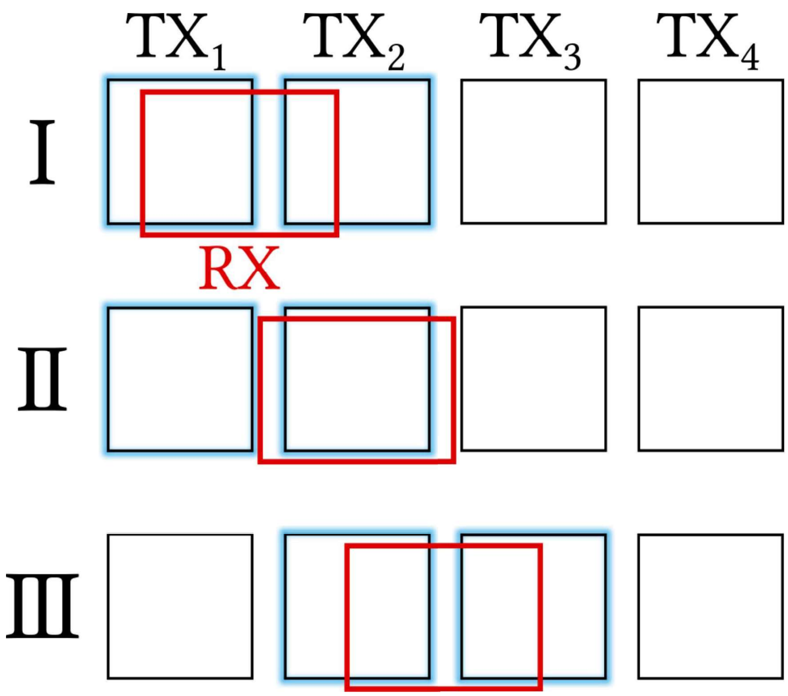

- The **powered** coils are **highlighted**
- The **RX slides** along the **whole path** (zero is RX/TX1 centres aligned)
- When the **RX aligns** with a new **TX** coil, the **previous** is turned **off** while the **next** is turned **on**
- The **behaviour** is thus **periodic** and can be **unlimited**

CONCURRENT TX AND RX COILS OPTIMIZATION

PREDICTED AND MEASURED COUPLING FACTOR FOR OPTIMIZED RX LAYOUT

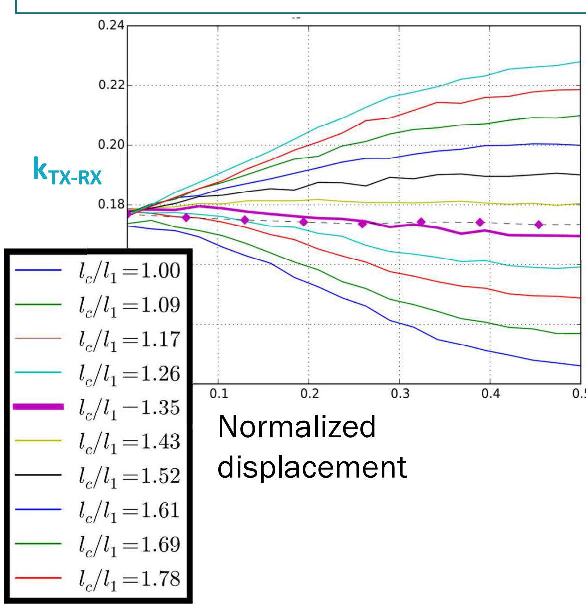

Normalized displacement

PREDICTED AND MEASURED COUPLING FACTOR FOR VARIABLE RX-TX DISTANCES

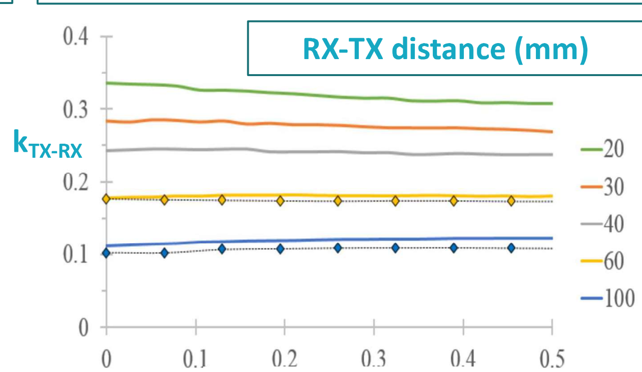

Normalized displacement

RX slides from a) to b) at a distance of 6 cm, facing two TX coils: EM based optimization

[1] Pacini, Mastri, Trevisan, Masotti, Costanzo, "Geometry optimization of sliding inductive links for position-independent wireless power transfer," IMS 2016.

DISTRIBUTED CURRENT SOURCES: ONE FOR EACH TX COIL

- The optimal **series connection** of two coils can be obtained ***virtually*** by forcing the **same current through them**
  - A stand-alone **Class EF** Inverter, designed in [2], provides a **constant current** source with a DC-AC efficiency better than **90% at 6.78MHz.**
  - The **load can vary BUT must** be **resistive** and **0< R_L< R_L^{MAX}**
- The inverter topology **is modified** to account for closely located coils when the RX is moving.

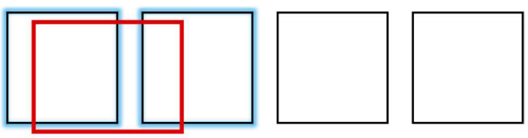

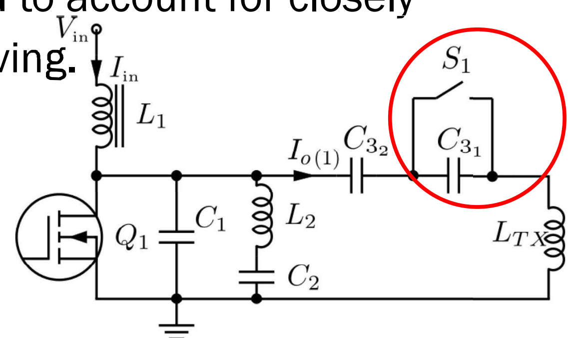

[2] Aldhaher, Mitcheson, Yates, "Load-independent Class EF inverters for inductive wireless power transfer," WPTC 2016.

INVERTER EMBEDDED NETWORK DESIGN

- The effective coil inductance seen from the inverter port (***virtuaL series connection of two coils)***

$$L_{TX}^{1} = L_{TX}(1 + k_{23}),$$

where k_{23} is the coupling factor between the two TX coils

$$C_3' = \frac{C_3}{\left(1 + \frac{\omega}{2\pi f_0}\right) k_{23}}$$

Compensating capacitor to provide the same residual inductance

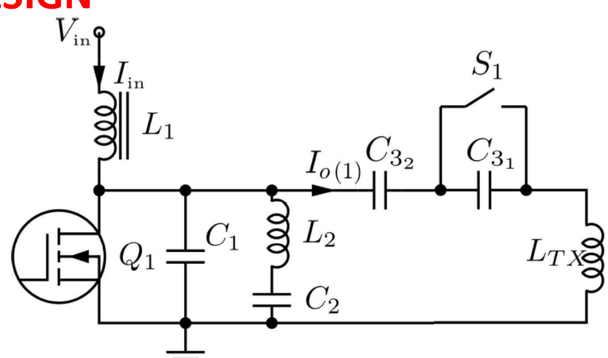

Inverter load need be inductive

Q_1 ON: f < f_0

Q_1 OFF: f > f_0

T_{ON}>T_{OFF}

f_0=6,78 MHz

WPW 2019

WPW SCHOOL

IDENTICAL RF CURRENT SOURCES: VIRTUAL SERIES CONNECTION

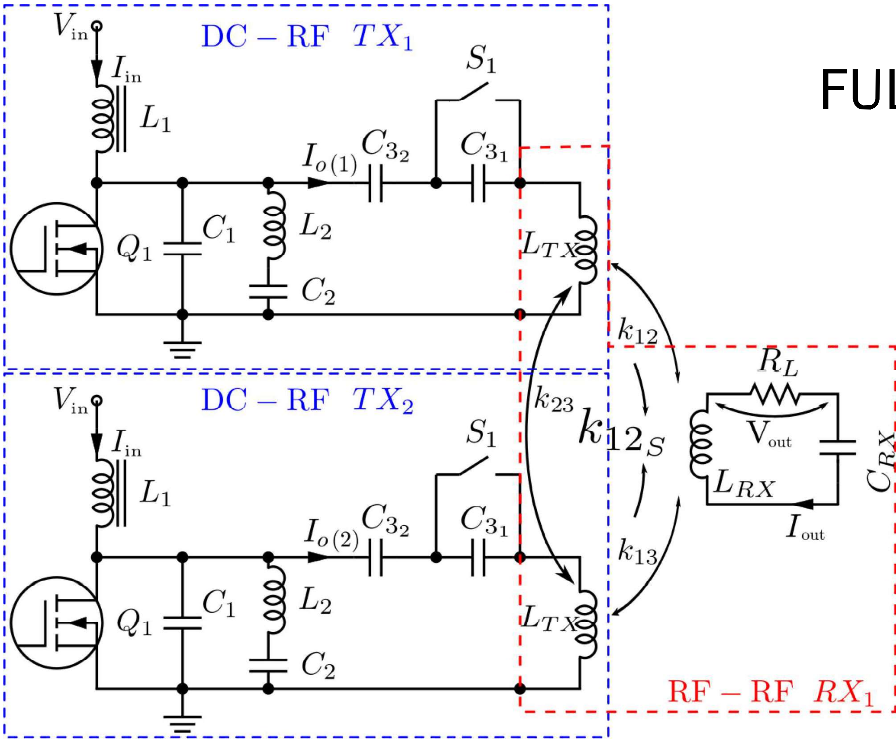

FULLY MODULAR DESIGN

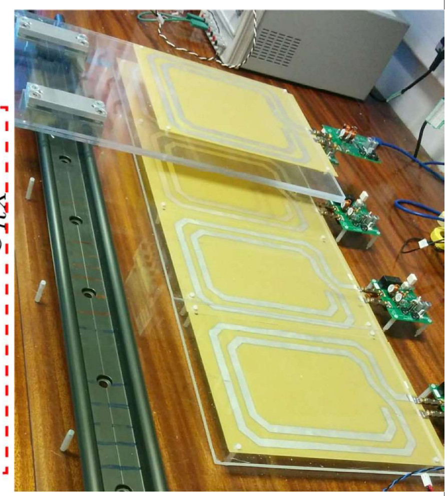

WPW 2019

WPW SCHOOL

MITIGATION OF PARASITIC CURRENTS IN INACTIVE COILS

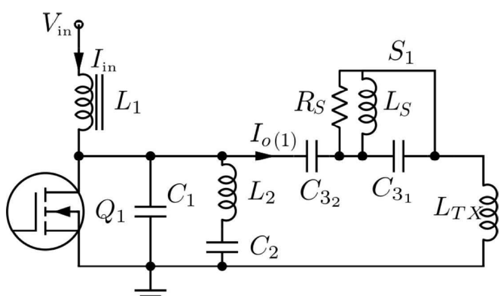

$$C_{3_2} = \alpha C_{3_1}$$

$$C_{3_2} = C_3(\alpha + 1)$$

$$C_{3_1} = C_3\left(\frac{\alpha + 1}{\alpha}\right)$$

- C_3 is **splitted** in two and a **switch** S_1 is parallel-connected to the lower capacitor ***to stress the impedance differentiation between active and non-active coils***
- ActiveTX coil -> **S_1 open**
- InactiveTX coil -> **S_1 closed**
- For **α=10**, the currents are **reduced** by one order of magnitude

MODIFIED LOAD_INDEPENDENT INVERTER

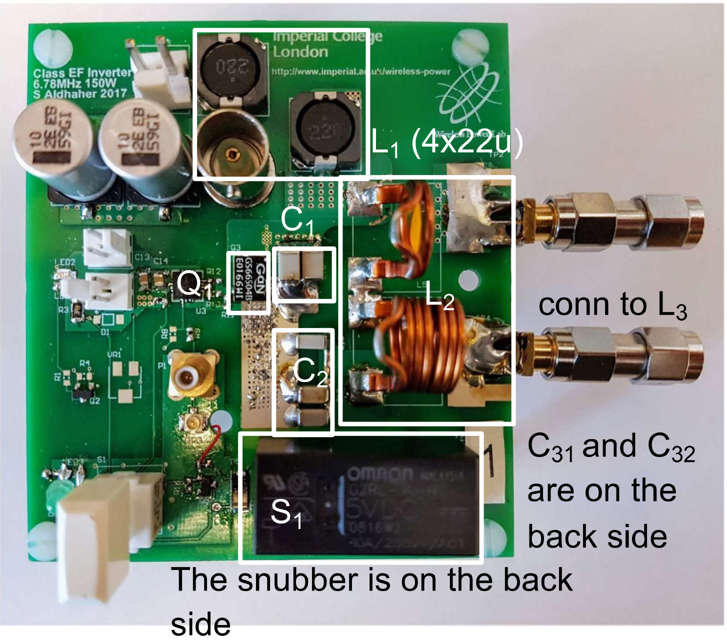

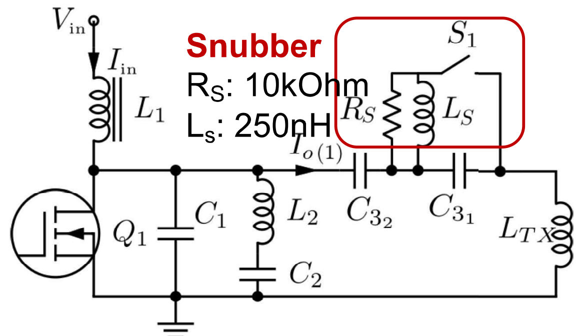

L_1: 88uH, Q_1: GaN E-HEMT Gan system GS66504B, S_1: G2RL-1A
C_1: 660pF, C_2: 696pF,
L_2: 283nH,
C_{32}: 4700pF, C_{31}: 526pF,
L_{TX}: 1.42uH (TX COIL),
Driver: ISL55111IRZ

SAME RF CURRENT FOR ANY RX POSITION AND MANY LOADS

- Currents in both TX coils are the same for any RX position and RX load (R_L > 30 Ohm and purely resistive)
- Constant output voltage and currents for 25 load and 20 different RX positions.

30>R_L>10k
All RX positions

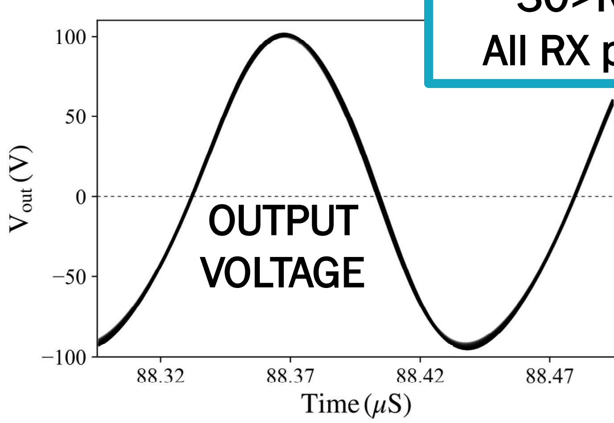

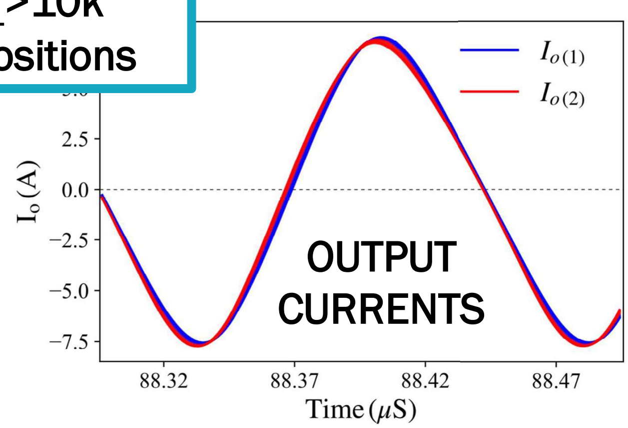

THE WHOLE DC-DC SYSTEM

- RF-to-DC resonant rectifier specs:
  - To have a constant input reactance
  - To act as A DC voltage source is challenging.
- The multiple nonlinearities need the rectifier to be optimised together with the whole DC- AC link to account for all the mutual effects
- HB design of the rectifier can reduce the simulation time by three orders
- Non uniform (amplitude) currents on the two TX coils would cause a major variation on the output voltage (valid for a variation of the position or load)
- Phase dfference between the TX coil currents results in strong idle losses: the quality factor of the transmitting coil is reduced by one half.

CLASS-E RECTIFIER DESIGN

THE RF-RF LINK IS AN IMPEDANCE INVERTER

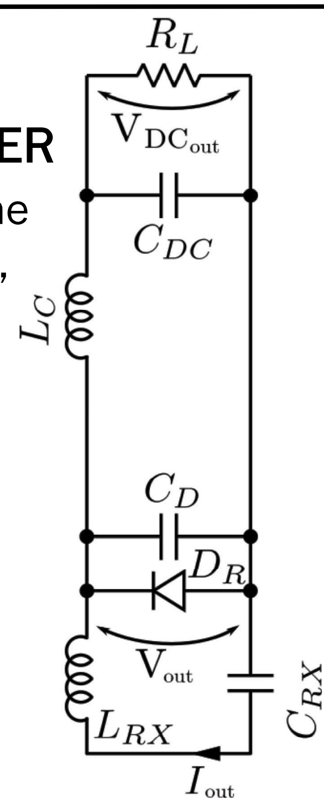

- The rectifier input is designed such that from the TX side is seen as a purely resistive impedance, for any RX position
- Nonlinear optimization with C_D and C_{RX} as the variables
- Zero-reactance ensures load-Independent operation of the Class EF Inverter.
- Soft switching and constant current

CLASS-E RECTIFIER PROTOTYPE

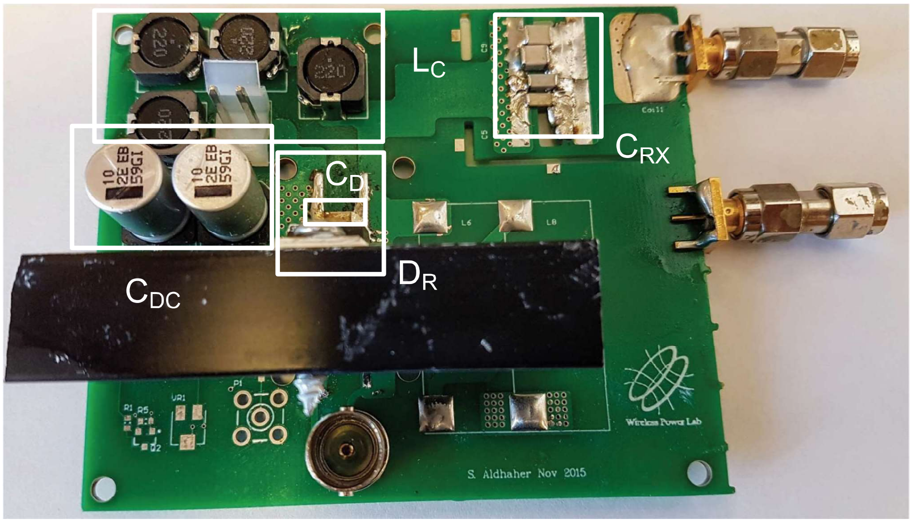

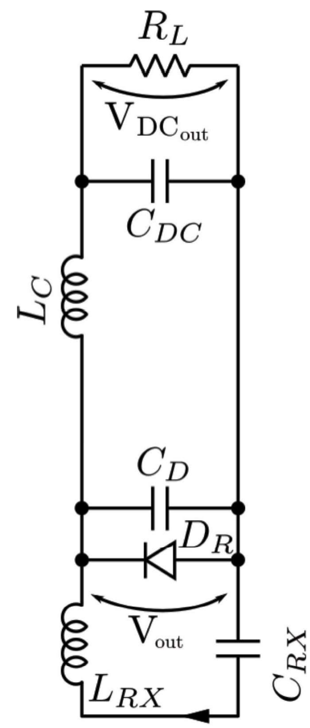

L_C: 88uH, D_R: C3D02060F, C_D: 33pF, C_{DC}: 20uF, C_{RX}: 498pF, L_{RX}: 1.7uH (RX COIL)

MEASURED DC OUTPUT VOLTAGE

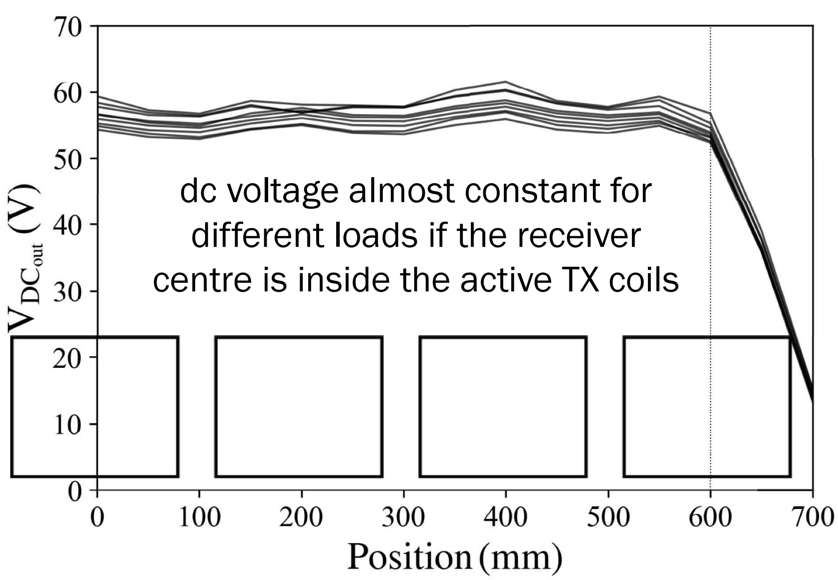

RX moves over the selected active coils

as the receiver moves out of the last active coil, the output voltage drops

this proves the effectiveness of the geometry optimisation

A. Pacini, A. Costanzo, S. Aldhaher, and P. D. Mitcheson, "Load- and Position-Independent Moving MHz WPT System Based on GaN- Distributed Current Sources", IEEE Transactions on Microwave The- ory and Techniques, vol. 65, no. 12, pp. 5367–5376, Dec. 2017. doi: 10.1109/tmtt.2017.2768031.

DC-DC EFFICIENCY

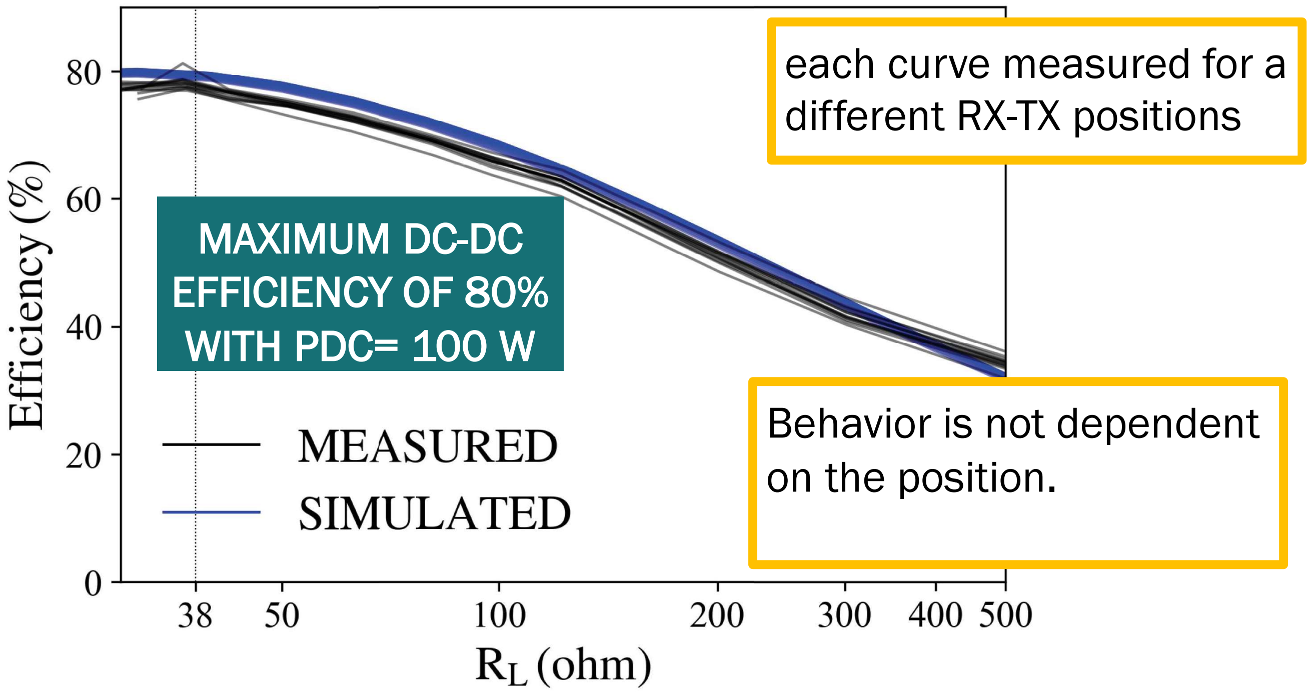

QUESTIONS ?

WPW SCHOOL

Wireless Grid Integration of EVs for V2G Applications : Challenges and Technologies

Udaya Madawala
University of Auckland

Electric vehicles (EVs) are gaining global acceptance as the means of future transport for sustainable living and as an alternative energy storage to stabilize the electricity network through the vehicle-to-grid (V2G) concept. For V2G applications, EVs essentially require a bi-directional power interface with the electricity network (grid) to allow for both storing (charging) and retrieval (discharging) of energy. This can be achieved by both wired and wireless means, but the latter, based primarily on Inductive Power Transfer (IPT) technology, is becoming more popular being convenient, safe, and ideal for both stationary and dynamic charging of EVs. The seminar discusses the standards, challenges and future directions of V2G technologies, and presents the latest advances in bi-directional wireless power transfer (BD-WPT) technology developed for V2G applications.

Wireless Grid Integration of EVs for V2G Applications :

Challenges & Technologies

Professor Udaya K Madawala

Email : u.madawala@auckland.ac.nz

Power Electronics Research Group
Department of Electrical & Computer Engineering

THE UNIVERSITY OF AUCKLAND
Te Whare Wānanga o Tāmaki Makaurau
NEW ZEALAND

Wireless EV Charging

Based on:

- *Inductive Power Transfer (IPT) technology*

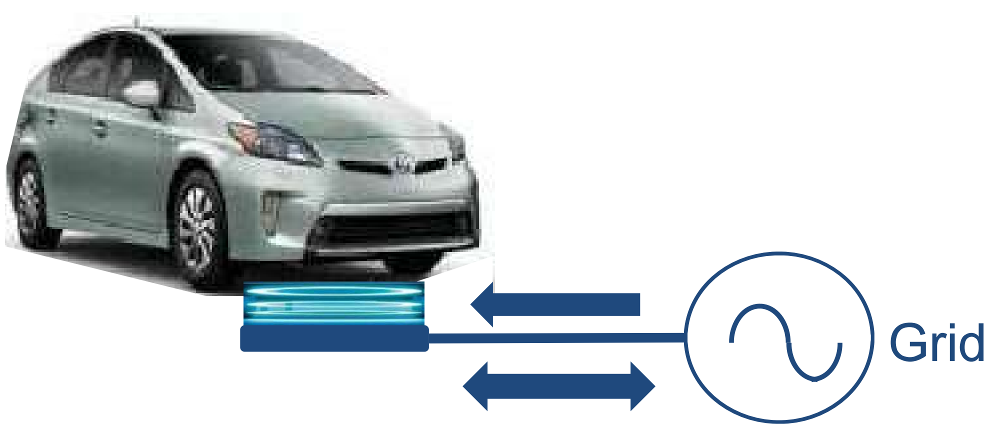

Wireless EV Charging

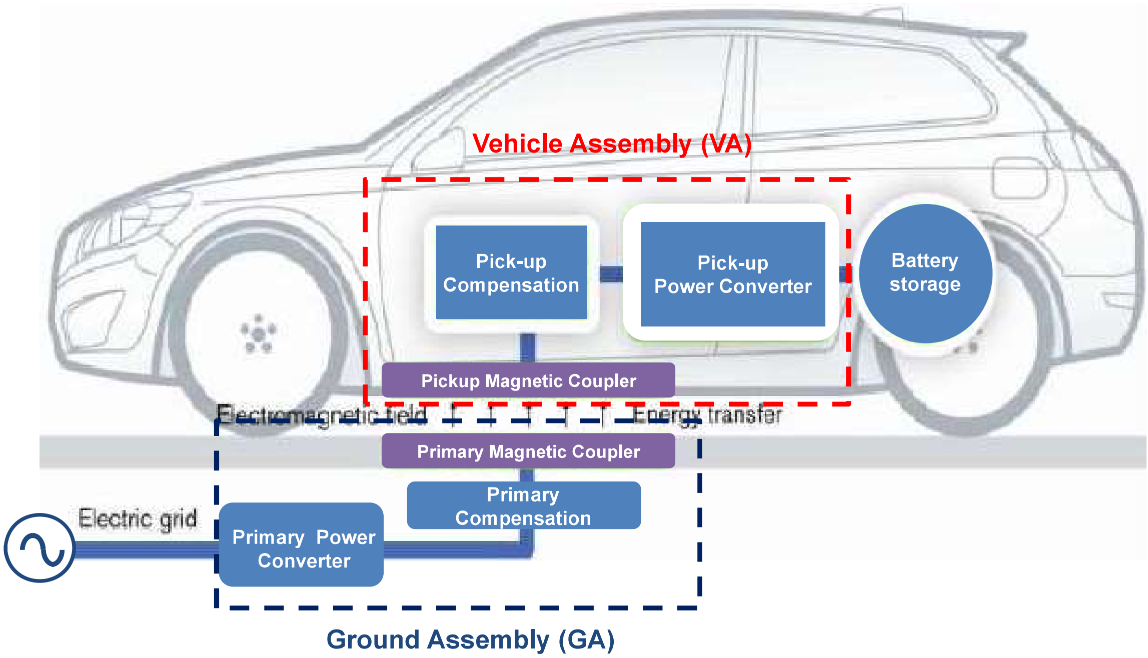

Challenges *(Wireless EV Charging)*

- Charging
  - *stationary, or both stationary & dynamic (~ 25 kW !)*
- Uni- or bi-directional power flow at high frequency operation
- Controlling power converters
  - *High order resonant (SS/SP/PP etc) circuits with active & passive control*
- Magnetic pad (coupler) design, interoperability & alignment
- Communication between VA & GA
  - *Tariff, synchronization, demand side management, etc.*
- Compliance with standards (ICNIRP) related to
  - *Safety, EMFs, FoD & LoD, radiated and conducted emissions, etc*
- Physical construction, cost, robustness etc

Standards *(Wireless EV Charging)*

- Being implemented by SAE : TIR J2954(LDEVs), J2954/2 (HDEVs)
  - *Safety, performance, interoperability, communication, control, EMF exposure, etc.*
- EVs are expected to be compatible with J1772 chargers
- Nominal frequency of operation is set as 85 kHz (79 kHz to 90.00 kHz)
- Minimum target efficiency is 85% (80% offset) for WPT1-3

Classification: Light duty EVs	WPT1	WPT2	WPT3	WPT4
Maximum VA rating	3.7 kVA	7.7 kVA	11 kVA	22 kVA

http://www.standardsuniversity.org/e-magazine/june-2016/sae-publishes-tir-j2954-wireless-power-transfer-evphev/

V2G Compatible EVs

➢ Main requirement is the 'bi-directional' charger with communication

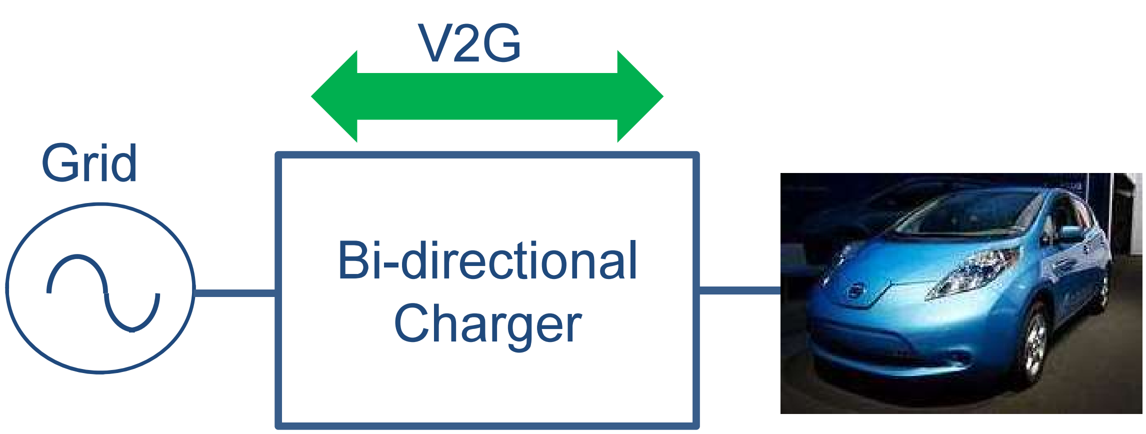

Source : http://newsroom.nissan-europe.com/uk/en-gb/media/pressreleases/145248/nissan-and-enel-launch-groundbreaking-vehicle-to-grid-project-in-the-uk

Standards & V2G Compatible EVs

- IEC standard for V2X systems is expected in 2019
- CHAdeMO is currently the only system that complies to standards (IEC 61851-23, EN50118), relevant to bi-directional energy flow
- Globally, except China, CHAdeMO is the most widely used charging system offering V2X chargers
- According to literature three EVs currently have V2G compatibility,
  - ✓ *Nissan Leaf, Nissan e-NV200, Mitsubishi Outlander*

Bi-directional WPT (BD-WPT) Systems for V2G Applications

A typical Bi-directional WPT System

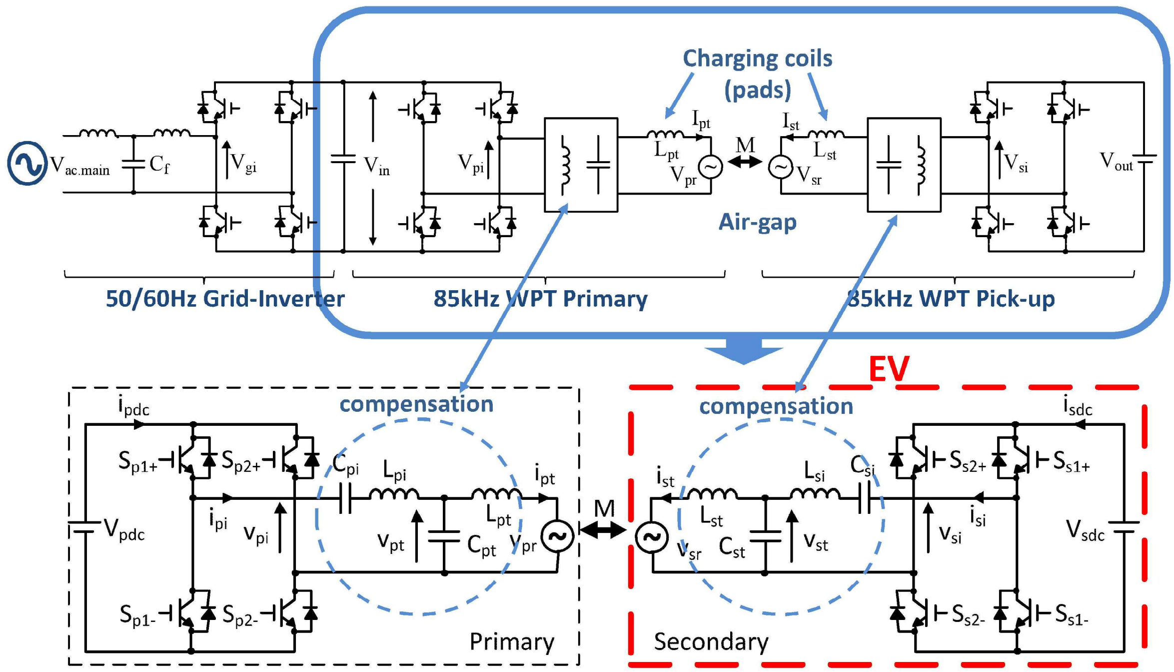

Control of Bi-directional WPT Systems

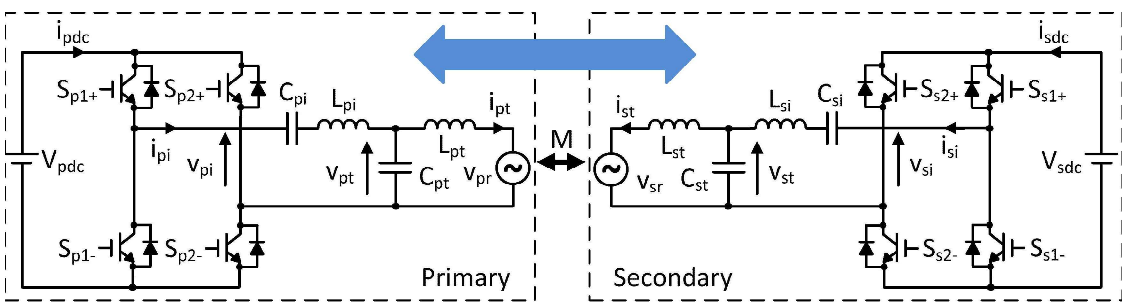

$$P_o = \frac{-M}{\omega_s L_{pt} L_{st}} \frac{8}{\pi^2} V_{pdc} V_{sdc} \sin(\theta) \sin\left(\frac{\phi_p}{2}\right) \sin\left(\frac{\phi_s}{2}\right)$$

- *An 8th order resonant (tuned) system*
- *Controlled with **phase-modulation***
- *Proper control and synchronization are vital*

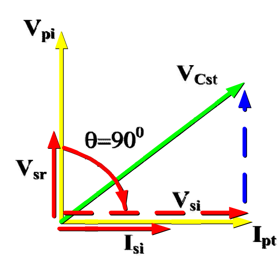

Control Techniques for BD-WPT Systems

Impact of Pad Misalignment

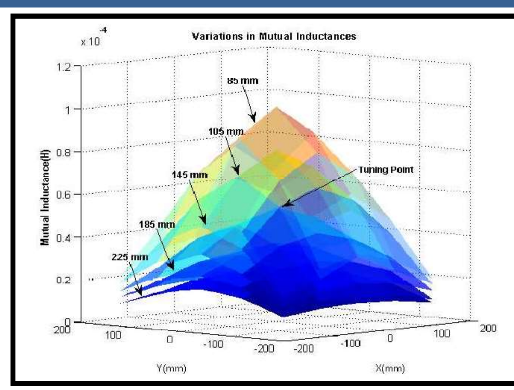

$$P_o = \frac{-M}{\omega_s L_{pt} L_{st}} \frac{8}{\pi^2} V_{pdc} V_{sdc} \sin(\theta) \sin\left(\frac{\phi_p}{2}\right) \sin\left(\frac{\phi_s}{2}\right)$$

- Self & mutual inductances vary due to pad misalignments in 3-D
  - *Detunes the system increasing losses and reducing power delivery*
  - ***May adopt special and large pads, but at an increased cost!***

A P-Q Controller

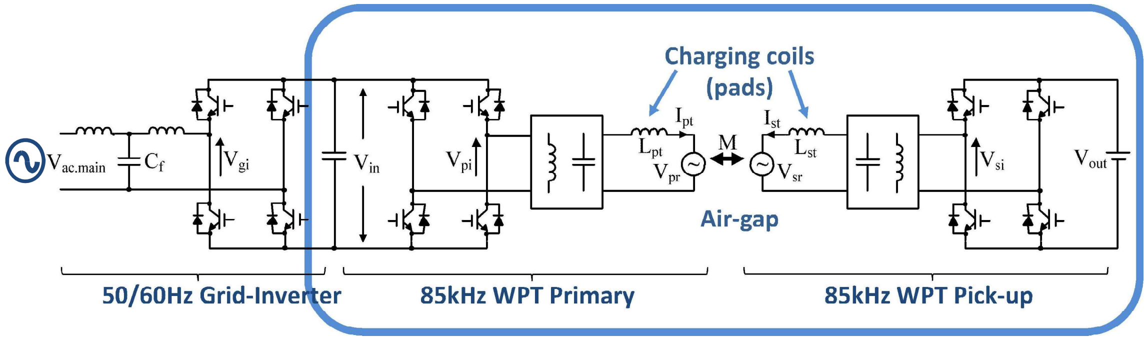

- *Regulates power flow in both directions*
- *Uses active (P) and reactive (Q) power on the pick-up side*
- *Provides synchronization without any direct communication*
- *Ensures operation at no or minimum Q*
- *Tolerant to pad-misalignment and variation in component values*

A P-Q Controller : Concept

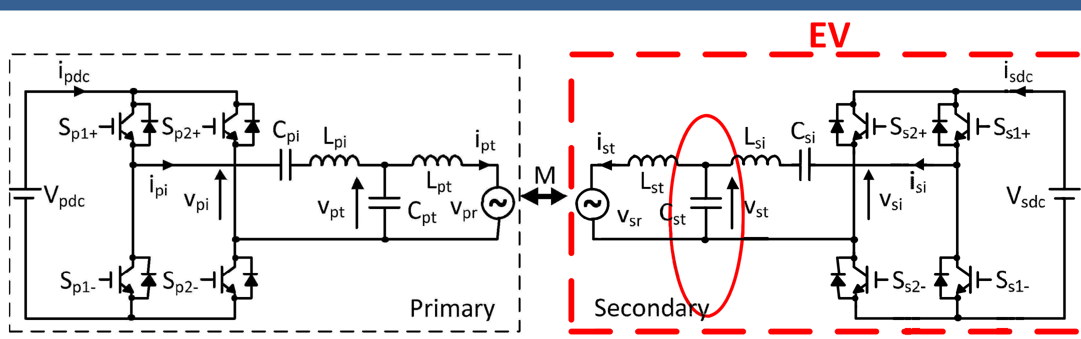

$$S_s = P_s + j\,Q_s \quad \text{and} \quad \theta_{power} = \cos^{-1}\left(\frac{P_s}{\sqrt{P_s^2 + Q_s^2}}\right) = F(\theta_c, \phi_p, \phi_s, \omega, Z_{p,s})$$

Under tuned conditions

$$P_s = \frac{-M}{\omega_s L_{pt} L_{st}} \frac{8}{\pi^2} V_{pdc} V_{sdc} \sin(\theta) \sin\left(\frac{\phi_p}{2}\right) \sin\left(\frac{\phi_s}{2}\right)$$

A P-Q Controller : Concept

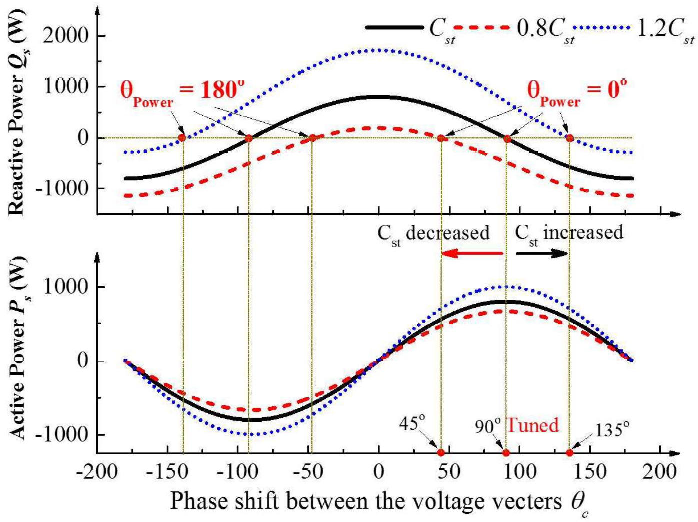

A P-Q Controller : Implementation

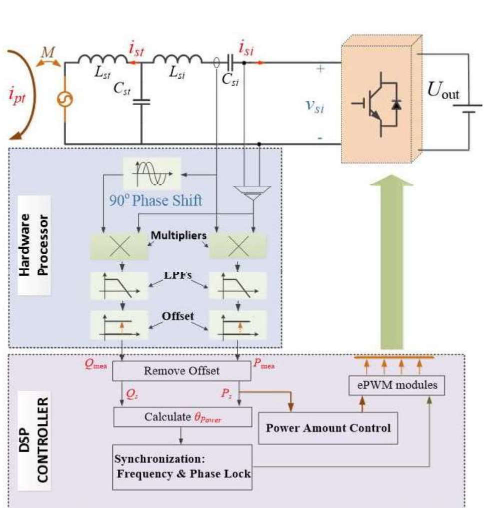

Proposed control technique

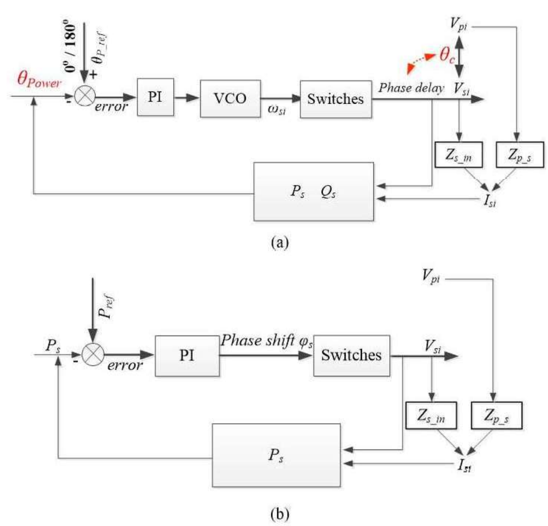

Control block diagrams (a) synchronization (b) amount of power transfer

A P-Q Controller : Results

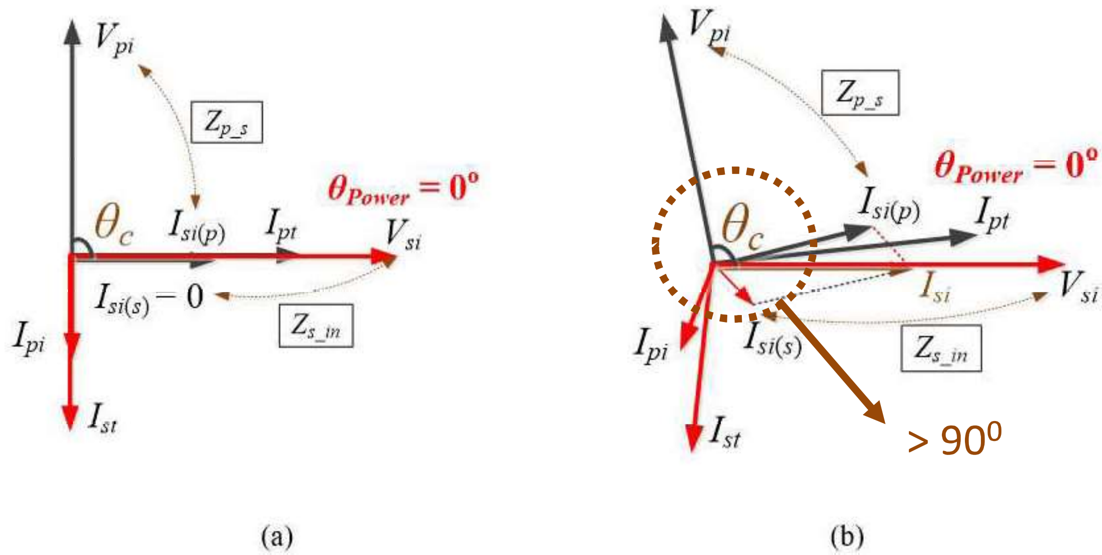

Phasor representations under (a) tuned (b) detuned conditions

A P-Q Controller : Results

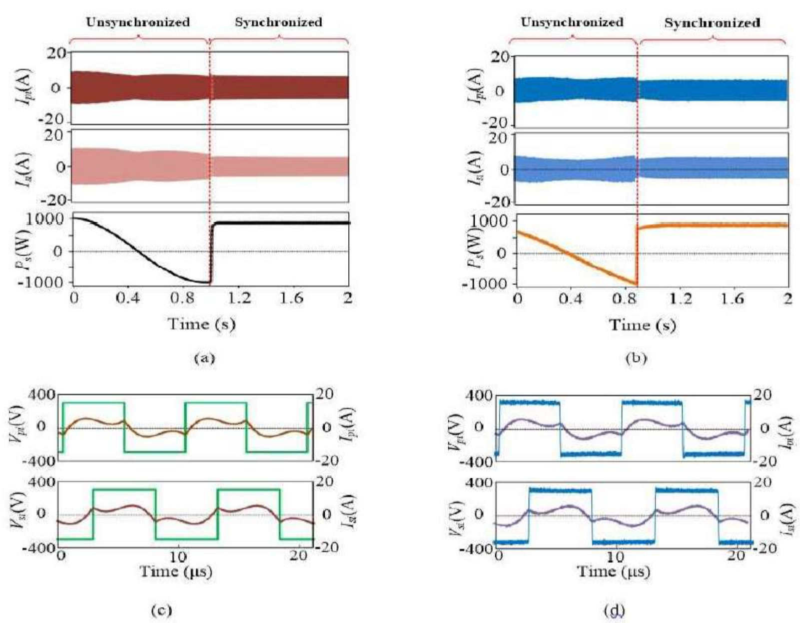

Waveforms of synchronizing process (a) Simulated (b) Experimental
Synchronized waveforms (c) Simulated (d) Experimental

A P-Q Controller : Results

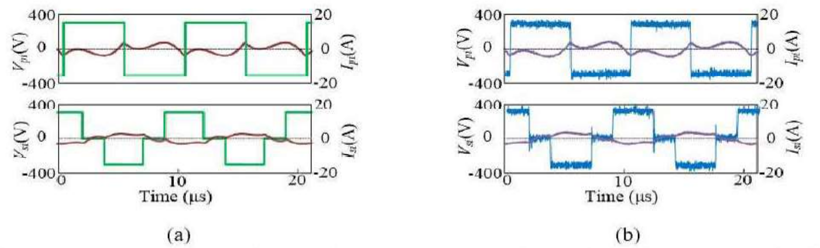

Waveforms for 450 W when pads are misaligned by 150mm (a) Simulated (b) Experimental

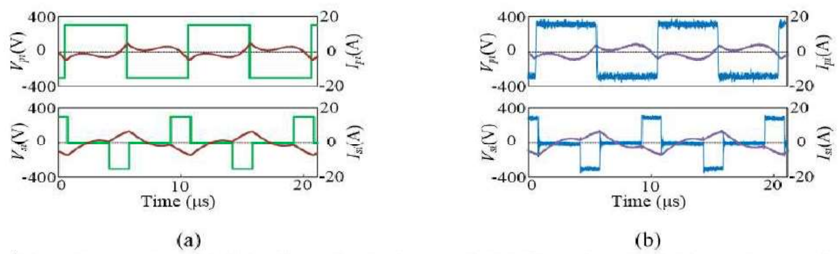

Waveforms for 450 W when C_{st} is detuned (a) Simulated (b) Experimental

A New P-Q Controller

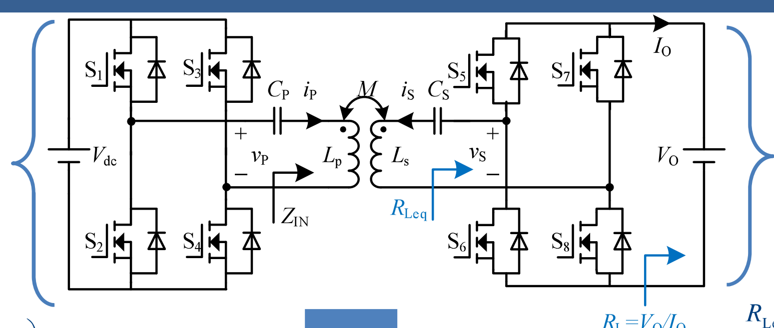

$$V_P = \frac{2\sqrt{2}}{\pi}\sin\left(\frac{\alpha}{2}\right)V_{dc}$$

$$R_{Leq} = \frac{8}{\pi^2}\sin\left(\frac{\beta}{2}\right)^2 R_L$$

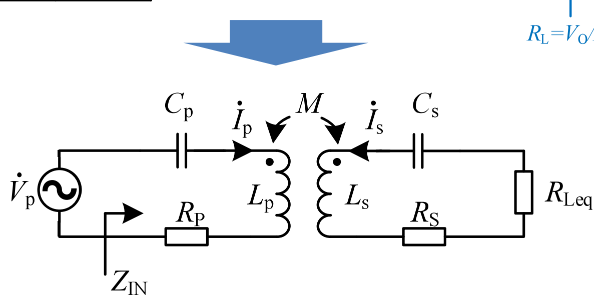

$$P_{out} = \frac{V_P^2\omega^2 M^2 R_{Leq}}{\left(X_P^2 + R_P^2\right)\left[\left(R_S + R_{Leq}\right)^2 + X_S^2\right] + 2\omega^2 M^2\left(-X_P X_S + R_P R_{Leq} + R_P R_S + \omega^2 M^2/2\right)}$$

A New P-Q Controller : Concept

- Secondary regulates power/voltage
  - *With fast response & no communication*
  - *Pout depends on RLeq controlled by β*

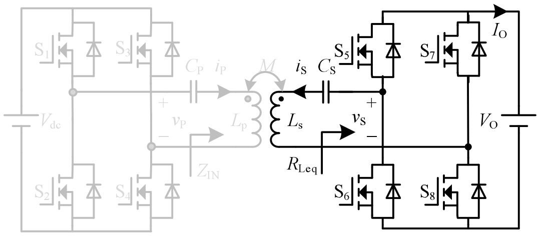

$$P_{out} = f\left(R_{\mathrm{Leq}}, M, \alpha\right)$$

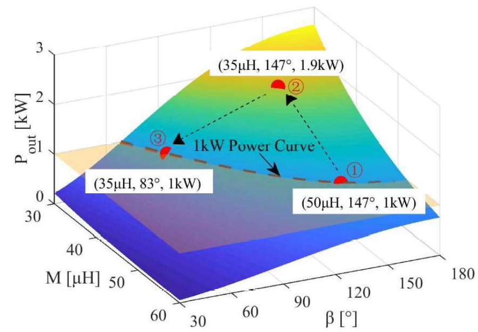

- Only one unique β

  for any given M & $\boldsymbol{\alpha}$!

- *Best combination of α & β ?*

A New P-Q Controller : Concept

- *Various 'α' gives various β_O (R_{LeqO}) for given P_{out}*
- *As α changes β_O changes too.*

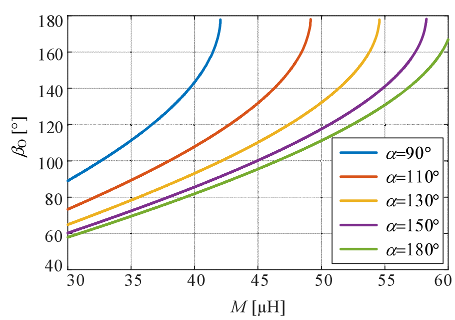

- Find R_{Leq} that gives primary ZPA

$$R_{\mathrm{LeqZ}}\Big|_{\mathrm{Im}(Z_{\mathrm{IN}})=0} = \sqrt{\frac{X_S}{X_P}} \cdot \sqrt{\omega^2 M^2 - X_P X_S} - R_S$$

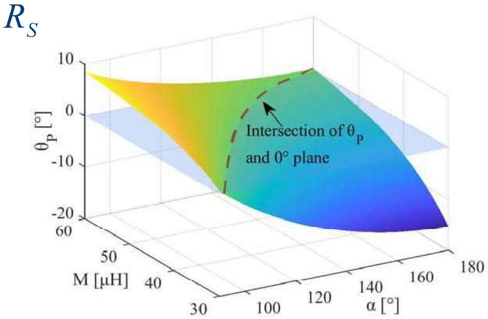

- *Changing* α to track ZPA means:

$$R_{\mathrm{LeqO}} = R_{\mathrm{LeqZ}}$$

THE UNIVERSITY OF AUCKLAND NEW ZEALAND WPW 2019

Source : Y. Liu & U. K. Madawala

Prepared by U. K. Madawala for WPW SCHOOL

A New P-Q Controller : Optimal ‘α_o’ & ‘β_o’

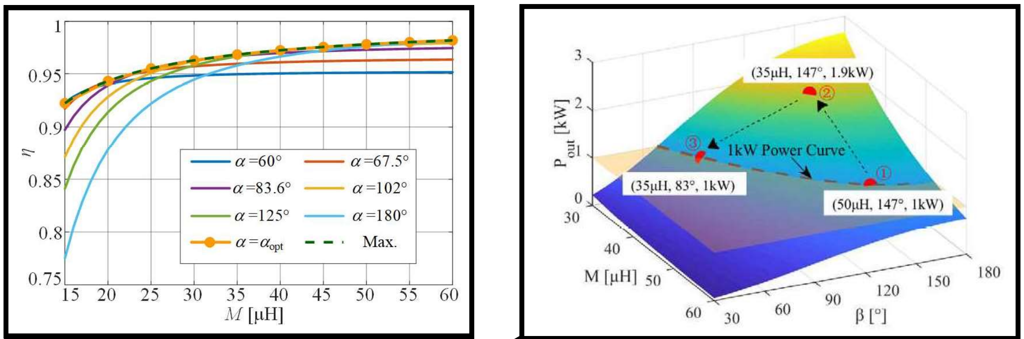

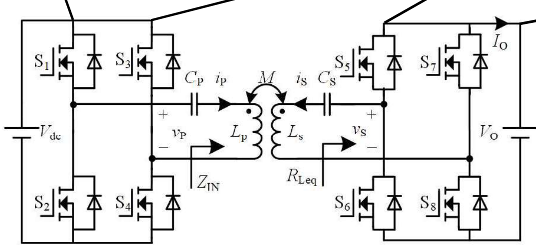

- Satisfies 2 goals simultaneously
  - *ZPA & constant output power*
  - *Optimal system efficiency*

$$R_{\mathrm{LeqO}} = R_{\mathrm{LeqZ}}$$

A New P-Q Controller : Results

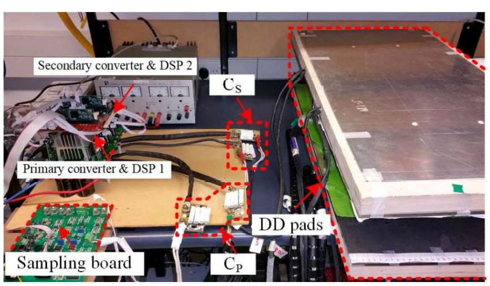

(a) Prototype

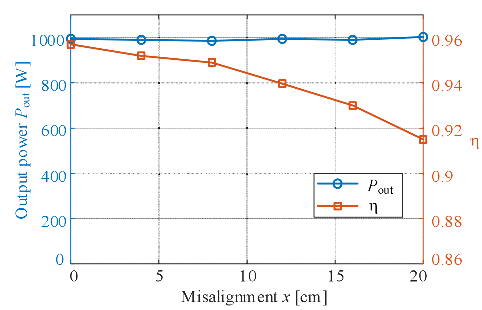

(b) Output power and system efficiency

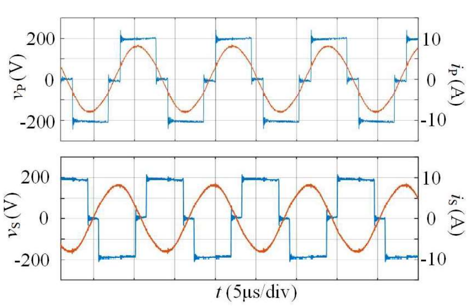

(c) Steady waveforms at x=8cm

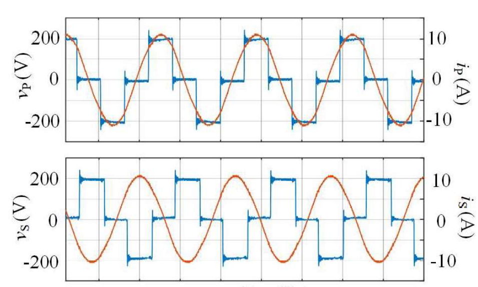

(d) Steady waveforms at x=20cm

A BD-WPT System based on Matrix Converters

A BD-WPT System

based on a matrix converter

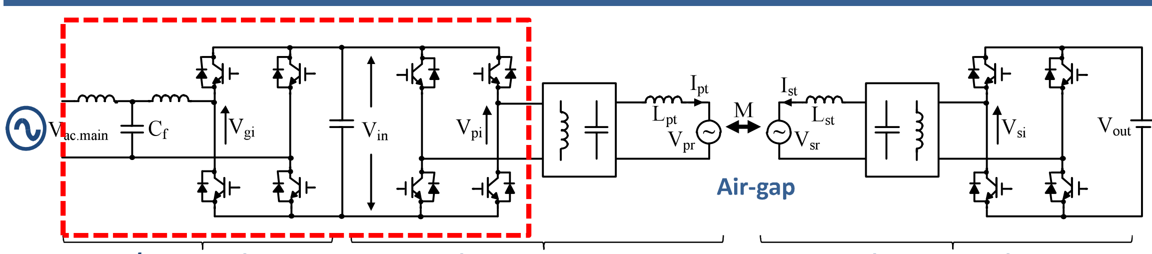

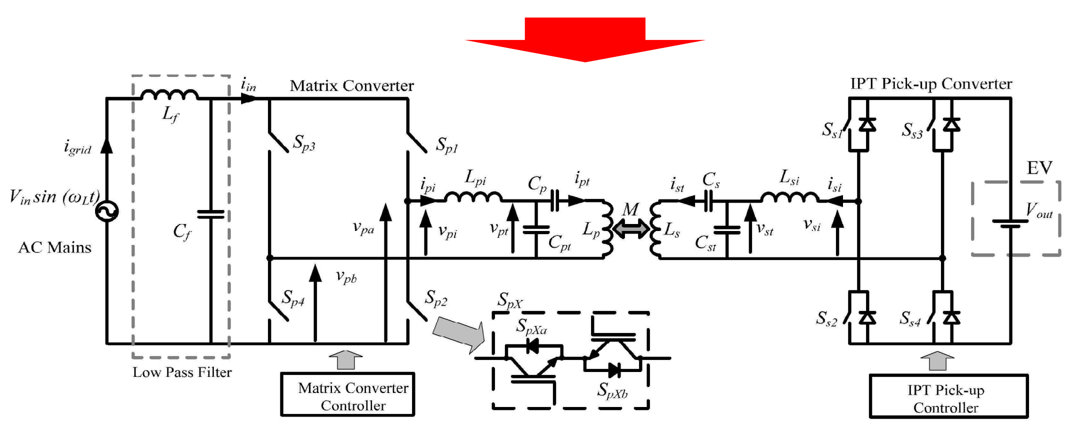

Source : S. Weerasinghe, U. K. Madawala & D. J. Thrimawithana

A BD-WPT System

based on a matrix converter

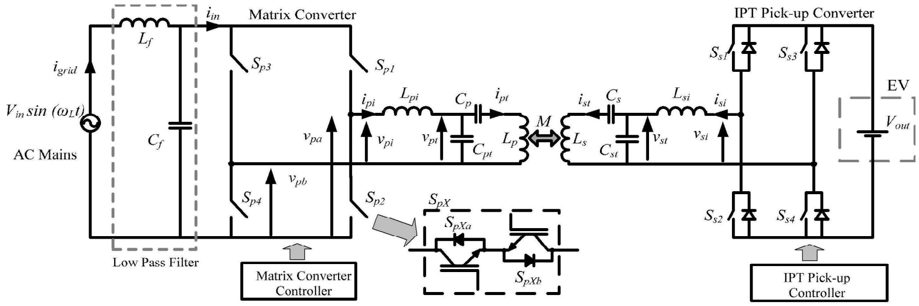

- Direct low frequency AC to high frequency AC conversion
  - *Does not require a large filter inductor or DC-link capacitors*
  - *Reduced number of conversion stages*
  - *Each bidirectional switch is operated at 50% duty cycle at resonant frequency*
  - *Employs a current direction based commutation algorithm*
  - *Complex control strategies required to ensure reliable operation*

$$i_{grid}(t)=\frac{V_{in}L_fC_f\omega_L\sin\left(\omega_Lt+\frac{\pi}{2}\right)}{1-\omega_L^2L_fC_f}-\frac{\psi\sin(2\omega_Tt+\theta)}{1-4\omega_T^2L_fC_f}-\psi\sin\theta \qquad P_{in+}=\frac{-16MV_{in}V_{out}}{\pi^3\omega_TL_{pt}L_{si}}\sin\left(\frac{\varphi_1}{2}\right)\sin\left(\frac{\varphi_2}{2}\right)\sin(\theta)$$

A BD-WPT System

based on a matrix converter

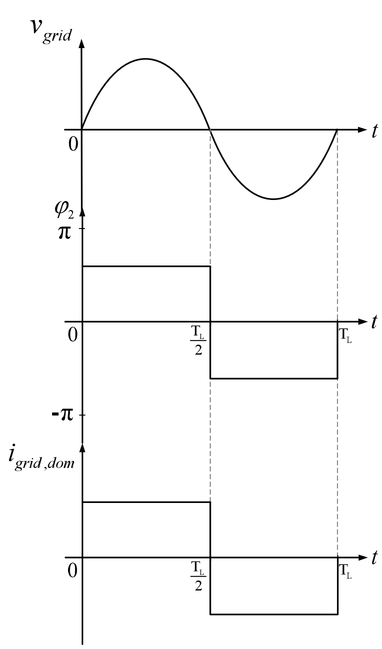

$$i_{grid,dom}(t)=\frac{8}{\pi^2}\frac{M}{\omega_TL_{pt}L_{si}}V_{out}\sin\left(\frac{\varphi_1}{2}\right)\sin\left(\frac{\varphi_2}{2}\right)\sin\theta$$

$THD \approx 48\%$

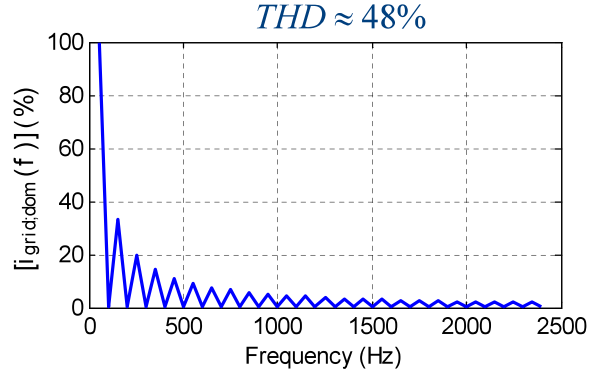

- ➢ *Attenuation of grid current harmonics is essential*
- ➢ *PWM based modulation techniques cannot be directly employed*

A BD-WPT System

based on a matrix converter

$$i_{grid,dom}(t) = \hat{i}_{grid,dom} sin\left(\frac{\varphi_2}{2}\right)$$

where

$$\hat{i}_{grid,dom} = \frac{8}{\pi^2}\frac{M}{\omega_T L_{pt} L_{si}} V_{out} \left| sin\left(\frac{\varphi_1}{2}\right) sin\theta \right|$$

$$\varphi_2 = \frac{4\pi}{T_L} t$$

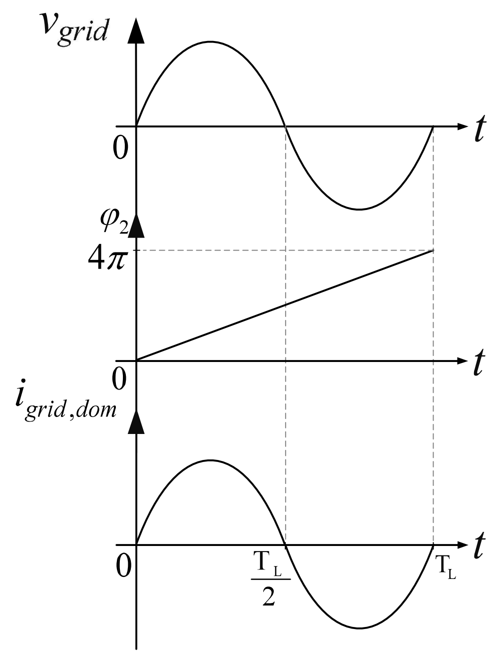

Forward & Reverse Power Flow

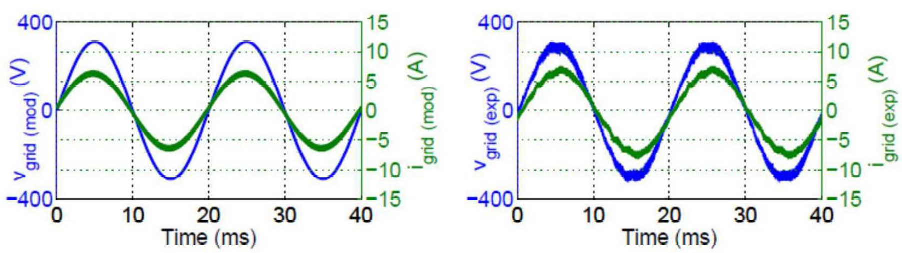

(a) (b)

i_{grid} for maximum power in forward direction at $\varphi_1 = \pi$ and $\theta = -\pi/2$ (a) theoretical and (b) experimental

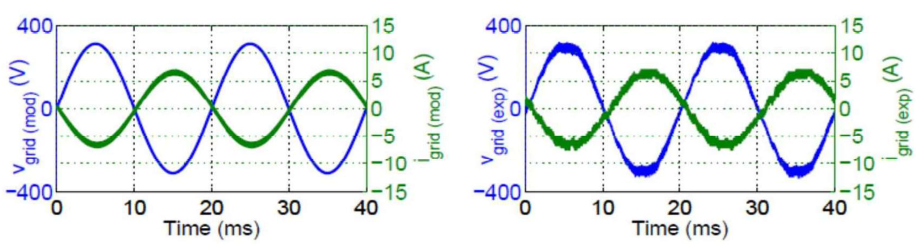

(a) (b)

i_{grid} for maximum power in reverse direction at $\varphi_1 = \pi$ and $\theta = \pi/2$ (a) theoretical and (b) experimental.

Dynamic EV Charging
with pulsed power

A Hybrid BD-WPT system
for dynamic charging

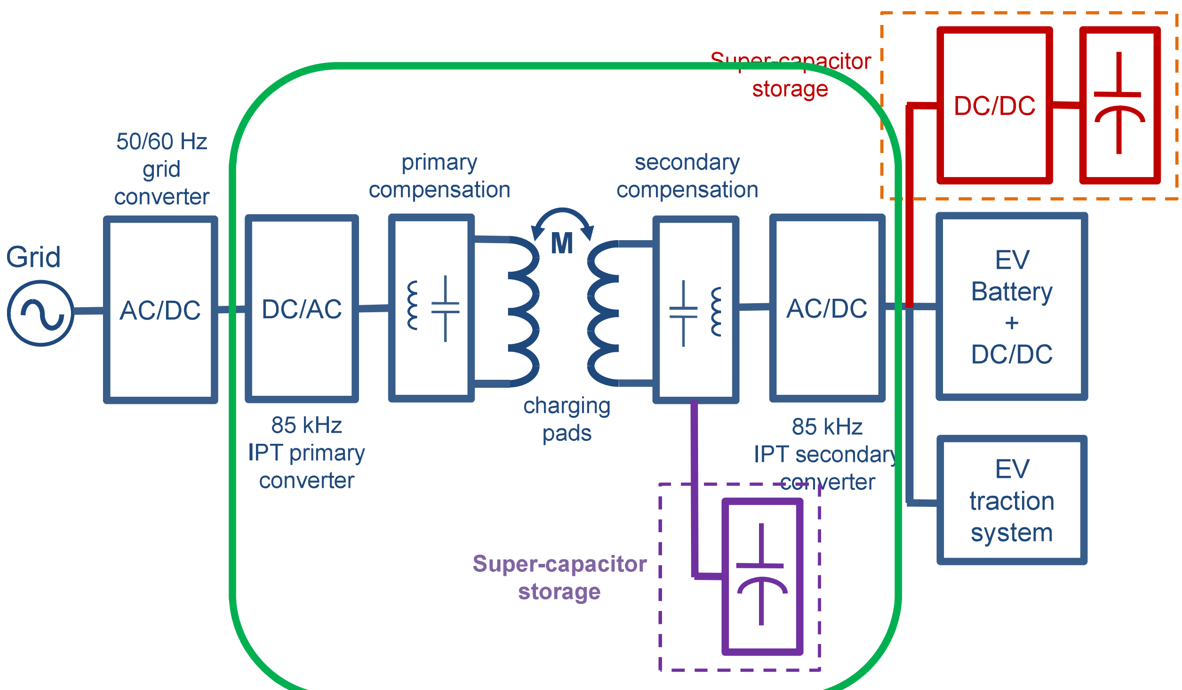

Source : S. Ruddlle, D. J. Thrimawithana & U. K. Madawala.

Prepared by U. K. Madawala for WPW SCHOOL

A Hybrid BD-WPT system

for dynamic charging

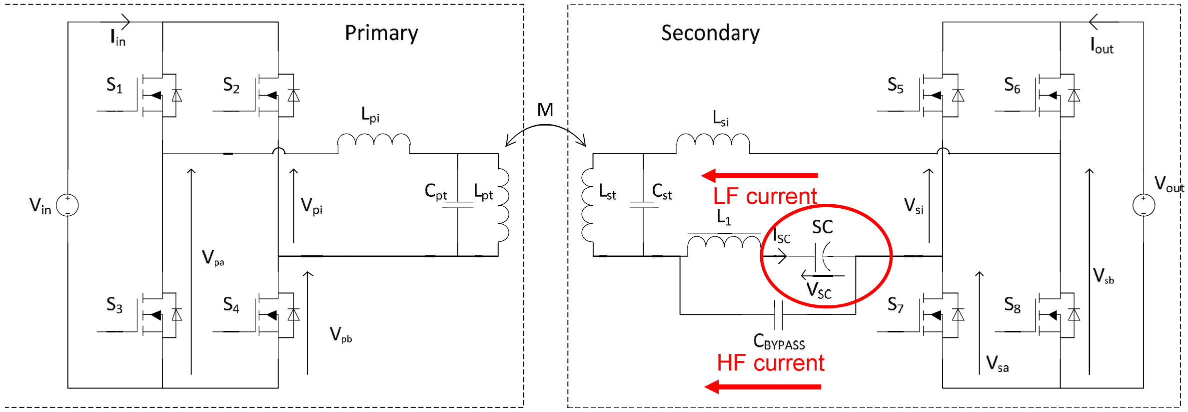

- An integrated (in primary or secondary) super-capacitor (SC) bank
- Eliminates the extra converter stage
- Allows for both storage and retrieval of energy in 9 modes of operations

Modes of Operation

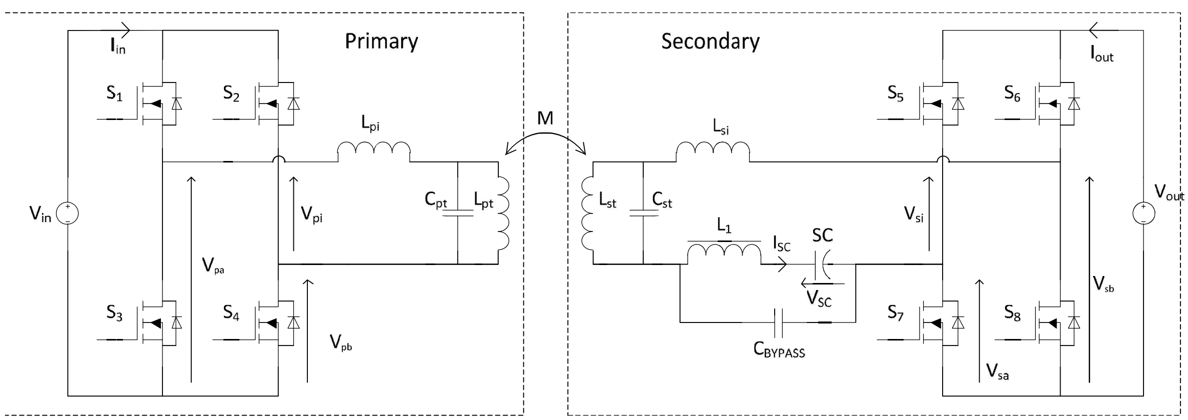

$$P_{out} = \frac{4MV_{in}V_{out}}{\pi^3 L_{pt} L_{st} f_{sw}} \sin\theta \sin\frac{\varphi_p}{2} \sin\frac{\varphi_s}{2} \cos\frac{\pi D}{2}$$

Where D is the Duty cycle offset between legs of secondary converter

Control

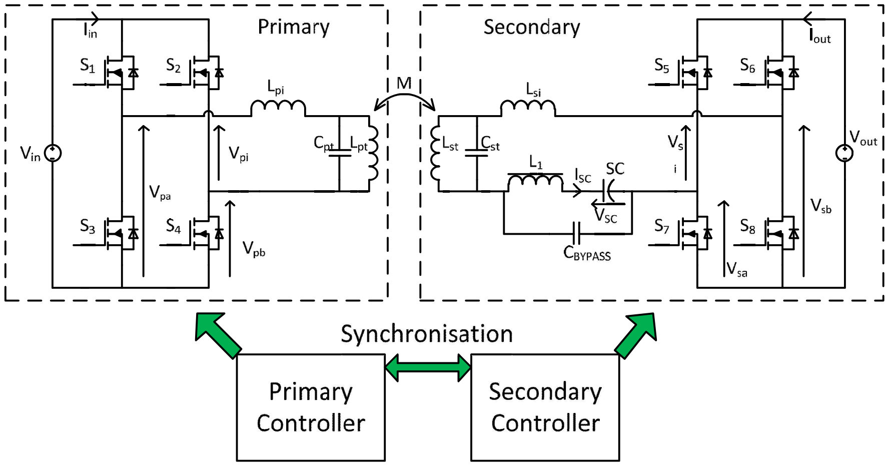

- Primary controller sets the power to/from grid
- Secondary controller sets the power to/from EV and SC
- Synchronisation to allow bi-directional power transfer

Experimental Results

- 3.7 kW nominal rating, LCL tuning, 90 F super capacitor

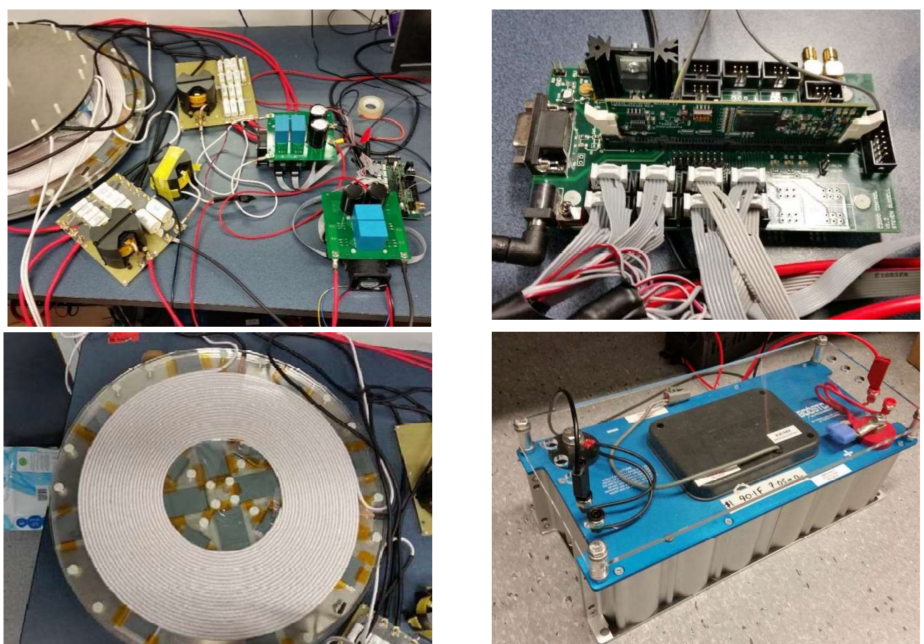

Experimental Results

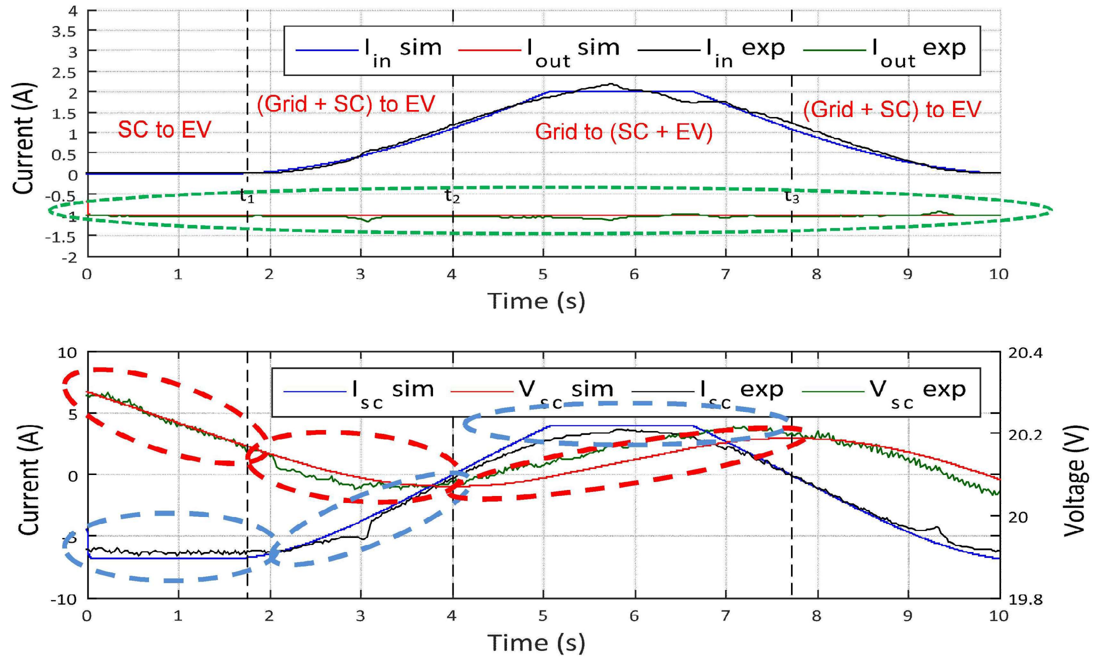

Source : S. Ruddell, D. J. Thrimawithana & U. K. Madawala.